國立臺灣大學醫學院藥學研究所

碩士論文

Graduate Institute of Pharmaceutical Sciences
College of Medicine
National Taiwan University

Master Thesis

合成具有活性，選擇性之鈉依賴型葡萄糖共同運輸通道抑制劑之碳-芳香環-D-呋喃葡萄糖苷作爲治療第二型糖尿病之藥物

Synthesis of C-aryl D-glucofuranosides as Potent, Selective Sodium-Dependent Glucose Cotransporter 2 (SGLT2) Inhibitors for Type 2 Diabetes Treatment

劉雅雯

Ya-Wen Liw

指導教授 ：梁碧惠 博士

Advisor: Pi-Hui Liang, Ph.D.

中華民國 100 年 7 月

July, 2011

Acknowlegdement

The completion of this Master's Thesis would not have been possible without the help, support and guidance of several individuals who in one way or another contributed and extended their valuable assistance during the process of study.

First and foremost, utmost gratitude to my supervisor, Dr. Pi-Hui, Liang for giving me the opportunity to work in her lab knowing that I have only little experience in the field of chemical synthesis. For being an endless and tireless mentor when I hurdle all the obstacles during the research work, I would say she is not only a great teacher but also great friend.

Dr. Tsui-Ling, Hsu from Genomics Research Center of Acedemia sinica for her kindness and passion in teaching me experimental techniques. I am indebted to all other fellows in lab 6L12 who have always helped me patiently, especially Sarah Cheung, Vince Huang, PK and Elvis.

Dr. Li-Jiuan Shen for her generosity for allowing me to use the culture room and the kindness of her students in providing me helps all the time.

Special thanks to my friends in R1247 and those who had helped and would like to stay anonymous, for your friendship and the positive energy you spread through the hard times.

Last but not the least, special thanks to my family and friends, words alone cannot express the thanks I owe to you.

中文摘要

目前大多數用於治療第二型糖尿病(T2DM)的藥物，並不足以維持血醣於理想範圍，即糖化血色素(Hb_{A1c})數值小於 7%。因此，亟需發展有別於目前治療機轉的其他藥物。第二型鈉依賴葡萄糖轉運蛋白(SGLT2)由 672 個氨基酸所組成，獨特地表現於腎近端小管 S1 部分，以高容量，低親和力的方式將大部分存在在腎小球濾液裏的腎糖再吸收， 因此推測抑制 SGLT2 能夠降低血糖濃度以達到血糖控制的效果。

先導化合物，Dapagliflozin **7**，具有碳－芳香環-六環葡萄糖苷之結構，可選擇性與 SGLT2 結合但不被轉運，是一個活性極高的抑制劑。先前已有研究指出，六環的 *N*-glucosides, *S*-glucosides, thio-*C*-glucosides and dioxa-bicyclo-[3.2.1]octane 皆對 SGLT2 有抑制的效果，但並未有文獻針對呋喃葡萄糖苷（水溶液中的糖有 1%是由呋喃葡萄糖苷組成的）的結構進行過討論。因此我們設計並合成了一系列由碳-芳香環-D-呋喃葡萄糖苷組成的化合物。兩個關鍵的中間物，分別為 D－葡萄糖酸－γ－內酯 **46** 為偶聯反應所用及 *C*－苯甲醛－葡萄糖 **65** 為格氏反應所用。

利用穩定表達 hSGLT1 的 COS-7 細胞，我們針對化合物 **32a**–**32r** 進行了 ^{14}C-AMG 攝取抑制測試；然而結果顯示這些分子在 5μM 的濃度中，對 hSGLT1 並無抑制效果。另外，針對 hSGLT2 的細胞測試仍在進行中。

Abstract

A wide range of medications available for type 2 diabetes (T2DM) are inadequate to maintain the glycemic control at Hb_{A1c} <7%, hence development of novel drug with different mechanism of action is desirable. Type 2 sodium-dependent glucose co-transporter (SGLT2) is a 672-amino acid, high capacity, low affinity transporter express nearly exclusively in the S1 segment of the renal proximal tubule. Since SGLT2 mediates the majority of renal glucose reabsorption from the glomerular filtrate, inhibiting SGLT2 is believed to be able to decrease the glucose level to achieve glycemic control.

Dapagliflozin (**7**), a leading compound with a structure of C-arylglucoside, can bind to but not be transported by SGLT2, andacts as a potent and selective SGLT2 inhibitor. Various glycoform, such as *N*-glucosides, *S*-glucosides, thio-*C*-glucosides and dioxa-bicyclo-[3.2.1]octane have been studied for their effect on SGLT2 inhibitions but no report was published on glucofuranosides which contain 1% composition of sugars in aqueous solution. Herein, we designed and synthesized a series of novel (1*S*)-1,4-anhydro-1-*C*-aryl-D-glucitol derivatives. To get these compounds, 2 key intermediates—perbenzylated D-glucono-gamma-lactone **46** and *C*-benzylaldehyde glucoside **65,** were synthesized and they were sequentially subjected to the coupling reaction and Grignard reaction to afford the desired structures.

The inhibitory effect of compounds **32a-32r** on the uptake of [^{14}C]-AMG were tested in COS-7 cell stably expressing hSGLT1, the results showed no inhibitory activity of these compounds at 5 μM against hSGLT1. Further study on the cell-based assay of hSGLT2 is still in progress.

Table of Contents

List of Figures

List of Tables

List of Schemes

List of Abbreviations

DMP	Dess-Martin periodinane
DMAP	4-Dimethylaminopyridine
DMF	*N*, *N*-Dimethylforamide
DPP-4	Dipeptidyl peptidase-4
EA	Ethyl acetate
EGFP	Green fluorescent protein
GLP-1	Glucagon-like peptide-1
MsOH	Methanesulfonic acid
NMM	*N*-methylmorpholine
PCC	pyridinium chlorochromate
SAR	Structure-activity relationship
SLC5A	Solute carrier family 5
SMIT	Sodium/inositol cotransporter
TBAF	Tetra-*n*-butylammonium fluoride
TBAI	Tetra-*n*-butylammonium iodide
THF	Tetrahydrofuran
TIPSCl	Triisopropylsilyl chloride
TMSCl	Trimethylsilyl chloride
Vdss	Volume of distribution at steady state

1. Introduction

1.1 Type 2 Diabetes Mellitus (T2DM)

Type 2 diabetes mellitus (T2DM), formerly non-insulin-dependent diabetes mellitus (NIDDM) or adult-onset diabetes is a highly prevalent disease affecting more than 150 million people worldwide especially in developed countries.[1] However, the number of patient has been rapidly increasing in developing countries.[2]

Chronic hyperglycemia not only presents as the hallmark of T2DM diagnosis, it is also shown to be the main cause of two defects: β-cells failure & insulin resistance.[3] This glucotoxicity effect is the major risk factor for the microvascular complications including retinopathy, neuropathy, nephropathy and heart failure which are the main causes of morbidity and mortality in T2DM.[4] As been shown by the United Kingdom Prospective Diabetes Study (UKPDS), all of these complications are directly proportional to the level of glycosylated hemoglobin (Hb_{A1c}) which should be controlled between 6.5-7% in diabetic subject.[5] Therefore, a good control of blood glucose level can not only reduce the risk of microvascular complications but also improves the developed metabolic abnormalities. Although control of diet and exercise may improve the condition, combination with medical regimen is necessary to achieve the optimal effect.

The initial therapy strategies have been shifting from insulin secretogougues and α-glucosidase inhibitor which prevents digestion of carbohydrates to monosaccharides to insulin sensitizers such as metformin and the thiazolidinediones (TZDs, Figure 1).[6] As an old drug with generic form available, metformin continues to be the most favorable prescription drug due to its low cost and efficacious. Metformin exerts its glycemic effect

by suppressing the glucose production in liver (hepatic glucogenesis),[7] increasing insulin sensitivity, increasing peripheral uptake of glucose[8] and decreasing absorption of glucose from gastrointestinal tract. Other than that, metformin may promote weight loss compared to TZDs which had found to be associated with weight gain,[9, 10] fractures and an increased risk of congestive heart failure.[11,12] The contraindication of metformin being the risk of lactic acidosis in patient with kidney, lung or liver disease,[13] but this can be easily avoided as long as it is not prescribed to the known high-risk groups. Combination regimen (e.g. metformin, sulfonylurea, TZDs, meglitinides, DPP-4 inhibitors and GLP-1 receptor agonists) is often used in diabetic treatment in order to achieve sufficient control of blood sugar but it is found that none of these combinations is showing prevailing effect over the others. Moreover, most of these agents are unable to maintain their glycemic control after 3-9 years' time which might be caused by the decline of β -cell function where the effectiveness of these drugs relies on insulin action.[14] Thus, new strategies, especially those works independently from insulin is urging to be discovered.

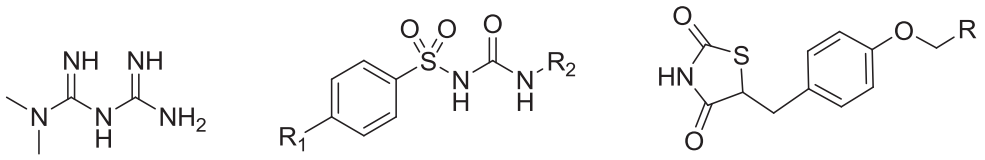

Metformin **Sulfonylurea** **Thiazolidinedione (TZD)**

Figure 1. Structure of anti-diabetic drugs

1.2 Sodium-Glucose Cotransporter (SGLTs)

1.2.1 Glucose Transporters Description

Glucose being the key fuel for cellular metabolism has to be well reserved in living body. With its high polarity, glucose is unable to cross the lipid bilayer in living cell, hence in order to transport from the extracellular to intracellular space, it needs assistance from protein transporters. There are two distinct classes of glucose transporters present: 1) Facilitative glucose transporter (GLUTs), consists of 12 transmembrane domains, facilitate the passive transport of glucose across the membrane along its concentration gradient, hence no energy is required;[15,16] 2) Sodium-glucose co-transporter (SGLTs), 14 transmembrane protein spanning α-helices,[17,18] translocate glucose across the cellular membrane against the concentration gradient, where it consumes energy provided from sodium transport along its electrochemical gradient.[15, 16] So far there are 6 different genes encoded for SGLTs being identified (Table 1)[19] in human, SGLT type 1 & 2 encoded by the solute carrier genes SLC5A1 and SLC5A2, respectively, are more well-studied and its function under both physiological and pathological conditions are being extensively elucidated.

Table 1. The sodium- glucose co-transporter family[19]

Co-transporter	Gene	Substrate	Tissue distribution
SGLT1	**SLC5A1**	**Glucose, galactose**	**Intestine, trachea, kidney, heart, brain, testis, prostate**
SGLT2	**SLC5A2**	**Glucose**	**Kidney, brain, liver, thyroid, muscle and heart**
SGLT4	**SLC5A9**	**Glucose, mannose**	**Intestine, kidney, liver, brain, lung, trachea, uterus,pancreas**
SGLT5	**SLCA10**	**Not known**	**Kidney**
SGLT6	**SMIT2/SLC5A11**	**Glucose, myo-inositol**	**Brain, kidney, intestine**
SMIT1	**SLC5A3**	**Glucose, myo-inositol**	**Brain, heart, kidney, lung**

SGLT1

The human SGLT1 (hSGLT1) is a 75 kDa heavily glycosylated protein and its gene encodes for 670 amino acids with the extracellular N-terminus and intramembrane C-terminus. There are 2 glucose binding and translocation domains with one on the extracellular face and another on the intracellular face located in the 5 transmembrane regions (X, XI, XIII, XIV) nearest to C-terminus.[19] The N-terminal segment 4-5 domain is responsible for the sodium recognition as well as the coupling of sodium electrochemical gradient to the sugar translocation during the cotransport (Figure 2). It is a primarily expressed in the S3 segment of renal proximal tubule and intestinal mucosa where it transports both glucose & galactose with similar affinity.[20]

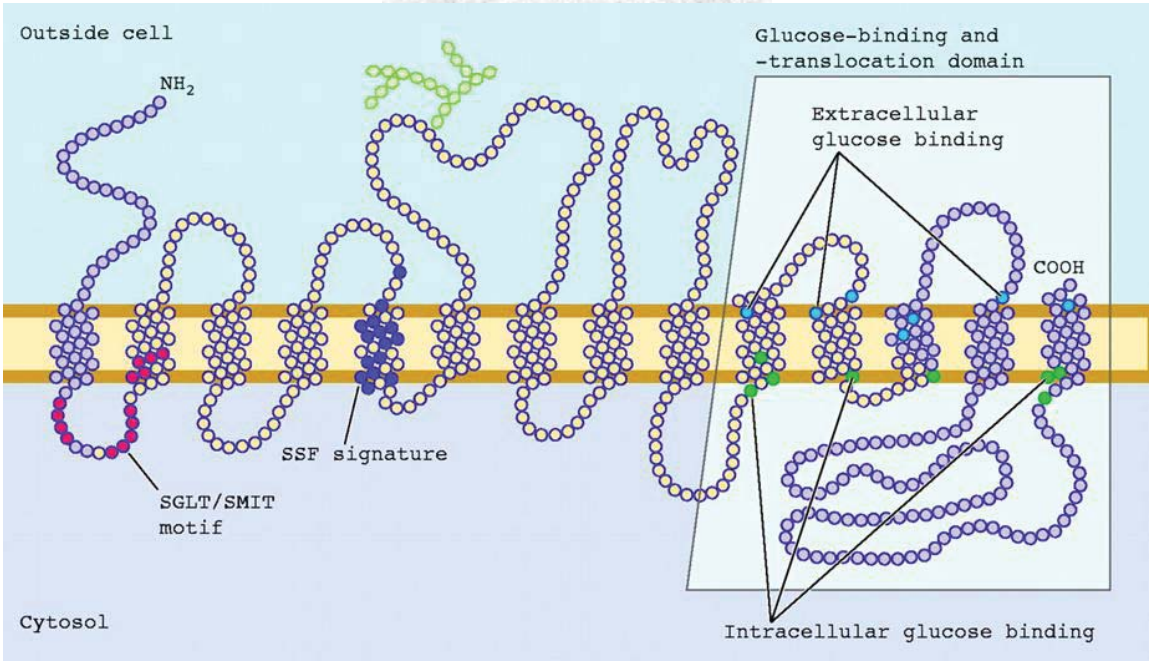

Figure 2. The secondary structure of SGLT1[20]

SGLT2

The human SGLT2 (hSGLT2) is identified in the year of 1991, 4 years after SGLT1 identification. It has approximately 58 % amino acids sequence homology to SGLT1 and it displays the least homology with other SGLTs in the family.[21] The gene encodes for a protein of ~75 kDa which consisted of 672 amino acids. SGLT2 is primarily expressed on the epithelial cell in S1 segment of the proximal tubule.[19] It is also expressed in low level in the brain & liver.[22] SGLT2 only transports D-glucose rather than both glucose and galactose as in SGLT1.[23]

1.2.2 Glucose Reabsorption in Kidney

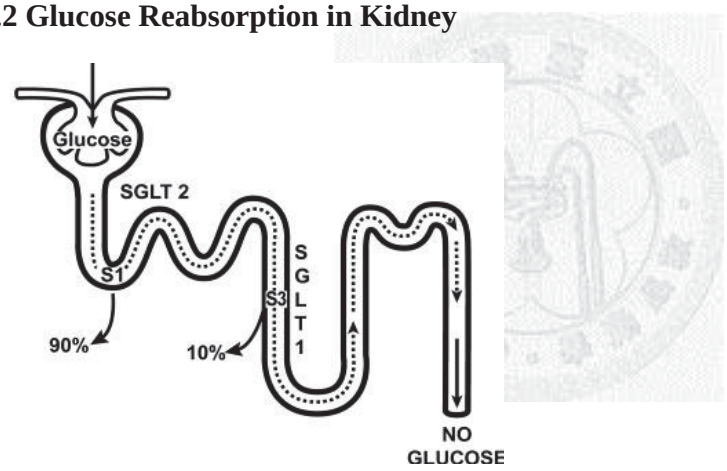

Figure 3. SGLTs role in glucose reabsorption [24]

The kidney serves a pivotal role in maintaining blood glucose in normal subjects. The glomerulus filtered approximately 180 liters of plasma with glucose concentration of 90 mg/dl each day. About a total of 180 g of glucose is reabsorbed in the proximal tubule in normal glucose-tolerant subjects. 90% of work is done by SGLT2 in early convoluted S1 segment in a high capacity-low affinity (Tmax = 10 nmol/mg protein·min, *K*m = 2 mM) mode while SGLT1 in the distal S3 segment is account for the reuptake of 10% remaining

glucose the mode of low capacity-high affinity (Tmax = 2 nmol/mg protein·min, *K*m = 0.2 mM) [Figure 3].[22,25,26] The glucose reabsorbed through brush border membrane will be then transported back into peritubular capillary *via* exocytosis or efflux through GLUT1 in late proximal tubule and GLUT2 in early proximal tubule.[27] The Na^+/K^+ pump functions to maintain the low level of intracellular Na^+ level in order generate the electrochemical gradient for SGLTs function (Figure 4). [22,24]

The maximum glucose transport capacity (Tm) of kidney varies among individuals but the average value is approximately 375 mg/min. In normal glucose-tolerant subjects, the filtered glucose load is below 375 mg/min, thus all the filtered glucose will be reuptake back to the blood and no glucose will be presented in urine. However, in diabetic patient, the plasma glucose concentration is directly related to the amount of filtered glucose which is often exceed the threshold of Tm (375 mg/min), hence the excess filtered glucose will be passed out with urine. The glucose excreted in urine is directly proportional to the amount of filtered glucose. [24]

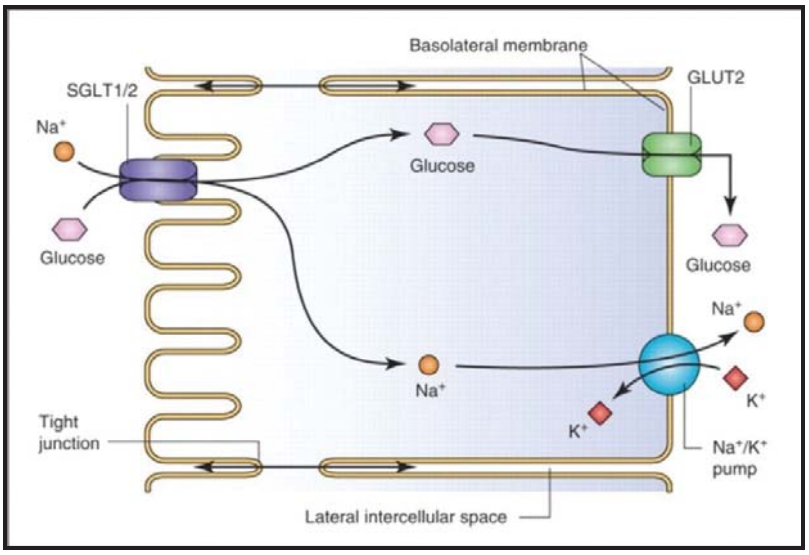

Figure. 4 Mechanism of glucose reuptake[28]

1.2.3 Hyperglycemia Effects in SGLT2 & GLUT2 Gene Expression

In theoretical view, hyperglycemia will increase both the interstitial & blood glucose concentration and would attenuate the concentration gradient across the basolateral membrane (BLM) which will then leads impairment of glucose efflux from epithelial cell and as a whole, less glucose reuptake to bloodstream. However, experiments in diabetic animal model consistently disapproved this theoretical standpoint. It was found that, in uncontrolled diabetic animal model, the rate of glucose reabsorption increased above the threshold (375 mg/min). [29-31] It has been also been reported that, under hyperglycemic environment, the molecular mechanism adapted by increasing the expression of SGLT2 gene the renal proximal tubule cells both in experimental animals & humans.[32] The elevated expressions of SGLT2 mRNA and protein have also been demonstrated to correlate with higher glucose reabsorption (Figure 5).[32] The treatment with insulin & phlorizin had shown to reversed the elevated SGLT2 gene expression by correcting the hyperglycemic environment.

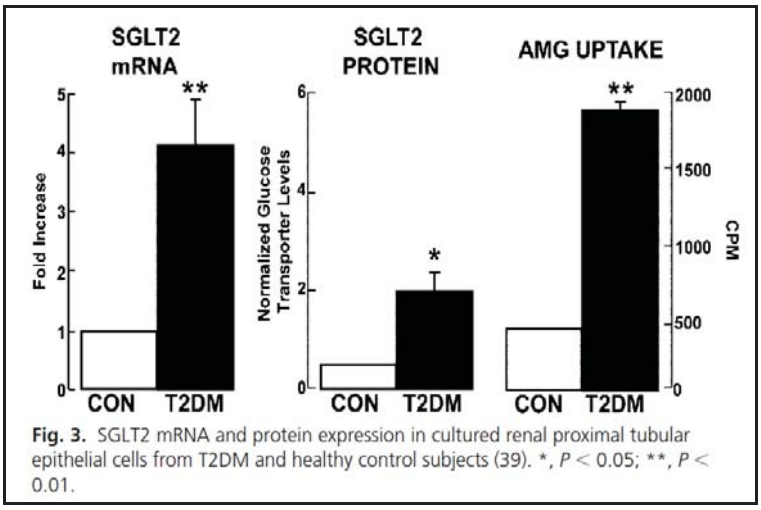

Fig. 3. SGLT2 mRNA and protein expression in cultured renal proximal tubular epithelial cells from T2DM and healthy control subjects (39). *, $P < 0.05$; **, $P < 0.01$.

Figure 5. SGLT2 mRNA and protein expression and glucose uptake level in healthy versus diabetic subjects[32]

In subject with normal glucose tolerance, the reabsorption of glucose in kidney to maintain the energy reservoir is of great benefit to the brain which can only utilize glucose to generate energy for neuronal function. However, the data from above experiments showed that, the adaptive mechanism in kidney had become the backfire under hyperglycemic environment. Instead of exacerbating the condition, it would be desirable for the kidney to excrete the excessive glucose as what have been predicted in theoretical stand and restore normoglycemia.

1.2.4 Genetic Disorders

There are 2 types of genetic disorder involving SCL5A1[33,34] and SCL5A2[35,36] genes respectively: 1) Glucose-Galactose Malabsorption (GGM, MIM 182380); 2) Familial Renal Glucosuria (FRG, MIM233100). GGM is inherited in an autosomal recessive pattern, the missense mutation caused SGLT1 protein misfolding that impaired the trafficking to the plasma membrane. GGM is a rare disorder found in infancy and is characterized by watery diarrhea which may lead to dehydration and death if left untreated. The treatment is immediately removal of lactose, glucose and galactose-containing substances from the diet, and replacement with fructose-based formula. Some of the affected infant may be able to tolerate glucose & galactose. FRG is also an autosomal recessive disease which appears to be a benign condition characterized with glycosuria in the absence of hyperglycemia and other proximal tubule dysfunction. There are 21 different gene mutation have been described for SGLT2, majority of the defects are caused by missense and frameshift mutations which result in disruption of transmembrane domains 10-13 of SGLT2 for the

binding and translocation of sugar moiety.[35] The severity of glycosuria differs among individual, ranging from 20~200 g of glucose excreted per day. Despite, the affected subjects are generally asymptomatic, except for some unusual and rare case of polyuria or hypoglycemia.

SGLT2 gene knockout mice were generated in order to investigate the physiological impact in the absence of this protein. Compared to WT mice, *Sglt2*$^{-/-}$ mice showed glycosuria, polyuria, increased uptake of food & water without affecting the plasma glucose level, glomerular filtration rate (GFR), urinary excretion of other proximal tubular substrates.[37] This result has provided a proof of concept that inhibition of SGLT2 is a safe and potential strategy in sustaining normal blood glucose level free from hypoglycemia and insulin control.

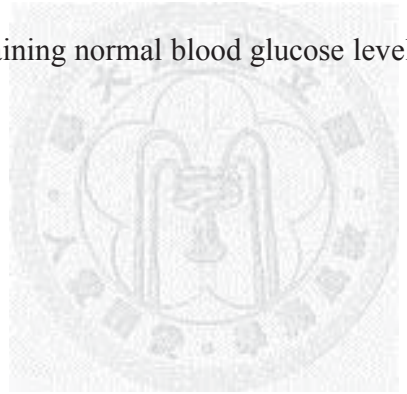

1.3 SGLT2 Inhibitors

Understanding of the interaction binding affinity and stoichiometry of sugar upon SGLTs during the translocation serves a pivotal role in molecular based design of potent inhibitors. Hence, extensive studies have been carried out on different sugar moiety to define the substrate specificity.

Sugar can only be transported through the transporter in hexose and D-configuration except for fructose, which means all others L-conformation sugars will not be transported through the sodium-glucose cotransporter. Beta positioning of -OH group and the functional group itself are crucial at C1 showing by the 10-fold loss of affinity by 1-deoxy-D-glucose.[19]

However, short aliphatic in alpha confirmation such as alpha-methyl D-glucose may be tolerated. In addition, the binding of beta-glucosides with larger aromatic aglycones are well accommodated with the domain at loop 13 of the transporter but not translocated.[19] In this case, beta-glucoside such as phlorizin (**1**, Figure 6) is a potent inhibitor for sodium/glucose cotransport.

The equatorial –OH group at C2 and C3 are required for the transport as D-mannose, *N*-glucosamine, D-allose, and 3-deoxy-D-glucose are not transported or transported only at a limited extend. The positioning at C4 is of less importance for SGLT1 but not so in SGLT2 as it has very much lower affinity for galactose. 6-Deoxy-D-glucose is transported but not pentose D-xylose which means the $–CH_2$ group has a more significant role then the –OH group here.[38] Moreover, at the binding site for C6 to SGLT2 there seems to have a hydrophobic pocket for an alkyl group[38] which provides a chance in designing an inhibitor selectively against SGLT2 over SGLT1.

1.3.1 Evolution of SGLT2 Inhibitors: *O*-glucosides, *C*-arylglucosides and Other Agents

Phlorizin (**1**, Figure 6) is a glucoside linked to phloretin (**2**, dihydrochalcone) and was found from the bark of apple trees in the year of 1835. Initially it was proposed as drugs for fever, infectious disease, and malaria. However, within 50 years, it was found out to be causing diabetic-like symptoms such as glycosuria, polyuria and weight loss when administered at high doses. Start from then, it was used as a tool in evaluating the renal physiology.[28]

The interaction of **1** with the isolating SGLTs showed a competitive inhibition at the D-glucose binding site while the **2** binds to the receptor in a non-competitive form with low affinity.[39] The aglycone binding site was investigated in rabbit SGLT1 by mutagenesis and transport studies in transfected cells. The region between amino-acids amino acids 602-610 was showed to involve in binding of **1** but not D-glucose.[40] The same conclusion was reached at the finding of major conformation changes at the position of 602-609 on the isolated human SGLT1 with the binding of **1** or **2** but only minor changes was observed with D-glucose.[41] AAs from 606 to 630 represents the late part of loop XIII & XIV formed a condensed conformation which increased in hydrophobicity upon the binding of **1**.[42]

The most important point of this molecular studies have to be the differences between hSGLT1 and hSGLT2 as there are many sequence similarity and conservative replacement in the transmembrane region. The extramembranous loop are more various, particularly at the C-terminus which is binding site of aglycone.[43] Compared to hSGLT1, hSGLT2 has 10 more AAs and 2 more cysteines at loop XIII & XIV close to the assumed binding site. Several hydrophilic groups have been replaced by hydrophobic groups in hSGLT2 which explained a higher affinity of **1**.[44]

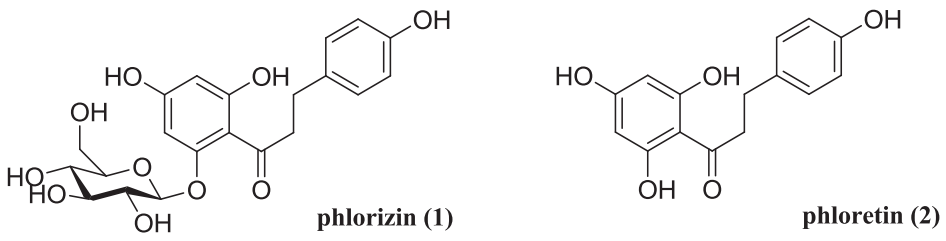

Figure 6. Phlorizin (**1**) and the aglycone (**2**)

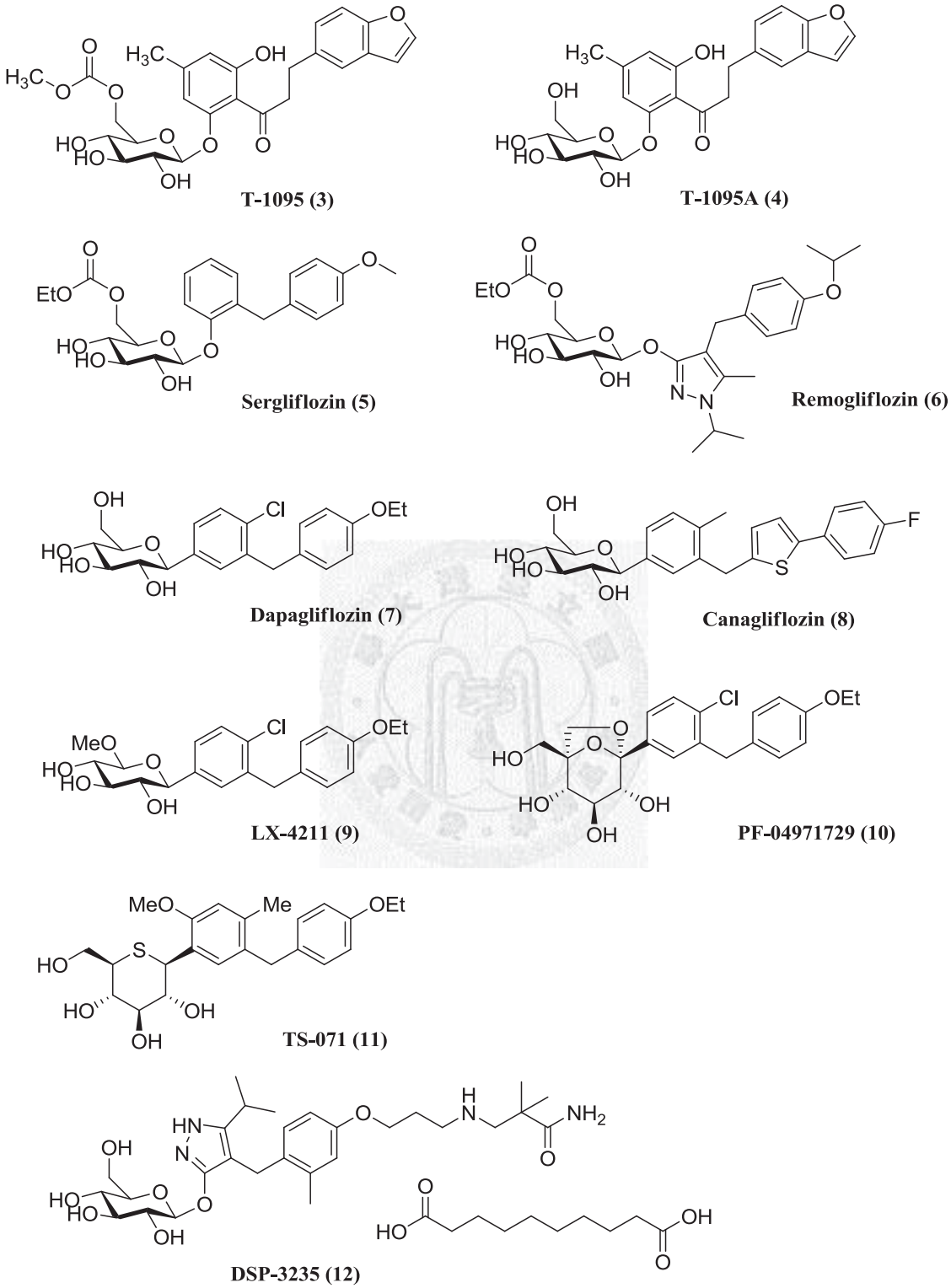

Figure 7. Structure available for SGLT2 inhibitors[48]

A. *O*-glucosides

*Phlorizin **(1)***

Phlorizin (**1**) (Figure 6) with the ability to normalize the fasting and postprandial glucose concentration and reverse insulin resistance in diabetic patient *via* inhibition of SGLT2 however it had not been pursued to clinical trial for treatment of diabetes. This is due to its poor absorption in the gastrointestinal tract in the presence of *β*-glucosidase which will cleave the *O*-glucoside linkage.[45] The cleavage will release the aglycone phoretin (**2**) which has shown to antagonize GLUT1, the main glucose transporter in blood brain barrier, may lead to serious neurology defects.[46] Lastly, **1** binds to SGLT1 although in a lower affinity but is sufficient to cause fetal diarrhea.[47] Based on these limitations, **1** has become the lead compound in developing other glycosides with greater bioavailability and higher selectivity for SGLT2.

*T-1095 **(3)***

With an addition of methyl carbonate group to C6 of phlorizin, a new drug T-1095 (**3**) was produced. **3** is a prodrug developed by Tanabe Seiyaku Co. (Figure 7)[48] to prevent the action of glucosidase in the gut to produce a higher bioavailability after oral administration.[49] The prodrug will be metabolized into T-1095A (**4**), the active form that inhibits SGLT2 with 30-fold higher specifity over SGLT1 to produce glucosuria. The maximal glucosuria effect (1g/100g body weight per 24 h) in normal and diabetic rats was achieved by a dose of 300 mg/Kg.[48] Due to the insufficient selectivity upon SGLT2, **3** was discontinued after phase II clinical trials.

*Sergliflozin (KGT-1251) (**5**)*

Sergliflozin (**5**) was initially developed by Kissei Pharmaceutical Co. but later on being developed by GlaxoSmithKline (GSK) for the indication of diabetes.[48] Similar to **3**, it has also been designed as a prodrug, sergliflozin etabonate with a methyl spacer between 2 aromatic rings (Figure 7). With the modification on the aglycones, both **3** & **5** avoid the antagonistic effect on GLUT.[50] Most importantly, **5** showed a significantly higher selectivity of 296-fold over SGLT1 (K_i = 2.39 nM over 708 nM) in human cells expressing both SGLT subtypes.[24] Oral administration in animal models including rats, mice and dog, **5** demonstrated a dose dependent glucosuria. An oral dose of 30 mg/Kg caused glocosuria in a unit of 1 g/Kg/day in dogs and 2 g/Kg/day in rat.[50] However, in pharmacodynamics/pharmacokinetic studies in human under fasting and after glucose-loading, the 24-h glucose excretion at the highest doses of 500 mg was only 18-27% of the glomerular filtration amount.[51] Hence, it had been discontinued after phase II clinical trial and the indication was changed to obesity.

*Remogliflozin (**6**)*

Remogliflozin etabonate is a prodrug as **3** & **5** with a structure of benzylpyrazole glucoside (Figure 7). Compared to **1**, **6** showed 2 times greater potency towards rat SGLT2 with a ratio of selectivity of 38 against SGLT1. Even greater selectivity was shown for hSGLT2 with the K_i value of hSGLT1/hSGLT2 equals to 365. Without stimulating insulin, **6** inhibited the raise of plasma glucose after glucose loading. With a chronic treatment of **6**, db/db mice showed reduced levels of fasting glucose and Hb_{A1c} through ameliorating

glucosuria.[52] However, the clinical trial initiated by GSK was discontinued after phase II as a result of evaluating circumstances including the development status of SGLT2 inhibitors by competitors while they chose to develop KGA-3235/DSP-3235 (**12**, Figure 7), a SGLT1 inhibitor instead under the license from Kissei Pharmaceuticals.[48]

B. *C*-arylglucosides

In order to further improve the bioavailability of SGLT2 inhibitors, avoiding the metabolic instability of the *O*-glucoside linkage, a new generation of drugs consisted of *C*-arylglucosides was developed.

*Dapagliflozin (BMS-512148) (**7**)*

Dapagliflozin (**7**, Figure 7) is a competitive, reversible and highly selective SGLT2 inhibitor which is the furthest advanced compound in development of SGLT2 inhibitor class. This drug is being studied by Bristol-Myers Squibb in partnership with AstraZeneca and was accepted for review by U.S. Food and Drug Administration in March 2011 with a Prescription drug User Fee Act (PDUFA) date set for October 2011 (Table 3).[48]

In rats animal model studies, **7** showed 84% bioavailability and a pharmacological half-life of 4.6 h.[53] *In vitro* studies in CHO cells expressing SGLT1 and SGLT2, **7** showed 1200-fold selectivity biased for SGLT2 (K_i = 1.1 *vs.* 1390 nM for SGLT2 & SGLT1, respectively) with 6- and 8-fold greater potency compared to **3** and **5**, respectively. However, the selectivity dropped to 200-fold in rat *in vivo* study.[53] **7** caused a dose-dependent glucosuria in normal and diabetic rats. With an oral dose of 0.1, 1 and 10 mg/kg in normal rats, the glucose excretion increased to 2.75, 5.5 and 9.5 g/Kg/day.[54]

In preclinical studies, **7** found to have good permeability across Caco-2 cell membranes. Although it was found to be a substrate for P-glycoprotein, it did not show significant inhibition effect against it. In interaction study with cytochrome-P450 enzymes, **7** was neither an inhibitor nor inducer of them. When incubated with mice, rats, dogs, monkeys, and human hepatocyte, **7** showed highest turnover in rat hepatocytes and was most stable in human hepatocytes. The prominent metabolic pathways observed *in vitro* were glucuronidation, hydroxylation (in C2-OH or C6-OH position) and *O*-deethylation.[55] The pharmacokinetics profile of **7** showed good oral absorption, adequate clearance and elimination half-life without any residual metabolites with significant pharmacological activity.[55,56] All these characteristics of **7** have provided the potential for single daily dosing in humans.

In 2007, phase IIa clinical trial was enrolled by recruiting 47 T2DM patients with unimpaired renal function between the age of 18-70 years old, and were either drug-naïve or on stable dose of metformin. The study was conducted in a randomized, double-blind state with a daily oral dose of 5, 25, 100 mg or placebo. Results showed that **7** demonstrated dose-dependent urinary glucose excretion (UGE) and clinical meaningful improvement in fasting blood glucose and oral glucose tolerance.[57]

Subsequent to these studies, an international, randomized, double-blind, placebo-controlled, dose-ranging (2.5, 5. 10, 20 and 50 mg/day) study was initiated in 389 drug-naïve T2DM patients with elevated Hb_{A1c} value. After 12 weeks of study, patients receiving showed dose-dependent UGE (52-85g/day) and a reduction of Hb_{A1c} of -0.55 to 0.90% from baseline (7.6-8%) compared to the placebo group. These results proved the effectiveness and tolerance of **7** in the dose-range of 2.5-50 mg/day.[58]

In Phase II clinical trial examined the efficacy of **7** in T2DM patients who had not responded adequately to combined therapy of high-dose of insulin and insulin sensitizer, **7** showed reduced Hb_{A1c} (-0.70 and -0.78%), fasting plasma glucose (FPG) [+2.4 to -9.6 mg/dl *vs.* +17.8 in placebo], postprandial glucose (-34.3 to -42.9 mg/dl *vs.* +18.7 in placebo), further body weight decrease (-4.5 to -4.3 kg *vs.* -1,9 kg in placebo) at dose of 10 and 20 mg, respectively.[59]

In phase III trials, studies had been carried on the effect of **7** on the patients with inadequate glycemic control on metformin (>1500 mg/day), insulin therapy, sulfonylurea glimepiride. All the studies showed significant reduced in Hb_{A1c} and FPG, causing further weight loss and increased UGE. [60-63]

The ongoing trials are designed to investigate the efficacy and safety of **7** as monotherapy and as combination regimen. There are 2 phase III trials examining the safety and efficacy of **7** in patients with cardiovascular (CV) disease, added to the existing medications. There are also studies designed for patients with moderate renal impairment; comparison of glomerular filtration rate with hydrochlorothiazide which is a first-line diuretic drug. [64]

*Canagliflozin (**8**)*

Canagliflozin (**8**) is designed as a structure of *C*-glucoside with an additional of thiophene ring compared to **7** (Figure 7). It has been developed by Johnson & Johnson and currently has also reached phase III clinical trial (Table 3).[48]

In several phase II studies, **8** were given as dose-escalated 30, 100, 200 and 400 mg once daily, 300 mg twice daily, sitagliptin 100 mg once daily and placebo to 451 T2DM patients. After 12 weeks treatment, the placebo adjust baseline of FPG and Hb_{A1c} decreased significantly for both **8** and sitagliptin treatment. However, weight loss had only been shown in the group of patients receiving **8**. Adverse events (AEs) were showing similar frequency and severity among all groups, except for symptomatic genital infections report for **8** (8%) were slightly higher compared to 2% in both placebo and sitagliptin groups. Results had shown the effect of **8** in the improvement of β-cell function where insulin secretion rate had increased significantly.[65]

Ongoing Phase III trials have been designed to investigate the efficacy, safety and tolerability of **8** as monotherapy or in combination therapy with metformin plus sulfonylurea or monotherapy in T2DM patients with moderate renal impairment. A long-term of up to 4 years phase III study will be launched to assess the CV risk for major adverse cardiac events when **8** is added to the standard therapy in T2DM patients.[66]

*LX-4211 (**9**)*

LX-4211 (**9**) is developed by Lexicon pharmaceuticals with a replacement of hydroxymethylene with methyl ether at C6 of **7** (Figure 7).[48] It is a dual SGLT1/SGLT2 inhibitor with ~20-fold selectivity favouring SGLT2. In phase IIa studies, 38 patients with T2DM were randomized to receive **9** (150 or 300 mg) or placebo once daily for 28 days. **9** treated patients exhibited increased daily UGE throughout the study period relative to the placebo group. Both Hb_{A1c} and FPG were also decreased significantly in both doses of **9**.[67]

In addition, effect of **9** in blood pressure and triglycerides reduction may distinguish it from other SGLT2 inhibitors. **9** exhibited a favorable profile without dose-limiting toxicities. Currently no additional phase II or III studies are being registered.

*PF-04971729 (**10**)*

PF-04971729 (**10**) belongs to a novel class of potent and selective SGLT2 inhibitor incorporating a dioxa-bicyclo-[3.2.1]octane (briged ketal) with exactly the same aglycone group with **7** (Figure 7). It demonstrated ~2200 folds of selectivity on hSGLT2 over hSGLT1 expressed in CHO cells. **10** is being developed by Pfizer Inc. and is currently in phase II clinical trial (Table 3).[68]

Prior to the discovery of this compound, the same research team had synthesized a series of C-5-spirocyclic *C*-glycoside SGLT2 inhibitors (Figure 8)[69] showing good potency and selectivity for hSGLT2 [IC_{50} = 6.98 nM, 1540 nM for hSGLT2 & hSGLT1, respectively].[68] Unfortunately, the lead compound **13** suffered from suboptimal PK profile with $t_{1/2}$ = 1.9 h and predicted a daily dose of >100 mg is needed to produce near maximal UGE (60 g/day) in healthy volunteers.[70] Studies showed that the elimination of **13** is largely mediated through hepatic metabolism ($CL_{plasma/renal/hepatic}$ = 22.3/1.80/20.5 mL/min/Kg). The *in vitro* stability study which revealed an apparent higher value of intrinsic clearance ($CL_{int\ app}$) in human hepatocytes (HHEP) relative to human liver microsome (HLM) indicated a non-CYP mediated metabolic elimination. Indeed, the *in vitro* metabolite in HHEP was identified as a single glucuronide conjugate of **13**.[68]

SAR studies showed that when the oxetane ring in **13** was replaced by an azetidine to form compound **14**, the $CL_{int\ app}$ (HHEP) was markedly reduced with the lipophilicity remains unchanged. This phenomenon suggested a probability that the missing of H-bond donor in compound **13** was the culprit of increase metabolism in human body. This hypothesis was confirmed by the marked reduction of CL_{int} app (HHEP) in both compound **15** & **16** with similar lipophilicity (Figure 8).[68]

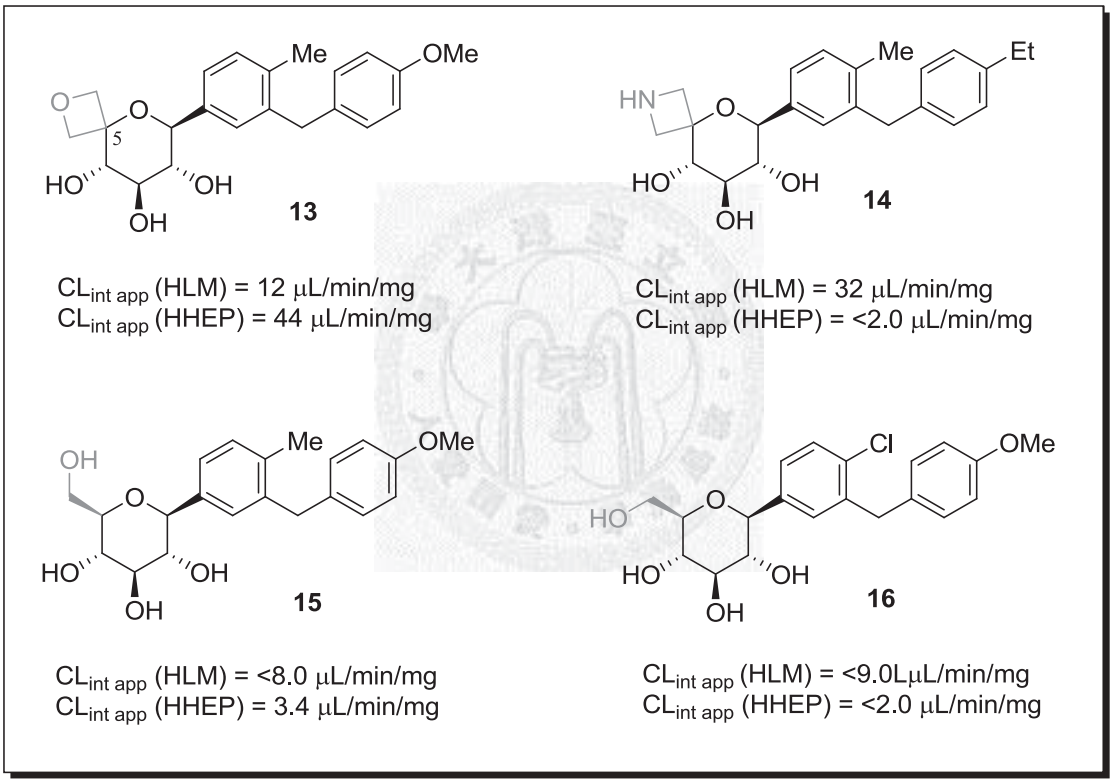

Figure 8. *In vitro* $CL_{int\ app}$ considerations for compound **13-16**[68]

These findings had led the group to focus on the synthesis of dioxa-bicyclo[3.2.1]octane derivatives because they hypothesized that the bridge ketal would confer rigidity to the compound and produce SGTL2 inhibitors with higher potency and

selectivity. In addition, the presence of hydroxymethylene group at the initial position of the spirocycle is anticipated to reduce the phase 2 metabolism in human.[68]

C. Other Agents

There are some of the compounds which are already in clinical trials but their structures are not available to public. The compounds are as follow:

i) BI-10773 & BI-44847

Both of them has entered the phase II clinical trial and are being developed by Boehringer Ingelheim (Table 3).[48] Although these 2 compounds came out at almost the same time, the clinical activity seems to be centered on BI-10773 where the preclinical data demonstrated great blockade of SGLT2 with an IC_{50} of 3.1±0.7 nM.[71] There are active phase II trials registered for BI-10773 but not for BI-44847.[72]

ii) ASP-1941

ASP-1941 are being developed by Astellas Pharma and there are 2 ongoing phase III trials taking place in Japan assessing the efficacy, safety and tolerability of this drug in Japanese T2DM patients (Table 3).[48, 73]

iii) Antisense oligonucleotide inhibitor (ISIS-388626)

ISIS-388626 is an RNAase H chimeric with 12 length of nucleotide sequence developed by Isis pharmaceuticals.[48] The antisense oligonucleotide is complementary to mRNA of SGLT2, upon binding it prevents the production of SGLT2 protein specifically

without affecting expression of SGLT1. Earlier animal studies showed that ISIS- 388626 increased urinary excretion at 14 to 130-fold at the dose of 1-30 mg/Kg in normoglycaemic mice.[74] The administration of ISIS-388626 weekly demonstrated ~80% reduction in renal SGLT2 mRNA expression.[75] 6 months consecutive treatment with ISIS-388626 in Zucker diabetic fatty rats showed no accumulation in cardiac, liver or intestinal tissue, indicating that the selectivity of this agent towards the renal proximal tubule.[75] Significant reduction in Hb_{A1c} from 10.9±0.3% to 6.3±0.8% accompanied with marked glucosuria and plasma glucose reduction in these rats were also observed.[48] The phase I trial is currently recruiting to evaluate the safety and tolerability in normal subjects with single subcutaneous injection at four increasing dose levels (50, 100, 200, 400 mg) and with multiple dosing weekly continues for 6 or 13 weeks.[76]

iv) *TS-071 (**11**) (Structure shown in Figure 7)*

A series of derivatives of a novel scaffold, C-phenyl 1-thio-D-glucitol were synthesized and evaluated for their activities against SGLT2 and SGLT1 activities. SAR studies of substituents on the aromatic rings afforded TS-071 (**11**) with good absorption and distribution profile and is stable in human cryopreserved hepatocyte.[77] The pharmacokinetic parameters of **11** after oral and intravenous administration of rats and dogs are being compared with **7**. As shown in Table 2, the $T_{max,}$ bioavailability (F), Vdss are comparable with **7** but the half-life ($t_{1/2}$) of **11** was shorter most probably due to the faster clearance rate (36.3 ± 2.67 mL/min/Kg) compare to 1.5 ± 0.2 mL/min/Kg for **7**.[55]

Table 2. PK profile of TS-071 (11) versus dapagliflozin **(7)**[77]

Compounds	11 (rats)	11 (dogs)	7 (dogs)
Dose (mg/kg)	1	1	6.6
C_{max} (ng/mL)	35.7 ± 17.0	914 ± 73.4	10700 ± 1600
T_{max} (h)	0.5 ± 0.00	0.67 ± 0.29	0.6 ± 0.4
$t_{1/2}$ (h)	2.93 ± 2.00	4.07 ± 0.25	7.4 ± 1.2
***F* (%)**	35.3	92.7	83 ± 2
Vd_{ss} (L/kg)	2.63 ± 0.57	0.80 ± 0.06	0.80 ± 0.1
Cl (mL/min/kg)	36.3 ± 2.67	3.19 ± 0.26	1.5 ± 0.2

At a dose of 3 mg/Kg in rats, **11** demonstrated 24-30 folds higher distribution in kidney, the target organ and being excreted within 24 h with no detection of leftover in liver, heart or brain. A single dose of **11** (1mg/Kg) in Zucker fatty rats after glucose loading induced 30-fold increase in urinary glucose output (180 mg/day) compared to vehicle control (6 mg/day) and 180-fold increase in normal control Zucker lean rats (1 mg/day). Even higher increment of 2600-fold found in diabetic compared to normal dogs, most probably contributed by higher *F* (%) in dogs described previously.[77] **11** is currently being developed by Taisho pharmaceuticals and is currently undergoing phase II clinical trial.[48]

Table 3. SGLT2 inhibitors in the clinical development[48]

Drug	Alternative name	Company	Development Phase
Dapagliflozin (7)	BMS-512148	Bristol-Myers Squibb/AstraZeneca	IV
Dapagliflozin (7)/ metformin	BMS-512148/metformin	Bristol-Myers Squibb/AstraZeneca	III (USA)
Canagliflozin (8)	TA-7284/JNJ-28431754	Johnson & Johnson/ Mitsubitshi Tanabe Pharma	III
LX-4211 (9)		Lexicon Pharmaceuticals	II (USA)
ASP-1941		Astellas/Kotobuki	III (Japan)
PF-04971729 (10)		Pfizer Inc.	II
BI-10773		Boehringer Ingelheim	II
BI-44847		Boehringer Ingelheim (under license from Ajinomoto)	II
TS-071 (12)		Taisho Pharmaceuticals	II (Japan)
ISIS-SGLT2Rx	ISIS-388626	Isis Pharmaceuticals	I

Data obtained from http://clinical.gov/ which is a registry and results database of federally and privately supported clinical trials conducted in the United States and around the world

D. Newly Designed Agents

Other than the above compounds which are going through clinical trials, in recent years there are some others newly synthesized compound seeking to find a novel compound with comparable or higher potency, improved coefficient (log P) value thus decrease plasma protein binding than those current agents in clinical trials.

JinHwa Lee et. al.

This team had published a few compounds with proximal and distal aglycone ring replaced with heterocyclic rings and cyclic diarylpolynoid **(17-21, 24, 25)** to study the SARs.[78-81, 83]

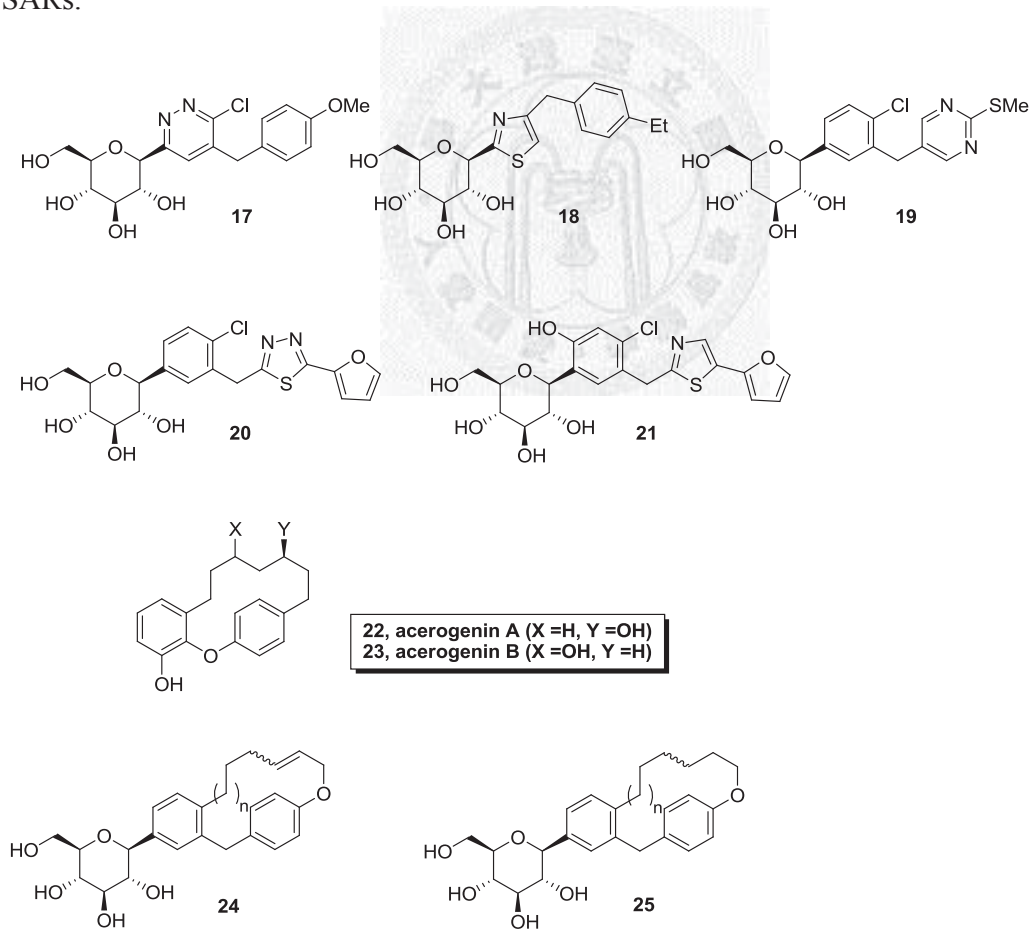

Figure 9. Compounds **17-23** with modified biphenyl rings[78-83]

The team had proposed that the replacement of proximal or distal ring with heterocyclic ring might be able to provide an electronic environment that would increase the log P value and potentially decrease the plasma protein binding which might lead to an improved pharmacokinetic profile.

In the year of 2010, they synthesized compounds **17** and **18** by replacing the proximal ring with pyridazine and thiazole moieties, respectively (Figure 9). Unfortunately, neither of these surrogates showed improvement in the hSGLT2 inhibition (with IC_{50} = 610 nM & 121 nM, respectively) due to the unfavourable electronic environment.[78]

Same year, they synthesized compounds **19** and **20** by replacing the distal ring with pyrimidine and 1,3,4-thiadiazolyl rings, respectively (Figure 9).[79,80] Although both of these compounds showed better IC_{50} (10.7 nM and 7.03 nM) compared to **17** and **18** but still weaker than **7**. In addition, compound **20** showed merely 1.4-fold increase in urine volume *in vivo* compared to 5.7-fold increased showed by **7**. Extended from that, they synthesized a series of analouges comprised of thiazolylmethyl ortho-substituted phenyl glucosides and found compound **21** (IC_{50} = 0.797 nM) with most outstanding *in vitro* inhibitory activity against hSGLT2 in this series.[81] This finding suggested that the presence of hydrogen donor at the *ortho*-position of proximal ring might be beneficial.

In the midst of exploring SGLT2 inhibitors, two cyclic diarylheptanoids, acreogenin A **(22)** and B **(23)** has been reported from the bark of *Acer nekoense* as inhbitors of both SGLT1 and SLGT2 but with much stronger activity against SGLT1 (Figure 9).[82] Despite, the resemblance of **22** and **23** to the structure of diaryl or heteroaryl part of reported SGLT2 inhibitors provided a hint that the combination of cyclic diaryl with glucoside could lead to

a novel potent SGLT2 inhibitors. Disappointingly, all of the anologues of **24** and **25** (Figure 9) showed modest *in vitro* inhibitory activity against SGLT2 with the best IC_{50} of 59.5 nM showed by analogue of **24** with n=0.[83]

Yuanwei Chen et. al.

This team synthesized 3 different series of compounds with the core structure of 6'-*O* (**26,27**) and 2'-*O*-sprio *C*-aryl glucosides (**28**)[84] and 4'-position substituted *C*-aryl glucosides (**29,30**)[85,86]. (Figure 10)

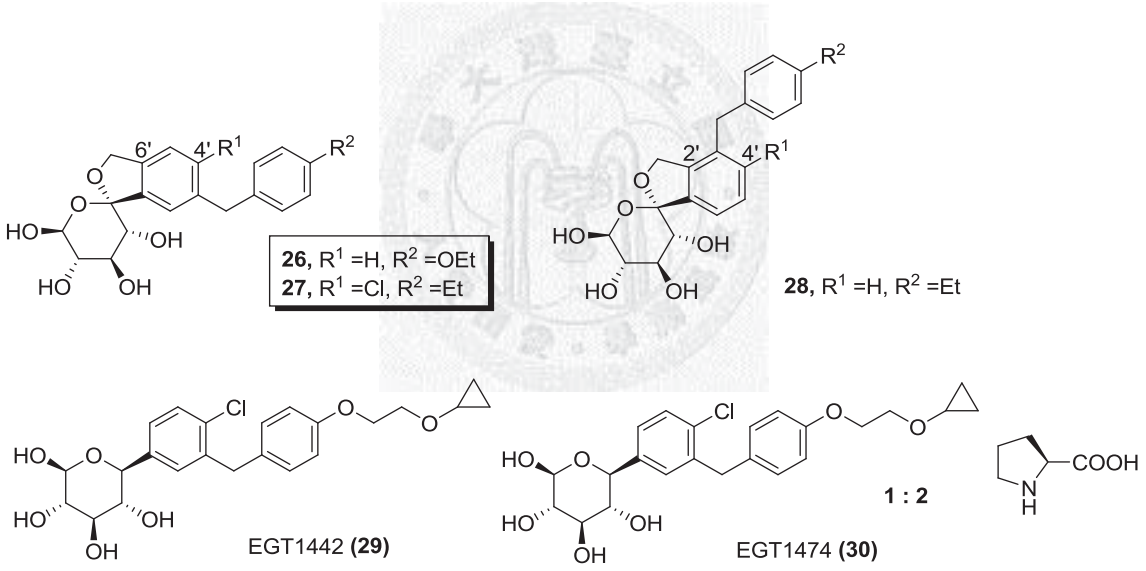

Figure 10. Compounds synthesized by *Yuanwei Chen et. al.*[84-86]

As stated in Table 4, 2'-*O*-spiro *C*-aryl glucosides showed no *in vitro* hSGLT2 inhibitory activity at a screening concentration of 1 μM. However, one of the analogues of 6'-*O*-spiro *C*-aryl glucoside **26** exhibited similar inhibitory activity and a slight reduced in selectivity compared to **7**.[84]

Table 4. *In vitro* data for hSGLT inhibitory activity and selectivity[84]

Compounds	hSGLT2 IC_{50} (nM)	hSGLT1 IC_{50} (nM)	Selectivity (hSGLT1/hSGLT2)
Dapagliflozin 7	6.7	885	132
26	71	10,000-100,000	141-1410
27	6.6	620	94
28	0%[a]	38%[b]	-

[a] Inhibition at a screening concentration of 1 μM.

[b] Inhibition at a screening concentration of 100 μM.

This year, the same team reported a series of *C*-aryl glucosides substituted at the 4'-position and found the most potent compound **29** (hSGLT2, IC_{50} =2.3 nM) in this series of compound with 12,600-fold selectivity versus hSGLT1.[85] **29** is co-crystallized with L-proline to form **30** in 1:2 stoichiometry. In animal studies, **30** demonstrated increased urinary glucose excretion in healthy rats and dogs model with sustained blood glucose and Hb_{A1c} reducing effect in diabetic mice. No body weight gain, diarrhea or hypoglycaemia was observed. Moreover, **30** was found to significantly prolong the survival of spontaneously hypertensive stroke prone (SHRSP) rats on a stroke-promoting diet.[86] This has made **30** as a potential drug for treating diabetic patient with hypertension comorbidity.

JinChyi Lee et. al.

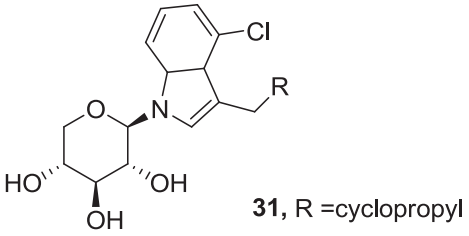

31, R =cyclopropyl

Figure 11. *N-β*-D-Xylosylindole derivatives[87]

This team focused on exploring *N*-linked D-Xylose SAR on SGLT2 inhibition. The results showed that compounds in this series inhibited hSGLT2 at lower potency and weak selectivity over hSGLT1 with the best compound **31** (IC_{50} =161 nM) showed only 1.3-fold selectivity over hSGLT1.[87]

1.3.2 Potential Side Effects and Future Perspective

Overall studies of SGLT2 inhibitors demonstrated that the benefit of this novel group of drugs is able to compensate the limitations of current drugs available for diabetes such as hypoglycaemia and weight gain. However, the mechanism of action of SGLT2 might develop other side effects such as urinary tract infection (UTI), fungal genitourinary infections as well as deterioration of renal function.

The diuresis involving SGLT2 inhibitors treatment might be caused by sodium loss or osmotic effect. Until now, the diuresis seems to be modest and without clinical significances. The slight elevation also observed in serum magnesium, serum phosphate and hematocrit[58] which might be due to slight volume depletion but still it did not cause clinically significant electrolyte imbalance.[24,88] Hence, patients should be educated with the importance of hydration under this treatment. As this clinical data was collected from short-term clinical trials (up to 48 weeks), long term monitoring is necessary due to the concern arise from the slight diuretic-like effect of the SGLT2 inhibitors might cause renal impairment in long-term usage.

Another concern is raised from the increase of urinary tract infection (UTI) which can be easily predicted as i) high concentration of glucose may promote bacterial growth, ii)

chronic hyperglycemia may inhibits phagocytic effect of white blood cell. Same here, long term trials have to be performed in order to accurately evaluate the chance of getting UTI under SGLT2 inhibitors treatment.[24,88] Nonetheless, the risk of UTI can be tackled with antibiotic therapy and improvement of phagocytic effect. Or else, patients with history of frequent UTI or autonomic neuropathy and neurogenic bladder would have to be considered excluded from this kind of treatment.

In summary, selective inhibition of SGLT2 appears to be an intriguing strategy in treating T2DM. SGLT2 inhibitors also show potential indications for treating T1DM and obesity. However, a question remains that to what extent, inhibiting SGLT1 along with SGLT2 would yield the greatest clinical improvement but we know that over inhibition of SGLT1 will cause the treatment-limiting gastrointestinal (GI) symptoms. There are still rooms for researchers to focus on the physiological properties of SGLTs and synthesize novel compounds to study the SARs of SGLT2 inhibitors.

1.4 Purpose & Aim

Extensive researches had been carried out in modifying the glycosides (eg. *N*-xylosides, *s*-glycosides, dioxa-bicyclo[3.2.1]octance) in order to produce novel compounds that could avoid infringement of registered patents.

Glucose exists as pyranose for more than 99% in aqueous solution while the open-chain form is limited to about 0.25% and furanose exists only in negligible amounts.[89] Based on this physical property, glucopyranose will have the highest chance of transport through SGLT2. However, it was previously showed that five-membered iminocyclitols carrying hydroxyl groups with specific orientation mimicking the shape and charge of the transition state of the reacting glucopyranose moiety showed significant inhibitory effects on both glycosyltransferase- and glycosidase- catalyzed reactions.[90] Extended from the above phenomena, it is hypothesized that glucofuranosides would have comparable inhibitory activity with glucopyranosides against SGLT2. Therefore, we designed a novel (1*S*)-1,4-anhydro-1-*C*-aryl-D-glucitol derivatives based on the synthesis of **7** to evaluate the tolerability of SGLT2 on glucofuranose.

Based on the SAR studies of substitutions on the biphenyl ring with methyl spacer reported by Yamamoto, K. and his team,[77] we designed and synthesized analogues (**32a-h**) which were predicted to possess considerable potency and selectivity towards SGLT2 (Figure 12). The SARs of the biphenyl ring will be discussed in section 2.1.2.

In order to quickly build up the library, we chose 8 Grignard reagents to introduce substituted, heteroaryl and benzofused rings at the distal ring position (**32i-q**).[87] Details will be discussed in section 2.1.4. With all these compounds available, extensive studies would

be conducted on these analogues in order to find out whether D-glucofuranoside offered high binding affinity and selectivity towards SGLT2 to produce desirable glucosuria effect in treating diabetes.

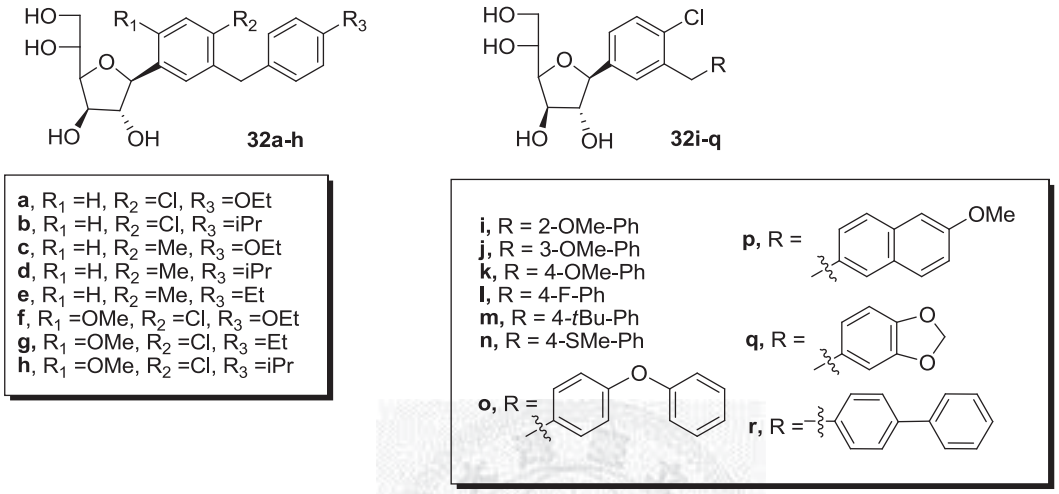

Figure 12. Synthesis of analogues **32a-32r**

2. Results and Discussion

2.1 Proposed Scheme for the Synthesis of *C*-Glucofuranoside Analogues

The previous SAR studies revealed that the meta-substituted diarylmethane to be superior SGLT2 ligand at the biphenyl and 1,2-diarylethane binding site.[57] A series of analogues with preferred C-4′ and C-4 substitutions were synthesized and evaluated, from there, a potent and selective SGLT2 inhibitor, dapagliflozin **7**, which currently progressed furthest in clinical trial for type 2 diabetes, was found. Taking **7** as our reference compound, we resynthesized it based on the reported method (Scheme 1) and proposed a scheme of *C*-glucofuranoside analogues (Scheme 2).

The synthesis of **7** was commenced by the preparation of persilylated gluconolactone **33** from the commercially available gluconolactone. The commercially available benzoic acid **34** was converted to benzoyl chloride with oxalyl chloride and under Friedel-Crafts acylation with phenetole generated a 7:1 mixture of regioisomors in favor of the desired *p*-benzophenone **49a**, which was purified by recrystallization from ethanol twice in a 64% yield. Reduction of **49a** with BF_3•OEt_2 and Et_3SiH yielded aglycon **50a** in a 62% yield which followed by lithium halogen exchange to form nascent lithiated aromatic rings. Addition of the activated aglycone to **33** gave a mixture of lactols which were converted *in situ* by methansulfonic acid in methanol to form desilylated *O*-methyl lactols **35** in a 85% yield (2 steps). Again reduction of the anomeric methoxy group with BF_3•OEt_2 and Et_3SiH gave de-methoxy intermediate which followed by peracetylation to yield tetraacetate **36**. **36** was recrystallized with EtOH for the purpose of removal of small

amount of α-anomer formed during reduction. Deacetylation was achieved by lithium hydroxide to yield **7**.

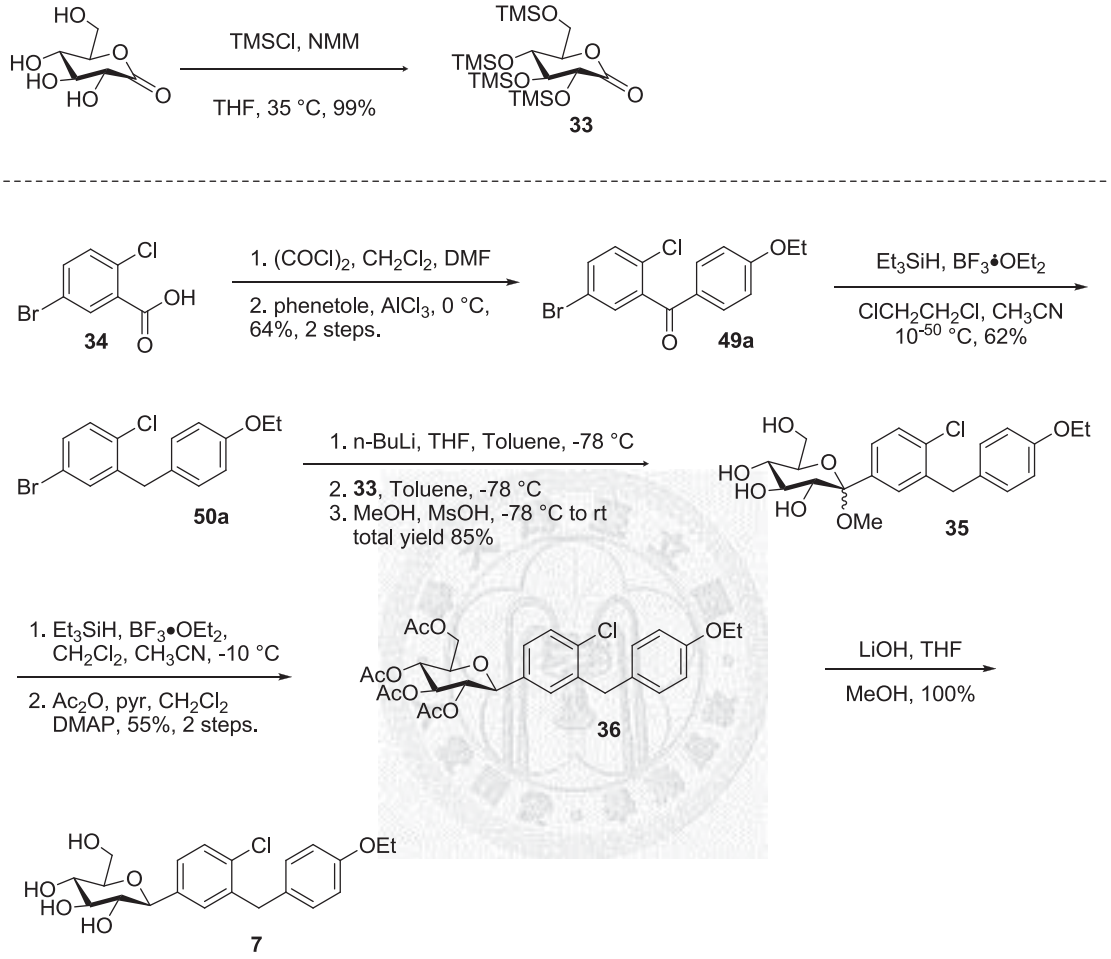

Scheme 1. Synthesis of dapagliflozin **7**[53]

2.1.1 Synthesis of D-glucono-gamma-lactone

As proposed in Scheme 2, in order to generate protected gluco-gamma-lactone for the coupling reaction with biphenyl, we have prepared 5,6,-*O*-isopropylidene-D-glucono-1,4-lactone **37** from gluconolactone using 2,2-dimethoxypropane under a promoter-$SnCl_2$.[91]

Persilylated lactone **38** was obtained by treating **37** TMSCl and NMM. Nucleophilic addition of **50a** with compound **38** was conducted by using n-BuLi in THF and toluene. This reaction was expected to form a mixture of corresponding *O*-methyl lactols **39**. However, compound **35** was obtained instead, due to the hydrolysis of acetonide caused by addition of MsOH and then five-membered ting was opened to form 6-membered ring **35**. Hence, we concluded that this scheme cannot lead us to our final steps due to the conversion of glucofuranoside back to glucopyranoside. In addition, **37** was not an ideal intermediate as it was not stable under $SnCl_2$ which cannot be removed through extraction or evaporation, also it was not stable through the process of silica gel column chromatography.

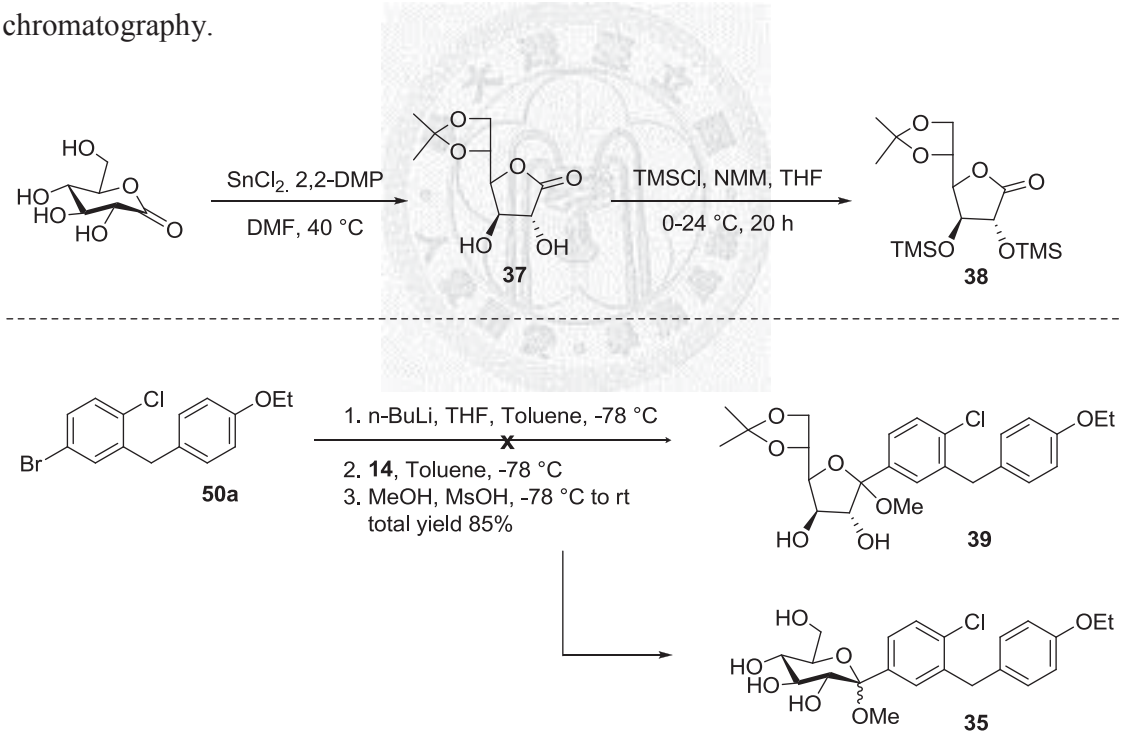

Scheme 2. Proposed scheme for synthesis of *C*-glucofuranoside

Herein, we proposed another scheme by preparing perbenzylated gluco-gamma-lactone as an intermediate for the coupling reaction (Scheme 3). With the characteristics of being easily introduced with high yield, benzyl ether has demonstrated good stablility under

most of the acidic and alkaline conditions and it can be easily removed with Pd/C hydrogenesis.

As shown in Scheme 3, compound **42** was obtained through the hydrolysis of 5,6-acetonide of the commercially available diacetone-D-glucose **40** followed by protection of the three hydroxyl groups with benzyl chloride and NaH. The 1,2-acetonide was then removed and anomeric methylation was achieved by treating with 2.0 M HCl in MeOH to yield **43.** It was followed by benzylation of C2-OH with benzyl chloride and NaH to get compound **44** and acid hydrolysis yielded compound **45**. Oxidation of compound **45** with Dess-Martin periodinane (DMP) produced the perbenzylated lactone **46.** Later, this process was optimized (Scheme 4) with some minor changes. a) The hydrolysis of acetonide at the very beginning was replaced with benzylation reaction in order to obtain a product **47** that can be extracted with organic solvent to achieve crude purification. b) For the consideration of yield and time consumed, benzyl bromide was used instead of benzyl chloride for benzylation. c) For time-saving purpose, DMP as the oxidizing reagent at the final step was replaced by PCC.

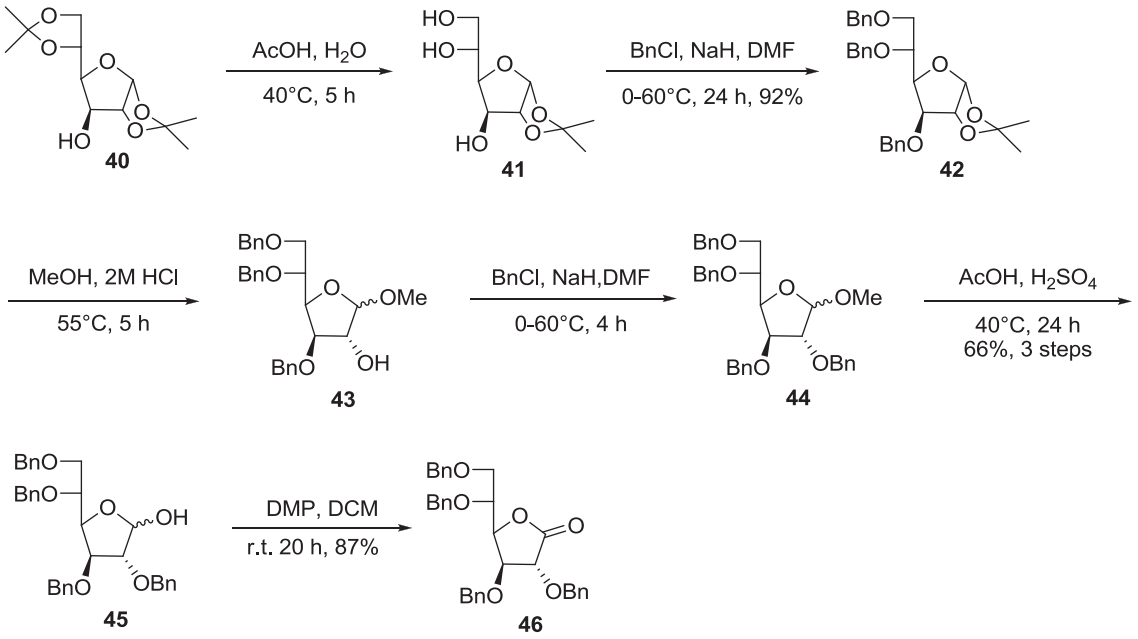

Scheme 3. Synthesis of perbenzylated glucono-gamma-lactone

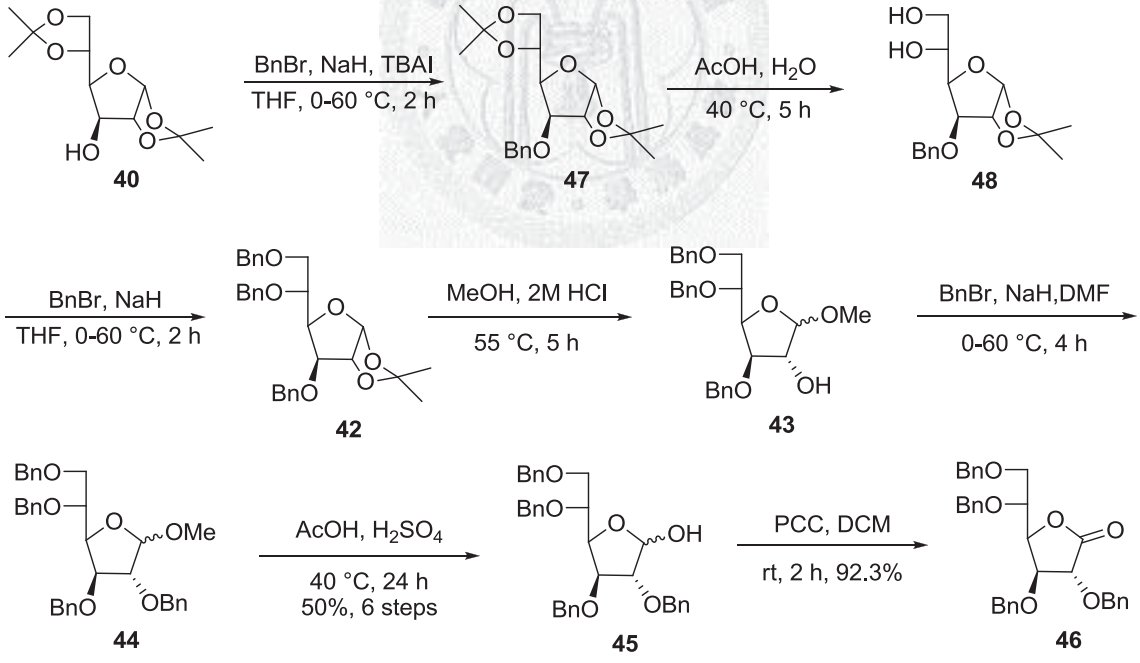

Scheme 4. Modified scheme for synthesis of perbenzylated glucono-gamma-lactone

2.1.2 Synthesis of Aglycones

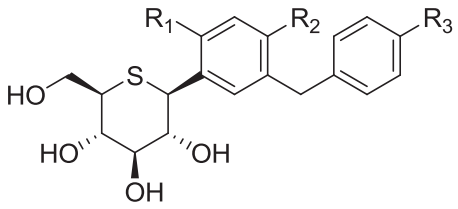

Figure 13. SARs of aglycone of TS-071 (**11**)

It was previously described in the synthesis of TS-071 (**11**), substitution of methoxy group at R_1 and a bulky group such as isopropyl and *tert*-butyl group in R_3 confer greater selectivity to SGLT2, and the methyl or chloro group at R_2 is responsible for the increased potency towards SGLT2 (Figure 13).[77] Based on the mentioned SAR, we synthesized 8 meta-substituted diarylmethane (**50a-h)** with preferred C-2, C-4 and C-4' substitutions (Scheme 5). The di-substituted biphenyl was prepared according to the procedure described for compound **50a**. The tri-substituted biphenyl was prepared from the Friedel-Crafts acylation of benzoylchloride **52-54** with compound **51** prepared from methylation of commercially available 2-bromo-5-chlorophenol (Scheme 5).

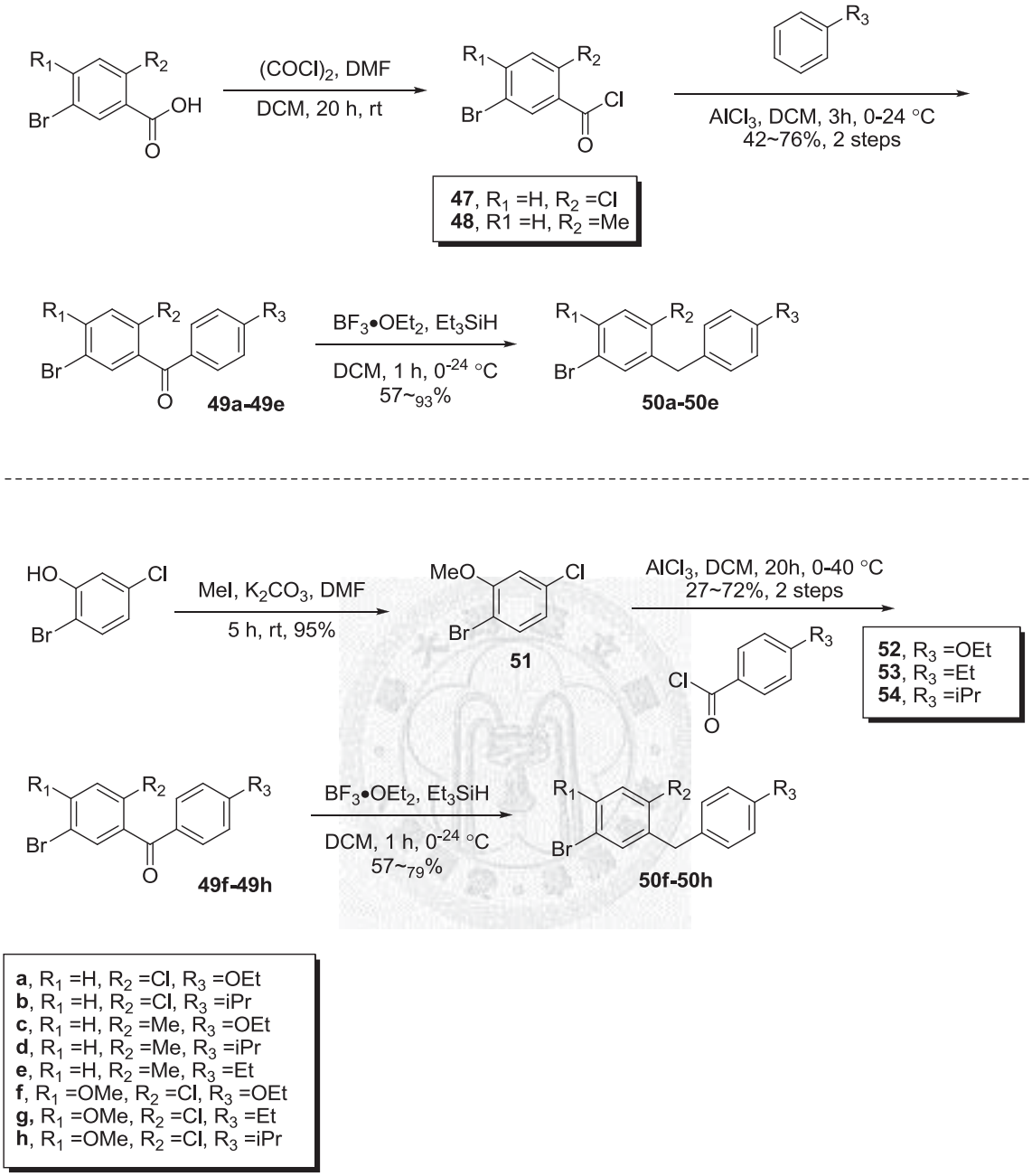

Scheme 5. Synthesis of aglycones **50a-50h**

2.1.3 Coupling of D-glucono-gamma-lactone & Biphenyl

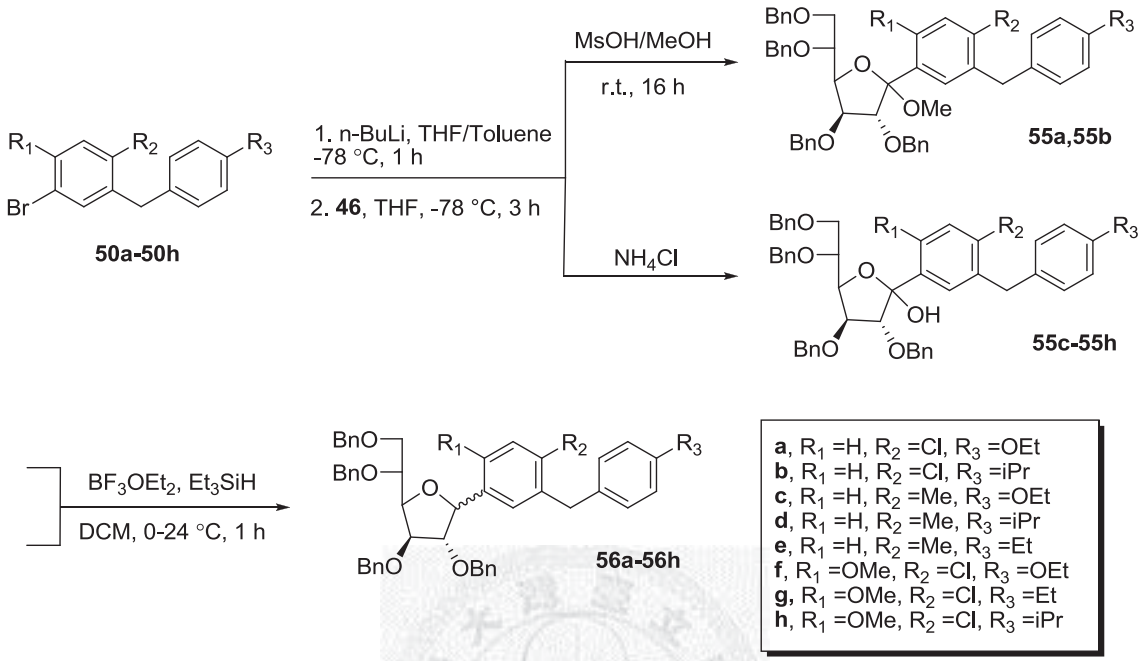

Scheme 6. Coupling reaction to afford compounds **56a-56h**

The coupling of **50a** & **50b** with compound **46** was based on the synthesis method of **7** where the lactol was converted to *O*-methyl lactol *in situ*. Later on, we found out that this step can be saved by directly reduction of the lactol to afford compound **56c-56h** (Scheme 6).[79] Compounds **56a-56h** were mixture of anomers, due to their different polarities of the biphenyl groups, **56f-56h** can be separated in their perbenzylated forms through column chromatography on silica gel, but **56a-56e** have to be converted in to tetra-acetates **59a-59e** and then to be separated by column chromatography on silica gel to afford the β-anomers (Scheme 7). The debenzylation of perbenzylated *C*-glucoside were carried out in the hard acid (BF_3) and soft nucleophile (EtSH) system[92] to obtain **32f-32h** and **58a-58e**.

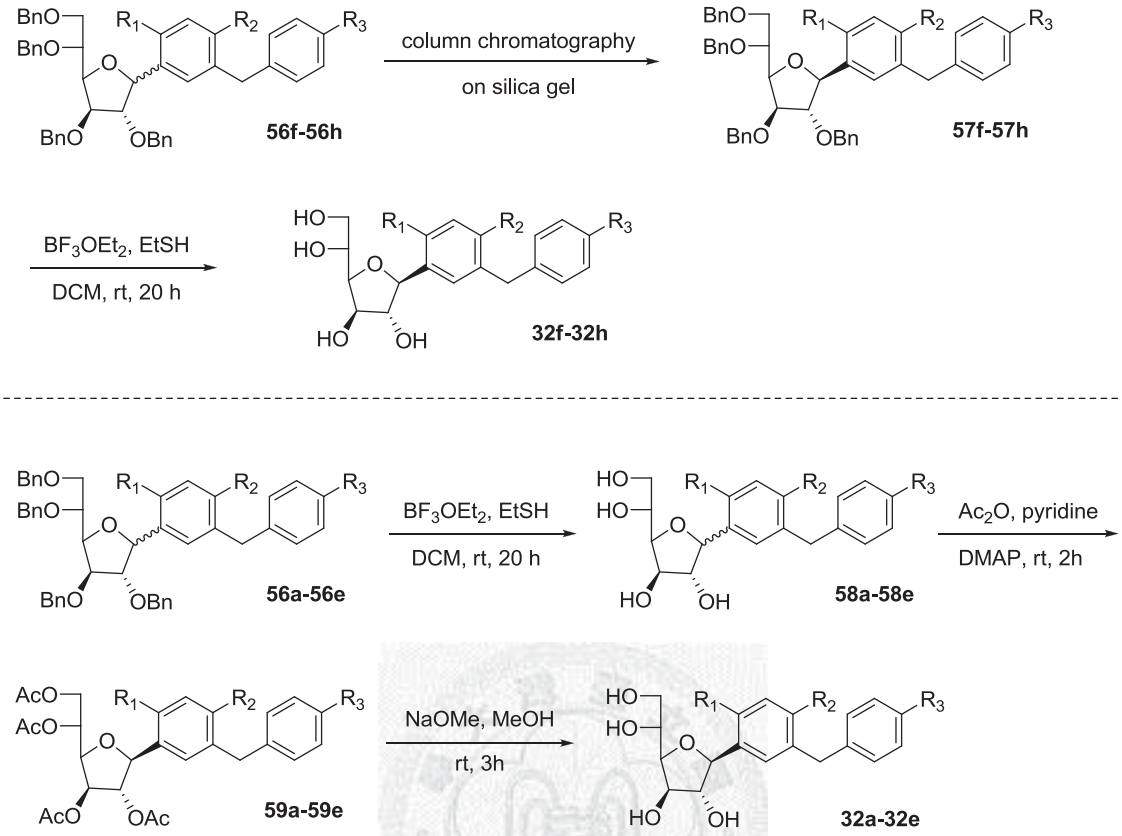

Scheme 7. Purification of mixture of anomers

As what we proposed earlier that one of the advantages in using benzyl as protective group is that it can be easily removed by Pd/C hydrogenation with the least side products to achieve high yields. However, this strategy was not applicable in this case as Pd/C hydrogenation will cause de-chlorination and the opening of *C*-glucosides at the C1 position which was also a benzylidic position to form a long chain glucitol, instead of five-membered rings. The NMR data (Figure 14) suggested that the peaks between 2.5-3.0 ppm to be 2H at C1 position. The high resolution mass spectra (Figure 15) indicated that a mass of 385.1616 was the open ring structure **32j-1** (Figure 15).

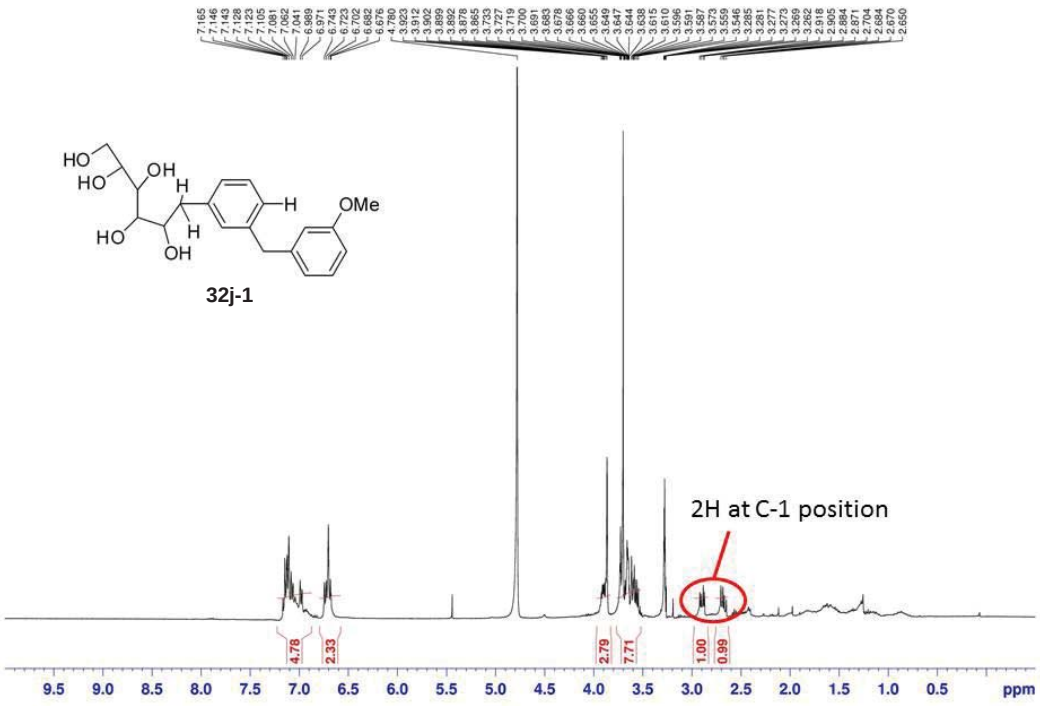

Figure 14. H-NMR of example open-ring product **32j-1**

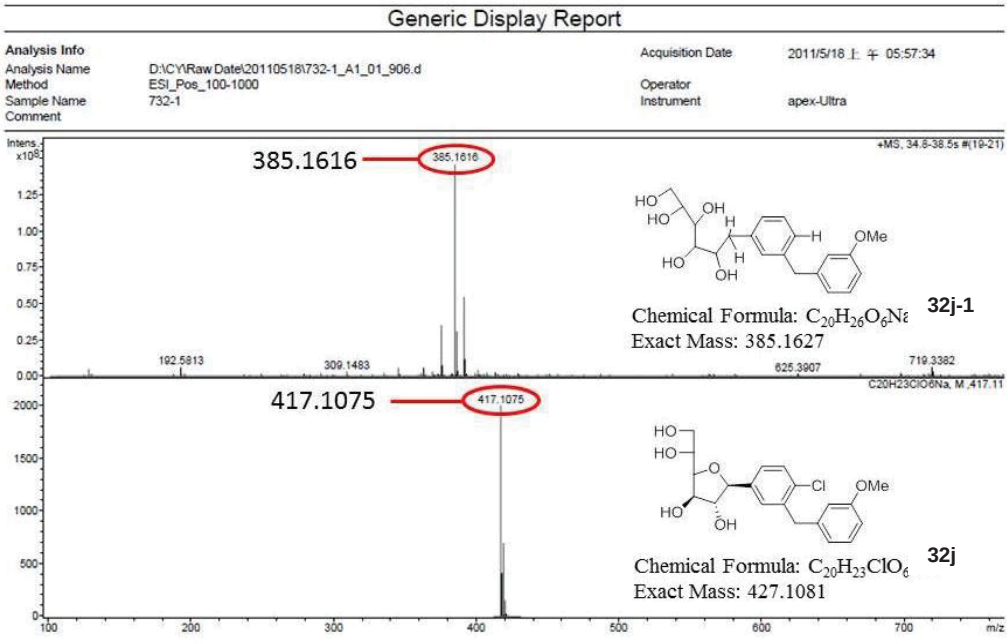

Figure 15. High resolution ESI-TOF of example open-ring product **32j-1**

2.1.4 Building up Library with Grignard Reactions

Besides synthesis of the biphenyl substitutions with known SARs, we were also interested in the effect of substitutions at C-2' and C-3'and the presence of heteroaryl and benzofused ring at the distal ring. The present of another benzene ring at the distal position may evaluate the tolerability of the aglycone binding site for a larger hydrophobic group, if yes, this may confer to a more rigid binding and result in strong binding activity of these inhibitors.

During the course of synthesis, we found that the coupling reactions as shown in Scheme 5 and 6 were not a good way to build the library. As we looked at Scheme 5 & 6, in order to produce eight final compounds we need to go through eight Friedel-Crafts acylations and eight coupling reactions plus eight times purification to afford β-anomers which will not be cost effective. Therefore, we came up with another method by combining ideas on the synthesis of *N*-xylosides proposed by Lee, J. C. team[87] and *C*-glucoside alcohol intermediate by Lee, J. H. team[79] as shown in Scheme 8 and 9.

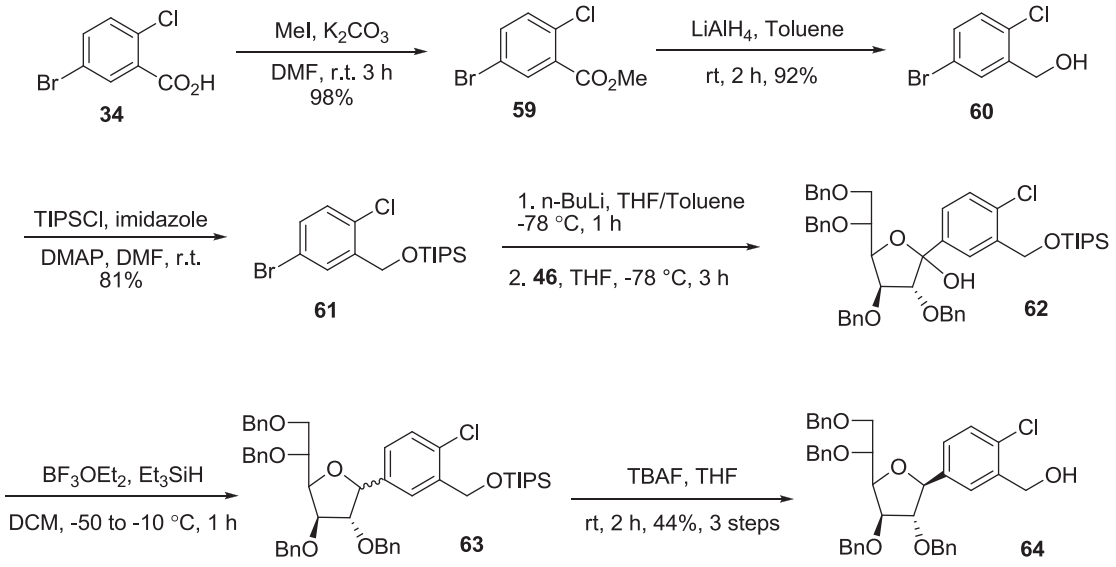

Scheme 8. Preparation of β-*C*-glucoside intermediate **64**

The preparation of the β-*C*-glucoside intermediate prior to the Grignard reaction is shown in Scheme 8. The commercially available benzoic acid **34** was converted to methyl benzoate **59**, which was then reduced with $LiAlH_4$ to form benzyl alcohol **60**. The subsequent silylation of **60** with TIPSCl in the presence of imidazole and DMAP generated **61**. Lithium-halogen exchanged, followed by the addition of the nascent lithiated aromatic compound to perbenzylated glucono-gamma-lactone **46** produced a mixture of corresponding lactols. The lactols were reduced in the conditions of BF_3•OEt_2 and Et_3SiH to give compound **63**, which was desilylated using TBAF and finally purified with column chromatography on silica gel to afford alcohol **64** in a single β-anomer at 44% yield over 3 steps. With the single β-anomer **64** on hand, intensive column chromatography for the separation of each anomer as shown in Scheme 7 was not necessary.

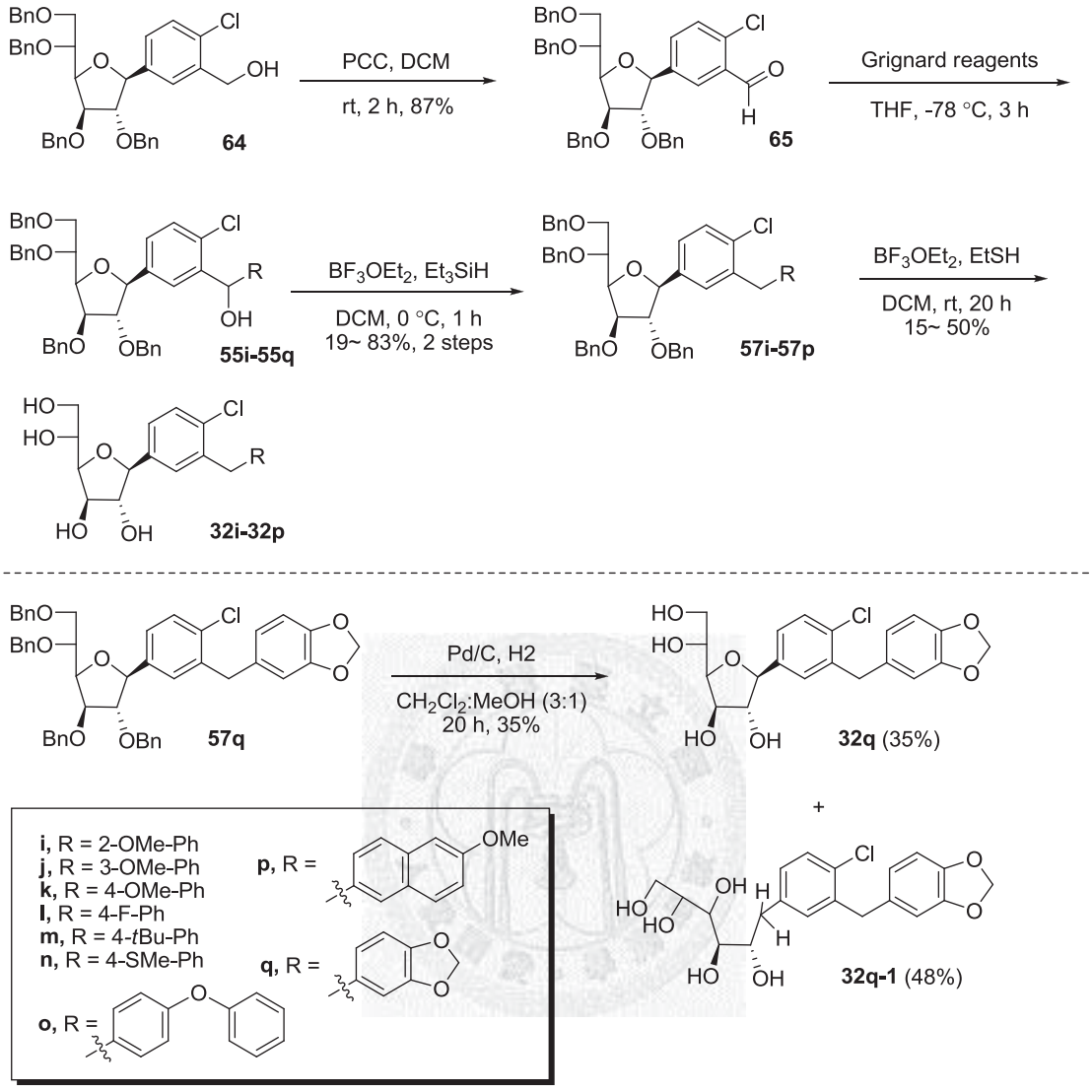

Scheme 9. Grignard reactions to afford final compound **32i-32q**

The alcohol **64** was oxidized by PCC to form aldehyde **41** in a 87% yield. Addition of various Grignard reagents to **65** to introduce the substituted, heteroaryl and benzofused rings at the distal ring position. The resulting alcohol **55i-55q** were reduced under standard conditions (BF_3•OEt_2 and Et_3SiH) to generate **57i-57p** which were debenzylated by using hard acid (BF_3) and soft nucleophile (EtSH) system to form the desired products **32i-32p**.[92] Except for compound **57q**, as the methylene group will also be removed under the hard acid

condition, we had tried debenzylation through hydrogenation with Pd/C to obtain desired product, **32q** in a 35% yield with an open-ring side product, **37q-1** in a 48% yield. To achieve complete debenzylation while avoiding dechlorination and the formation of side product with opened ring at C-1 position, time course of hydrogenation must be controlled within 16 to 20 hrs.

Some of the aromatic Grignard reagents were not commercially available so we have to prepare it *in situ* as illustrated in Scheme 10. The Grignard reagents were prepared from commercially available 4-bromobiphenyl and 4-bromo-4'-methoxybiphenyl by magnesium and a catalytic amount of iodine under reflux. The aldehyde **65** was added *in situ* to the Grignard reagent to give the desired product **55r.** Other than this, the following reduction and debenzylation steps are exactly the same as Scheme 9.

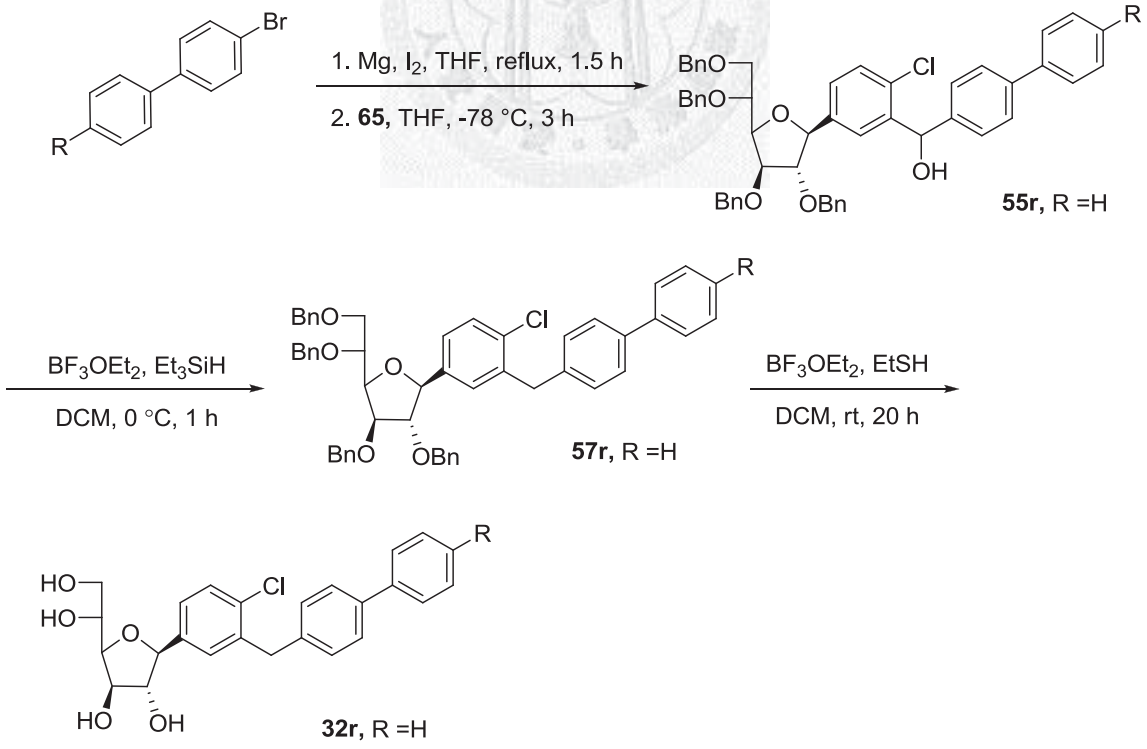

Scheme 10. Preparative tri-aryl compounds by Grignard reaction

2.2 Biological Activity

The biological assay was carried out in the laboratory of Dr. Lih-Ching, Hsu, carried out by the master student, Hong-Chi Chang. The *in vitro* inhibitory activities of the synthesized analogues were tested in COS-7 cells transiently or stably expressing hSGLT1 and hSGLT2 by measuring the inhibition of sodium-dependent uptake of [^{14}C]-labeled-α-methyl-D-glucopyranoside (AMG) into the cells. The COS-7 cells stably expressing hSGLT2 was prepared by me under the help of Dr. Sherry Hsu in Academia Sinica.

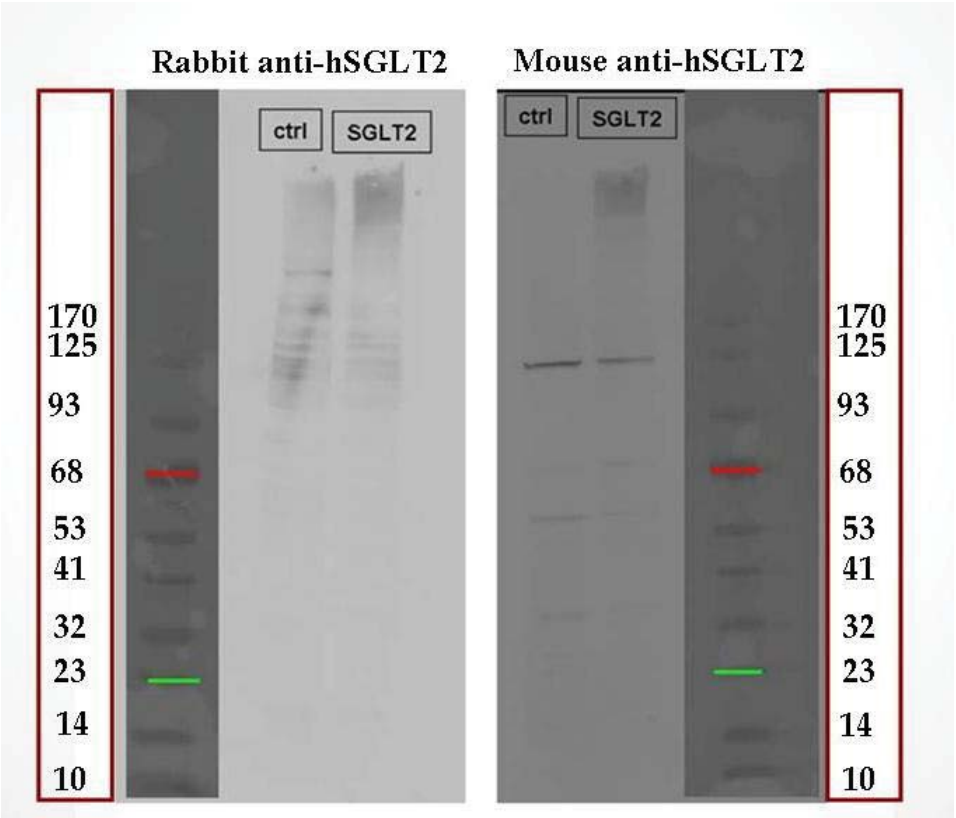

Figure 16. Western blot results of hSGLT2 and backbone (ctrl) transient transfection COS-7 cell

Due the lacking of good hSGLT2 antibodies, we have tried 2 different antibodies for western blot. From the picture shown above, the rabbit anti-hSGLT2 (US Biological) is not a good antibody for western blot as it showed a lot of nonspecific binding. Although the mouse anti-hSGLT2 (abcam) showed a better profile, the desirable band at 72 kDa can barely be seen. However, compared to backbone transfected cell (ctrl), the cell transfected with hSGLT2 showed smearing at the top which might be caused by the aggregation of overexpression hSGLT2 protein.

2.2.1 hSGLT1 *In vitro* assay

Using phlorizin **1** (0.5 μM) and dapagliflozin **7** (0.5 μM) as reference compounds, all of the inhibitory effects of the synthesized **32a-32r** against hSGLT1 were test at a concentration of 0.5 μM. The uptake activity were measured with 1 μM [^{14}C]AMG for 90 mins at 18 ºC. As SGLTs are sodium dependent transporter, positive control were set up by adding [^{14}C]AMG into sodium buffer in the absence of any synthesized analogue or reference compound, whereas the negative control were carried out in sodium-free buffer replaced by choline buffer.

Results were shown in Figure 16 where only phlorizin **1** showing significant inhibition (approx. 70%) on the [^{14}C]AMG uptake. Dapagliflozin **7** inhibited 20% on the uptake of isotope. All of the other tested compounds (**32a-32r**) did not exhibit any inhibitory effect on hSGLT1 at this concentration.

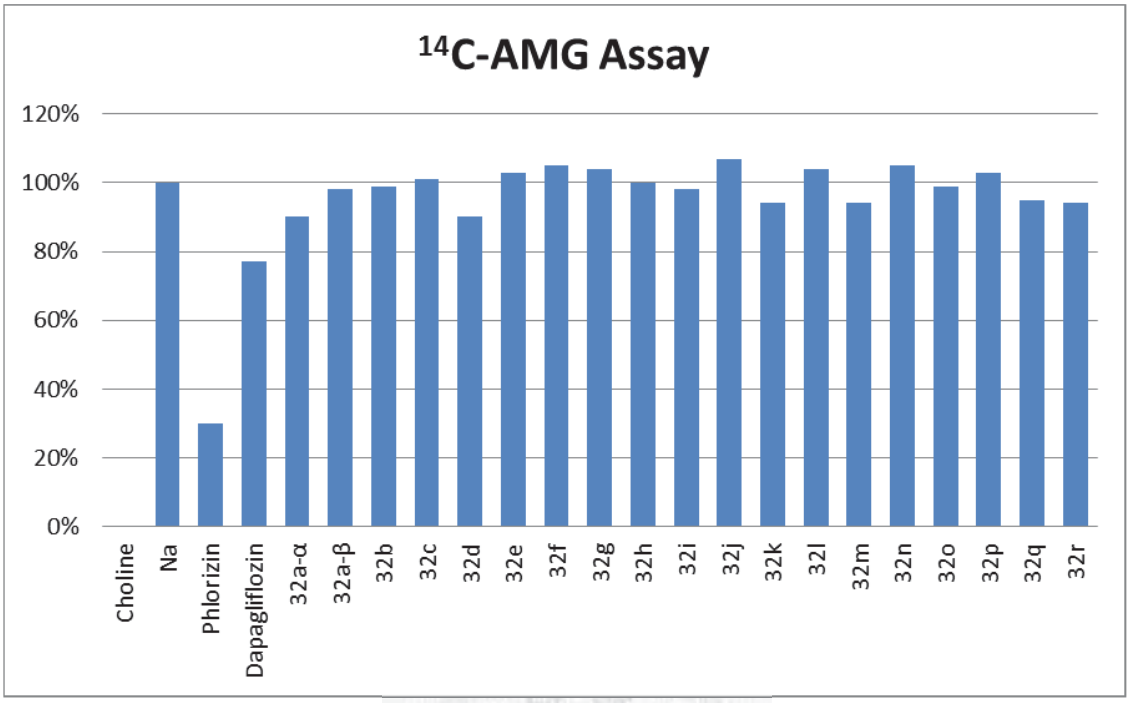

Figure 17. Inhibitory effects of **32a-32r** against hSGLT1

COS-7 cells transiently transfected with a hSGLT1 expression vector. All inhibitory assays are carried out in sodium buffer except for choline buffer control. The total glucose uptakes are calculated in unit of percentage in relative to positive control (Na).

2.2.2 hSGLT2 *In vitro* assay

The results of hSGLT2 *in vitro* assay are still pending.

3. Conclusion

A series of compounds (**32a-32r**) containing furanose-type glucose and C-linked diaryl and tri-aryl rings had been designed and successfully synthesized. In the course of synthesis, we had developed an optimized 7-step scheme using diacetone glucose as a starting material, with only one purification step required to obtain a novel glucofuranoside, D-glucono-gamma-lactone **46**. Besides, we also found the Grignard reaction as a quick way to synthesize this serial of compounds without extensive column chromatography to obtain the desired single anomer through the key intermediate **65**.

The *in vitro* assay showed that the five-membered ring analogues, **32a-32r** did not inhibit hSGLT1. Future study of the SAR on the substitutions on C-5' and C-6' position of five-membered ring glucoside and the presence of an additional aromatic ring at the distal position of biphenyl will be a worthy approach if the hSGLT2 assay shows promising result.

4. Experimental Section

4.1 Materials

4.1.1 Chemistry

All reagents were purchased at the highest commercial quality and used without further purification, unless otherwise indicated.

Acros:

TBAI, benzyl bromide, AcOH, MeOH (dry), THF (dry), CH_2Cl_2 (dry), DMF (dry), CH_3CN (dry), toluene (dry), 2M HCl in ether, 5-bromo-2-chlorobenzoic acid, oxalyl chloride, phenetole, $AlCl_3$, NaOH, cumene, BF_3•OEt_2, Et_3SiH, MsOH, NH_4Cl, EtSH, NaH, 4-ethylbenzoic acid, 4-isopropylbenzoic acid, $LiAlH_4$, imidazole, DMAP, TIPSCl, TBAF

Sigma-Aldrich:

2-methoxyphenylmagnesium bromide, 3-methoxyphenylmagnesium bromide, 4-methoxy-phenylmagnesium bromide, 4-fluorophenylmagnesium bromide, 4-*tert*-butylphenyl-magnesium bromide, 4-thioanisolemagnesium bromide, 3,4-(methylenedioxy)phenyl-magnesium bromide, 4-phenoxyphenylmagnesium bromide, 6-Methoxy-2-naphthyl-magnesium bromide

Alfa:

Diacetone-D-glucose, NaOMe, 4-ethoxybenzoic acid

Chemetall:

n-BuLi (2.5 M in hexane)

J.T. Baker:

KOH, K_2CO_3, ether (20L, ACS grade)

Fisher Scientific:

$NaHCO_3$

Matrix Scientific:

5-bromo-2-methylbenzoic acid

RDH:

Molecular sieves 4 Å, Celite, $MgSO_4$, Na_2SO_4

Mallinckrodt Chemicals: (20L, ACS grade solvent)

CH_2Cl_2, *n*-hexane, EA, MeOH, $CHCl_3$, diethyl ether, toluene

Merck: (4L, HPLC grade solvent)

CH_3CN, MeOH

Silicycle:

Silica gel (230 – 400 mesh)

友和貿易（股）公司:

Ethanol (95%)

林純藥工業株式會社:

Iodomethane

4.1.2 General Instrument and Methods

TLC, Thin layer chromatography:

Merck silica gel plates (60F-254), UV light (245 nm), anisaldehyde, cerium molydate solution as visualizing agents.

NMR Spectra:

DPX-200 (200 MHz), Bruker AMX-400 (400 MHz), AVIII-600 (600 MHz). Chemical shifts in part per million (ppm) are reported relative to the residual $CDCl_3$ (^1H = 7.24 ppm, ^{13}C = 77.0 ppm), CD_3OD (^1H = 4.78 ppm, ^{13}C = 49.0 ppm) . Splitting patterns are described as following abbreviations: s, singlet; d, double; t, triplet; q, quartet; dd, double doublet; m, multiplet. Coupling constant (*J*) are reported in hertz (Hz).

Melting Point:

Fargo, melting point apparatus, MP-1D

High resolution Mass Spectra:

BioTOF II in Genomics Research Center, Academia Sinica.

HPLC:

Hitachi L-2130 pump, L-2420 UV-Vis detector, L-2200 autosampler, Mightysil RP-18 GP 250-4.6 5 (μM) column, Flow rate = 1.0 mL/min, UV detection = 224 nm.

4.1.3 COS-7 cell culture

COS-7 cells (African Green Monkey Kidney Cells; American Type culture Collection)

Invitrogen, GIBCO:

Phosphate buffer saline (PBS), High Glucose DMEM (Dulbecco's Modified Eagle's Medium HG), FBS (Fetal bovine serum), NEAA (non-essential amino acids), 0.05% Trypsin-EDTA

Corning Life Sciences:

6-well plates, 12-well plates, 24-well plates, 10 mm dish, T25 flask

4.1.4 Transformation and Isolation of Plasmid DNA

Sigma:

Ampicillin

ECOS-101:

Competent cell

GeneCopoeia™:

hSGLT2 plasmid (OmicsLink™ Expression Clone Datasheet of EX-C0047-M02), eGFP plasmid (OmicsLink™ Expression Clone Datasheet of EX=EGFP-M02)

QIAGEN:

QIAprep® Miniprep

4.1.5 Digestion and Ligation

Thermo Scientific:

Nanodrop 2000, FastDigest® Restriction Enzymes, FastDigest® Green buffers

Fermentas:

DNA blunting enzyme (CloneJET™ PCR Cloning Kit #K1231, #K1232), Rapid DNA Ligation Kit

4.1.6 Transfection & Stable Clone Selection

Mirus:

*Trans*IT®-LT1 Transfection Reagent

Invitrogen:

Opti-MEM® medium, High Glucose DMEM (Dulbecco's Modified Eagle's Medium HG), FBS (Fetal bovine serum), NEAA (non-essential amino acids), G418, Geneticin®

4.1.7 Western Blot

Pierce:

BCA™ Protein Assay Kit

Abcam:

Mouse hSGLT2 antibody (ab58298)

United States Biological:

Rabbit hSGLT2 antibody

Acros:

2-Mercaptoethanol

Invitrogen:

NuPAGE® Novex 4-12% Bis-Tris Gel 1.0 mm, 12 well, NuPAGE® NOPS SDS Running Buffer (for Bis-Tris Gels only) (20x),

Bio-Rad®:

SDS, Tris-base, Glycine , Tween-20

4.2 Methods

4.2.1 Chemistry

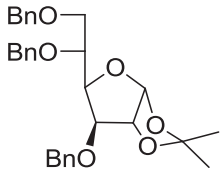

Chemical Formula: $C_{30}H_{34}O_6$
Exact Mass: 490.2355
Molecular Weight: 490.5874

3,5,6-*O*-Tribenzyl-1,2-*O*-isopropylidene-D-glucofuranose (42)

To the solution diacetone-D-glucose (50.0 g, 192 mmol) in THF (250 mL) was added TBAI (3.55g, 9.61 mmol). The mixture was incubated in ice bath for 10 mins before adding NaH (60% in mineral oil, 14.2 g, 355 mmol) followed by benzyl bromide (26 mL, 211.7 mmol). The temperature of reaction was raised to 60 ℃ for 2 h. After the reaction was completed, the mixture was incubated in 0 ℃ and quenched with MeOH and extracted with EA. The organic layer were washed with H_2O, ammonium chloride and sat. $NaHCO_3$, dried over $MgSO_4$, filtered and concentrated in vacuo to afford crude **47** as a yellow oil.

To the solution of crude **47**, water (200 mL) was added AcOH (400 mL) and stirred at 40 ℃ for 5 h. After the reaction was completed, water (200 mL) was added before concentrated in vacuo to avoid acetylation. Finally toluene (150 mL) and MeOH (50 mL) was added and concentrated in vacuo to afford crude **48**.

The crude compound **48** in THF (250 mL) was subjected to NaH (60% in mineral oil, 28.4 g, 710 mmol) followed by benzyl bromide (52 mL, 423 mmol) at 0 ℃. After 2 h when the reaction was completed, the mixture was incubated in 0 ℃ and quenched with MeOH and extracted with EA. The organic layer were washed with H_2O, ammonium chloride and sat. $NaHCO_3$, dried over $MgSO_4$, filtered and concentrated in vacuo to afford crude **42** as a yellow oil. Analytical sample was purified by column chromatography (EA/*n*-

hexane = 1/10 to 1/8). ^{1}HNMR (400 MHz, $CDCl_3$) δ 7.39-7.24 (m, 15H), 5.94 (d, J = 3.7 Hz, 1H), 4.85 (d, J = 9.2 Hz, 1H), 4.67-4.61 (m, 4H), 4.53 (d, J = 4.2 Hz, 1H), 4.50 (d, J = 4.4 Hz, 1H), 4.34 (dd, J = 9.3, 2.9 Hz, 1H), 4.15 (d, J = 2.9 Hz, 1H), 4.12-4.08 (m, 1H), 3.95 (dd, J = 10.6, 1.32 Hz, 1H), 3.72 (q, J = 5.88 Hz, 1H), 1.51 (s, 3H), 1.34 (s, 3H). HRMS (ESI) calcd. for $C_{30}H_{34}O_6Na^+$ $[M+Na]^+$: 513.2253, found: 513.2258.

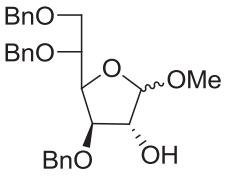

Chemical Formula: $C_{28}H_{32}O_6$
Exact Mass: 464.2199
Molecular Weight: 464.5501

Methyl 3,5,6-*O*-tribenzyl-D-glucofuranoside (43)

In the solution of crude **42** (max 192 mmol) in dry MeOH (575 mL) was added 2.0 M HCl in diethy ether (28 mL) and stirred for 4 h at 55 ℃. After the reaction completed, solvent was removed under reduced pressure, H_2O was added from time to time when half of the solvent was removed and this was repeated for 5 times. Finally, the mixture was extracted with EA, $NaHCO_3$ and brine to afford crude **43** as a yellow oil. Analytical sample was purified by column chromatography (EA/*n*-hexane= 1/16 to 1/10). ^{1}HNMR (200 MHz, d_4-MeOH) δ 7.21-7.14 (m, 15H), 4.81 (d, J = 4.3 Hz, 1H), 4.59 (dd, J = 11.6, 3.4 Hz, 2H), 4.39-4.33 (m, 4H), 4.22 (dd, J = 7.6, 4.9 Hz, 1H), 4.11 (dd, J = 4.3, 3.1 Hz, 1H), 3.95 (dd, J = 5.1, 3.1 Hz, 1H), 3.90-3.82 (m, 1H), 3.74 (dd, J = 10.6, 2.1 Hz, 1H), 3.55 (q, J = 5.1 Hz, 1H), 3.29 (s, 3H). ^{13}C-NMR (50 MHz, d_4-MeOH) δ 129.29, 128.67, 128.49, 104.01, 84.91, 78.25, 77.71, 77.48, 74.24, 73.34, 72.83, 71.67, 56.02. HRMS (ESI) calcd. for $C_{28}H_{32}O_6Na^+$ $[M+Na]^+$: 487.2091, found: 487.2092.

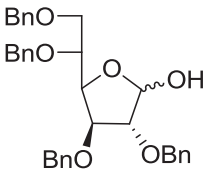

Chemical Formula: $C_{34}H_{36}O_6$
Exact Mass: 540.2512
Molecular Weight: 540.6460

2,3,5,6-*O*-Tetrabenzyl-D-glucofuranose (45)

To the solution **43** (max. 192 mmol) in THF (250 mL) was added TBAI (3.55g, 9.61 mmol). The mixture was incubated in ice bath for 10 mins before adding NaH (60% in mineral oil, 14.2 g, 355 mmol) followed by benzyl bromide (26 mL, 211.7 mmol). The temperature of reaction was raised to 60 ℃ for 2 h. After the reaction was completed, the mixture was incubated in 0 ℃ and quenched with MeOH and extracted with EA. The organic layer were washed with H_2O, ammonium chloride and sat. $NaHCO_3$, dried over $MgSO_4$, filtered and concentrated in vacuo to afford crude **44**.

To the solution of **44** in AcOH (500 mL), 20 % H_2SO_4 (150 mL) was added and stirred at 40 ℃ for 20 h. Upon completion, 100 mL H_2O was added and concentrated in vacuo to until half of the reaction mixture was evaporated. The reaction mixture was extracted with toluene (250 mL) twice, dried over $MgSO_4$, filtered and concentratedin vacuo. The resulting mixture was purified by column chromatography (400 g silica gel, EA/*n*-hexane = 1/8 to 1/5) to afford **45** (52.0 g, 96.2 mmol, 50% yield over 6 steps) as a colorless oil. ^{1}H-NMR (200 MHz, $CDCl_3$) δ 7.38-7.20 (m, 20H), 5.57-5.28 (m, 1H), 4.99-4.80 (m, 1H), 4.71-4.28 (m, 8H), 4.21-4.06 (m, 2H), 4.04-3.85 (m, 2H), 3.84-3.71 (m, 1H). ^{13}C-NMR (50 MHz, $CDCl_3$) δ 128.55, 128.52, 128.40, 128.36, 128.24, 128.20, 128.17, 128.10, 127.94, 127.86, 127.83, 127.79, 127.56, 127.52, 127.39, 127.36, 101.42, 83.72, 80.91, 80.45, 80.15, 79.94, 77.78, 76.68, 75.86, 73.37, 73.27, 73.00, 72.68, 72.22, 72.13, 71.66, 71.13, 70.78. HRMS (ESI) calcd. for $C_{34}H_{36}O_6Na^+$ $[M+Na]^+$: 563.2404, found: 563.2409.

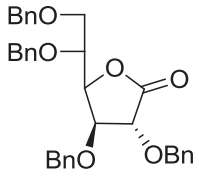

Chemical Formula: $C_{34}H_{34}O_6$
Exact Mass: 538.2355
Molecular Weight: 538.6302

2,3,5,6-*O*-Tetrabenzyl-glucono-gamma-lactone (46)

4 Å molecular sieves (60 g) were dried under vacuum and heated at 300 ℃ for 2 h. To the molecular sieve were added compound **45** (52.0 g, 96.2 mmol) in solution of dry CH_2Cl_2 (500 mL) and PCC (36.0 g, 167 mmol). The reaction mixture was stirred at room temperature for 5 h. After the reaction was completed, it was evaporated to remove solvent under reduced pressure and the residue was filtered through silica gel (50 g) and and the filter cake was washed with CH_2Cl_2. The combined filtrate were concentrated in vacuo to afford compound **46** (47.9 g, 88.8 mmol, 93% yield) as a colorless oil. ^{1}H-NMR (400 MHz, $CDCl_3$) δ 7.43-7.17 (m, 20H), 4.92 (d, J = 11.7 Hz, 1H), 4.80 (dd, J = 6.3, 5.4 Hz, 1H), 4.76 (d, J = 11.2 Hz, 1H), 4.63 (d, J = 11.6 Hz, 1H), 4.60-4.45 (m, 5H), 4.35-4.27 (m, 2H), 4.14-4.07 (m, 1H), 3.87-3.71 (m, 2H). ^{13}C-NMR (50 MHz, $CDCl_3$) δ 172.87, 137.96, 137.90, 136.92, 136.61, 128.40, 128.36, 128.31, 128.26, 128.12, 128.04, 127.88, 127.64, 127.59, 127.52, 79.11, 78.73, 76.78, 76.39, 73.35, 72.99, 72.33, 72.22, 69.51. HRMS (ESI) calcd. for $C_{34}H_{34}O_6Na^+$ $[M+Na]^+$: 561.2248, found: 561.2257.

Compound **49a-49h, 50a-50h, 51, 59, 60 and 61** were having the same data characteristics with compounds reported by Yamamoto, K. *et. al*[77], therefore only H-NMR were included.

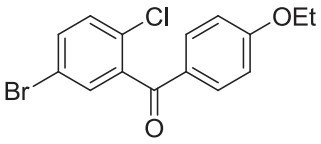

Chemical Formula: $C_{15}H_{12}BrClO_2$
Exact Mass: 337.9709
Molecular Weight: 339.6116

(5-Bromo-2-chlorophenyl)(4-ethoxyphenyl)methanone (49a)

To a stirred suspension of 5-bromo-2-chlorobenzoic acid (927 mg, 3.94 mmol) in CH_2Cl_2 (10 mL) was added oxalyl chloride (406 µL, 4.73 mmol) and DMF (15 µL, 0.20 mmol). The resulting mixture was stirred for 20 h at r.t. After the reaction was completed, the mixture was concentrated to afford compound **47** (1.00 g, max. 3.94 mmol) as a yellowish solid.

To the solution of crude **47** in CH_2Cl_2 (10 mL) were added phenetole (500 µL, 3.94 mmol) followed by $AlCl_3$ (525 mg, 3.94 mmol) batchwise so that the temperature do not exceed 0 ℃. After being stirred at 5 ℃ for 3 h, ice water was added to quench reaction. The resulting mixture were extracted by CH_2Cl_2, then washed with 1N HCl, H_2O, 1N NaOH, brine, dried over $MgSO_4$, filtered and concentrated in vacuo. The residual solid was recrystallized from 95% EtOH to give **49a** (556 mg, 1.64 mmol, 42 % over 2 steps) as a white solid. mp: 62 ℃. ^{1}H-NMR (400 MHz, $CDCl_3$) δ 7.76-7.72 (m, 2H), 7.51 (dd, J = 8.5, 2.4 Hz, 1H), 7.46 (d, J =2.4 Hz, 1H), 7.30 (d, J = 8.6 Hz, 1H), 6.93-6.89 (m, 2H), 4.10 (q, J = 7.0 Hz, 2H), 1.43 (t, J = 7.0 Hz, 3H).

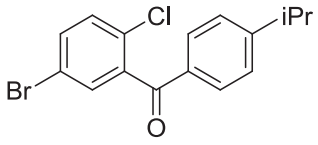

Chemical Formula: $C_{16}H_{14}BrClO$
Exact Mass: 335.9917
Molecular Weight: 337.6388

(5-Bromo-4-chlorophenyl)(4-isopropylphenyl)methanone (49b)

Compound **49b** (544 mg , 1.61 mmol, 76% yield over 2 steps) as a white solid was prepared according to the method described for the synthesis of **49a** using 5-bromo-2-chlorobenzoic acid (500 mg, 2.12 mmol) and cumene (295 µL, 2.12 mmol). mp: 93 ºC. ^{1}H-NMR (200 MHz, $CDCl_3$) δ 7.66 (d, J = 8.0 Hz, 2H), 7.49-7.33 (m, 2H), 7.30-7.10 (m, 3H), 2.85 (m, 1H), 1.16 (d, J = 6.87, 6H).

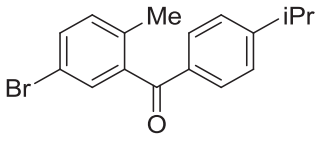

Chemical Formula: $C_{17}H_{17}BrO$
Exact Mass: 316.0463
Molecular Weight: 317.2203

`

(5-Bromo-2-methylphenyl)(4-isopropylphenyl)methanone (49d)

Compound **49d** (453 mg, 1.43 mmol, 57% yield over 2 steps) as a green oil was prepared according to the method described for the synthesis of **49a** using 5-bromo-2-methylbenzoic acid (539 mg, 2.51 mmol) and cumene (350 µL, 2.51 mmol) ^{1}H-NMR (400 MHz, $CDCl_3$) δ 7.71 (d, J = 8.1 Hz, 2H), 7.48 (dd, J = 8.3, 2.2 Hz), 7.40 (d, J = 2.3 Hz, 1H), 7.30 (d, J = 8.2 Hz, 2H), 7.14 (d, J = 8.0 Hz, 1H), 2.97 (m, 1H), 2.23 (s, 3H), 1.27 (d, J = 6.9 Hz, 6H).

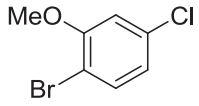

Chemical Formula: C_7H_6BrClO
Exact Mass: 219.9291
Molecular Weight: 221.4789

1-Bromo-4-chloro-2-methoxybenzene (51)

In the solution of 2-bromo-5-chlorophenol (500 mg, 2.41 mmol) in DMF (5 mL), K_2CO_3 (333 mg, 2.41 mmol) and MeI (188 μL, 3.01 mmol) was added subsequently. After stirring the mixture at ambient temperature for 6 h, ice water was added to quench reaction. The resulting mixture was extracted with EA twice and the combined organic layers were washed with H_2O and brine to afford **51** as a yellow solution (507 mg, 2.29 mmol, 95% yield) as colorless oil. ^{1}H-NMR (400 MHz, $CDCl_3$) δ 7.42 (d, J = 8.5 Hz, 1H), 6.86 (d, J = 2.2 Hz, 1H), 6.81 (dd, J = 8.3, 2.2 Hz, 1H), 3.86 (s. 3H).

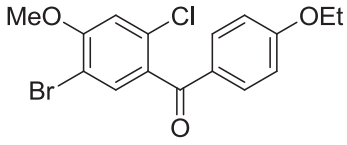

Chemical Formula: $C_{16}H_{14}BrClO_3$
Exact Mass: 367.9815
Molecular Weight: 369.6376

(5-Bromo-2-chloro-4-methoxyphenyl)(4-ethoxyphenyl)methanone (49f)

Crude **52** (max. 5.25 mmol) as a yellow solution, was prepared according to the procedure described for the synthesis of crude **47** using 4-ethoxybenzoic acid (872 mg, 5.25 mmol).

Compound **49f** (1.39g, 3.76 mmol, 72% yield over 2 steps) as a white solid, was prepared according to the procedure described for the synthesis of **49a** using compound **51** (1.16 g, 5.25 mmol) and crude **52** (max. 5.25 mmol). The crude product is purified with column chromatography (25 g silica gel, EA/*n*-hexane = 1/20 to 1/15 to 1/10). mp: 80 ºC. ^{1}H-NMR (400 MHz, $CDCl_3$) δ 7.71 (d, J = 8.7 Hz, 2H), 7.52 (s, 1H), 6.91 (s, 1H), 6.87 (d, J = 8.9 Hz, 2H), 4.05 (q, J = 7.0 Hz, 2H), 3.90 (s, 3H), 1.38 (t, J = 7.0 Hz, 3H).

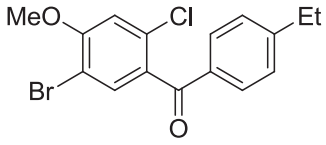

Chemical Formula: $C_{16}H_{14}BrClO_2$
Exact Mass: 351.9866
Molecular Weight: 353.6382

(5-Bromo-2-chloro-4-methoxyphenyl)(4-ethylphenyl)methanone (49g)

Crude **53** (max. 3.13 mmol) was prepared according to the procedure described for the synthesis of crude **47** using 4-ethylbenzoic acid (470 mg, 3.13 mmol) as a starting material.

Compound **49g** (356 mg, 1.01 mmol, 32% yield over 2 steps) as a colorless oil was prepared according to the procedure described for the synthesis of **49a** using compound **51** (658 mg, 2.97 mmol) and crude **53** (max. 3.13 mmol). The crude product is purified with column chromatography (6 g silica gel, EA/*n*-hexane = 1/20 to 1/15 to 1/10). ^{1}H-NMR (200 MHz, $CDCl_3$) δ 7.68 (d, J = 8.0 Hz, 2H), 7.54 (s, 1H), 7.24 (d, J = 8.3 Hz, 2H), 6.93 (s, 1H), 3.90 (s, 3H), 2.67 (q, J = 7.6 Hz, 2H), 1.21 (t, J = 7.6 Hz, 3H).

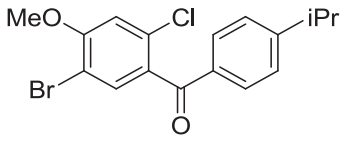

Chemical Formula: $C_{17}H_{16}BrClO_2$
Exact Mass: 366.0022
Molecular Weight: 367.6647

(5-Bromo-2-chloro-4-methoxyphenyl)(4-isopropylphenyl)methanone (49h)

Crude **54** (max. 3.31 mmol) was prepared according to the procedure described for the synthesis of crude **47** using 4-isopropylbenzoic acid (543 mg, 3.31 mmol) as a starting material.

Compound **49h** (331 mg, 0.90 mmol, 27% yield over 2 steps) as a yellow oil was prepared according to the procedure described for the synthesis of **49a** using compound **51** (658 mg, 2.97 mmol) and **54** (max. 3.31 mmol). The crude product is purified with column chromatography (6 g silica gel, EA/*n*-hexane = 1/20 to 1/15 to 1/10). ^{1}H-NMR (200 MHz, $CDCl_3$) δ 7.70 (d, J = 8.2 Hz, 2H), 7.55 (s, 1H), 7.29 (d, J = 8.2 Hz, 2H), 6.94 (s, 1H), 3.92 (s, 3H), 2.94 (m, 1H), 1.24 (d, J = 6.9 Hz, 6H).

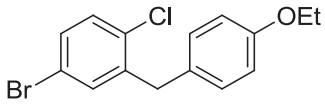

Chemical Formula: $C_{15}H_{14}BrClO$
Exact Mass: 323.9917
Molecular Weight: 325.6281

4-Bromo-1-chloro-2-(4-ethoxybenzyl)benzene (50a)

To a stirred suspension of **49a** (15.6 g, 45.8 mmol) in CH_2Cl_2 (100 mL) was added Et_3SiH (11.2 mL, 96.2 mmol), followed by BF_3•OEt_2 (8.6 mL, 60.9 mmol) at 0 ℃. The reaction mixture was then returned to r.t. and stirred for 1 h. After the reaction was completed, 7.0 N KOH was added to quench the reaction and the resulting mixture was extracted with CH_2Cl_2. The organic layer was then washed with 10% brine, sat. brine, dried over $MgSO_4$ and filtered before concentrated in vacuo. The resulting solids were recrystallized with 95% EtOH to afford compound **50a** (9.95g, 30.6 mmol, 67% yield) as a white solid. mp: 78 ºC. ^{1}H-NMR (200 MHz, $CDCl_3$) δ 7.26-7.20 (m, 3H), 7.11-7.02 (m, 2H), 6.87-6.77 (m, 2H), 3.99 (q, J =6.9 Hz, 2H), 3.97 (s, 2H), 1.39 (t, J = 7.0 Hz, 3H).

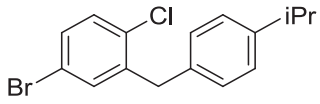

Chemical Formula: $C_{16}H_{16}BrCl$
Exact Mass: 322.0124
Molecular Weight: 323.6552

4-Bromo-1-chloro-2-(4-isopropylbenzyl)benzene (50b)

Compound **50b** (476 mg, 1.47 mmol, 93% yield) as a white solid was prepared according to the method described for the synthesis of **50a** using compound **49b** as a starting material. mp: 95 ºC ^{1}H-NMR (400 MHz, $CDCl_3$) δ 7.31-7.25 (m, 2H), 7.24-7.21 (m, 1H), 7.20-7.09 (m, 4H), 4.03 (s, 2H), 2.95-2.83 (m, 1H), 1.25 (d, J = 6.95, 6H).

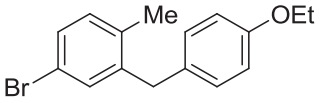

Chemical Formula: $C_{16}H_{17}BrO$
Exact Mass: 304.0463
Molecular Weight: 305.2096

4-Bromo-2-(4-ethoxybenzyl)-1-methylbenzene (50c)

Crude **49c** (600 mg , max. 1.88 mmol) as a green oil was prepared according to the method described for the synthesis of **49a** using 5-bromo-2-methylbenzoic acid (539 mg, 2.51 mmol) and phenetole (318 μL, 2.51 mmol) as starting materials.

Compound **50c** (522 mg, 1.71 mmol, 68% yield over 3 steps) as a colorless oil was prepared according to the method described for the synthesis of **50a** using crude **49c** (max, 1.88 mmol) as a starting material. ^{1}H-NMR (400 MHz, $CDCl_3$) δ 7.30-7.20 (m, 2H), 7.00 (d, J = 8.1 Hz, 3H), 6.87-6.78 (m, 2H), 3.99 (q, J = 7.0 Hz, 2H), 3.85 (s, 2H), 1.39 (t, 7.0 Hz, 3H).

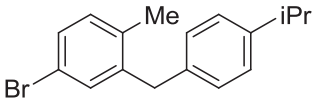

Chemical Formula: $C_{17}H_{19}Br$
Exact Mass: 302.0670
Molecular Weight: 303.2368

4-Bromo-2-(4-isopropylbenzyl)-1-methylbenzene (50d)

Compound **50d** (250 mg, 0.82 mmol) as a yellow oil was prepared according to the method described for the synthesis of **50a** using compound **49d** (453 mg, 1.43 mmol) as a starting material. ^{1}H-NMR (400 MHz, $CDCl_3$) δ 7.32-7.27 (m, 2H), 7.22-7.16 (m, 2H), 7.10-7.03 (m, 3H), 3.94 (s, 2H), 2.98-2.86 (m, 1H), 2.23 (s, 3H), 1.28 (d, J = 6.9 Hz, 6H).

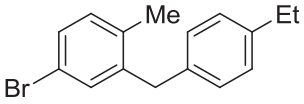

Chemical Formula: $C_{16}H_{17}Br$
Exact Mass: 288.0514
Molecular Weight: 289.2102

4-Bromo-2-(4-ethylbenzyl)-1-methylbenzene (50e)

Crude **49e** (438mg, max. 1.44 mmol) as a pink solution was prepared according to the method described for the synthesis of **49a** using 5-bromo-2-methylbenzoic acid (524 mg, 2.44 mmol) and ethylbenzene (300 μL, 2.44 mmol).

Compound **50e** (215 mg, 0.74 mmol, 31% yield over 3 steps) as a yellowish oil was prepared according to the method described for the synthesis of **50a** using crude **49e** (max. 1.44 mmol) as a starting material. ^{1}H-NMR (200 MHz, $CDCl_3$) δ 7.35-7.26 (m, 2H), 7.21-7.11 (m, 2H), 7.11-7.00 (m, 3H), 3.93 (s, 2H), 2.66 (q, J = 7.6 Hz, 2H), 2.22 (s, 3H), 1.26 (t, 3H).

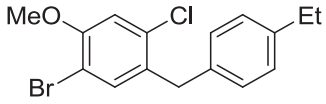

Chemical Formula: $C_{16}H_{16}BrClO$
Exact Mass: 338.0073
Molecular Weight: 339.6546

1-Bromo-4-chloro-5-(4-ethylbenzyl)-2-methoxy-benzene (50g)

Compound **50g** (273 mg, 0.80 mmol, 79% yield) as an off-white solid was prepared according to the method described for the synthesis of **50a** using compound **49g** (356 mg, 1.01 mmol) as a starting material. mp: 87 ºC. ^{1}H-NMR (200 MHz, $CDCl_3$) δ 7.32 (s, 1H), 7.18-7.03 (m, 4H), 6.90 (s, 1H), 3.97 (s, 2H), 3.86 (s, 3H), 2.62 (q, J = 7.7 Hz 2H), 1.22 (t, J = 7.5 Hz, 3H).

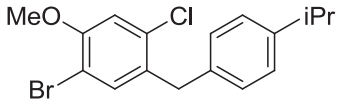

Chemical Formula: $C_{17}H_{18}BrClO$
Exact Mass: 352.0230
Molecular Weight: 353.6812

1-bromo-4-chloro-5-(4-isopropylbenzyl)-2-methoxy-benzene (50h)

Compound **50h** (182 mg, 0.51 mmol, 57% yield) as a colorless oil was prepared according to the method described for the synthesis of **50a** using compound **49h** (331 mg, 0.90 mmol) as a starting material. ^{1}H-NMR (200 MHz, $CDCl_3$) δ 7.34 (s, 1H), 7.21-7.04 (m, 4H), 6.91 (s, 1H), 3.97 (s, 2H), 3.86 (s, 3H), 3.00-2.76 (m, 1H), 1.24 (d, J = 7.0 Hz, 6H).

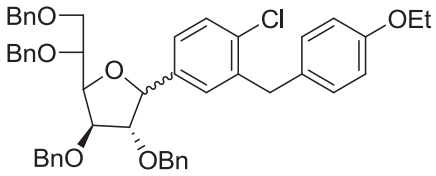

Chemical Formula: $C_{49}H_{49}ClO_6$
Exact Mass: 768.3218
Molecular Weight: 769.3628

1,4-Anhydro-2,3,5,6-tetra-*O*-benzyl-1-*C*-[4-chloro-3-(4-ethoxybenzyl)-phenyl]-D-glucitol (56a)

To a stirred -78 °C solution of **50a** (604 mg, 1.86 mmol) in 1:2 THF/toluene (15 mL) under N_2 gas was added *n*-BuLi (2.5 M in hexane, 742 μL, 1.86 mmol) dropwisely. After 1 h, to this mixture was added **46** (1.00 g, 1.86 mmol) in toluene (10 mL) while maintaining the temperature under -78 °C. After 1 h, MsOH (0.6 N in MeOH, 15 mL) was added; whereupon, the reaction was slowly warmed to ambient temperature over 16 h. After the reaction was completed, the mixture was quenched with sat. $NaHCO_3$ and later extracted with CH_2Cl_2. The organic layer was then washed with H_2O, brine, dried over $MgSO_4$, filtered and concentrated under reduced pressure to afford crude **55a**.

Compound **56a** (264 mg, 0.34 mmol, 18% yield over 2 steps) as a colorless oil which comprised of a 1:2 mixture of anomers was prepared according to the procedure of the synthesis of **50a** using crude **55a** as a starting material. The purification was carried out by column chromatography (10 g silica gel, EA/*n*-hexane = 1/20). ^{1}H-NMR (400 MHz, $CDCl_3$) δ 7.51-7.28 (m, 20H), 7.26-7.19 (m, 2H), 7.18-7.05 (m, 4H), 6.84 (d, J = 8.6 Hz, 2H), 4.99-4.87 (m, 2H), 4.77-4.51 (m, 6H), 4.49-4.28 (m, 3H), 4.27-4.17 (m, 2H), 4.16-3.95 (m, 7H), 3.81 (q, J = 5.6 Hz, 1H), 1.43 (t, J = 7.0 Hz, 3H). ^{13}C-NMR (100 MHz, $CDCl_3$) δ 157.27, 139.65, 138.86, 138.75, 138.51, 137.59, 137.43, 132.81, 131.16, 129.80, 129.63, 129.16, 128.88, 128.38, 128.33, 128.18, 128.16,128.11, 127.80, 127.69, 127.56, 127.51, 127.47, 127.44, 127.31, 125.41, 114.28, 88.43, 85.78, 82.39, 80.83, 77.20, 75.91,

73.32, 72.48, 71.63, 71.26, 70.93, 63.16, 38.23, 14.78. HRMS (ESI) calcd. for $C_{49}H_{49}ClO_6Na^+$ $[M+Na]^+$: 791.3110, found: 791.3110.

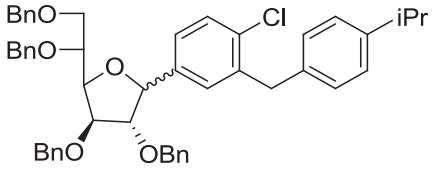

Chemical Formula: $C_{50}H_{51}ClO_5$
Exact Mass: 766.3425
Molecular Weight: 767.3899

1,4-Anhydro-2,3,5,6-tetra-*O*-benzyl-1-*C*-[4-chloro-3-(4-ethoxybenzyl)-phenyl]-D-glucitol (56b)

Crude **55b** was prepared according to the procedure described for the synthesis of crude **55a** using **50b** (476 mg, 1.47 mmol) and **46** (712 mg, 1.32 mmol) as starting materials.

Compound **56b** (159 mg, 0.21 mmol, 16% yield over 2 steps) as a colorless oil which comprised of a 1:3 mixture of anomers was prepared according to the procedure of the synthesis of **50a** using **55b** (223 mg, 0.28 mmol) as a starting material. The purification was carried out by column chromatography (10 g silica gel, EA/*n*-hexane = 1/20) ^{1}H-NMR (400 MHz, $CDCl_3$) δ 7.53-7.22 (m, 21H), 7.22-7.09 (m, 6H), 4.98-4.88 (m, 2H), 4.75-4.52 (m, 5H), 4.49-4.35 (m, 2H), 4.33-4.20 (m, 2H), 4.20-4.07 (m, 3H), 4.07-3.96 (m, 2H), 3.90-3.78 (m, 1H). 2.99-2.87 (m, 1H). 1.30-1.29 (m, 6H). ^{13}C-NMR (100 MHz, $CDCl_3$) δ 146.44, 138.96, 138.54, 138.12, 137.96, 137.73, 137.26, 136.91, 136.76, 133.95, 130.82, 128.95, 128.87, 128.47, 128.22, 128.13, 128.09, 127.62, 127.50, 127.46, 127.42, 127.34, 127.24, 126.32, 125.23, 110.49, 86.69, 82.05, 81.72, 76.58, 73.37, 72.36, 71.99, 71.88, 71.47, 38.81, 33.55, 23.94. HRMS (ESI) calcd. for $C_{50}H_{51}ClO_5Na^+$ $[M+Na]^+$: 789.3323, found: 789.3318.

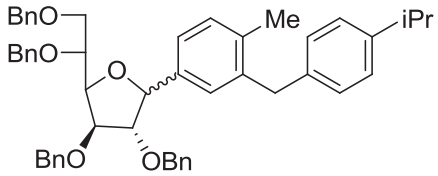

Chemical Formula: $C_{51}H_{54}O_5$
Exact Mass: 746.3971
Molecular Weight: 746.9715

2,3,5,6-tetra-*O*-benzyl-1-*C*-[3-(4-isopropylbenzyl)-4-methylphenyl]-D-gluco-furanoside (56d)

To a stirred -78 °C solution of **50d** (250 mg, 0.82 mmol) in THF (3 mL) under N_2 gas was added n-BuLi (2.5 M in hexane, 360 μL, 1.01 mmol) dropwisely. After 1 h, to this mixture was added **46 (**355 mg, 0.66 mmol) in THF (1.5 mL) while maintaining the temperature under -78 °C. After stirring for 3 h, NH_4Cl was added to quench reaction and resulting mixture was extracted with CH_2Cl_2 and washed with H_2O, brine, dried over $MgSO_4$, filtered and concentrated under reduced pressure to afford crude **55d**.

To the solution of crude **55d** in CH_2Cl_2 (5 mL) at -50 °C, was added Et_3SiH (158 μL, 0.99 mmol), followed by BF_3•OEt_2 (76.8 μL, 0.66 mmol) slowly to maintain the temperature below -40 °C. The resulting suspension was allowed to warm to -10 °C over 1 h prior to quenching with K_2CO_3. After concentrated in vacuo, the resulting mixture was extracted with ethyl acetate and washed with brine, dried over $MgSO_4$, filtered and purified with column chromatography (5 g silica gel, ethyl acetate/*n*-hexane = 1/20) to afford **56d** (75 mg, 0.10 mmol, 15% yield over 2 steps) as a colorless oil which comprised of a 1:3. ^{1}H-NMR (400 MHz, $CDCl_3$) δ 7.43-6.95 (m, 27H), 4.88 (d, J = 2.8 Hz, 1H), 4.85 (d, J = 11.5 Hz, 1H), 4.68-4.50 (m, 5H), 4.50-4.35 (m, 2H), 4.32-4.15 (m, 3H), 4.05-3.90 (m, 4H), 3.77 (dd, J = 10.7, 5.6 Hz, 1H), 2.93-2.80 (m, 1H), 2.24 (s, 3H), 1.23 (d, J = 7.0 Hz, 6H). ^{13}C-NMR (100 MHz, $CDCl_3$) δ 146.29, 139.01, 138.90, 138.65, 138.45, 137.85, 137.56, 136.89, 130.26, 128.49, 128.40, 128.31, 128.23, 128.20, 127.75, 127.56, 127.50, 127.34, 127.31,

126.30, 124.59, 88.84, 86.62, 82.83, 80.80, 76.06, 73.37, 72.67, 71.68, 71.40, 71.19, 39.07, 33.61, 24.01, 19.39. HRMS (ESI) calcd. for $C_{51}H_{54}O_5Na^+$ $[M+Na]^+$: 769.3863, found: 769.3833.

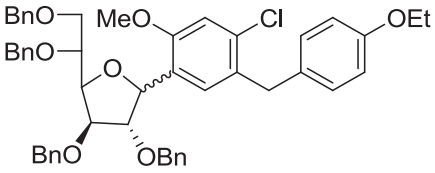

Chemical Formula: $C_{50}H_{51}ClO_7$
Exact Mass: 798.3323
Molecular Weight: 799.3887

1,4-Anhydro-2,3,5,6-tetra-*O*-benzyl-1-*C*-[4-chloro-5-(4-ethoxybenzyl)-2-methoxyphenyl]-D- glucitol (56f)

Crude **50f** (360 mg, max. 1.01 mmol) was prepared accordimg to the method described for the synthesis of **50a** using **49f** (609 mg, 1.65 mmol) as a starting material.

Crude **55f** was prepared according to the method described for the synthesis of crude **55d** using crude **50f** and **46** (436 mg, 0.81 mmol) as starting materials.

Compound **56f** (319 mg, 0.40 mmol, 49% yield over 3 steps) as a yellow oil which comprised of a 1:1.3 mixture of anomers was prepared according to the procedure of the synthesis of **56d** using crude **55f** as a starting material. ^{1}H-NMR (400 MHz, $CDCl_3$) δ 7.52-7.02 (m, 20H), 6.97-6.83 (m, 3H), 6.81 (d, J = 6.7 Hz, 1H), 6.79-6.67 (m, 2H), 5.53-5.32 (m, 1H), 4.94-4.78 (m, 1H), 4.78-4.49 (m, 5H), 4.49-4.41 (m, 1H), 4.33-4.19 (m, 2H), 4.19-3.84 (m, 8H), 3.81 (s, 2H), 3.73-3.62 (m, 2H), 1.45-1.30 (m, 3H). ^{13}C-NMR (400 MHz, $CDCl_3$) δ 157.10, 157.05, 154.67, 154.29, 139.07, 139.03, 138.69, 138.67, 138.16, 137.93, 137.73, 132.71, 132.38, 132.17, 131.51, 130.63, 130.30, 130.26, 130.01, 129.54, 129.42, 128.30, 128.19, 128.17, 128.15, 128.05, 127.78, 127.62, 127.54, 127.52, 127.48, 127.43,

127.29, 127.25, 125.68, 114.19, 114.17, 110.84, 110.78, 85.64, 82.48, 82.34, 80.95, 80.90, 80.57, 79.39, 76.30, 76.00, 73.39, 73.34, 72.38, 72.12, 71.93, 71.71, 71.28, 71.23, 70.57, 63.21, 63.06, 55.38, 55.31, 37.77, 37.47, 14.80. HRMS (ESI) calcd. for $C_{50}H_{51}ClO_7Na^+$ $[M+Na]^+$: 821.3221, found: 821.3212.

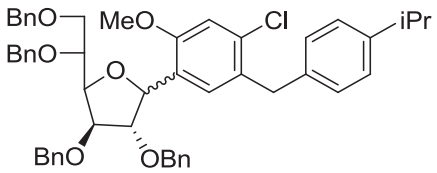

Chemical Formula: $C_{51}H_{53}ClO_6$
Exact Mass: 796.3531
Molecular Weight: 797.4159

1,4-Anhydro-2,3,5,6-tetra-*O*-benzyl-1-*C*-[4-chloro-5-(4-isopropylbenzyl)-2-methoxyphenyl]-D- glucitol (56h)

Crude **55h** was prepared according to the method described for the synthesis of crude **55d** using **50h** (182 mg, 0.51 mmol) and **46** (220 mg, 0.41 mmol) as starting materials.

Compound **56h** (127 mg, 0.16 mmol, 40% yield over 2 steps) as a yellow oil which comprised of a mixture of 1:3 anomers was prepared according to the procedure of the synthesis of **56d** using crude **55h** as a starting material. ^{1}H-NMR (400 MHz, $CDCl_3$) δ 8.20-7.78 (m, 2H), 7.64-6.76 (m, 24H), 4.95-4.28 (m, 7H), 4.28-3.50 (m, 13H), 2.91-2.74 (m, 1H), 1.28-1.17 (m, 6H). ^{13}C-NMR (100 MHz, $CDCl_3$) δ 137.13, 134.50, 133.49, 133.26, 130.08, 129.77, 128.96, 128.73, 128.34, 128.22, 128.12, 128.09, 127.61, 127.56, 127.49, 127.34, 126.25, 85.94, 80.96, 80.65, 80.61, 77.20, 76.02, 73.41, 71.35, 71.26, 70.94, 55.43, 33.60, 29.67. HRMS (ESI) calcd. for $C_{51}H_{53}ClO_6Na^+$ $[M+Na]^+$: 819.3423, found 819.3389.

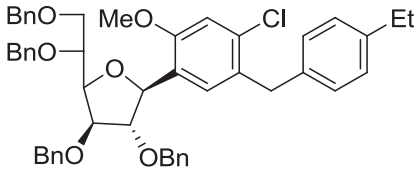

Chemical Formula: $C_{50}H_{51}ClO_6$
Exact Mass: 782.3374
Molecular Weight: 783.3893

(1*S*)-1,4-Anhydro-2,3,5,6-tetra-*O*-benzyl-1-*C*-[4-chloro-5-(4-ethylbenzyl)-2-methoxyphenyl]-D-glucitol (57g)

Crude **55g** was prepared according to the procedure described for the synthesis of crude **55d** using **50g** (273 mg, 0.80 mmol) and **46 (**346 mg, 0.64 mmol) as starting materials.

Crude **56g** which comprised of a mixture of 1:3 anomers was prepared according to the procedure described for the synthesis of **56d** using crude **55g** as a starting material.

Compound **57g** (94.0 mg, 0.12 mmol, 19% yield over 2 steps) was obtained through the purification of crude **56g** (2g silica gel, EA/*n*-hexane = 1/20 to 1/15). ^{1}H-NMR (400 MHz, $CDCl_3$) δ 7.38-7.09 (m, 21H), 6.96-6.86 (m, 4H), 6.83 (s, 1H), 5.25 (s, 1H), 4.76-4.64 (m, 2H), 4.63-4.50 (m, 3H), 4.45 (d, J = 11.3 Hz, 1H), 4.35 (dd, J = 9.3, 3.2 Hz, 1H), 4.18 (s, 2H), 4.05 (d, J = 3.3 Hz, 1H), 3.98-3.88 (m, 3H), 3.85-3.79 (m, 2H), 3.76 (s, 3H), 3.58 (dd, J = 10.7, 5.2 Hz, 1H), 2.48 (q, J = 7.7 Hz, 2H), 1.11 (t, J = 7.6 Hz, 3H). ^{13}C-NMR (100 MHz, $CDCl_3$) δ 154.75, 141.57, 139.08, 138.69, 138.21, 137.97, 137.44, 132.85, 130.44, 130.06, 129.01, 128.42, 128.35, 128.25, 128.19, 128.10, 127.69, 127.64, 127.57, 127.51, 127.49, 127.35, 127.29, 125.72, 125.28, 110.81, 82.53, 80.95,79.43, 77.81, 76.36, 73.43, 72.47, 72.16, 71.97, 71.85, 55.36, 38.25, 28.38, 15.56. HRMS (ESI) calcd. for $C_{50}H_{51}ClO_6Na^+$ $[M+Na]^+$: 805.3266, found: 805.3234.

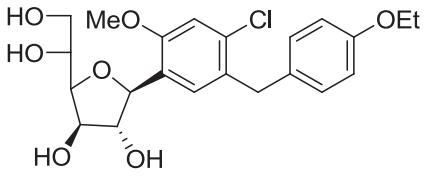

Chemical Formula: $C_{22}H_{27}ClO_7$
Exact Mass: 438.1445
Molecular Weight: 438.8986

(1*S*)-1,4-Anhydro-1-[4-chloro-5-(4-ethoxybenzyl)-2-methoxyphenyl]-D-glucitol (32f)

Compound **57f** (180 mg, 0.22 mmol, 56% yield) was obtained after purification of **56f (**319 mg, 0.40 mmol) with column chromatography (6 g silica gel, EA/*n*-hexane = 1/20 to 1/15).

To the solution of **57f** in CH_2Cl_2 (2 ml), BF_3•OEt_2 (893 μL, 7.04 mmol) and EtSH (318 μL, 4.40 mmol) was added and stirred for 20 h. After the reaction was completed, H_2O was added to quench reaction, the resulting mixture was extracted with CH_2Cl_2 and the aqueous layer was extracted with EA. The combine organic layers was concentrated in vacuo and the resulting oil was purified with column chromatography (2 g silica gel, CH_2Cl_2/d_4-MeOH = 20/1) to obtain **32f** (28.0 mg, 0.064 mmol, 29% yield) as a colorless oil. ^{1}H-NMR (400 MHz, d_4-MeOH) δ 7.32 (d, J =13.5 Hz, 1H), 7.02-6.95 (m, 2H), 6.87 (s, 1H), 6.74-6.67 (m, 2H), 4.25 (dd, J = 13.7, 3.4 Hz, 1H), 4.10-3.84 (m, 7H), 3.77 (s, 2H), 3.75 (s, 3H), 3.58 (q, J =5.4 Hz, 1H), 1.29 (t, J = 7.0 Hz, 3H). ^{13}C-NMR (100 MHz. d_4-MeOH) δ 158.64, 133.75, 133.41, 131.67, 131.44, 130.77, 130.61, 129.53, 126.85, 115.31, 112.09, 82.43, 81.24, 79.77, 78.56, 71.51, 65.55, 64.43, 38.56, 15.20. HRMS (ESI) $C_{22}H_{27}ClO_7Na^+$ $[M+Na]^+$:461.1338, found: 461.1380.

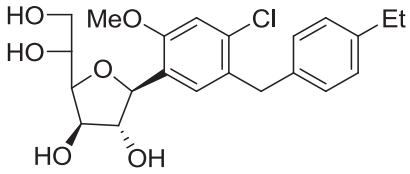

Chemical Formula: $C_{22}H_{27}ClO_6$
Exact Mass: 422.1496
Molecular Weight: 422.8992

(1*S*)-1,4-Anhydro-1-[4-chloro-5-(4-ethylbenzyl)-2-methoxyphenyl]-D-glucitol (32g)

Compound **32g** (4.00 mg, 0.009 mol, 27% yield) was prepared according to the procedure of the synthesis of **32f** using **57g** (15.3 mg, 0.035 mmol) as a starting material. ^{1}H-NMR (400 MHz, d_4-MeOH) δ 7.37 (s, 1H), 7.02-6.97 (m, 4H), 6.87 (s, 1H), 4.90-4.88 (m, 1H), 4.06 (dd, J = 3.0, 1.1 Hz, 1H), 4.03-3.92 (m, 3H), 3.89 (s, 2H), 3.76 (s, 3H), 3.73 (dd, J = 11.7, 3.4 Hz, 1H), 3.57 (dd, J = 11.5, 5.4 Hz, 1H), 2.52 (q, J = 7.7 Hz, 2H), 1.13 (t, J = 7.7 Hz, 3H). ^{13}C-NMR (150 MHz, d_4-MeOH) δ 156.64, 143.05, 138.69, 133.81, 131.51, 130.60, 129.58, 128.72, 112.23, 84.24, 84.46, 82.46, 78.90, 71.32, 65.40, 39.04, 29.44. HRMS (ESI) calcd. for $C_{22}H_{27}ClO_6Na^+$ $[M+Na]^+$: 445.1388, found, 445.1368.

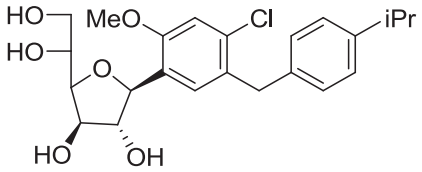

Chemical Formula: $C_{23}H_{29}ClO_6$
Exact Mass: 436.1653
Molecular Weight: 436.9258

(1*S*)-1,4-Anhydro-1-[4-chloro-5-(4-isopropylbenzyl)-2-methoxyphenyl]-D-glucitol (32h)

Compound **57h** (68.9 mg, 0.086 mmol, 54% yield) was obtained after purification of **56h (**127 mg, 0.16 mmol) with column chromatography (6 g silica gel, EA/toluene/*n*-hexane = 1/1/20 to 1/1/15).

Compound **32h** (17mg, 0.039 mmol, 45% yield was prepared according to the procedure of the synthesis of **32f** using **57h** as a starting material. ^{1}H-NMR (600 MHz, d_4-MeOH) δ 7.06-7.00 (m, 4H), 6.91 (d, J = 1.9 Hz, 1H), 6.76 (s, 1H), 4.49 (s, 1H), 3.96-3.92 (m ,1H), 3.77 (s, 3H), 3.72 (s, 3H), 3.67 (dd, J = 11.1, 3.4 Hz, 1H), 3.64-3.58 (m, 3H), 3.57 (dd, J = 7.6, 1.7 Hz, 1H), 3.52 (dd, J = 11.3, 5.7 Hz, 1H), 2.81-2.74 (m, 1H), 1.15 (d, J = 6.9 Hz, 6H). ^{13}C-NMR (150 MHz, d_4-MeOH) δ 157.65, 147.70, 140.74, 134.91, 133.21, 129.89, 129.87, 129.05, 128.11, 127.46, 111.63, 84.40, 82.59, 79.09, 71.52, 65.64, 64.51, 36.03, 35.13, 24.66. HRMS (ESI) calcd. for $C_{23}H_{29}ClO_6Na^+$ $[M+Na]^+$: 459.1550, found, 459.1548.

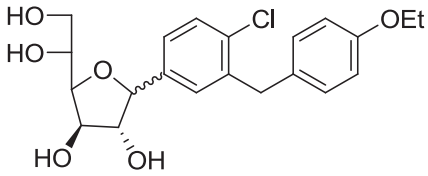

Chemical Formula: $C_{21}H_{25}ClO_6$
Exact Mass: 408.1340
Molecular Weight: 408.8726

1,4-Anhydro-2,3,5,6-tetra-*O*-benzyl-1-[4-chloro-3-(4-ethoxybenzyl)phenyl]-D-glucitol (58a)

Compound **58a** (19 mg, 0.046 mmol, 43% yield) was prepared according to the procedure of the synthesis of **32f** using **56a** (84 mg, 0.11 mmol) as a starting material. ^{1}H-NMR (400 MHz, d_4-MeOH) δ 7.31-7.19 (m, 3H), 7.04-6.99 (m, 2H), 6.77-6.71 (m, 2H), 4.51 (d, J = 3.8 Hz, 1H), 4.16-.411 (m, 1H), 3.99-3.91 (m, 6H), 3.87 (dd, J = 3.8, 2.1 Hz, 1H), 3.75 (dd, J = 11.4, 3.0 Hz, 1H), 3.60 (dd, J = 11.4, 5.2 Hz, 1H), 1.30 (t, J = 7.1 Hz, 3H). ^{13}C-NMR (100 MHz, d_4-MeOH) δ 158.86, 133.85, 132.85, 131.09, 130.83, 130.81, 130.25, 130.16, 126.77, 115.47, 88.15, 86.10, 82.35, 79.50, 71.41, 65.23, 64.45, 39.22, 15.19. HRMS (ESI) calcd. for $C_{21}H_{25}ClO_6Na^+$ $[M+Na]^+$: 431.1232, found: 431.1228.

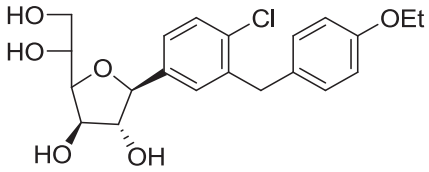

Chemical Formula: $C_{21}H_{25}ClO_6$
Exact Mass: 408.1340
Molecular Weight: 408.8726

(1*S*)-1,4-Anhydro-1-[4-chloro-3-(4-ethoxybenzyl)phenyl]-D-glucitol (32a)

To the solution of **58a** (19 mg, 0.046 mmol) in pyridine (1 mL), Ac_2O (100 μL, 1.06 mmol) and DMAP (1mg, 0.010 mmol) were added and the resulting mixture was stirred at ambient temperature for 3 h. After the reaction was completed, H_2O was added to quench reaction and the resulting mixture was extracted with EA. The organic layer was then was with 1.0 N HCl, 1.0 N NaOH, H_2O and brine and concentrated in vacuo. The resulting oil was purified by column chromatography (500 mg silica gel, EA/*n*-hexane = 1/2 to 1/1) to afford **34a** (17 mg, 0.029 mmol, 66% yield) as a white solid.

To the solution of **34a** in MeOH (2 mL) was added NaOMe (3 mg) and the resulting mixture was stirred at ambient temperature for 3 h. After the reaction was completed, the resulting mixture was extracted with EA and the organic layer was washed with 1.0 N HCl, $NaHCO_3$, H_2O and brine. The resulting solid was purified with column chromatography (200 mg silica gel, MeOH/CH_2Cl_2 = 1/10) to obtain **5a** (12.0 mg, 0.029 mmol, 97% yield) as a colorless oil. ^{1}H-NMR (400 MHz, d_4-MeOH) δ 7.29-7.18 (m, 3H), 7.04-6.98 (m, 2H), 6.77-6.71 (m, 2H), 4.51 (d, J = 3.8 Hz, 1H), 4.11 (q, J = 1.7 Hz, 1H), 3.99-3.89 (m, 6H), 3.87 (dd, J = 3.7, 1.7 Hz, 1H), 3.77-3.72 (m, 1H), 3.59 (dd, J = 11.4, 5.4 Hz, 1H), 1.29 (t, J = 7.0 Hz, 3H). ^{13}C-NMR (150 MHz, d_4-MeOH) δ 159.01, 141.55, 140.25, 134.00, 133.01, 130.99, 130.40, 130.32, 126.93, 115.63, 88.30, 86.25, 82.51, 79.66, 71.57, 65.38, 64.61, 39.37, 15.34. HRMS (ESI) calcd. for $C_{21}H_{25}ClO_6Na^+$ $[M+Na]^+$: 431.1232, found: 431.1231.

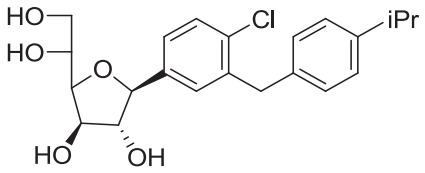

Chemical Formula: $C_{22}H_{27}ClO_5$
Exact Mass: 406.1547
Molecular Weight: 406.8998

(1*S*)-1,4-Anhydro-1-[4-chloro-3-(4-isopropylbenzyl)phenyl]-D-glucitol (32b)

Crude **58b** (19 mg, 0.046 mmol, 42% yield) was prepared according to the procedure described for the synthesis of **32f** using **56b** (159 mg, 0.206 mmol) as a starting material.

Crude **59b** was prepared according to the procedure described the synthesis of **59a** using crude **58b** as a starting material

Compound **32b** (3 mg, 0.007 mmol, 15% yield over 3 steps) was prepared according to the procedure described for the synthesis of **32a** using crude **59b** as a starting material. ^{1}H-NMR (400 MHz, d_4-MeOH) δ 7.30-7.19 (m, 2H), 7.08-7.00 (m, 5H), 4.50 (d, J = 3.8 Hz, 1H), 4.11 (q, J = 1.8 Hz, 1H), 4.04-3.89 (m, 3H), 3.86 (dd, J = 3.7, 1.5 Hz, 1H), 3.82 (s, 1H), 3.74 (dd, J = 11.3, 3.0 Hz, 1H), 3.58-3.54 (m, 1H). ^{13}C-NMR (100 MHz, d_4-MeOH) δ 141.40, 140.39, 130.37, 130.19, 129.83, 129.80, 127.39, 127.36, 126.85, 88.16, 86.13, 82.35, 79.52, 74.34, 71.41, 42.45, 35.01, 24.49. HRMS (ESI) calcd. for $C_{22}H_{27}ClO_5Na^+$ $[M+Na]^+$: 429.1439, found: 429.1456.

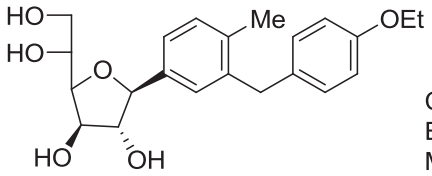

Chemical Formula: $C_{22}H_{28}O_6$
Exact Mass: 388.1886
Molecular Weight: 388.4541

(1*S*)-1,4-Anhydro-1-[3-(4-ethoxybenzyl)-4-methylphenyl]-D-glucitol (32c)

Compound **55c** (588 mg, 0.77 mmol, 45% yield) as a colorless oil was prepared according to the procedure described for the synthesis of **55d** using **50c** (522 mg, 1.71 mmol) and **22** (921 mg, 1.71 mmol) as starting materials.

Compound **56c** (414 mg, 0.55 mmol, 71.8% yield) as a colorless oil was prepared according to the procedure of the synthesis of **55d** using **55c** (588 mg, 0.77 mmol) as a starting material.

Compound **58c** (97.0 mg, 0.25 mmol, 46% yield) as a colorless oil was prepared according to the procedure described for the synthesis of **32f** using **56c** as a starting material.

Compound **59c** (93.5 mg, 0.17 mmol, 68% yield) was prepared according to the procedure described for the synthesis of **59a** using **58c** as a starting material.

Compound **32c** (62.4 mg, 0.16 mmol, 94% yield) was prepared according to the procedure described for the synthesis of **32a** using **59c** as a starting material. ^{1}H-NMR (400 MHz, d_4-MeOH) δ 7.17-7.10 (m, 2H), 7.05-6.99 (m, 1H), 6.96-6.89 (m. 2H), 6.73-6.67 (m, 2H), 4.48 (d, J = 4.2 Hz, 1H), 4.14 (dd, J = 3.8, 1.8 Hz, 1H), 4.01-3.94 (m, 1H), 3.94-3.86 (m, 4H), 3.82 (s, 2H), 3.76 (dd, J = 11.5, 3.3 Hz, 1H), 3.59 (dd, J = 11.5, 5.9 Hz, 1H), 2.09 (s, 3H), 1.27 (t, J = 7.0 Hz, 3H). ^{13}C-NMR (150 MHz, d_4-MeOH) δ 158.69, 140,62, 139.63, 137.05, 133.90,131.25, 130.72, 129.37, 125.70, 115.54, 88.74, 86.31, 82.23, 79.86, 71.60, 65.31, 64.63, 39.71, 19.58, 15.34. HRMS (ESI) calcd. for $C_{22}H_{28}O_6Na^+$ $[M+Na]^+$: 411.1778,

411.1775.

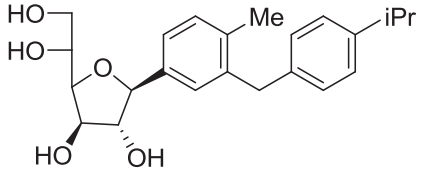

Chemical Formula: $C_{23}H_{30}O_5$
Exact Mass: 386.2093
Molecular Weight: 386.4813

(1*S*)-1,4-Anhydro-1-[3-(4-isopropylbenzyl)-4-methylphenyl]-D-glucitol (32d)

Compound **58d** (16.6 mg, 0.043 mmol, 43% yield) as a colorless oil was prepared according to the procedure described for the synthesis of **32f** using **56d** as a starting material.

Compound **59d** (15.0 mg, 0.027 mmol, 63% yield) was prepared according to the procedure described for the synthesis of **59a** using **58d** as a starting material.

Compound **32d** (10.0 mg, 0.026 mmol, 95% yield) was prepared according to the procedure described for the synthesis of **32a** using **59d** (75mg, 0.10 mmol) as a starting material. ^{1}H-NMR (400 MHz, d_4-MeOH) δ 7.22-7.03 (m, 2H), 7.03-6.90 (m, 5H), 4.78 (d, J = 4.2 Hz, 1H), 4.13 (q, J = 1.9 Hz, 1H), 4.02-3.94 (m, 1H), 3.93-3.87 (m, 2H), 3.81-3.86 (m, 2H), 3.76 (dd, J = 11.2, 3.2 Hz, 1H), 3.59 (dd, J = 11.5, 6.2 Hz, 1H), 2.79-2.69 (m, 1H), 2.09 (s, 3H), 1.13 (d, J = 6.9 Hz, 6H). ^{13}C-NMR (100 MHz, d_4-MeOH) δ 147.55, 140.25, 139.56, 139.14, 131.10, 129.59, 127.25, 125.61, 88.64, 86.22, 82.10, 79.76, 71.49, 65.22, 40.04, 34.95, 24.50, 19.47. HRMS (ESI) calcd. for $C_{23}H_{30}O_5Na^+$ $[M+Na]^+$: 409.1985, found: 409.1999.

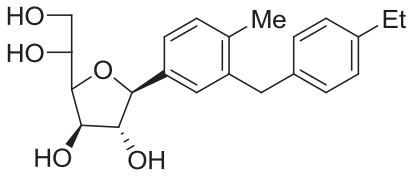

Chemical Formula: $C_{22}H_{28}O_5$
Exact Mass: 372.1937
Molecular Weight: 372.4547

(1*S*)-1,4-Anhydro-1-[3-(4-ethylbenzyl)-4-methylphenyl]-D-glucitol (32e)

Compound **55e** (450 mg, 0.59 mmol, 80% yield) as a colorless oil was prepared according to the procedure described for the synthesis of **55d** using **50e** (215 mg, 0.74 mmol) and **46 (**320 mg, 0.59 mmol) as starting materials.

Compound **56e** (235 mg, 0.32 mmol, 55% yield) as a colorless oil was prepared according to the procedure of the synthesis of **56d** using **55e** as a starting material.

Compound **58e** (50.0 mg, 0.13 mmol, 42% yield) as a colorless oil was prepared according to the procedure described for the synthesis of **32f** using **56e** as a starting material.

Compound **59e** (44.0 mg, 0.081 mmol, 61% yield) was prepared according to the procedure described for the synthesis of **59a** using **58e** as a starting material.

Compound **32e** (29.0 mg, 0.078 mmol, 96% yield) was prepared according to the procedure described for the synthesis of **32a** using **59e** as a starting material. ^{1}H-NMR (400 MHz, d_4-MeOH) δ 7.20-7.13 (m, 2H), 7.05-6.98 (m, 3H), 6.97-6.92 (m, 2H), 4.48 (d, J = 4.2 Hz, 1H), 4.13 (dd, J = 3.9, 1.8 Hz, 1H), 4.00-3.95 (m ,1H), 3.94-3.90 (m, 1H), 3.87 (s, 2H), 3.76 (dd, J = 11.3, 3.4 Hz, 1H), 3.60 (dd, J = 11.5, 5.9 Hz, 1H), 2.51 (q, J = 7.6 Hz, 2H), 2.11 (s, 3H), 1.12 (t, J = 7.5 Hz, 3H). ^{13}C-NMR (150 MHz, d_4-MeOH) δ 142.97, 140.29, 139.60, 139.03, 136.95, 131.10,, 129.64,129.36, 128.75, 125.62, 88.68, 86.25, 82.15, 79.80, 71.53, 65.25, 40.07, 29.42, 19.45, 16.23. HRMS (ESI) calcd. for $C_{22}H_{28}O_5$ $[M+Na]^+$: 395.1829, 395.1827.

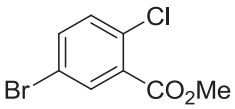

Chemical Formula: $C_8H_6BrClO_2$
Exact Mass: 247.9240
Molecular Weight: 249.4890

Methyl 5-bromo-2-chlorobenzoate (59)

To the solution of 5-bromo-2-chlorobenzoic acid (23.6 g, 0.10 mol) and K_2CO_3 (13.8 g**,** 0.10 mol) in DMF (50 mL), MeI (17.7 g, 0.13 mol) was added and the resulting suspension was stirred for 3h at rt. After the reaction was completed, ice was added to quench reaction and the resulting mixture was extracted with EA (2x). The conbined organic layers were washed with brine, dried over $MgSO_4$ filtered and concentrated in vacuo to obtain crude **35** (24.5 g, 0.098 mol, 98% yield). ^{1}H-NMR (400 MHz, $CDCl_3$) δ 7.87 (d, J = 2.4 Hz, 1H), 7.44 (dd, J = 8., 2.5 Hz, 1H), 7.23 (d, J = 8.5 Hz, 1H), 3.86 (s, 3H).

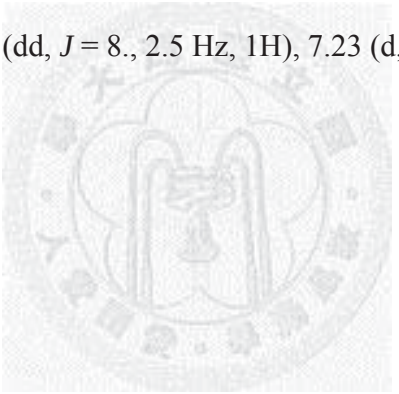

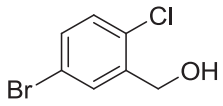

Chemical Formula: C_7H_6BrClO
Exact Mass: 219.9291
Molecular Weight: 221.4789

(5-Bromo-2-chlorophenyl)methanol (60)

To the solution of **59** (24.5 g, 0.098 mol) in toluene (100 mL), $LiAlH_4$ (4.10 g, 0.11 mol) was added at 0 °C and the resulting mixture was returned to room temperature and stirred for 2 h. After the reaction was completed, H_2O was added to quench reaction and the resulting mixture was extracted with EA. The organic layer was washed with 1.0 N NaOH, H_2O and brine and concentrated to yield **60** (20.0 g, 0.090 mol, 92% yield) as a white solid. mp: 70 ºC. ^{1}H-NMR (400 MHz, $CDCl_3$) δ 7.62 (d, J = 2.3 Hz, 1H), 7.32 (dd, J = 8.4, 2.5 Hz, 1H), 7.18 (d, J = 8.4 Hz, 1H), 4.71 (s, 2H).

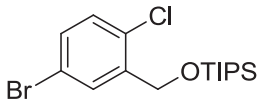

Chemical Formula: $C_{16}H_{26}BrClOSi$
Exact Mass: 376.0625
Molecular Weight: 377.8195

(5-Bromo-2-chlorobenzyloxy)triisopropylsilane (61)

To the solution of **60** (17.0 g, 76.8 mmol) in DMF (50 mL), imidazole (10.5 g, 154 mmol), DMAP (470 mg, 3.80 mmol) and TIPSCl (20.2 mL, 94.4 mmol). The resulting mixture was stirred at ambient temperature for 12 h. After the reaction was completed, the reaction was quenched with NH_4Cl and extracted with EA. The organic layer was then washed with H_2O and brine, dried over $MgSO_4$, filtered and concentrated in vacuo to afford **61** (23.5 g, 62.3 mmol, 81% yield) as a colorless oil. ^{1}H-NMR (400 MHz, $CDCl_3$) δ 7.81-7.74 (m, 1H), 7.30 (dd, J = 8.4, 2.4 Hz, 1H), 7.14 (d, J = 8.4 Hz, 1H), 4.84 (s, 2H), 1.15-1.04 (m, 21H).

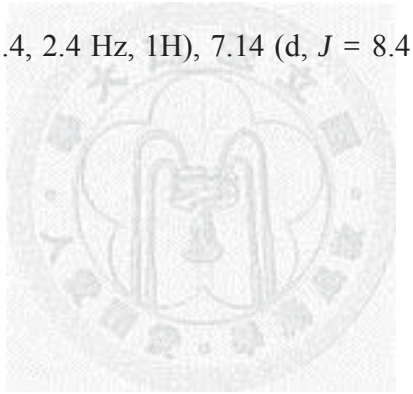

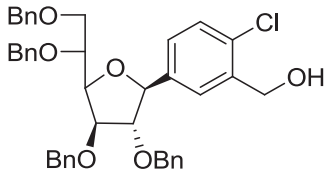

Chemical Formula: $C_{41}H_{41}ClO_6$
Exact Mass: 664.2592
Molecular Weight: 665.2136

(1*S*)-1,4-Anhydro-2,3,5,6-tetra-*O*-benzyl-1-*C*-[(4-chloro-3-hydroxymethyl)-phenyl]-D-glucitol (64)

Crude **62** as yellow oil was prepared according to the procedure described for the synthesis of **56f** using **61** (6.44 g, 17.0 mmol) and **46** (7.35 g, 13.6 mmol) as starting materials.

To the solution of crude **62** in CH_2Cl_2 (10 mL) at -50 °C, was added Et_3SiH (4 mL, 25.0 mmol), followed by BF_3•OEt_2 (3.2 mL, 27.5 mmol) slowly to maintain the temperature below -40 °C. The resulting suspension was allowed to warm to -10 °C over 1 h prior to quenching with K_2CO_3. After concentrated in vacuo, the resulting mixture was extracted with EA and washed with brine, dried over $MgSO_4$, filtered and concentrated to afford crude **63** as a yellow oil.

To the solution of crude **63** in THF (10 mL) was added TBAF (1.0 M in THF, 17.0 mL, 17.0 mmol) and the reaction mixture was stirred at ambient temperature for 2 h. After removal of organic volatiles under reduced pressure, the residue was extracted twice between EA and NH_4Cl. The combined organic layers were then washed with brine, dried over $MgSO_4$, filtered and purified with column chromatography (200 g silica gel, EA/toluene/*n*-hexane = 1/1/8) to afford 6**4** (4.0 g, 6.01 mmol, 44% yield over 3 steps) as a colorless oil. ^{1}H-NMR (400 MHz, $CDCl_3$) δ 7.59-7.28 (m, 21H), 7.25-7.14 (m, 2H), 5.01 (d, J = 2.6, 1H), 4.94 (d, J = 11.3 Hz, 1H), 4.79-4.56 (m, 7H), 4.54-4.39 (m, 3H), 4.37-4.31 (m, 1H), 4.27 (d, J = 3.2 Hz, 1H), 4.13-4.02 (m, 2H), 3.87 (dd, J = 5.6, 10.6 Hz, 1H). ^{13}C-NMR

(100 MHz, $CDCl_3$) δ 139.77, 138.73, 138.37, 138.02, 137.54, 137.39, 131.31, 128.93, 128.35, 128.16, 128.14, 127.77, 127.56, 127.50, 127.48, 127.46, 127.30, 126.65, 126.56, 88.41, 85.95, 82.37, 80.87, 75.85, 73.30, 72.54, 71.69, 71.20, 71.06, 62.40.

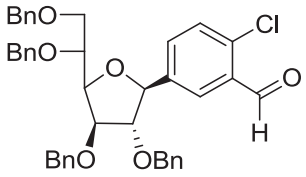

Chemical Formula: $C_{41}H_{39}ClO_6$
Exact Mass: 662.2435
Molecular Weight: 663.1978

(1*S*)-1,4-Anhydro-2,3,5,6-tetra-O-benzyl-1-C-(4-chloro-3-oxomethylphenyl)-D-glucitol (65)

Compound **65** (3.47 g, 5.23 mmol, 87% yield) was prepared according to the procedure described for the synthesis of **46** using **64** (4.0 g, 6.01 mmol) as a starting material. ^{1}H-NMR (400 MHz, $CDCl_3$) δ 7.93-7.76 (m, 1H), 7.55 (dd, J = 8.2, 1.6 Hz, 1H), 7.45-7.15 (m, 19H), 7.11-6.83 (m, 2H), 5.02-4.79 (m, 2H), 4.71-4.45 (m, 5H), 4.38 (s, 1H), 4.35 (dd, J = 9.1, 3.2 Hz, 1H), 4.30-4.20 (m, 1H), 4.20-3.87 (m, 4H), 3.79 (dd, J = 10.7, 5.5 Hz, 1H). ^{13}C-NMR (100 MHz, $CDCl_3$) δ 189.54, 140.68, 138.77, 138.46, 137.47, 137.28, 136.52, 133.15, 132.01, 130.44, 128.51, 128.46, 128.27, 128.25, 128.23, 127.98, 127.65, 127.62, 127.59, 127.56 127.46, 127.42, 127.11, 88.29, 85.35, 82.27, 81.12, 75.88, 73.44, 72.61, 71.88, 71.49, 71.00. HRMS (ESI) calcd. for $C_{41}H_{39}ClO_6$ $[M+Na]^+$: 685.2333, found : 685.2288.

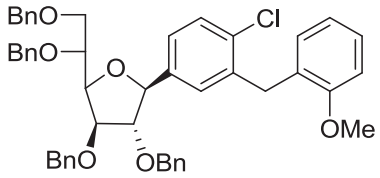

Chemical Formula: $C_{48}H_{47}ClO_6$
Exact Mass: 754.3061
Molecular Weight: 755.3362

(1*S*)-1,4-Anhydro-2,3,5,6-tetra-*O*-benzyl-1-*C*-[4-chloro-3-(2-methoxybenzyl)-phenyl]-D-glucitol (57i)

To the solution of **65** (150 mg, 0.23 mmol) in anhydrous THF (2 mL) under N_2 atmosphere was added a solution of 2-methoxyphenylmagnesium bromide (0.80 mL, 0.80 mmol, 1.0 M in THF) drop wisely at -78℃. After stirring for 2.5 h under -78 ℃, NH_4Cl was added to quench reaction and the resulting mixture was extracted with CH_2Cl_2. The organic phase was removed under reduced pressure and co-evaporated with toluene twice to afford crude **55i**.

Compound **57i** (145 mg, 0.19 mmol, 83% yield over 2 steps) as a colorless oil was prepared according to the procedure described for the synthesis of **56d** using crude **55i** as a starting material. ^{1}H-NMR (400 MHz, $CDCl_3$) δ 7.50-7.23 (m, 22H), 7.18-7.10 (m, 2H), 7.07-7.01 (m, 1H), 6.97-.689 (m, 2H), 4.97 (d, J = 2.7 Hz, 1H), 4.94 (d, J = 11.6 Hz, 1H), 4.74-4.65 (m, 2H), 4.65 (d, J = 11.6 Hz, 1H), 4.58 (s, 2H), 4.50-4.42 (m, 2H), 4.40 (dd, J = 9.1, 3.4 Hz, 1H), 4.28-4.23 (m, 2H), 4.18 (s, 2H), 4.07- 4.01 (m, 2H), 3.87-3.80 (m, 4H). ^{13}C-NMR (100 MHz, $CDCl_3$) δ 157.33, 139.44, 138.85, 138.51, 137.94, 137.58, 137.43, 133.12, 130.01, 129.04, 128.96, 128.36, 128.17, 128.15, 127.77, 127.63, 127.52, 127.47, 127.30, 125.30, 120.31, 110.11, 88.51, 85.85, 82.45, 80.80, 75.86, 73.31, 72.51, 71.59, 71.24, 71.04, 55.10, 33.28. HRMS (ESI) calcd. for $C_{48}H_{47}ClO_6$ $[M+Na]^+$: 777.2953, found: 777.2928

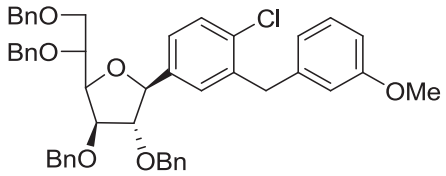

Chemical Formula: $C_{48}H_{47}ClO_6$
Exact Mass: 754.3061
Molecular Weight: 755.3362

(1*S*)-1,4-Anhydro-2,3,5,6-tetra-*O*-benzyl-1-*C*-[4-chloro-3-(3-methoxybenzyl)-phenyl]-D- glucitol (57j)

Crude **55j** was prepared according to the procedure described for the synthesis of **55i** using **65** (150 mg, 0.23 mmol) and 3-methoxyphenylmagnesium bromide (0.80 mL, 0.80 mmol, 1.0 M in THF).

Compound **57j** (33 mg, 0.044 mmol, 19% yield over 2 steps) as a colorless oil was prepared according to the procedure described for the synthesis of **56d** using crude **55j** as a starting material. ^{1}H-NMR (400 MHz, $CDCl_3$) δ 7.38-7.11 (m, 22H), 7.04-6.98 (m, 2H), 6.74-6.67 (m, 3H), 4.84 (d, J = 2.6 Hz, 1H), 4.81 (d, J = 11.4 Hz, 1H), 4.63-4.42 (m, 5H), 4.39-4.30 (m, 2H), 4.26 (dd, J = 9.1, 3.4 Hz, 1H), 4.15-4.09 (m, 2H), 4.01 (s, 2H), 3.95-3.88 (m, 2H), 3.72 (dd, J = 11.0, 5.2 Hz, 1H), 3.69 (s, 3H). ^{13}C-NMR (100 MHz, $CDCl_3$) δ 159.67, 141.00, 139.78, 138.95, 138.62, 138.14, 137.68, 137.52, 133.02, 129.32, 129.09, 128.47, 128.26, 128.24, 127.88, 127.64, 127.60, 127.58, 127.56, 127.39, 125.70, 121.31, 114.82, 111.41, 88.59, 85.88, 82.49, 80.94, 76.01, 73.42, 72.60, 71.77, 71.37, 71.12, 55.03, 39.18, 29.68. HRMS [ESI] calcd. for $C_{48}H_{47}ClO_6$ $[M+Na]^+$: 777.2953, found: 777.2914.

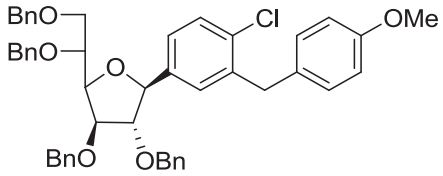

Chemical Formula: $C_{48}H_{47}ClO_6$
Exact Mass: 754.3061
Molecular Weight: 755.3362

(1*S*)-1,4-Anhydro-2,3,5,6-tetra-*O*-benzyl-1-*C*-[4-chloro-3-(4-methoxybenzyl)-phenyl]-D-glucitol (57k)

Crude **55k** was prepared according to the procedure described for the synthesis of **55i** using **65** (150 mg, 0.23 mmol) and 4-methoxyphenylmagnesium bromide (1.60 mL, 0.80 mmol, 0.5 M in THF).

Compound **57k** (138 mg, 0.18 mmol, 79% yield over 2 steps) a yellowish oil was prepared according to the procedure described for the synthesis of **56d** using crude **55k** as a starting material. ^{1}H-NMR (400 MHz, $CDCl_3$) δ 7.49-7.29 (m, 18H), 7.28-7.22 (m, 3H), 7.15-7.08 (m, 4H), 6.89-6.83 (m, 2H), 4.97 (d, J = 2.6 Hz, 1H), 4.93 (d, J = 11.4 Hz, 1H), 4.69 (d, J = 2.1 Hz, 2H), 4.64 (d, J = 11.6 Hz, 1H), 4.62-4.52 (m, 2H), 4.45 (d, J = 3.0 Hz, 2H), 4.41 (dd, J = 9.0, 3.4 Hz, 1H), 4.27-4.21 (m, 2H), 4.09.4.00 (m, 4H), 3.83 (dd, J = 10.6, 5.6 Hz, 1H), 3.78 (s, 3H). ^{13}C-NMR (100 MHz, $CDCl_3$) δ 157.91, 139.68, 138.88, 138.71, 138.52, 137.60, 137.45, 132.81, 131.31, 129.80, 129.17, 128.86, 128.37, 128.17, 128.15, 127.79, 127.55, 127.49, 127.45, 127.30, 127.28, 125.43, 113.73, 88.46, 85.76, 82.43, 80.86, 77.20, 75.92, 73.32, 72.47, 71.64, 71.26, 70.96, 54.99, 38.23. HRMS (ESI) calcd. for $C_{48}H_{47}ClO_6$ $[M+Na]^+$: 777.2953, found: 777.2903

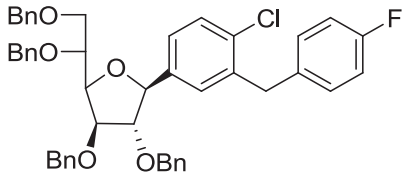

Chemical Formula: $C_{47}H_{44}ClFO_5$
Exact Mass: 742.2861
Molecular Weight: 743.3007

(1*S*)-1,4-Anhydro-2,3,5,6-tetra-*O*-benzyl-1-*C*-[4-chloro-3-(4-fluorobenzyl)-phenyl]-D-glucitol (57l)

Crude **55l** was prepared according to the procedure described for the synthesis of **55i** using **65** (150 mg, 0.23 mmol) and 4-fluorophenylmagnesium bromide (0.80 mL, 0.80 mmol, 1.0 M in THF).

Compound **57l** (134 mg, 0.18 mmol, 78% yield over 2 steps) as a colorless oil was prepared according to the procedure described for the synthesis of **56d** using crude **55l** as a starting material. ^{1}H-NMR (400 MHz, $CDCl_3$) δ 7.24-7.19 (m, 20H), 7.17 (d, J = 2.0 Hz, 1H), 7.10-7.02 (m, 4H), 6.96-6.89 (m, 2H), 4.91 (d, J = 2.5 Hz, 1H), 4.88 (d, J = 11.4 Hz, 1H), 4.64 (s, 2H), 4.61-4.49 (m, 3H), 4.40 (s, 2H), 4.34 (dd, J = 9.1, 3.4 Hz, 1H), 4.18 (d, J = 3.4 Hz, 2H), 4.02 (s, 2H), 3.99 (dd, J = 10.8, 2.0 Hz, 1H), 3.96 (d, J = 2.6 Hz, 1H), 3.77 (dd, J = 10.7, 5.5 Hz, 1H). ^{13}C-NMR (100 MHz, $CDCl_3$) δ 162.57, 160.14, 139.88, 138.89, 138.55, 138.14, 137.63, 137.63, 137.47, 135.03, 135.00, 132.90, 130.29, 130.21, 129.33, 128.92, 128.45, 128.24, 127.89, 127.64, 127.56, 127.54, 127.51, 127.37, 125.75, 115.20, 114.99, 88.50, 85.79, 82.44, 80.96, 75.95, 73.41, 72.56, 71.73, 71.34, 71.07, 38.36. HRMS (ESI) calcd. for $C_{47}H_{44}ClFO_5$ $[M+H]^+$: 743.2940, found: 743.2904.

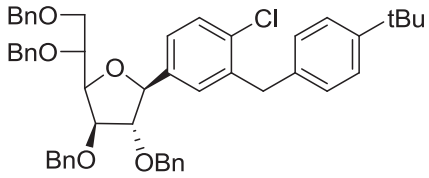

Chemical Formula: $C_{51}H_{53}ClO_5$
Exact Mass: 780.3582
Molecular Weight: 781.4165

(1*S*)-1,4-Anhydro-2,3,5,6-tetra-*O*-benzyl-1-*C*-[4-chloro-3-(4-*tert*-butylbenzyl)-phenyl]-D-glucitol (57m)

Crude **55m** was prepared according to the procedure described for the synthesis of **55i** using **65** (150 mg, 0.23 mmol) and 4-*tert*-butylphenylmagnesium bromide (1.60 mL, 0.80 mmol, 0.5 M in THF).

Compound **57m** (125 mg, 0.16 mmol, 70% yield over 2 steps) as a colorless oil was prepared according to the procedure described for the synthesis of **56d** using crude **55m** as a starting material. ^{1}H-NMR (400 MHz, $CDCl_3$) δ 7.47-7.20 (m, 23H), 7.14-7.06 (m, 4H), 4.92-4.84 (m, 2H), 4.66-4.56 (m, 3H), 4.55-4.47 (m, 2H), 4.45-4.36 (m, 2H), 4.32 (dd, J = 9.0, 3.4 Hz, 1H), 4.25-4.19 (m, 1H), 4.18 (d, J = 3.4 Hz, 1H), 4.06 (s, 2H), 3.99 (dd, J = 10.8, 1.9 Hz, 1H), 3.95 (d, J = 2.8 Hz,), 3.77 (dd, J = 10.6, 5.6 Hz, 1H), 1.31 (s, 9H). ^{13}C-NMR (100 MHz, $CDCl_3$) δ 148.85, 139.70, 138.87, 138.54, 138.44, 137.64, 137.48, 136.33, 133.05, 129.33, 129.12, 128.44, 128.41, 128.25, 128.23, 128.22, 127.86, 127.60, 127.55, 127.54, 127.37, 125.66, 125.23, 85.54, 85.94, 82.49, 80.89, 75.95, 73.39, 72.60, 71.72, 71.30, 71.10, 38.63, 34.28, 31.32. HRMS (ESI) calcd. for $C_{51}H_{53}ClO_5$ $[M+Na]^+$: 803.3474, found: 803.3442.

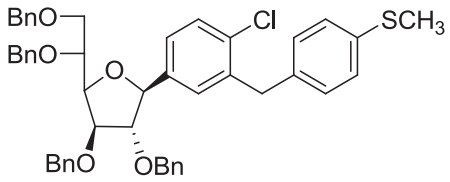

Chemical Formula: $C_{48}H_{47}ClO_5S$
Exact Mass: 770.2833
Molecular Weight: 771.4018

(1*S*)-1,4-Anhydro-2,3,5,6-tetra-*O*-benzyl-1-*C*-[4-chloro-3-(4-methylthiobenzyl)-phenyl]-D-glucitol (57n)

Crude **55n** was prepared according to the procedure described for the synthesis of **55i** using **65** (150 mg, 0.23 mmol) and 4-thioanisolemagnesium bromide (1.60 mL, 0.80 mmol, 0.5 M in THF).

Compound **57n** (102 mg, 0.13 mmol, 58% yield over 2 steps) was prepared according to the procedure described for the synthesis of **56d** using crude **55n** as a starting material. ^{1}H-NMR (400 MHz, $CDCl_3$) δ 7.44-7.27 (m, 19H), 7.25-7.15 (m, 4H), 7.10-7.05 (m, 4H), 4.94 (d, J = 2.5 Hz, 1H), 4.90 (d, J = 11.5 Hz, 1H), 4.66 (d, J = 1.5 Hz, 2H), 4.63-4.54 (m, 3H), 4.41 (d, J = 2.4 Hz, 2H), 4.37 (dd, J = 9.0, 3.3 Hz, 1H), 4.22-4.16 (m, 2H), 4.04 (s, 2H), 4.01 (dd, J = 10.7, 1.9 Hz, 1H), 3.98 (d, J = 2.5 Hz, 1H), 3.78 (dd, J = 10.7, 5.5 Hz, 1H), 2.44 (s, 3H). ^{13}C-NMR (100 MHz, $CDCl_3$) δ 139.76, 138.84, 138.51, 138.12, 137.58, 137.42, 136.27, 135.81, 132.86, 129.33, 129.92, 128.40, 128.19, 127.82, 127.58, 127.51, 127.49, 127.48, 127.31, 126.78, 125.61, 88.42, 85.74, 82.36, 80.84, 75.91, 73.33, 72.46, 71.65, 71.27, 70.86, 38.57, 15.89. HRMS (ESI) calcd. for $C_{48}H_{47}ClO_5S$ $[M+H]^+$: 771.2905, found: 771.2879.

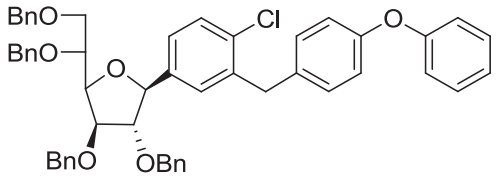

Chemical Formula: $C_{53}H_{49}ClO_6$
Exact Mass: 816.3218
Molecular Weight: 817.4056

(1*S*)-1,4-Anhydro-2,3,5,6-tetra-*O*-benzyl-1-*C*-[4-chloro-3-(4-phenoxybenzyl)-phenyl]-D-glucitol (57o)

Crude **55o** was prepared according to the procedure described for the synthesis of **55i** using **65** (150 mg, 0.23 mmol) and 4-phenoxyphenylmagnesium bromide (1.6 mL, 0.80 mmol, 0.5 M in THF).

Compound **57o** (131 mg, 0.16 mmol, 70% yield over 2 steps) as a yellowish oil was prepared according to the procedure described for the synthesis of **56d** using crude **55o** as a starting material. ^{1}H-NMR (400 MHz, $CDCl_3$) δ 4.48-7.27 (m, 20 H), 7.20-7.04 (m, 9H), 7.00-6.95 (m, 2H), 5.00 (d, J = 2.4 Hz, 1H), 4.95 (d, J = 11.4 Hz, 1H), 4.72-4.55 (m, 5H), 4.49-4.37 (m, 3H), 4.31-4.21 (m, 2H), 4.11 (s, 2H), 4.08 (dd, J = 10.7, 1.9 Hz, 1H), 4.04 (d, J = 2.7 Hz, 1H), 3.85 (dd, J = 10.6, 5.5 Hz, 1H). ^{13}C-NMR (100 MHz, $CDCl_3$) δ 157.25, 157.14, 155.41, 139.78, 138.83, 138.48, 138.30, 137.56, 137.41, 134.20, 132.89, 130.59, 130.02, 129.62, 129.57, 129.28, 128.96, 128.40, 128.19, 128.17, 127.83, 12758, 127.50, 127.48, 127.32, 125.66, 123.09, 122.95, 118.77, 118.61, 88.43, 85.79, 82.39, 80.87, 75.91, 73.33, 72.50, 71.65, 71.28, 70.95, 38.39. HRMS (ESI) calcd. for $C_{53}H_{49}ClO_6$ $[M+Na]^+$: 839.3110, found: 839.3074.

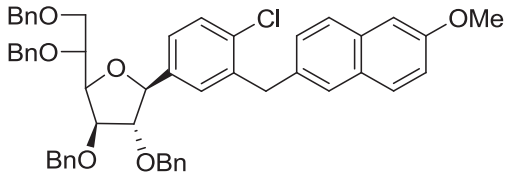

Chemical Formula: $C_{52}H_{49}ClO_6$
Exact Mass: 804.3218
Molecular Weight: 805.3949

(1*S*)-1,4-Anhydro-2,3,5,6-tetra-*O*-benzyl-1-*C*-[4-chloro-3-(6-methoxy-naphtha-len-2-yl)methyl] phenyl]-D-glucitol (57p)

Crude **55p** was prepared according to the procedure described for the synthesis of **55i** using **65** (150 mg, 0.23 mmol) and 6-Methoxy-2-naphthylmagnesium bromide solution (1.6 mL, 0.80 mmol, 0.5 M in THF).

Compound **57p** (120 mg, 0.15 mmol, 65% yield over 2 steps) as a yellowish oil was prepared according to the procedure described for the synthesis of **56d** using crude **55p** as a starting material. ^{1}H-NMR (400 MHz, $CDCl_3$) δ 7.83-7.45 (m, 5H), 7.37-7.25 (m, 13H), 7.23-7.13 (m, 7H), 7.10-6.91 (m, 4H), 4.91 (m, 1H), 4.70-4.64 (m, 1H), 4.60-4.51 (m, 2H), 4.50-4.43 (m, 2H), 4.37-4.23 (m, 3H), 4.09 (dd, J = 8.8, 3.5 Hz, 1H), 4.00-3.92 (m, 2H), 3.92-3.87 (m, 2H), 3.87-3.82 (m, 3H), 3.74-3.63 (n, 1H), 3.40-3.33 (m, 2H). ^{13}C-NMR (100 MHz, $CDCl_3$) δ 157.73, 138.92. 138.61, 137.50, 134.05, 132.11, 129.55, 128.57, 128.48, 128.26, 128.22, 127.87, 127.62, 127.59, 127.52, 127.39, 126.96, 126.61, 126.22, 126.17, 126.04, 125.71, 125.57, 118.79, 105.62, 88.48, 85.74, 82.35, 80.90, 76.03, 73.41, 72.58, 72.47, 71.72, 71.37, 57.14, 29.74. HRMS (ESI) calcd. for $C_{52}H_{49}ClO_6$ $[M+Na]^+$: 827.3110, found: 827.3217.

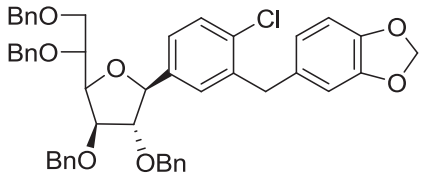

Chemical Formula: $C_{48}H_{45}ClO_7$
Exact Mass: 768.2854
Molecular Weight: 769.3197

(1*S*)-1,4-Anhydro-2,3,5,6-tetra-*O*-benzyl-1-*C*-[4-chloro-3-(3,4-methylenedioxy-benzyl)phenyl]-D-glucitol (57q)

Crude **55q** was prepared according to the procedure described for the synthesis of **55i** using **65** (150 mg, 0.23 mmol) and 3,4-(methylenedioxy)phenylmagnesium bromide (0.8 mL, 0.80 mmol, 1.0 M in THF/toluene = 1/1).

Compound **57q** (106 mg, 0.14 mmol, 60% yield over 2 steps) as a colorless oil was prepared according to the procedure described for the synthesis of **56d** using crude **55q** as a starting material. ^{1}H-NMR (400 MHz, $CDCl_3$) δ 7.41-7.20 (m, 19H), 7.20-7.15 (m, 2H), 7.07-7.02 (m, 2H), 6.69 (d, J = 7.9 Hz, 1H), 6.63-6.56 (m, 2H), 5.85 (dd, J = 5.2, 1.5 Hz, 2H), 4.88 (d, J = 2.6 Hz, 1H), 4.86 (d, J = 11.5 Hz, 1H), 4.62 (d, J = 1.3 Hz, 2H), 4.57 (d, J = 11.6 Hz, 1H), 4.51 (d, J = 7.1 Hz, 2H), 4.43-4.34 (m, 2H), 4.31 (dd, J = 9.0, 3.5 Hz, 1H), 4.20-4.14 (m, 2H), 3.99-3.94 (m, 3H), 3.93 (d, J = 2.6 Hz, 1H), 3.76 (dd, J = 10.8, 5.7 Hz, 1H). ^{13}C-NMR (100 MHz, $CDCl_3$) δ 189.54, 140.68, 138.77, 138.46, 137.47, 137.28, 136.52, 133.15, 132.01, 130.46, 128.51, 128.27, 128.25, 128.23, 127.98, 127.65, 127.62, 127.59, 127.56, 127.46, 127.42, 127.11, 88.29, 85.35, 82.27, 81.12, 75.88, 73.44, 72.61, 71.88, 71.49, 71.00. HRMS (ESI) calcd. for $C_{48}H_{45}ClO_7$ $[M+Na]^+$:791.2752, found: 791.2746.

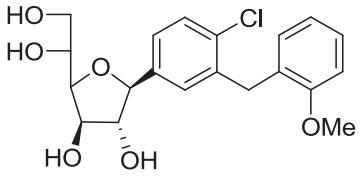

Chemical Formula: $C_{20}H_{23}ClO_6$
Exact Mass: 394.1183
Molecular Weight: 394.8460

(1*S*)-1,4-Anhydro-1-[4-chloro-3-(2-methoxybenzyl)phenyl]-D-glucitol (32i)

Compound **32i** (32.3 mg, 0.082 mmol, 43% yield) as a colorless oil was prepared according the procedure described for the synthesis of **32f** using **57i** (145 mg, 0.19 mmol) as a starting material. ^{1}H-NMR (400 MHz, d_4-MeOH) δ 7.27-7.18 (m, 2H), 7.17-7.09 (m, 2H), 6.92-6.83 (m, 2H), 6.79-6.72 (m, 1H), 4.46 (d, J = 3.7 Hz, 1H), 4.12-4.08 (m, 1H), 3.99-3.89 (m, 4H), 3.85 (dd, J = 3.8, 1.5 Hz, 1H), 3.77-3.68 (m, 4H), 3.61-3.52 (m, 1H). ^{13}C-NMR (100 MHz, d_4-MeOH) δ 158.87, 141.05, 139, 134.02, 131.59, 131.12, 130.81, 130.10, 129.90, 128.81, 128.76, 126.56, 121.39, 111.46, 88.08, 86.05, 82.22, 79.46, 71.33, 65.17, 55.80, 34.26. HRMS (ESI) calcd. for $C_{20}H_{23}ClO_6$ $[M+Na]^+$:417.1075, found: 417.1075.

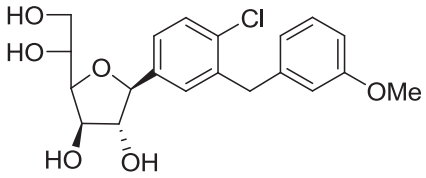

Chemical Formula: $C_{20}H_{23}ClO_6$
Exact Mass: 394.1183
Molecular Weight: 394.8460

(1*S*)-1,4-Anhydro-1-[4-chloro-3-(3-methoxybenzyl)phenyl]-D-glucitol (32j)

Compound **32j** (8.00 mg, 0.022 mmol, 50% yield) as a colorless oil was prepared according the procedure described for the synthesis of **32f** using **57j** (33 mg, 0.044 mmol) as a starting material. ^{1}H-NMR (400 MHz, d_4-MeOH) δ 7.33-.719 (m, 3H), 7.14-7.06 (m, 1H), 6.72-6.64 (m, 3H), 4.52 (d, J = 3.7 Hz, 1H), 4.12 (dd, J = 3.4, 1.6 Hz, 1H), 4.01-3.92 (m, 4H), 3.87 (dd, J = 2.7, 1.7 Hz, 1H), 3.75 (dd, J = 11.4, 3.0 Hz, 1H), 3.67 (s, 3H), 3.59 (dd, J = 11.4, 5.4 Hz, 1H). ^{13}C-NMR (100 MHz, d_4-MeOH) δ 161.24, 142.48, 141.46, 139.51, 133.92, 131.60, 131.25, 130.85, 130.36, 130.19, 126.93, 122.24, 115.58, 112.57, 88.13, 86.12, 82.36, 79.49, 71.40, 65.23, 55.55, 40.03. HRMS (ESI) calcd. for $C_{20}H_{23}ClO_6$ $[M+Na]^+$: 417.1075, found: 417.1075.

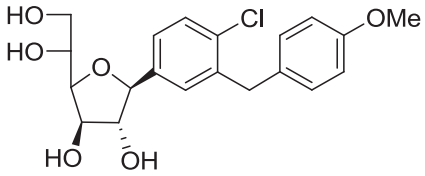

Chemical Formula: $C_{20}H_{23}ClO_6$
Exact Mass: 394.1183
Molecular Weight: 394.8460

(1*S*)-1,4-Anhydro-1-[4-chloro-3-(4-methoxybenzyl)phenyl]-D-glucitol (32k)

Compound **32k** (30.6 mg, 0.077 mmol, 43% yield) as a colorless oil was prepared according the procedure described for the synthesis of **32f** using **57k** (138 mg, 0.18 mmol) as a starting material. ^{i}H-NMR (400 MHz, d_4-MeOH) δ 7.29-7.19 (m, 3H), 7.07-6.99 (m, 2H), 6.79-6.71 (m, 2H), 4.51 (d, J = 3.6 Hz, 1H), 4.11 (dd, J = 3.4, 1.6 Hz, 1H), 4.01-3.91 (m, 4H), 3.87 (dd, J = 3.6, 1.6 Hz, 1H), 3.75 (dd, J = 11.3, 2.9 Hz, 1H), 3.69 (s, 3H), 3.59 (dd, J = 11.4, 5.3 Hz, 1H). ^{13}C-NMR (100 MHz, d_4-MeOH) δ 141.41, 140.09, 133.84, 132.92, 131.61, 131.25, 130.85, 130.25, 130.16, 126.79, 114.85, 88.15, 86.09, 82.36, 79.50, 71.41, 65.23, 55.65, 39.21. HRMS (ESI) calcd. for $C_{20}H_{23}ClO_6$ $[M+Na]^+$:417.1075, found: 417.1075.

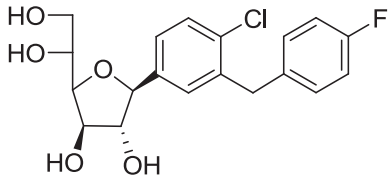

Chemical Formula: $C_{19}H_{20}ClFO_5$
Exact Mass: 382.0983
Molecular Weight: 382.8105

(1*S*)-1,4-Anhydro-1-[4-chloro-3-(4-fluorobenzyl)phenyl]-D-glucitol (32l)

Compound **32l** (27.6 mg, 0.072 mmol, 40% yield) as a colorless oil was prepared according the procedure described for the synthesis of **32f** using **57l** (134 mg, 0.18 mmol) as a starting material. ^{1}H-NMR (400 MHz, d_4-MeOH) δ 6.34-7.23 (m, 3H), 7.15-7.07 (m, 2H), 6.96-6.86 (m, 2H), 4.53 (d, J = 3.7 Hz, 1H), 4.13 (dd, J = 3.5, 1.7 Hz, 1H), 4.04-3.92 (m, 4H), 3.88 (dd, J = 3.7, 1.6 Hz, 1H), 3.76 (dd, J = 11.4, 3.0 Hz, 1H), 3.61 (dd, J = 11.3, 5.4 Hz, 1H). ^{13}C-NMR (100 MHz, d_4-MeOH) δ 141.55, 139.44, 136.87, 133.86, 131.59, 131.49, 131.41, 131.21, 130.82, 130.29, 130.27, 127.04, 116.05, 115.84, 88.10, 86.08, 82.37, 79.46, 71.39, 65.22, 39.23. HRMS (ESI) calcd. for $C_{19}H_{20}ClFO_5$ $[M+Na]^+$: 443.1596, found: 443.1598.

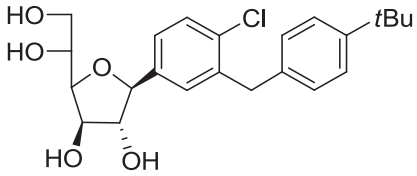

Chemical Formula: $C_{23}H_{29}ClO_5$
Exact Mass: 420.1704
Molecular Weight: 420.9264

(1*S*)-1,4-Anhydro-1-[4-chloro-3-(4-*tert*-butylbenzyl)phenyl]-D-glucitol (32m)

Compound **32m** (29.0 mg, 0.069 mmol, 43% yield) as a colorless oil was prepared according the procedure described for the synthesis of **32f** using **57m** (125 mg, 0.16 mmol) as a starting material. ^{1}H-NMR (400 MHz, d_4-MeOH) δ 7.47-7.41 (m, 3H), 7.24-7.21 (m, 2H), 7.06-7.01 (m, 2H), 4.51 (d J = 3.8 Hz, 1H), 4.12 (dd, J = 3.5, 1.7 Hz, 1H), 4.01-3.90 (m, 4H), 3.88 (dd, J = 3.7, 1.6 Hz, 1H), 3.76 (dd, J = 11.4, 3.1 Hz, 1H), 3.60 (dd, J = 11.4, 5.4 Hz, 1H), 1.23 (s, 9H). ^{13}C-NMR (100 MHz, d_4-MeOH) δ 141.39, 139.84, 137.88, 133.92, 131.61, 131.24, 130.84, 130.36, 130.18, 129.51, 126.84, 126.26, 88.14, 86.12, 82.33, 79.52, 71.41, 65.23, 44.40, 39.54, 35.18, 34.67, 31.86, 31.82. HRMS (ESI) calcd. for $C_{23}H_{30c}lO_5$ $[M+Na]^+$: 405.0876, found: 405.0876.

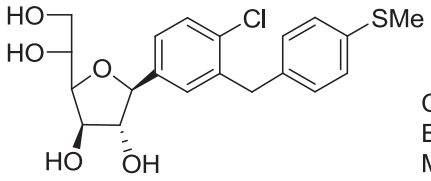

Chemical Formula: $C_{20}H_{23}ClO_5S$
Exact Mass: 410.0955
Molecular Weight: 410.9116

(1*S*)-1,4-Anhydro-1-[4-chloro-3-(4-methylthiobenzyl)phenyl]-D-glucitol (32n)

Compound **32n** (18.7 mg, 0.045 mmol, 35% yield) as a yellowish oil was prepared according the procedure described for the synthesis of **32f** using **57m** (102 mg, 0.13 mmol) as a starting material. ^{1}H-NMR (400 MHz, d_4-MeOH) δ 7.30-7.21 (m, 3H), 7.15-7.08 (m, 2H), 7.07-7.01 (m, 2H), 4.52 (d, J = 3.6 Hz, 1H), 4.12 (dd, J = 3.4, 1.6 Hz, 1H), 3.99-3.91 (m, 4H), 3.87 (dd, J = 3.7-1.7 Hz, 1H), 3.75 (dd, J = 11.3, 2.8 Hz, 1H), 3.59 (dd, J = 11.3, 5.3 Hz, 1H), 2.37 (s, 3H). ^{13}C-NMR (100 MHz, d_4-MeOH) δ 141.50, 139.53, 137.98, 137.51, 130.43, 130.32, 130.23, 128.01, 126.96, 88.13, 86.10, 82.37, 79.48, 71.41, 65.23, 39.53, 16.05. HRMS (ESI) $C_{20}H_{23}ClO_5S$ $[M+Na]^+$: 433.0847, found: 433.0869.

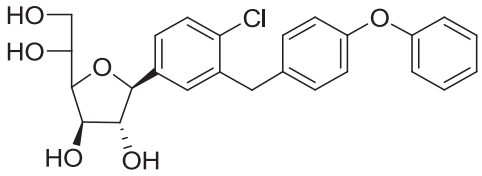

Chemical Formula: $C_{25}H_{25}ClO_6$
Exact Mass: 456.1340
Molecular Weight: 456.9154

(1*S*)-1,4-Anhydro1-[4-chloro-3-(4-phenoxybenzyl)phenyl]-D-glucitol (32o)

Compound **32o** (23.4 mg, 0.051 mmol, 32% yield) as a colorless oil was prepared according the procedure described for the synthesis of **32f** using **57o** (131 mg, 0.16 mmol) as a starting material. ^{1}H-NMR (400 MHz, d_4-MeOH) δ 7.31 (d, J = 1.8 Hz, 1H), 7.28-7.21 (m, 4H), 7.13-7.08 (m, 2H), 7.02-6.97 (m, 1H), 6.91-6.85 (m ,2H), 6.84-6.79 (m, 2H), 4.52 (d, J = 3.6 Hz, 1H), 4.12 (dd, J = 1.6, 3.5 Hz, 1H), 4.02-3.92 (m, 4H), 3.87 (d, J = 3.7, 1.6 Hz, 1H), 3.76 (dd, J = 11.3, 3.0 Hz, 1H), 3.60 (dd, J = 11.4, 5.6 Hz, 1H). ^{13}C-NMR (100 MHz, d_4-MeOH) δ 158.94, 157.00, 141.53, 139.70, 136.03, 133.90, 131.24, 130.81, 130.32, 130.25, 126.98, 124.15, 119.96, 119.90, 119.62, 88.16, 86.14, 82.39, 79.51, 71.42, 65.25, 39.36. HRMS (ESI) calcd. for $C_{25}H_{25}ClO_6$ $[M+Na]^+$: 479.1232, found: 479.1219.

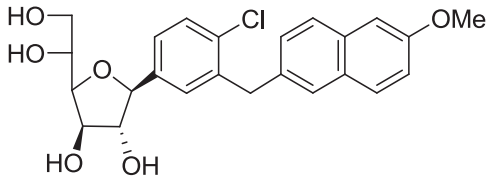

Chemical Formula: $C_{24}H_{25}ClO_6$
Exact Mass: 444.1340
Molecular Weight: 444.9047

(1*S*)-1,4-Anhydro-1-[4-chloro-3-(6-methoxy-naphthalen-2-yl)methyl]phenyl]-D-glucitol (32p)

Compound **32p** (10 mg, 0.023 mmol, 15% yield) as a colorless oil was prepared according the procedure described for the synthesis of **32f** using **57p** (120 mg, 0.15 mmol) as a starting material. ^{1}H-NMR (400 MHz, d_4-MeOH) δ 7.58 (dd, J = 13.7, 8.4 Hz, 2H), 7.45 (s, 1H), 7.36-7.18 (m, 4H), 7.11 (d, J = 2.4 Hz), 7.01 (dd, J = 9.0, 2.6 Hz, 1H), 4.51 (d, J = 3.6 Hz, 1H), 4.18-4.07 (m, 3H), 3.97-3.97 (m, 2H), 3.88 (dd, J = 3.6, 1.6 Hz, 1H), 3.81 (s, 3H), 3.73-3.67 (m, 1H), 3.60-3.52 (m, 1H). ^{13}C-NMR (100 MHz, d_4-MeOH) δ 158.87, 141.48, 139.71, 136.08, 134.76, 134.01, 130.52, 130.45, 130.25, 130.01, 128.87, 128.00 127.96, 126.93, 119.69, 106.64, 88.14, 86.09, 82.34, 79.48, 71.38, 65.18, 55.79, 40.02. HRMS (ESI) calcd. for $C_{24}H_{25}ClO_6$ $[M+Na]^+$: 469.1232, found: 479.1233.

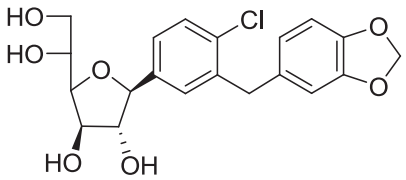

Chemical Formula: $C_{20}H_{21}ClO_7$
Exact Mass: 408.0976
Molecular Weight: 408.8295

(1*S*)-1,4-Anhydro-1-[4-chloro-3-(3,4-methylenedioxy-benzyl)phenyl]-D-glucitol (32q)

Compound **32q** (20 mg, 0.049 mmol, 35% yield) as a colorless oil was prepared according the procedure described for the synthesis of **32f** using **57q** (106 mg, 0.14 mmol) as a starting material. ^{1}H-NMR (400 MHz, d_4-MeOH) δ 7.32-7.19 (m, 3H), 6.68-6.54 (m, 3H), 5.81 (s, 2H), 4.51 (d, J = 3.7 Hz, 1H), 4.14-4.19 (m, 1H), 4.00-3.90 (m, 4H), 3.89-3.85 (m, 1H), 3.75 (dd, J = 11.3, 2.8 Hz, 1H), 3.59 (dd, J = 11.2, 5.2 Hz, 1H). ^{13}C-NMR (100 MHz. d_4-MeOH) δ 149.11,141.4345, 139.80, 134.72, 133.81, 130.23, 130.18, 126.89, 122.88, 110.16, 108.99, 102.11, 88.13, 86.07, 82.36, 79.46, 71.38, 65.20, 39.67. HRMS (ESI) calcd. for $C_{20}H_{21}ClO_7Na^+$ $[M+Na]^+$: 431.0868, found: 431.0876.

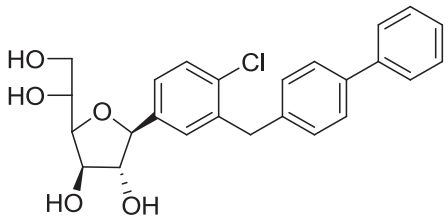

Chemical Formula: $C_{25}H_{25}ClO_5$
Exact Mass: 440.1391
Molecular Weight: 440.9160

(1*S*)-1,4-Anhydro-1-[4-chloro-3-(4-biphenylmethyl)phenyl]-D-glucitol (32r)

To a stirred suspension of magnesium (30.9 mg, 1.27 mmol) and 4-bromo-biphenyl (250 mg, 1.07 mmol) in THF (2 mL) was added I_2 (136 mg, 1.07 mmol) and reflux for 1.5 h. After colling to r.t., the resulting Grignard reagent was cooled to -78 ºC before adding **65** (0.51 mmol, 338 mg) in THF (1 mL). The resulting mixture was stirred at -78 ºC for 3 h and quenched with sat. NH_4Cl and extracted twice with EA. The combined organic layers were washed with brine, dired over $MgSO_4$ and concentrated to afford crude **55r**.

Crude **57r** was prepared according to the procedure described for the synthesis of **56f** using crude **55r** as a starting material.

Compound **32r** (4 mg, 0.010 mmol 1% yield over 4 steps) as a colorless oil was prepared according to the procedure described for the synthesis of **32f** using **57r (**76.9 mg, 0.096 mmol) as a starting material. ^{1}H-NMR (400 MHz, d_4-MeOH) δ 7.52 (d, J = 7.0 Hz, 2H), 7.49-7.43 (m, 3H), 7.37-7.31 (m, 3H), 7.29-7.25 (m, 2H), 7.20 (d, J = 8.3 Hz, 2H), 4.53 (d, J = 3.5 Hz, 1H), 4.12 (q, J = 1.7 Hz, 1H), 4.07 (s, 2H), 4.00-3.92 (m ,2H), 3.88 (dd, J = 3.7, 1.6 Hz, 1H), 3.75 (dd, J = 11.3, 2.9 Hz, 1H), 3.59 (dd, J = 11.4 ,5.2 Hz, 1H).

4.2.2 Transformation and Isolation of Plasmid DNA

The purchased hSGLT2 and EGFP plasmid came with the filter disc. The sample discs were placed separately in 1.5 mL microcentrifuge tubes and 50 µL of water were added and let stood at r.t. for 30 mins.

The frozen competent cell ECOS-101 was thawed on ice for 5 mins to obtain approximately 1/3 thawed state. 50 µL of ECOS-101 was extracted to another 1.5 mL microcentrifuge tube. Immediate after that, 5 µL of each plasmid was added separately to the 50 µL ECOS-101 prepared. The mixtures were tapped for 1 sec to homogenize and were immediately incubated at 42 ºC for 45 sec. Afterwards, the mixtures were again tapped for 1 sec before being transferred to chilled and dry agar plates (coated with Ampicillin), spreading by YB plating beads (autoclaved, dried, 4.0 mm diameter). The agar plates were immediately incubated at 37 ºC for 16 hrs.

5 colonies were selected from each plate and incubated in LB broth (1 mL) with ampicillin (final concentration 100mg/mL) at 37 ºC for 16 hrs. The isolation of plasmid DNA was carried out using QIAprep® Miniprep. The isolated plasmid DNA were treated with FastDigest® restriction enzymes (HindIII/EcORI for EGFP, SacI, SacI/XhoI, ScaI/NheI for hSGLT2) to confirm the band patterns are compatible to the plasmid sizes. The amount of DNA isolated was calculated with Nanodrop 2000.

4.2.3 Digestion and Ligation

In order to generate plasmid DNA without the open reading frame (ORF) of hSGLT2 for the transfection of control cell, the ORF sequence was removed with restriction enzymes, SacI and XhoI. The backbone and the ORF sequence were separated

with 10% agar electrophoresis. The extracted hSLGT2 backbone was treated with DNA blunting enzyme and re-ligated with Rapid DNA ligation Kit.

4.2.4 Transfection

A. Plate cells

COS-7 cells (2 x 10^5/well) were plated in 6-well plate in High-glucose DMEM (10%FBS, 1% NEAA, 0.5% PS) 20 hrs before transfection. 2 h before transfection replaced the existing medium with fresh medium.

B. Prepare TransIT-LT1 Reagent – DNA complex (amount stated for 1-well only)

This procedure was carried out immediately before the transfection. *Trans*IT-LT1 reagent was warmed to r.t. and was vortexed before use. 7.5 µL of *Trans*IT-LT1 reagent was added to 250 µL of serum-free Opti-MEM in a sterile tube. After pipetting and mixed gently, 2.5 µg of plasmid DNA (EGFP, hSGLT2, backbone) was added to the dilute *Trans*IT-LT1 reagent. After mixing gently, the mixtures were incubated at r.t. for 30 mins.

C. Add complexes to cells in complete growth medium

The mixtures prepared in step B were added dropwisely to the prepared cells in 6-well plate. After addition, culture vessels were rocked back and forth and form side to side to evenly distribute the *Trans*IT-LT1 reagent – DNA complexes. After 48 hrs of incubation, cells were harvest for stable clone selection and western blot.

4.2.5 Stable Clone Selection

Cells were dissociated by PBS wash and centrifuged at 300 rom for 5 mins. Different numbers of cells (10^4, $3x10^4$, 10^5/per well) were plated into 6-well plate. G418 with final concentration of 500 μg/mL was added to the culture medium for selection. After the single colonies were formed, they were picked up by pipetting and transferred into 96-well plate. When the cells were confluent in 96-well plate, they were transferred to 24-well plate. Again, they were transferred to 6-well plate and to T25 flask after the wells were confluent.

4.2.6 Western Blot

All protein concentrations were determined by BCA protein Assay Kit. Lysate buffer was added to the samples containing total 10 μg of protein to make up to total volume of 15 μL. To this mixture, 1μL of Beta-ME and 5 μL Laemmli buffer were added and heated to 90 ºC for 5 mins. The proteins were resolved by NuPAGE® Novex 4-12% Bis-Tris Gel 1.0 mm, 12 well, and transferred to nitrocellulose membrane. After blocking with 5% skimmed milk plus Tween-20, 0.1% for 30 mins, blots were probed in the same buffer with mouse anti-hSGLT2 (1:500) or anti-rabbit-hSLGT2 (1:500) for 1 hr at r.t. and washed with 0.05% Tween-20 4 times for 5 mins each. The blots were then incubated with secondary antibodies (1:2000) for 1 hr at r.t. Washes were performed as above and then visualized with an enhanced chemiluminscence kit.

5. References

1. King, H.; Aubert, R. E.; and Herman, W.H. Global burden of diabetes, 1995-2025: prevalence, numerical estimates, and projections. *Diabetes Care* **1998,** *21,* 1414-1431.

2. Source: IDF, Diabetes Atlas, 4th edition. "Diabetic facts" World Diabetes Foundation. http://www.worlddiabetesfoundation.org/composite-35.htm (07.07.2011).

3. Kaiser, N.; Leibowitz, G. J. Glucotoxicity and beta-cell failure in type 2 diabetes mellitus. *J. Pediatr. Endo. Metab.* **2003,** *16,* 5-22.

4. Morrish, N. J.; Wang, S. L.; Stevens, L. K.; Fuller, J. H.; Keen, H. Mortality and causes of death in the WHO multinational study of vascular disease in diabetes. *Diabetologia* **2001,** *44,* S14–S21.

5. Stratton, I. M.; Adler, A. I.; Neil, H. A.; Matthews, D. R.; Manley, S. E.; Cull, C. A.; Hadden, D.; Turner, R. C.; Holman, R. R. Association of glycemia with macrovascular and microvascular complications of type 2 diabetes (UKPDS 35): prospective observational study. *BMJ* **2000,** *321,* 405-412.

6. Bell, D. S. H. Type 2 diabetes mellitus: What is the optimal treatment regimen? *Am. J. Med.* **2004,** *116 (5 Suppl. 1),* 23S-29S.

7. Kirpichnikov, D.; McFarlane, S. I.; Sowers, J. R. Metformin: an update. *Ann. Intern. Med.* **2002,** *137,* 25-33.

8. Collier, C. A.; Bruce, C. R.; Smith, A. C.; Lopaschuk, G.; Dyck, D. J. Metformin counters the insulin-induced suppression of fatty acid oxidation and stimulation of triacylglycerol storage in rodent skeletal muscle. *Am. J. Physiol. Endocrinol. Metab.* **2006,** *291,* E182-E189.

9. Khan, M. A.; St. Peter, J. V.; Xue, J. L. A prospective, randomized comparison of the metabolic effects of pioglitazone or rosiglitazone in patients with type 2 diabetes who were previously treated with troglitazone. *Diabetes Care* **2002,** *25,* 708-711.

10. Goldberg, R. B.; Kendall, D. M.; Deeg; Buse, J. B.; Zagar, A. J.; Pinaire, J. A.; Tan, M. H.; Khan, M. A.; PErez, A. T.; Jacober, S. J.; GLAI Study Investigators. A comparison of lipid and glycemic effects of pioglitazone and rosiglitazone in patients with type 2 diabetes and dyslipidemia. *Diabetes Care* **2005,** *28,* 1547-1554.

11. Nissen, S. E.; Wolski, K. Effect of rosiglitazone on the risk of myocardial infarction anf death from cardiovascular casues. *N. Engl. J. Med.* **2007,** *356,* 2457-2471.

12. Singh, S.; Loke, Y. K.; Furberg, C. D. Long-term risk of cardiovascular events with rosiglitazone: a meta-analysis. *JAMA* **2007,** *298,* 1189-1195.

13. Jones, G.; Macklin, J.; Alexander, W. Contraindications to the use of metformin. *BMJ* **2003,** *326,* 4-5.

14. Turner, R. C.; Cull, C. A.; Frighi, V.; Holman, R. R. Glycemic control with diet, sulfonylurea, metformin, or insulin in patients with type 2 diabetes mellitus: progressive requirement for multiple therapies (UKPDS 49). UK Prospective Diabetes Study (UKPDS) Group. *JAMA* **1999,** *281,* 2005-2012.

15. Brown, G. K. Glucose transporters: structure, function, and consequences of deficiency. *J. Inherit. Metab. Dis.* **2000,** *23*, 237-246.

16. Wood, I. S.; Trayhurn, P. Glucose transporters (GLUT and SGLT): expanded families of sugar transport proteins. *Br. J. Nutr.* **2003,** *89,* 3-9.

17. Wright, E. M. Renal Na^+-glucose contransporters. *Am. J. Physiol. Renal Physiol.* **2001,** *280,* F10-F18.

18. Turk, E.; Wright, E. M. Membrane topological motifs in the SGLT contransporter family. *J. Membr. Biol.* **1997,** *159,* 1-20.

19. Wright, E. M.; Hirayama, B. A.; Loo, D. F. Active sugar transport in health and disease. *J. Intern. Med.* **2007,** *261,* 32-43.

20. Wright, E. M.; Loo, D. F. L.; Hirayama, B. A.; Turk, E. Surprising Versatility of Na^+-Glucose Cotransporter: SLC5. *Physiology* **2004,** *19,* 370-376.

21. Lee, Y. J.; Han, H. J. Regulatory mechanisms of Na^+/glucose cotransporters in renal proximal tubule cells. *Kidney Int* **2007,** *72,* S27-S35.

22. Turk, E.; Martin, M. G.; Wright, E. M. Structure of the human Na^+/glucose cotransporter gene SGLT1. *J. Biol. Chem.* **1994,** *269*, 15204-15209.

23. Kanai, Y.; Lee, W. S.; You, G.; Brown, D.; Hediger, M. A. The human kidney low affinity Na^+/glucose transporter SGLT2. Delineation of the major renal reabsorption mechanism for D-glucose. *J. Clin. Invest.* **1994,** *93,* 397-404.

24. Abdul-Ghani, M. A.; Norton, L.; DeFronzo, R. A. Role of Sodium-Glucose Cotransporter 2 (SGLT 2) Inhibitors in the Treatment of Type 2 Diabetes. *Endocrine Reviews* **2011**.

25. Valtin, H. Renal function: mechanisms preserving fluid and solute balance in health. Boston: Little, Brown and Company, 1983.

26. Hirayama, B. A.; Lostao, M. P.; Panayotova-Heiermann, M.; Loo, D. D.; Turk, E.; Wright, E. M. Kinetic and specificity differences between rat, human, and rabbit Na+-glucose cotransporters (SGLT-1). *Am. J. Physiol.* **1996,** *270,* G919-G926.

27. Gerich, J. E.; Meyer, C.; Woerle, H. J.; Stumvoll, M. Renal gluconeogenesis: its importance in human glucose homeostasis. *Diabetes Care* **2001,** *24,* 382-391.

28. White, J. R. Apple Trees to Sodium Glucose Co-Transporter Inhibitors: A Review of SGLT2 Inhibition. *Clinical Diabetes* **2010,** *28,* 5-10.

29. Dominguez, J. H.; Camp, K.; Maianu, L.; Feister, H.; Garvey, W. T. Molecular adaptations of GLUT1 and GLUT2 in renal proximal tubules of diabetic rats. *Am. J. Physiol.* **1994,** *266,* F283-F290.

30. Dominguez, J. H.; Song, B.; Maianu, L.; Garvey, W. T.; Qulali, M. Gene expression of epithelial glucose transporters: the role of diabetes mellitus. *J. Am. Soc. Nephrol.* **1994,** *5(5 Suppl. 1)*, S29-S36.

31. Noonan, W. T.; Shapiro, V. M.; Banks, R. O. Renal glucose reabsorption during hypertonic glucose infusion in female streptozotocin-induced diabetic rats. *Life Sci.* **2001,** *68,* 2967-2977.

32. Rahmoune, H.; Thompson, P. W.; Ward, J. M.; Smith, C. D.; Hong, G.; Brown, J. Glucose transporters in human renal proximal tubular cells isolated from the urine of patients with non-insulin-dependent diabetes. *Diabetes* **2005,** *54,* 3427-3434.

33. Melin, K.; Meeuwisse, G. W. Glucose-galactose malabsorption. A genetic study. *Acta. Paediatr. Scand.* **1969**, *188(Suppl.),* 19.

34. Turk, E.; Zabel, B.; Mundlos, S.; Dyer, J.; Wright, E. M. Glucose/galactose malabsorption caused by a defect in the Na^+/glucose cotransporter. *Nature* **1991,** *350,* 354-356.

35. Santer, R.; Kinner, M.; Lassen, C. L.; Schneppenheim, R.; Eggert, P.; Bald, M.; Brodehl, J.; Daschner, M.; Ehrich, J. H.; Kemper, M.; Li Volti, S.; Neuhaus, T.; Skovby, F.; Swift, P. G.; Schaub, J.; Klaerke, D. Molecular analysis of the SGLT2 gene in patients with renal glucosuria. *J. Am. Soc. Nephrol.* **2003,** *14,* 2873-2882.

36. Elsas, L. J.; Rosenberg, L. E. Familial renal glycosuria: a genetic reappraisal of hexose transport by kidney and intestine. *J. Clin. Invest.* **1969,** 48, 1845-1854.

37. Jurczak, M. J.; Lee, H. Y.; Birkenfeld, A. L.; Jornayvaz, F. R.; Frederick, D. W.; Pongratz, R. L.; Zhao, X.; Moeckel, G. W.; Samuel, V. T.; Whaley, J. M.; Shulman, G. I.; Kibbey, R. G. SGLT2 deletion improves glucose homeostasis and preserves pancreatic beta-cell function. *Diabetes* **2011,** *60,* 890-898.

38. Kipp, H.; Kinne-Saffran, E.; Bevan, C.; Kinne, R. K. Characteristics of renal Na(+)-D-glucose cotransport in the skate (Raja erinacea) and shark (Squalus acanthias). *Am. J. Physiol.* **1997,** *273,* R134-R142.

39. Vick, H.; Diedrich, D. F.; Baumann, K. Reevaluation of renal tubular glucose transport inhibition by phlorizin analogs. *Am. J. Physiol.* **1973,** *224,* 552-557.

40. Novakova, R.; Homerova, D.; Kinne, R. K.; Kinne-Saffran, E.; Lin, J. T. Identification of a region critically involved in the interaction of phlorizin with the rabbit sodium-D-glucose cotransporter SGLT1. *J. Membr. Biol.* **2001,** *184,* 55-60.

41. Tyagi, N. K.; Kumar, A.; Goyal, P.; Pandey, D.; Siess, W.; Kinne, R. K. D-Glucose-recognition and phlorizin-binding sites in human sodium/D-glucose cotransporter 1 (hSGLT1): a tryptophan scanning study. *Biochemistry-Us* **2007,** *46,* 13616-13628.

42. Puntheeranurak, T.; Kasch, M.; Xia, X.; Hinterdorfer, P.; Kinne, R. K. Three surface subdomains form the vestibule of the Na+/glucose cotransporter SGLT1. *J. Biol. Chem.* **2007,** *282,* 25222-25230.

43. Althoff, T.; Hentschel, H.; Luig, J.; Schutz, H.; Kasch, M.; Kinne, R. K. Na(+)-D-glucose cotransporter in the kidney of Squalus acanthias: molecular identification and intrarenal distribution. *Am. J. Physiol. Regul. Integr. Comp. Physiol.* **2006,** *290,* R1094-R1104.

44. Pajor, A. M.; Randolph, K. M.; Kerner, S. A.; Smith, C. D. Inhibitor binding in the human renal low- and high-affinity Na+/glucose cotransporters. *J. Pharmacol. Exp. Ther.* **2008,** *324,* 985-991.

45. Wuthrich, M.; Sterchi, E. E. Human lactase-phlorizin hydrolase expressed in COS-1 cells is proteolytically processed by the lysosomal pathway. *FEBS Lett.* **1997,** *405,* 321-327.

46. Leloup, C.; Orosco, M.; Serradas, P.; Nicolaidis, S.; Penicaud, L. Specific inhibition of GLUT2 in arcuate nucleus by antisense oligonucleotides suppresses nervous control of insulin secretion. *Brain Res. Mol. Brain Res.* **1998,** *57,* 275-280.

47. Ehrenkranz, J. R.; Lewis, N. G.; Kahn, C. R.; Roth, J. Phlorizin: a review. *Diabetes Metab. Res. Rev.* **2005,** *21,* 31-38.

48. Chao, E. C.; Henry, R. R. SGLT2 inhibition--a novel strategy for diabetes treatment. *Nat. Rev. Drug Discov.* **2010,** *9,* 551-559.

49. Oku, A.; Ueta, K.; Arakawa, K.; Ishihara, T.; Nawano, M.; Kuronuma, Y.; Matsumoto, M.; Saito, A.; Tsujihara, K.; Anai, M.; Asano, T.; Kanai, Y.; Endou, H. T-1095, an inhibitor of renal Na+-glucose cotransporters, may provide a novel approach to treating diabetes. *Diabetes* **1999,** *48,* 1794-1800.

50. Katsuno, K.; Fujimori, Y.; Takemura, Y.; Hiratochi, M.; Itoh, F.; Komatsu, Y.; Fujikura, H.; Isaji, M. Sergliflozin, a novel selective inhibitor of low-affinity sodium glucose cotransporter (SGLT2), validates the critical role of SGLT2 in renal glucose reabsorption and modulates plasma glucose level. *J. Pharmacol. Exp. Ther.* **2007,** *320,* 323-330.

51. Hussey, E. K.; Clark, R. V.; Amin, D. M.; Kipnes, M. S.; O'Connor-Semmes, R. L.; O'Driscoll, E. C.; Leong, J.; Murray, S. C.; Dobbins, R. L.; Layko, D.; Nunez, D. J. Single-dose pharmacokinetics and pharmacodynamics of sergliflozin etabonate, a novel inhibitor of glucose reabsorption, in healthy volunteers and patients with type 2 diabetes mellitus. *J. Clin. Pharmacol.* **2010,** *50,* 623-635.

52. Fujimori, Y.; Katsuno, K.; Nakashima, I.; Ishikawa-Takemura, Y.; Fujikura, H.; Isaji, M. Remogliflozin etabonate, in a novel category of selective low-affinity sodium glucose cotransporter (SGLT2) inhibitors, exhibits antidiabetic efficacy in rodent models. *J. Pharmacol. Exp. Ther.* **2008,** *327,* 268-276.

53. Meng, W.; Ellsworth, B. A.; Nirschl, A. A.; McCann, P. J.; Patel, M.; Girotra, R. N.; Wu, G.; Sher, P. M.; Morrison, E. P.; Biller, S. A.; Zahler, R.; Deshpande, P. P.; Pullockaran, A.; Hagan, D. L.; Morgan, N.; Taylor, J. R.; Obermeier, M. T.; Humphreys, W. G.; Khanna, A.; Discenza, L.; Robertson, J. G.; Wang, A.; Han, S.; Wetterau, J. R.; Janovitz, E. B.; Flint, O. P.; Whaley, J. M.; Washburn, W. N. Discovery of dapagliflozin: a potent, selective renal sodium-dependent glucose cotransporter 2 (SGLT2) inhibitor for the treatment of type 2 diabetes. *J. Med. Chem.* **2008,** *51,* 1145-1149.

54. Han, S.; Hagan, D. L.; Taylor, J. R.; Xin, L.; Meng, W.; Biller, S. A.; Wetterau, J. R.; Washburn, W. N.; Whaley, J. M. Dapagliflozin, a selective SGLT2 inhibitor,

improves glucose homeostasis in normal and diabetic rats. *Diabetes* **2008,** *57,* 1723-1729.

55. Obermeier, M.; Yao, M.; Khanna, A.; Koplowitz, B.; Zhu, M.; Li, W.; Komoroski, B.; Kasichayanula, S.; Discenza, L.; Washburn, W.; Meng, W.; Ellsworth, B. A.; Whaley, J. M.; Humphreys, W. G. In vitro characterization and pharmacokinetics of dapagliflozin (BMS-512148), a potent sodium-glucose cotransporter type II inhibitor, in animals and humans. *Drug Metab. Dispos.* **2010,** *38,* 405-414.

56. Kipnes, M. Dapagliflozin: an emerging treatment option in type 2 diabetes. *Expert Opin. Investig. Drugs* **2009,** *18,* 327-334.

57. Komoroski, B.; Vachharajani, N.; Feng, Y.; Li, L.; Kornhauser, D.; Pfister, M. Dapagliflozin, a novel, selective SGLT2 inhibitor, improved glycemic control over 2 weeks in patients with type 2 diabetes mellitus. *Clin. Pharmacol. Ther.* **2009,** *85,* 513-519.

58. List, J. F.; Woo, V.; Morales, E.; Tang, W.; Fiedorek, F. T. Sodium-glucose cotransport inhibition with dapagliflozin in type 2 diabetes. *Diabetes Care* **2009,** *32,* 650-657.

59. Wilding, J. P.; Norwood, P.; T'Joen, C.; Bastien, A.; List, J. F.; Fiedorek, F. T. A study of dapagliflozin in patients with type 2 diabetes receiving high doses of insulin plus insulin sensitizers: applicability of a novel insulin-independent treatment. *Diabetes Care* **2009,** *32,* 1656-16562.

60. Bailey, C. J.; Gross, J. L.; Pieters, A.; Bastien, A.; List, J. F. Effect of dapagliflozin in patients with type 2 diabetes who have inadequate glycaemic control with metformin: a randomised, double-blind, placebo-controlled trial. *Lancet* **2010,** *375,* 2223-2233.

61. Wilding, J. P. H.; Woo, V.; Soler, N. G.; Pahor, A.; Sugg, J.; Parikh, S. Dapagliflozin in patients with Type 2 diabetes poorly controlled on insulin therapy - efficacy of a novel insulin-independent treatment. *Diabetes* **2010,** *59(Suppl. 1),* A21-A22 (Abstract 78-OR)

62. Strojek, K.; Hruba, V.; Elze, M.; Langkilde, A.; Parikh, S. Efficacy and safety of dapagliflozin in patients with Type 2 diabetes mellitus and inadequate glycaemic control on glimepiride monotherapy. *Diabetologia* **2010,** *53(Suppl. 1).* Abstract 870 S347.

63. Nauck, M.; Del Prato, S.; Rohwedder, K.; Elze, M.; Parikh, S. Dapagliflozin vs glipizide in patients with Type 2 diabetes mellitus inadequately controlled on metformin: 52-week results of a double-blind, randomized, controlled trial. *Diabetologia* **2010,** *53(Suppl. 1),* Abstract 241.

64. "Dapagliflozin" ClinicalTrials.gov. http://clinicaltrials.gov/ct2/results?term=dapagliflozin (05.07.2011).

65. Rosenstock J.; Arbit, D.; Usiskin, K.; Capuano, G.; Canovatchel, W. Canagliflozin, an inhibitor od sodium-glucose co-transporter 2 (SGLT2), improves glycemic contorl and lowers bidy weight in subjects with Type 2 diabetes (T2D) on metformin. *Diabetes* **2010,** *59(Suppl. 1),* A21 (Abstract 0077-OR).

66. "Canagliflozin" ClinicalTrials.gov. http://clinicaltrials.gov/ct2/results?term=canagliflozin (05.07.2011)

67. Freiman, J.; Ruff, D. A.; Frazier, K. S.; Combs, K.; Turnage, A.; Shadoan, M.; Powell, D.; Zambrowicz, B.; Brown, P. LX4211, a dual SGLT2/SGLT1 inhibitor, shows rapid and significant improvements in glycemic control over 28 days in patients with type 2 diabetes (T2DM). *Diabetes* **2010,** *59 (Suppl. 1),* A511.

68. Mascitti, V.; Maurer, T. S.; Robinson, R. P.; Bian, J.; Boustany-Kari, C. M.; Brandt, T.; Collman, B. M.; Kalgutkar, A. S.; Klenotic, M. K.; Leininger, M. T.; Lowe, A.; Maguire, R. J.; Masterson, V. M.; Miao, Z.; Mukaiyama, E.; Patel, J. D.; Pettersen, J. C.; Preville, C.; Samas, B.; She, L.; Sobol, Z.; Steppan, C. M.; Stevens, B. D.; Thuma, B. A.; Tugnait, M.; Zeng, D.; Zhu, T. Discovery of a clinical candidate from the structurally unique dioxa-bicyclo[3.2.1]octane class of sodium-dependent glucose cotransporter 2 inhibitors. *J. Med. Chem.* **2011,** *54,* 2952-2960.

69. Mascitti, V.; Robinson, R. P.; Préville, C.; Thuma, B. A.; Carr, C. L.; Reese, M. R.; Maguire, R. J.; Leininger, M. T.; Lowe, A.; Steppan, C. M. Syntheses of C-5-spirocyclic C-glycoside SGLT2 inhibitors. *Tetrahedron Letters* **2010,** *51,* 1880-1883.

70. Robinson, R. P.; Mascitti, V.; Boustany-Kari, C. M.; Carr, C. L.; Foley, P. M.; Kimoto, E.; Leininger, M. T.; Lowe, A.; Klenotic, M. K.; Macdonald, J. I.; Maguire, R. J.; Masterson, V. M.; Maurer, T. S.; Miao, Z.; Patel, J. D.; Preville, C.; Reese, M. R.; She, L.; Steppan, C. M.; Thuma, B. A.; Zhu, T. C-Aryl glycoside inhibitors of SGLT2: Exploration of sugar modifications including C-5 spirocyclization. *Bioorg. Med. Chem. Lett.* **2010,** *20,* 1569-1572.

71. Grempler, R.; Thomas, L.; Eckhardt, M.; Himmelsbach, F.; Sauer, A.; Michael, M.; Eickelmann, P. *In vitro* properties and *in vivo* effect on unrinary glucose excretion of BI 10773, a novel selective SGLT2 inhibitor. *69th Scientific Sessions* **2009,** Abstract 521-9.

72. "BI-10773" ClinicalTrial.gov. http://clinicaltrials.gov/ct2/results?term=BI-10773 (06/07/2011).

73. "ASP-1941" ClinicalTrial.gov. http://clinicaltrials.gov/ct2/results?term=ASP-1941 (06/07/2011).

74. Bhanot, S.; Murray, S. F.; Booten, S. L.; Chakravarty, K.; Zanardi, T.; Henry, S.; Watts, L. M.; Wancewicz, E. V.; Siwkowsk, A.; Monia, B. P. ISIS 388626, an SGLT2 antisense drug, causes robust and sustained glucosuria in multiple species and is safe and well-tolerated. *69th Scientific Sessions* **2009,** Abstract 328-OR.

75. Wancewicz, E. V.; Siwkowsk, A.; Meibohm, B.; Yates, C. R.; Pearce, M.; Matson, J.; Booten, S.; Murray, S. F.; Hung, G.; Geary, R. S.; Bhanot, S.; Monia, B. P. *68th Scientific Sessions* **2008,** Abstract 334-OR.

76. "ISIS 388626" ClinicalTrial.gov. http://clinicaltrials.gov/ct2/results?term=isis+388626 (06/07/2011).

77. Kakinuma, H.; Oi, T.; Hashimoto-Tsuchiya, Y.; Arai, M.; Kawakita, Y.; Fukasawa, Y.; Iida, I.; Hagima, N.; Takeuchi, H.; Chino, Y.; Asami, J.; Okumura-Kitajima, L.; Io, F.; Yamamoto, D.; Miyata, N.; Takahashi, T.; Uchida, S.; Yamamoto, K. (1*S*)-1,5-anhydro-1-[5-(4-ethoxybenzyl)-2-methoxy-4-methylphenyl]-1-thio-D- glucitol (TS-071) is a potent, selective sodium-dependent glucose cotransporter 2 (SGLT2) inhibitor for type 2 diabetes treatment. *J. Med. Chem.* **2010,** *53,* 3247-3261.

78. Kang, S. Y.; Song, K. S.; Lee, J.; Lee, S. H. Synthesis of pyridazine and thiazole analogs as SGLT2 inhibitors. *Bioorg. Med. Chem.* **2010,** *18,* 6069-6079.

79. Lee, J.; Lee, S. H.; Seo, H. J.; Son, E. J.; Jung, M. E.; Lee, M.; Han, H. K.; Kim, J.; Kang, J. Novel C-aryl glucoside SGLT2 inhibitors as potential antidiabetic agents: 1,3,4-Thiadiazolylmethylphenyl glucoside congeners. *Bioorg. Med. Chem.* **2010,** *18,* 2178-2194. (81)

80. Lee, J.; Kim, J. Y.; Choi, J.; Lee, S. H.; Kim, J. Pyrimidinylmethylphenyl glucoside as novel C-aryl glucoside SGLT2 inhibitors. *Bioorg. Med. Chem. Lett.* **2010,** *20,* 7046-7049.

81. Lee, S. H.; Kim, M. J.; Kim, J.; Park, H. J.; Lee, J. Thiazolylmethyl ortho-substituted phenyl glucoside library as novel C-aryl glucoside SGLT2 inhibitors. *Eur. J. Med. Chem.* **2011,** *46,* 2662-2675.

82. Morita, H.; Deguchi, J.; Motegi, Y.; Sato, S.; Aoyama, C.; Takeo, J.; Shiro, M.; Hirasawa, Y. Cyclic diarylheptanoids as Na+-glucose cotransporter (SGLT) inhibitors from Acer nikoense. *Bioorg. Med. Chem. Lett.* **2010,** *20,* 1070-1074.

83. Kang, S. Y.; Kim, M. J.; Lee, J. S.; Lee, J. Glucosides with cyclic diarylpolynoid as novel C-aryl glucoside SGLT2 inhibitors. *Bioorg. Med. Chem. Lett.* **2011,** *21,* 3759-3763.

84. Xu, B.; Lv, B.; Feng, Y.; Xu, G.; Du, J.; Welihinda, A.; Sheng, Z.; Seed, B.; Chen, Y. *O*-Spiro *C*-aryl glucosides as novel sodium-dependent glucose co-transporter 2 (SGLT2) inhibitors. *Bioorg. Med. Chem. Lett.* **2009,** *19,* 5632-5635.

85. Xu, B.; Feng, Y.; Cheng, H.; Song, Y.; Lv, B.; Wu, Y.; Wang, C.; Li, S.; Xu, M.; Du, J.; Peng, K.; Dong, J.; Zhang, W.; Zhang, T.; Zhu, L.; Ding, H.; Sheng, Z.; Welihinda, A.; Roberge, J. Y.; Seed, B.; Chen, Y. *C*-Aryl glucosides substituted at the 4'-position as potent and selective renal sodium-dependent glucose co-transporter 2 (SGLT2) inhibitors for the treatment of type 2 diabetes. *Bioorg. Med. Chem. Lett.* **2011**.

86. Zhang, W.; Welihinda, A.; Mechanic, J.; Ding, H.; Zhu, L.; Lu, Y.; Deng, Z.; Sheng, Z.; Lv, B.; Chen, Y.; Roberge, J. Y.; Seed, B.; Wang, Y. X. EGT1442, a potent and selective SGLT2 inhibitor, attenuates blood glucose and HbA(1c) levels in db/db mice and prolongs the survival of stroke-prone rats. *Pharmacol. Res.* **2011,** *63,* 284-293.

87. Yao, C. H.; Song, J. S.; Chen, C. T.; Yeh, T. K.; Hung, M. S.; Chang, C. C.; Liu, Y. W.; Yuan, M. C.; Hsieh, C. J.; Huang, C. Y.; Wang, M. H.; Chiu, C. H.; Hsieh, T. C.; Wu, S. H.; Hsiao, W. C.; Chu, K. F.; Tsai, C. H.; Chao, Y. S.; Lee, J. C. Discovery of Novel *N*-*β*-D-Xylosylindole Derivatives as Sodium-Dependent Glucose Cotransporter 2 (SGLT2) Inhibitors for the Management of Hyperglycemia in Diabetes. *J. Med. Chem.* **2010,** *54,* 166-178.

88. Kipnes, M. S. Sodium-glucose cotransporter 2 inhibitors in the treatment of Type 2 diabetes: a review of Phase II and III trials. *J. Clin. Invest.* **2011,** *1,* 145-156.

89. Pazur, J. H.; Miskiel, F. J.; Liu, B. The identification of furanose and pyranose ring forms of the reducing units of oligosaccharides. *Anal Biochem* **1988,** *174,* 46-53.

90. Saotome, G.; Wong, C. H.; Kanie, O. Combinatorial library of five-membered iminocyclitol and the inhibitory activities against glyco-enzymes. *Chem. & Biol.* **2001**, *8*, 1061-1070.

91. Yang, W. B.; Patil, S. S.; Tsai, C. H.; Lin, C. H.; Fang, J. M. The synthesis of L-gulose and L-xylose from D-gluconolactone. *Tetrahedron* **2002,** *58,* 253-259.

92. Fuji, K.; Ichikawa, K.; Node, M.; Fujita, E. Hard acid and soft nucleophile system. New efficient method for removal of benzyl protecting group. *JOC* **1979,** *44,* 1661-1664.

6. Appendices

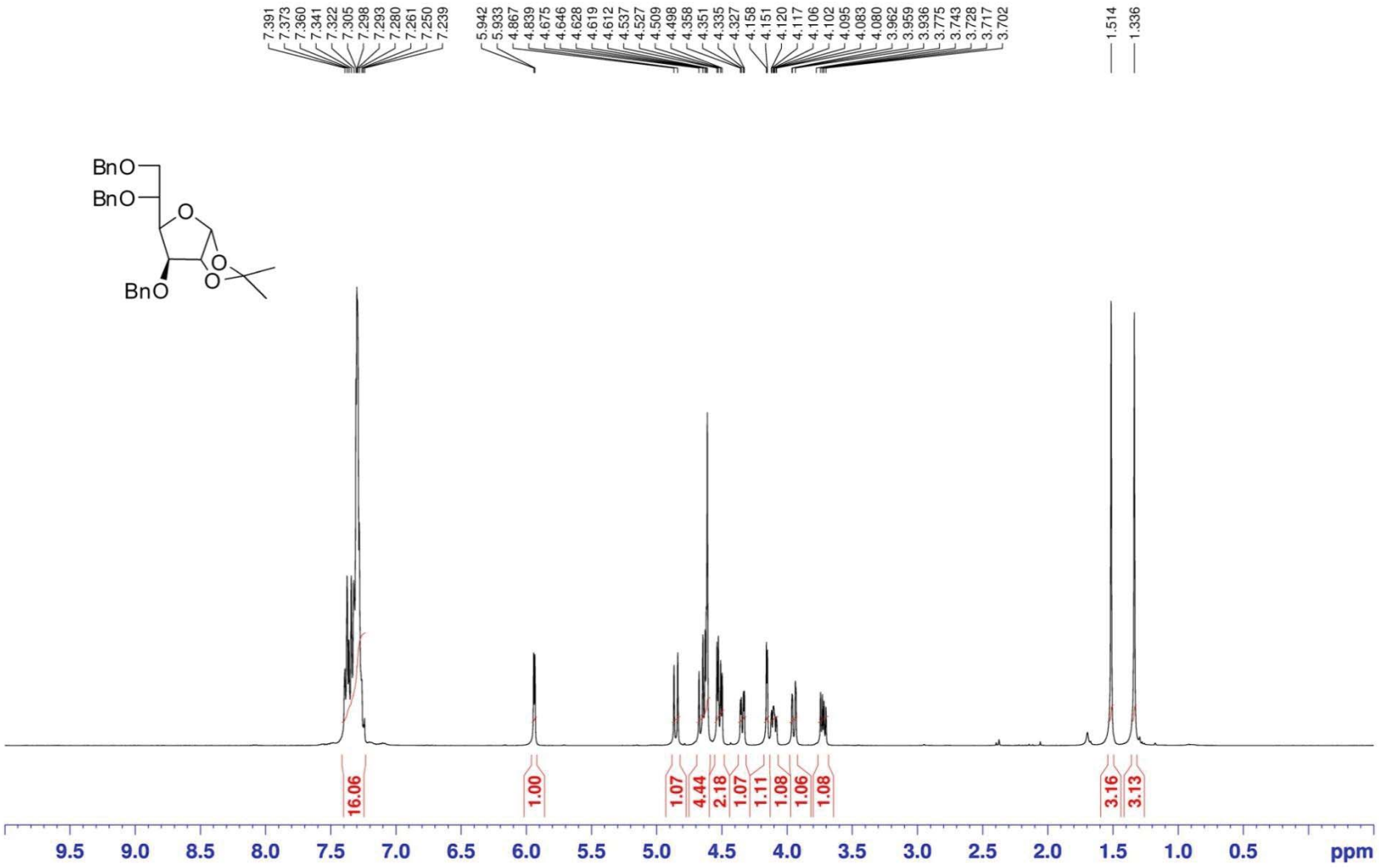

Appendix 1. ^{1}H-NMR spectra of **42** (400 MHz, $CDCl_3$)

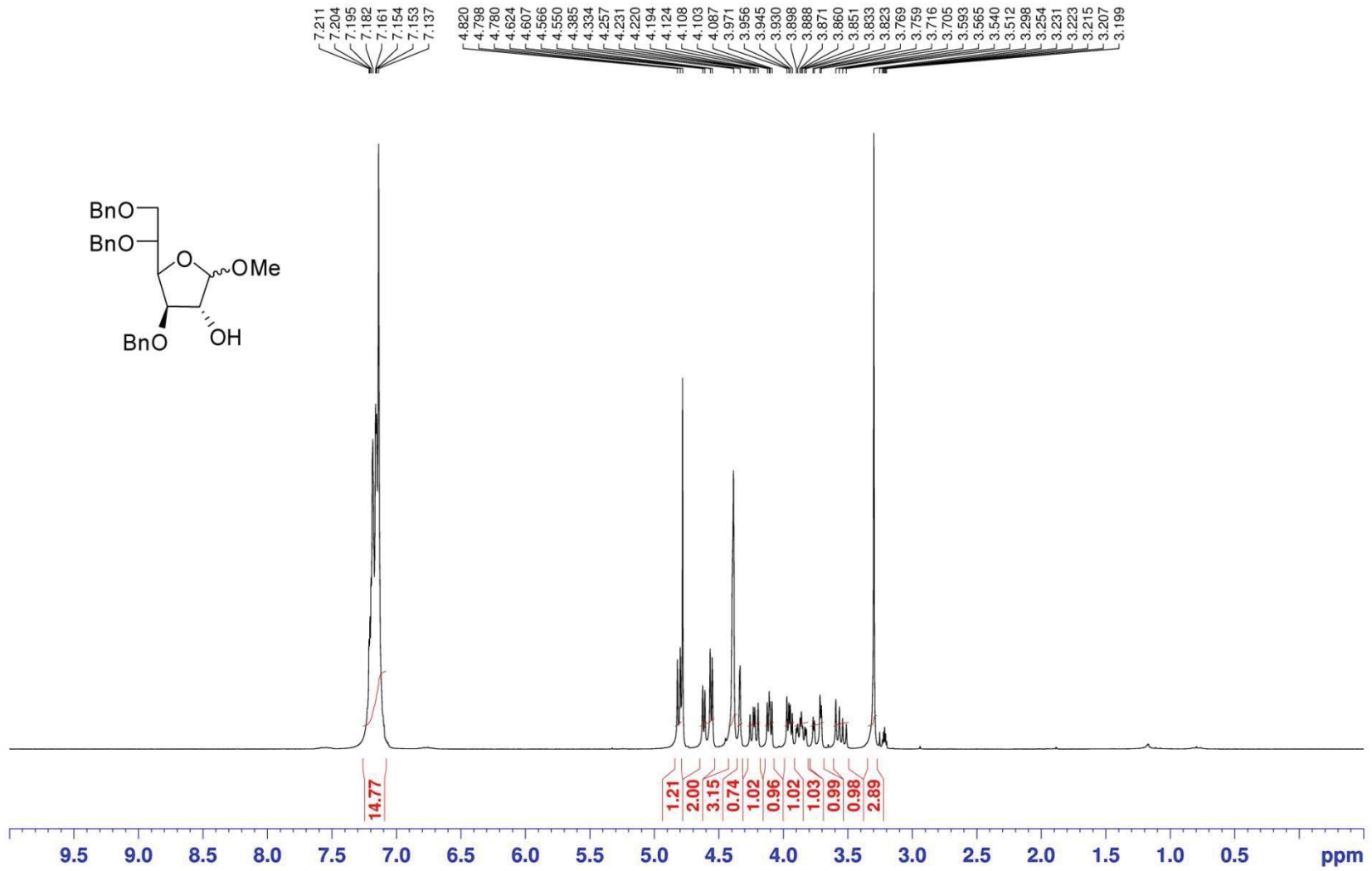

Appendix 2. ^{1}H-NMR spectra of **43** (200 MHz, d_4-MeOH)

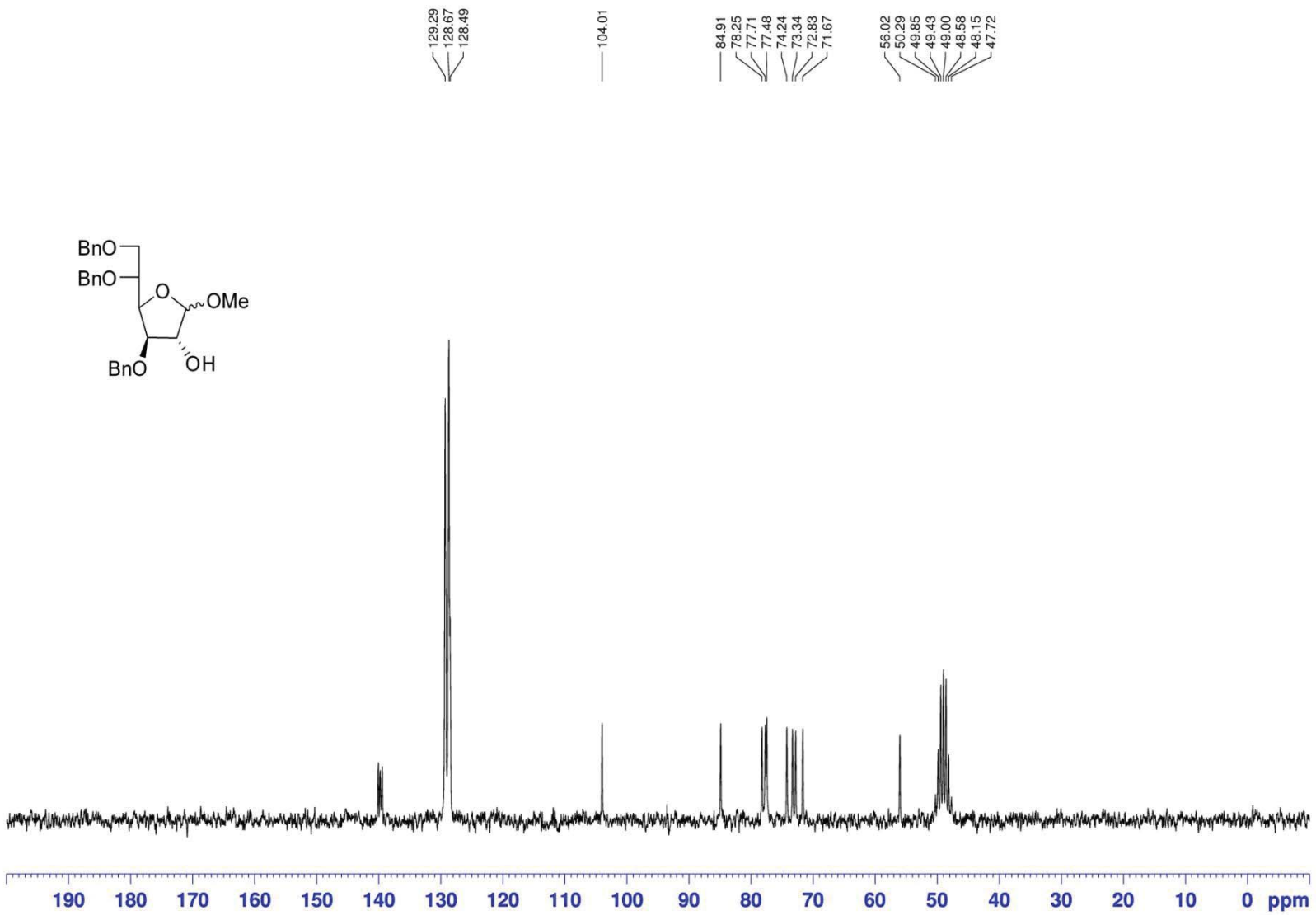

Appendix 3. ^{13}C-NMR spectra of **43** (50 MHz, d_4-MeOH)

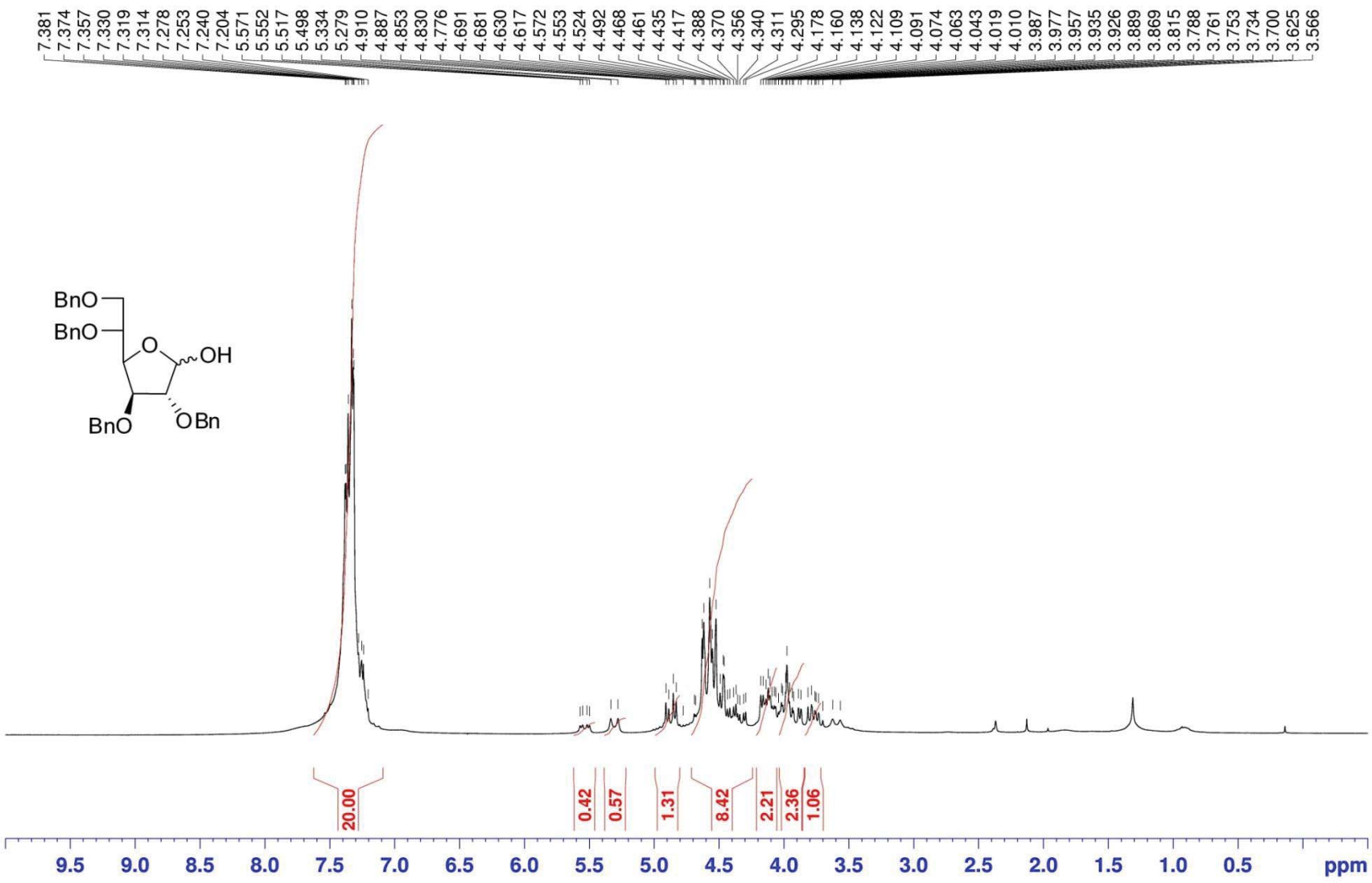

Appendix 4. ^{1}H-NMR spectra of **45** (200 MHz, $CDCl_3$)

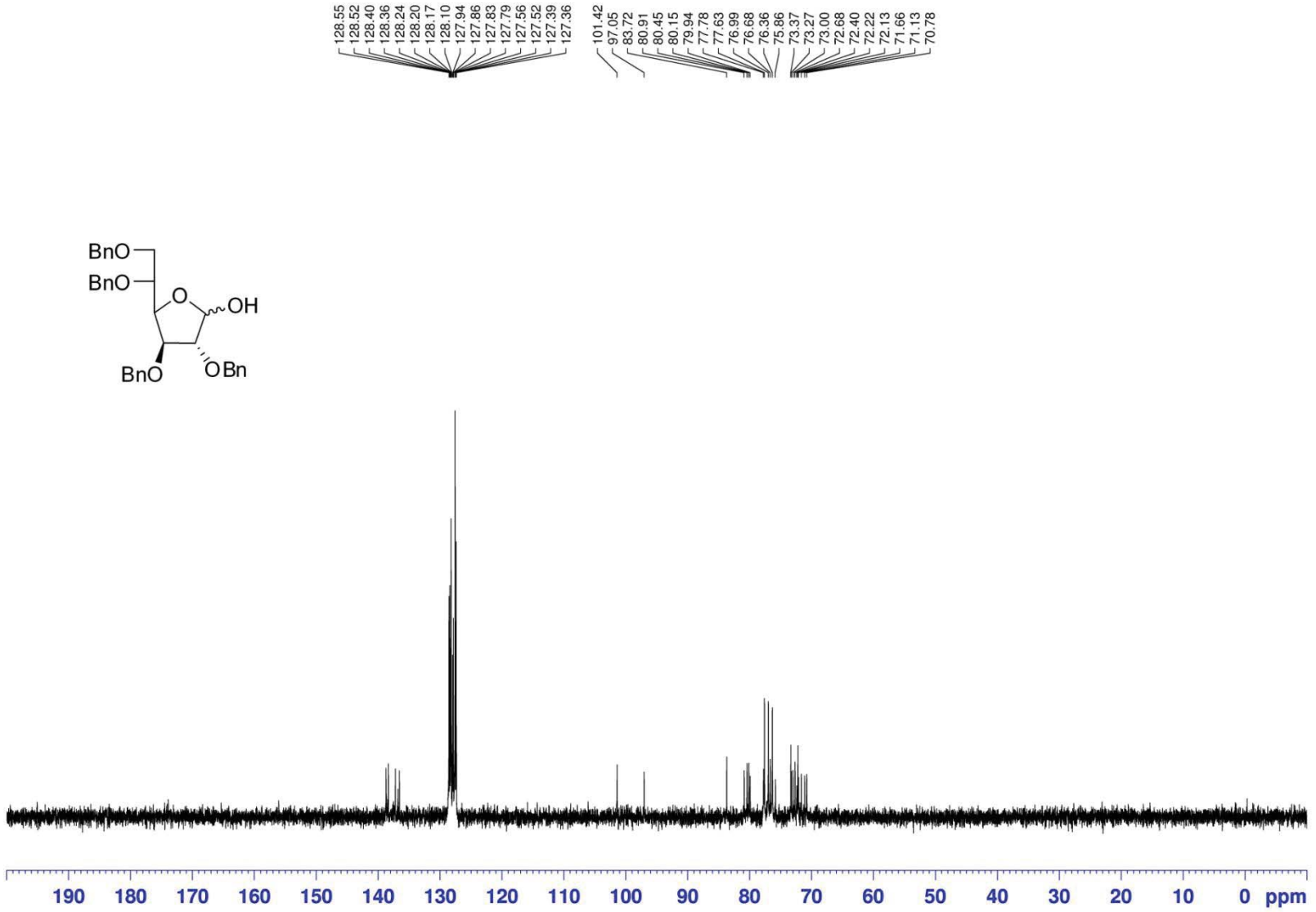

Appendix 5. ^{13}C-NMR spectra of **45** (50 MHz, $CDCl_3$)

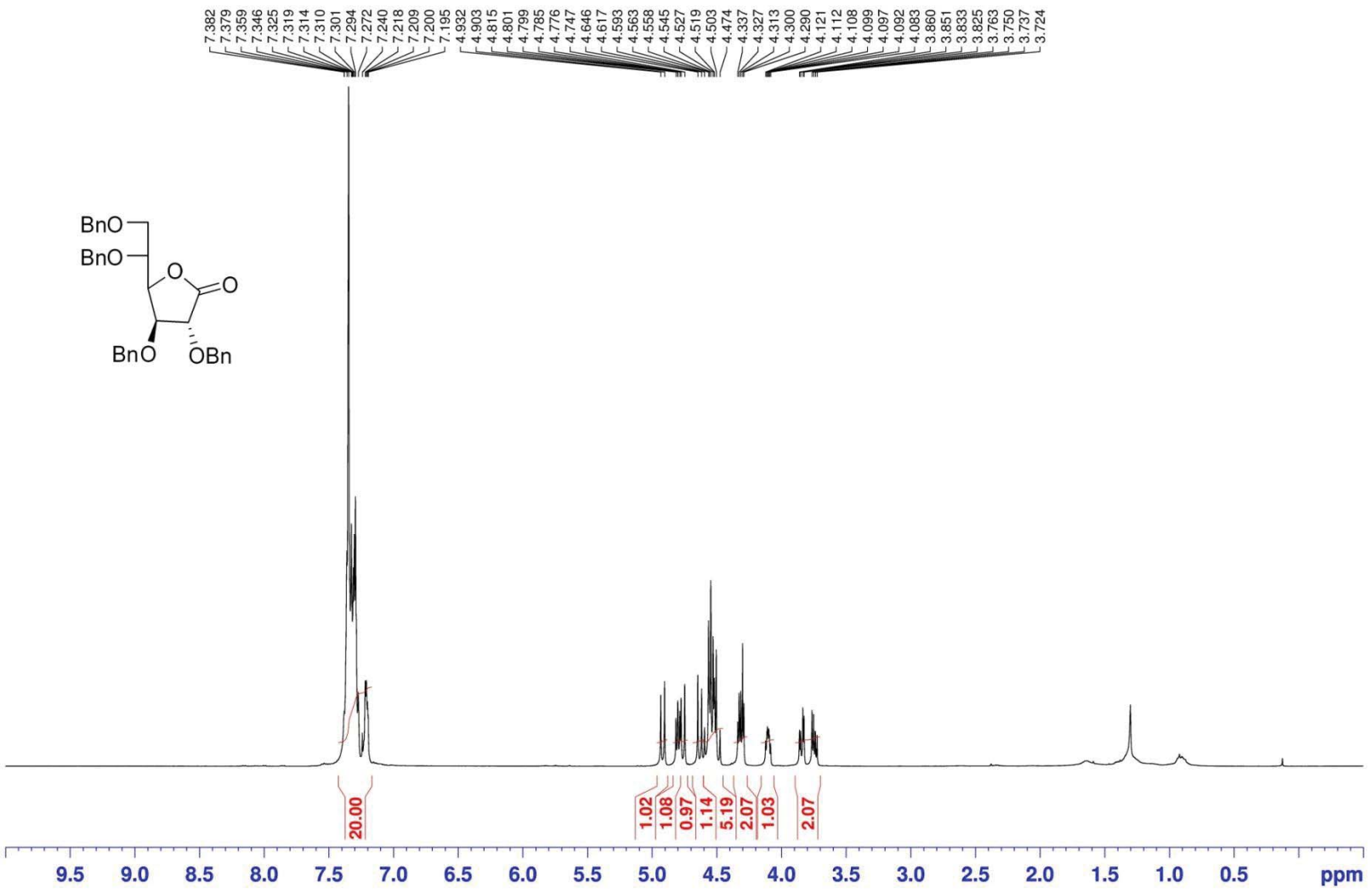

Appendix 6. ^{1}H-NMR spectra of **46** (400 MHz, $CDCl_3$)

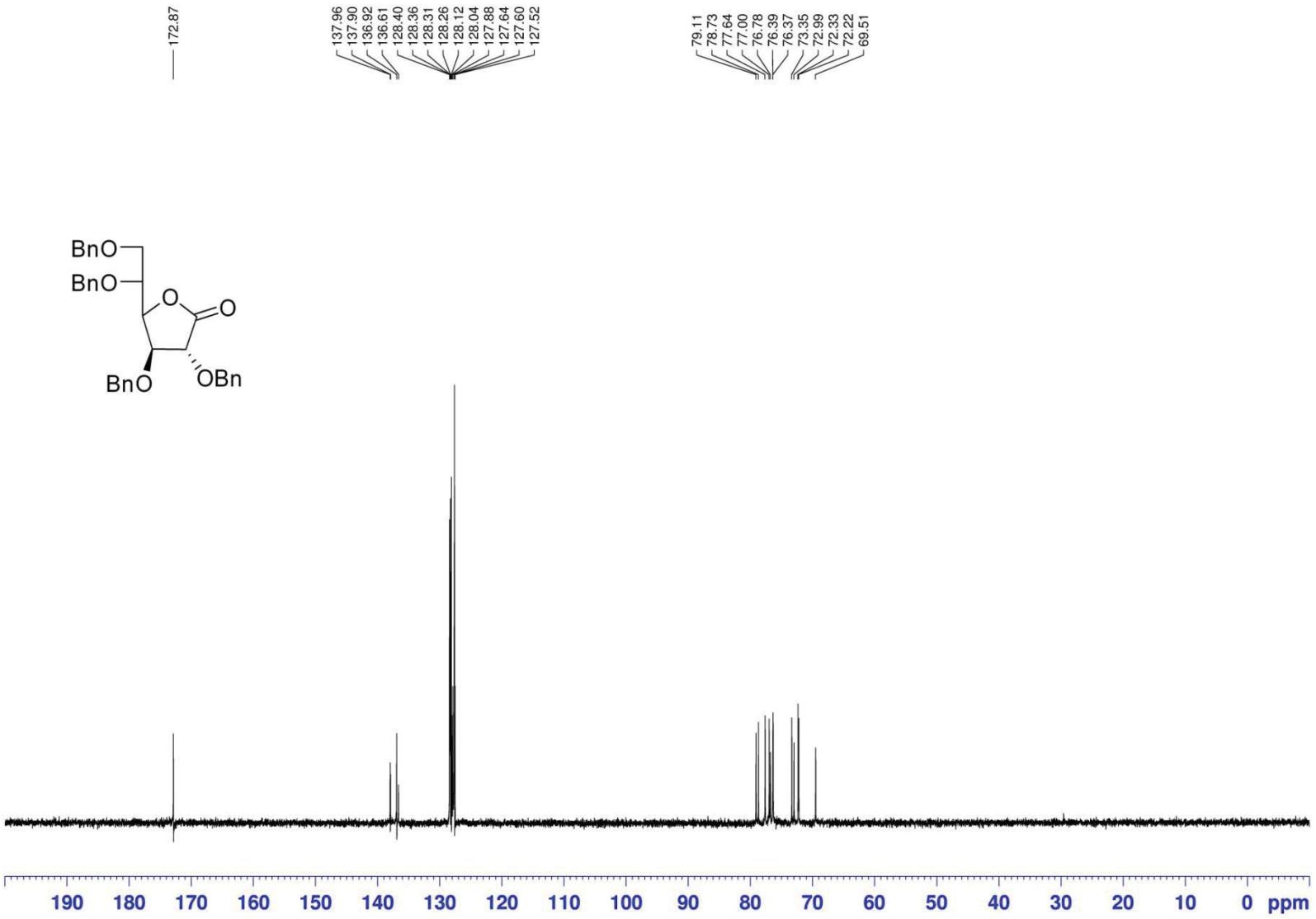

Appendix 7. ^{13}C-NMR spectra of **46** (50 MHz, $CDCl_3$)

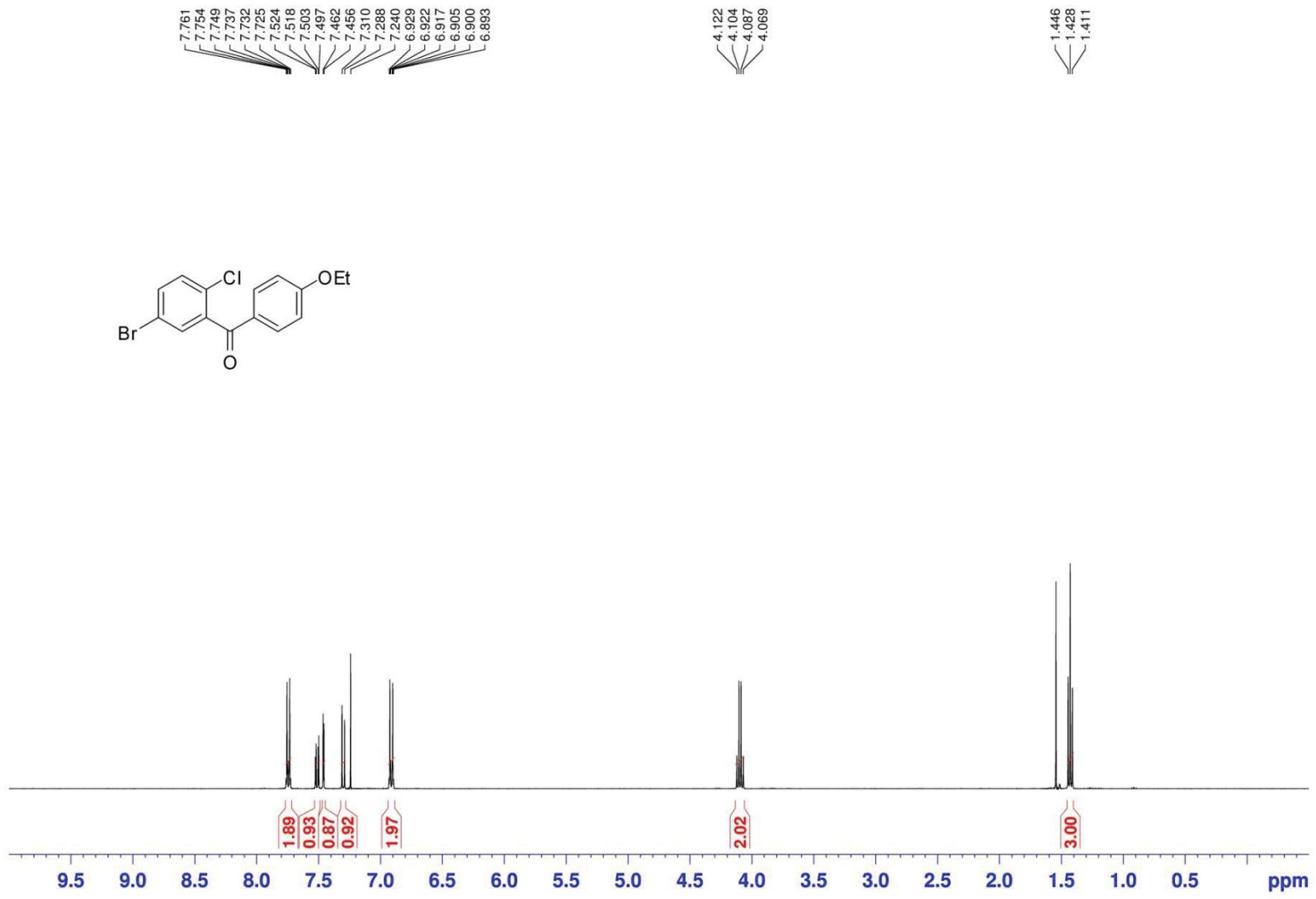

Appendix 8. ^{1}H-NMR spectra of **49a** (400 MHz, $CDCl_3$)

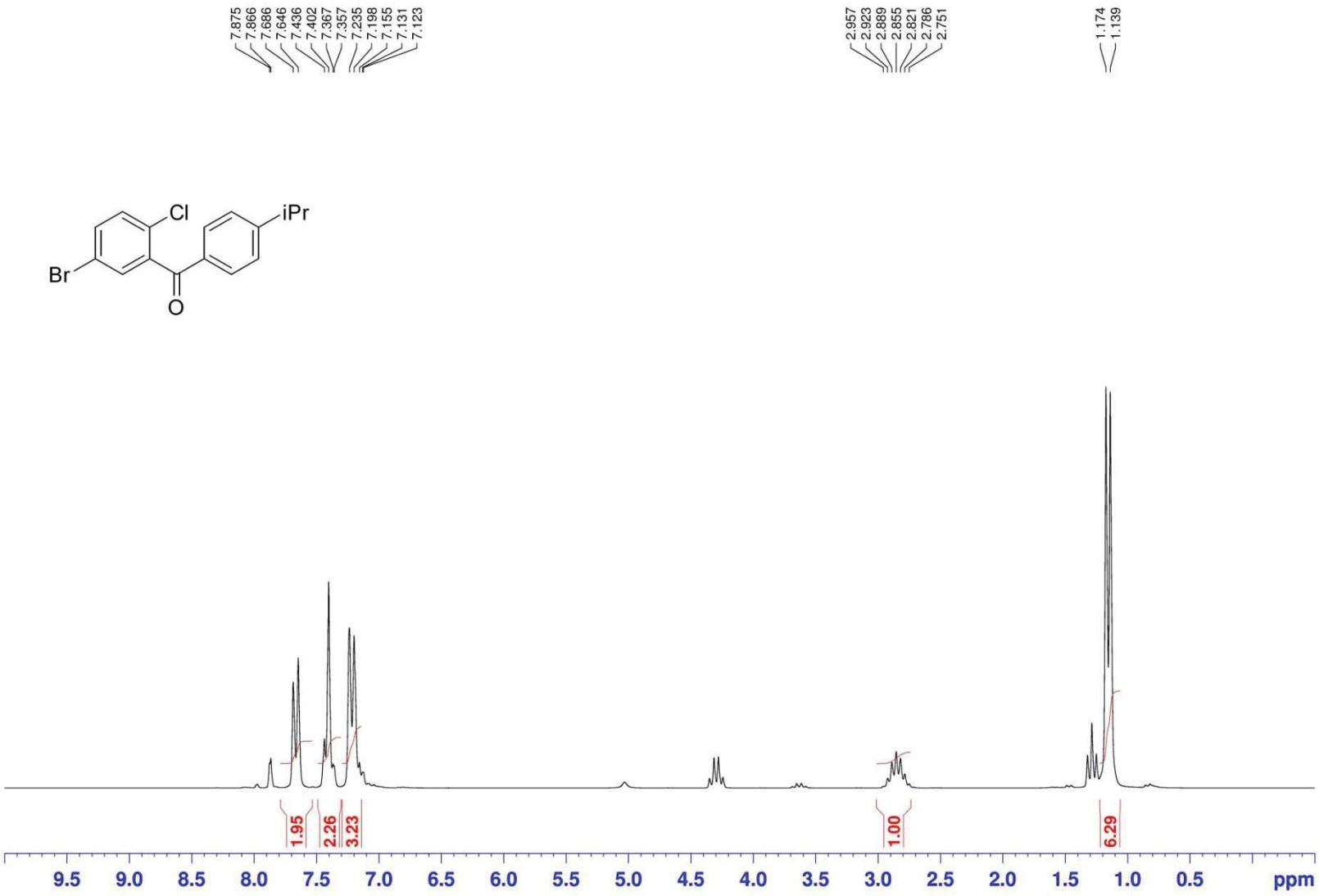

Appendix 9. ^{1}H-NMR spectra of **49b** (200 MHz, $CDCl_3$)

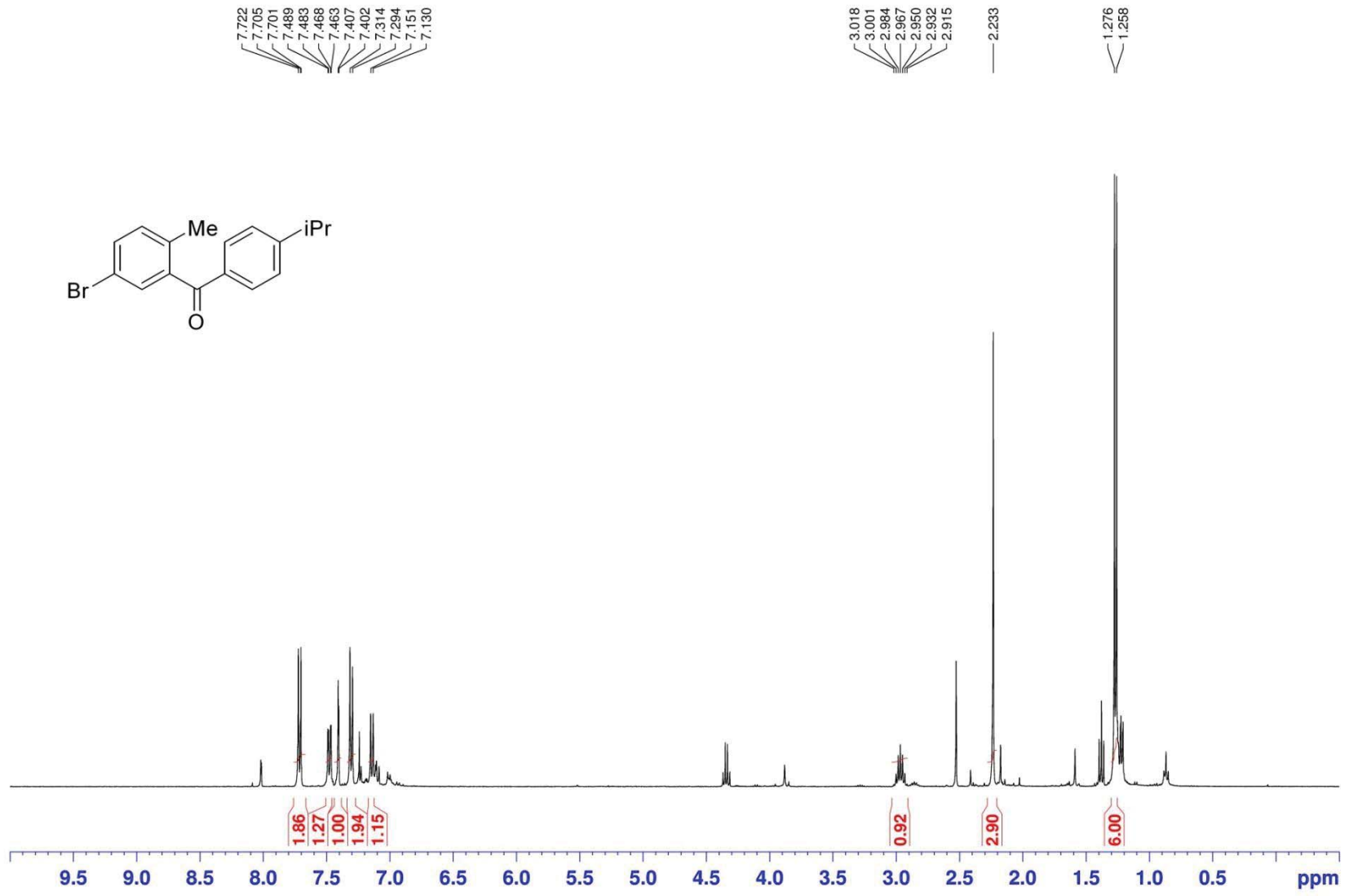

Appendix 10. ^{1}H-NMR spectra of **49d** (400 MHz, $CDCl_3$)

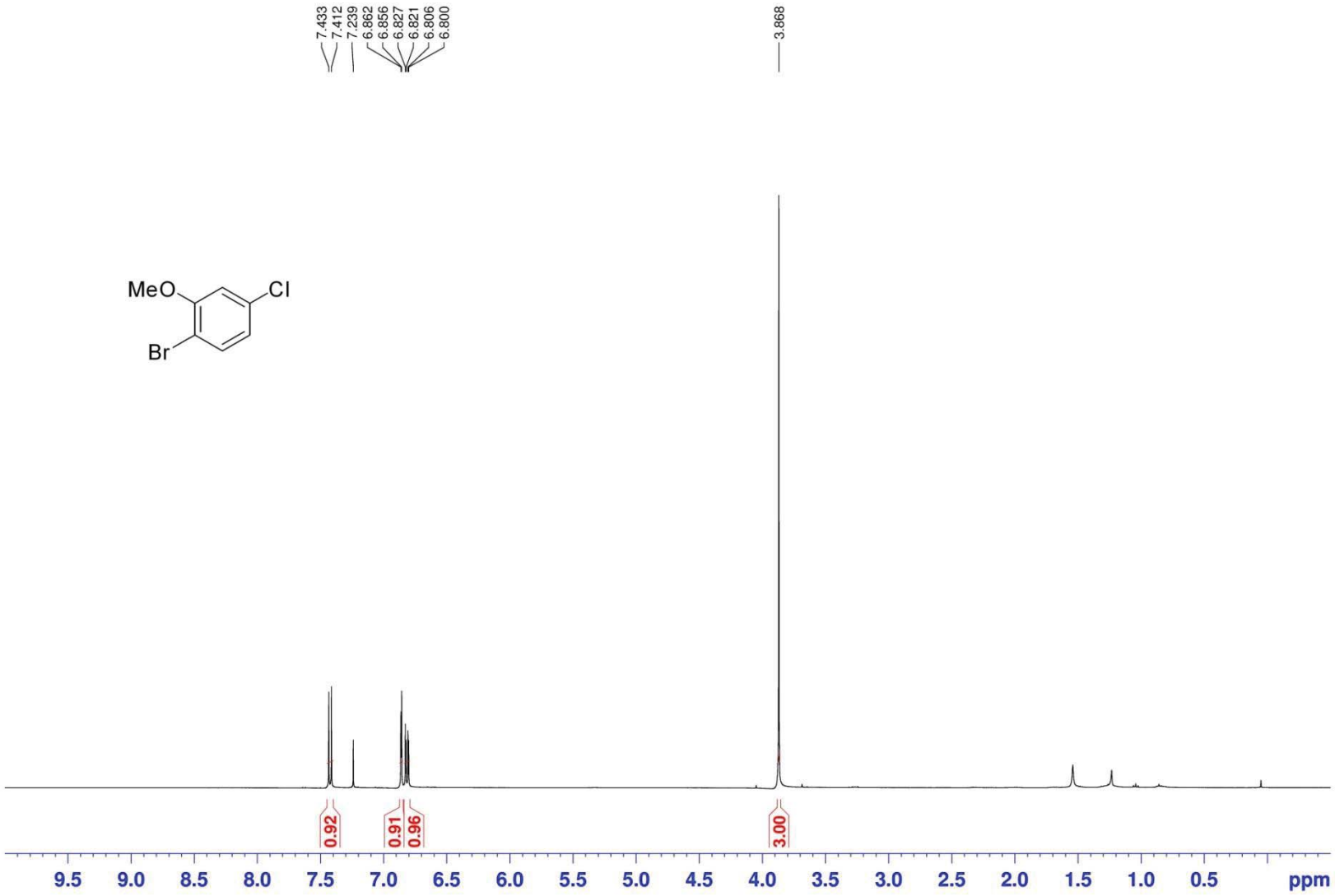

Appendix 11. ^{1}H-NMR spectra of **51** (400 MHz, $CDCl_3$)

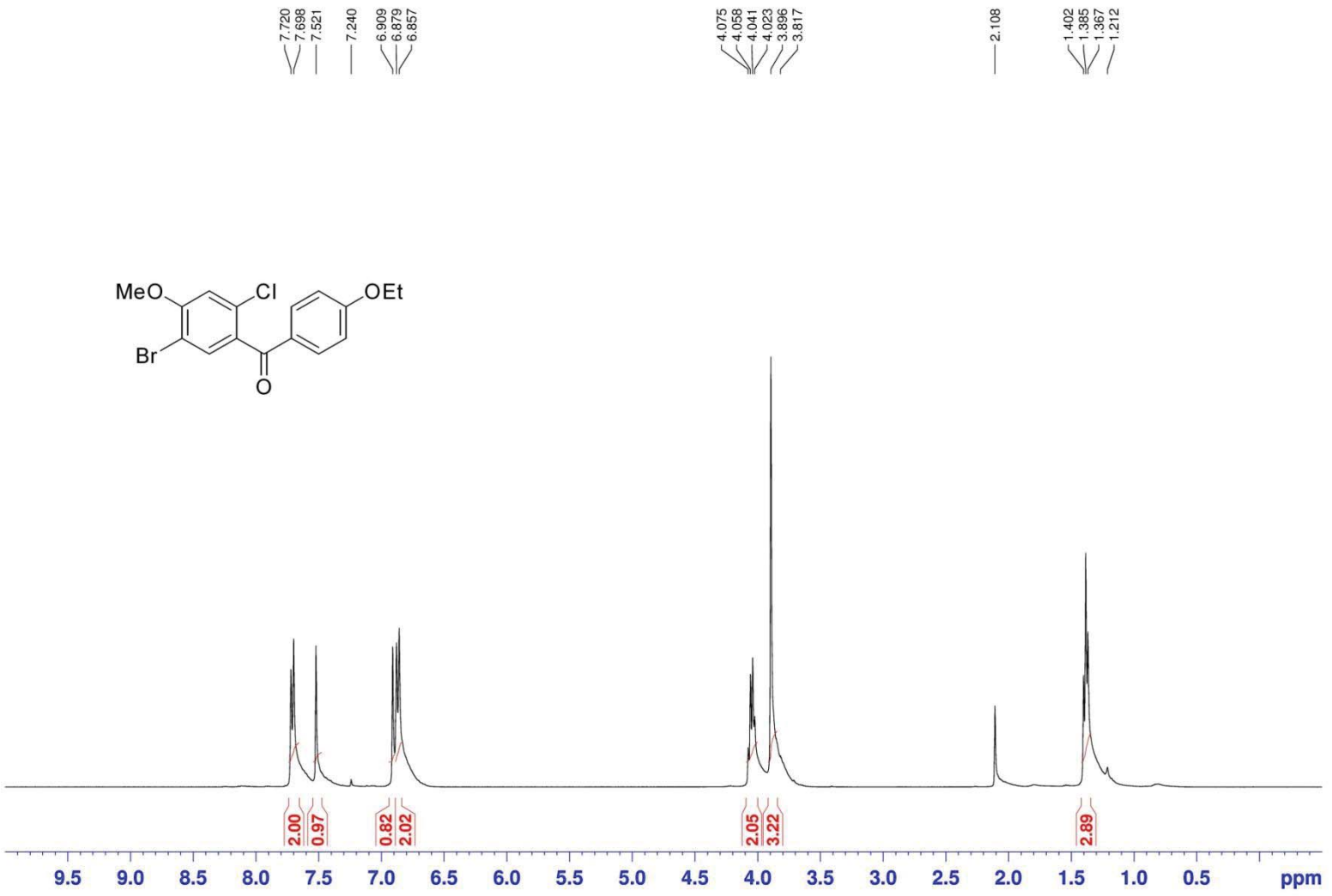

Appendix 12. ^{1}H-NMR spectra of **49f** (400 MHz, $CDCl_3$)

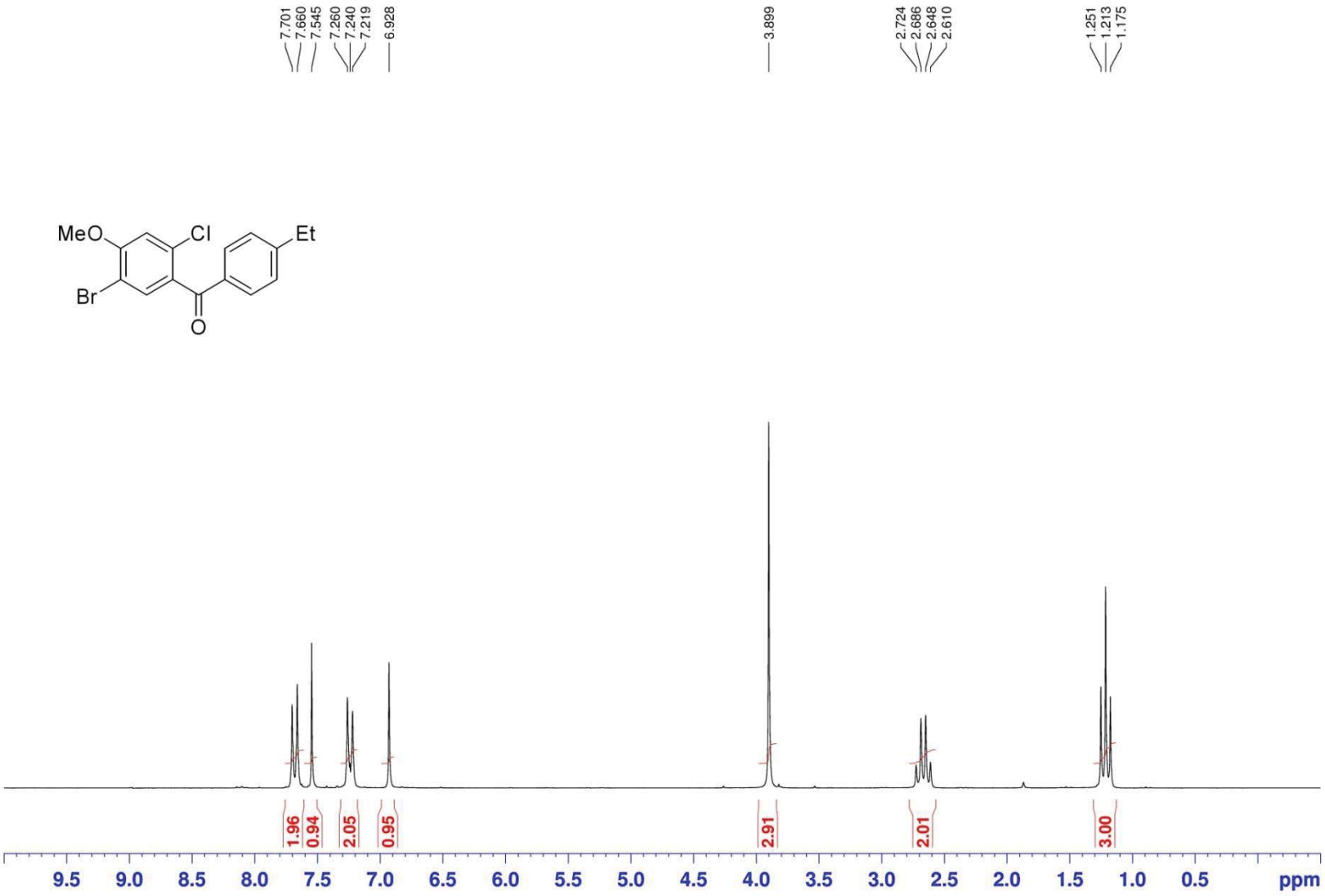

Appendix 13. ^{1}H-NMR spectra of **49g** (200 MHz, $CDCl_3$)

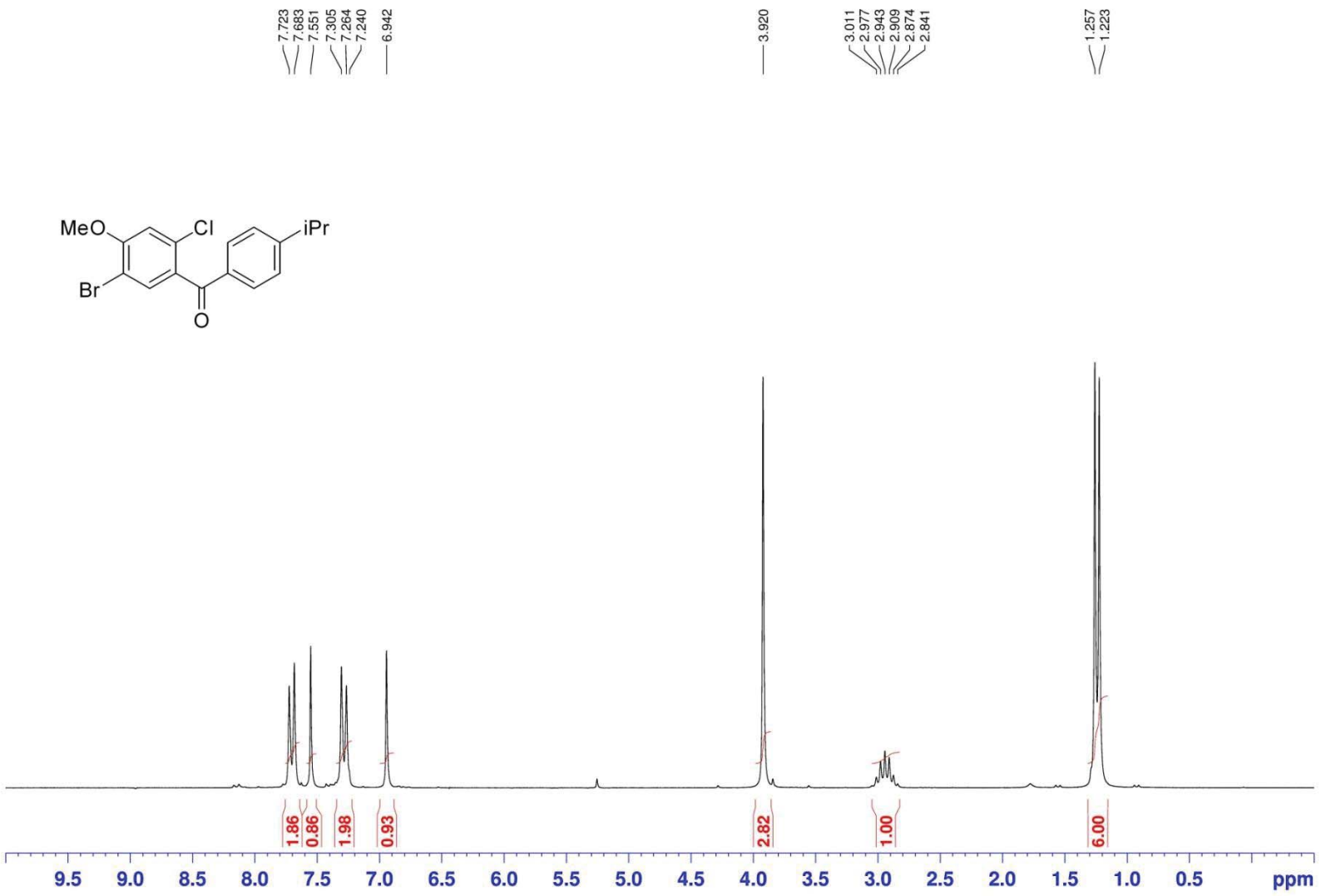

Appendix 14. ^{1}H-NMR spectra of **49h** (200 MHz, $CDCl_3$)

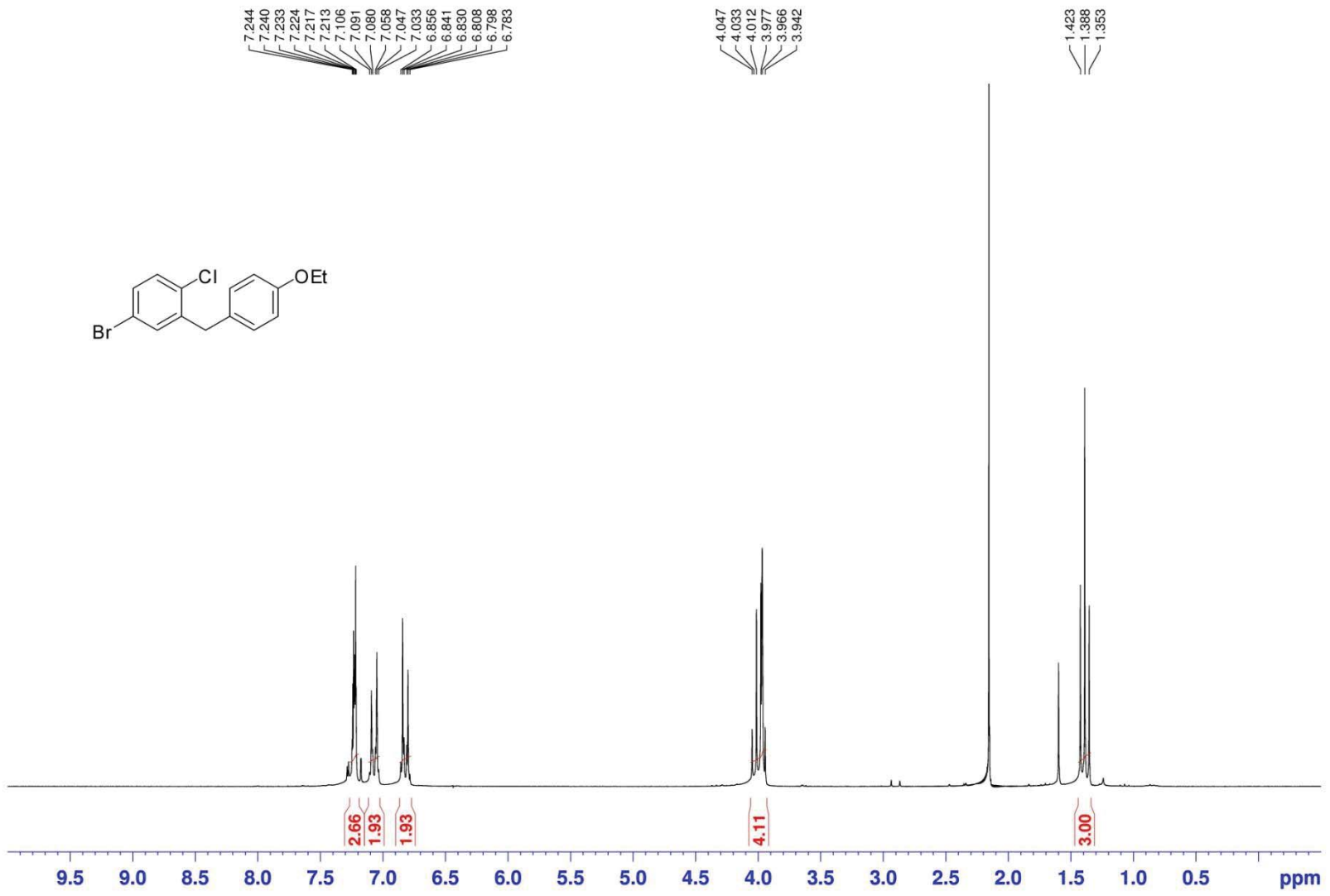

Appendix 15. ^{1}H-NMR spectra of **50a** (200 MHz, $CDCl_3$)

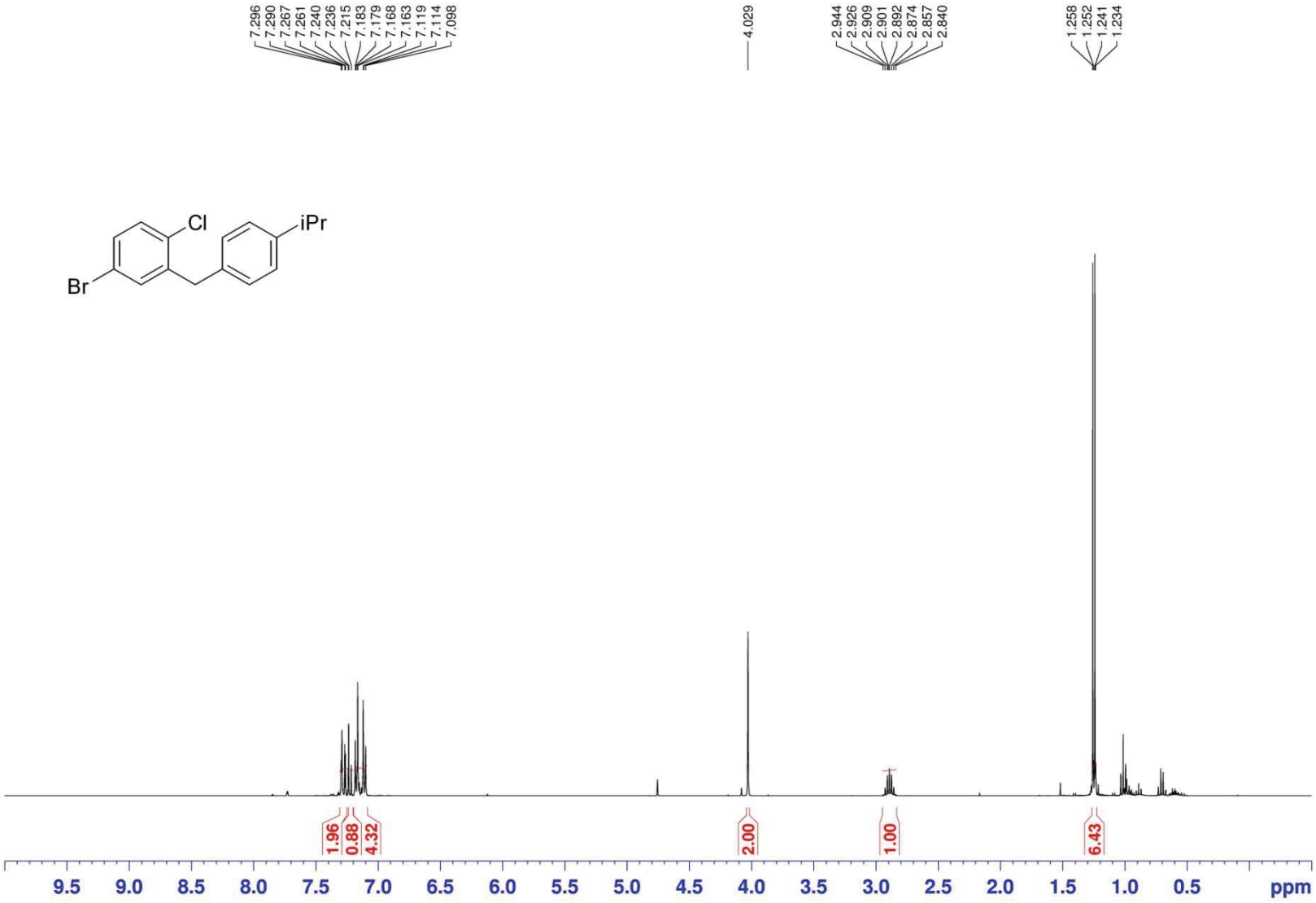

Appendix 16. ^{1}H-NMR spectra of **50b** (400 MHz, $CDCl_3$)

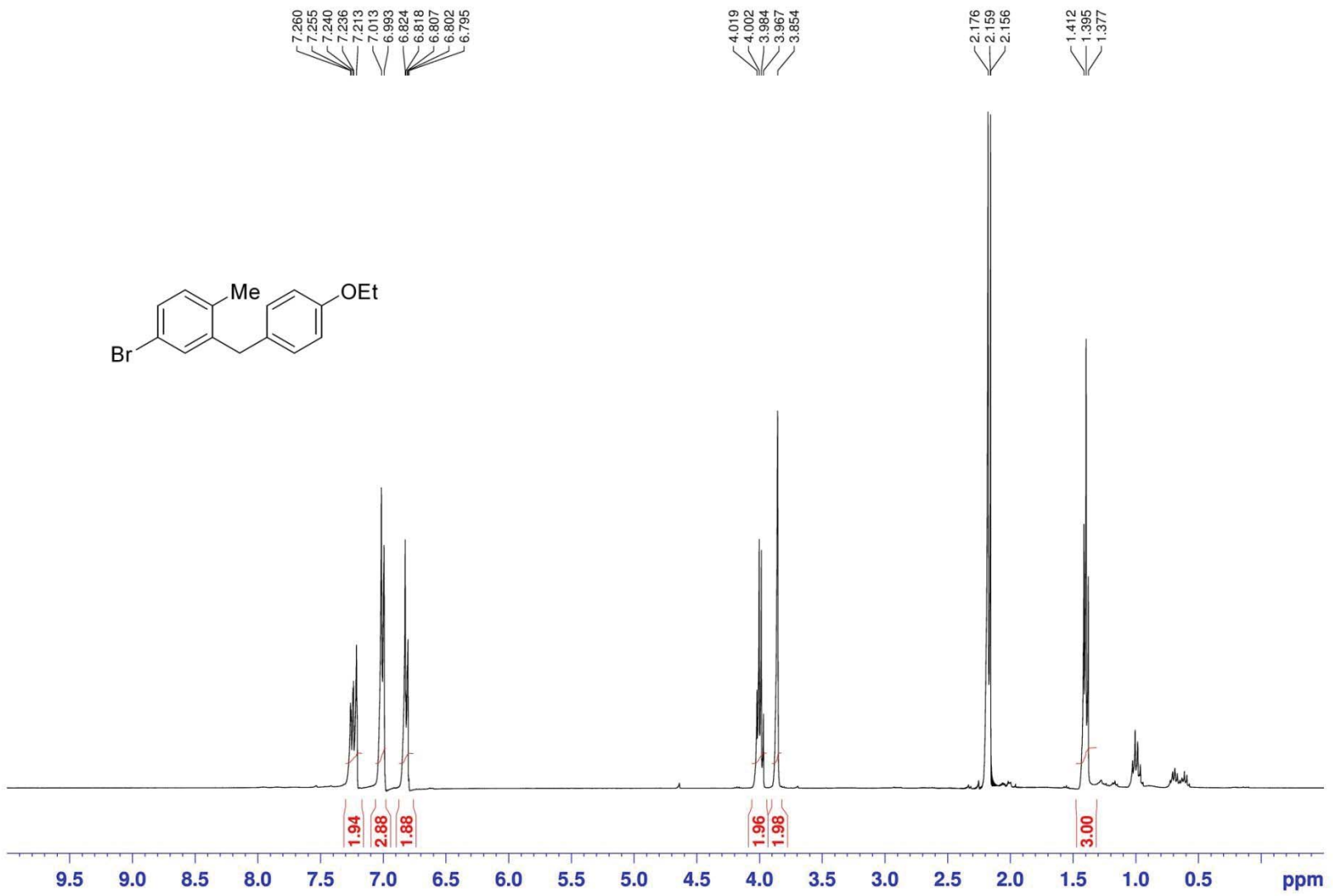

Appendix 17. ^{1}H-NMR spectra of **50c** (400 MHz, $CDCl_3$)

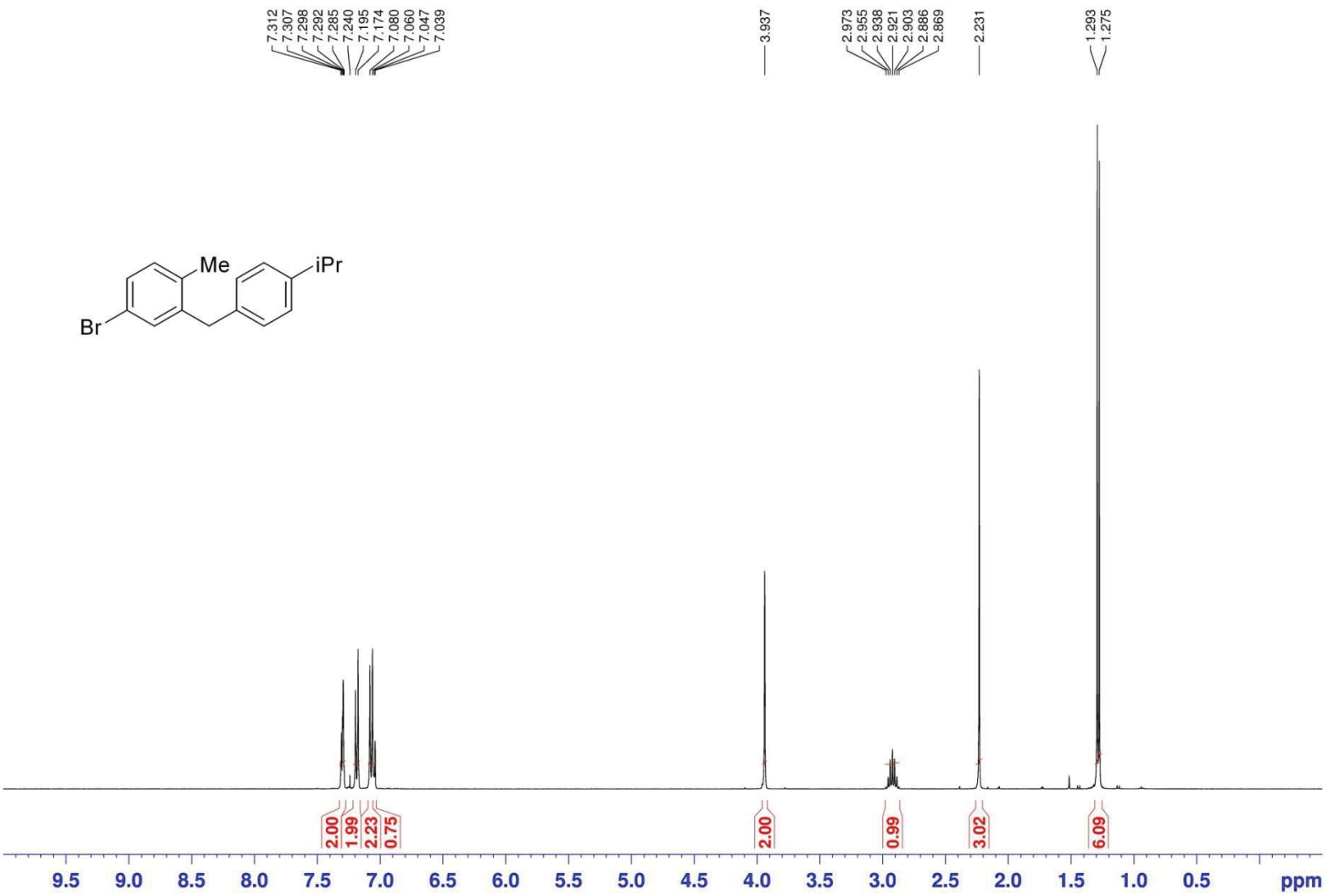

Appendix 18. ^{1}H-NMR spectra of **50d** (400 MHz, $CDCl_3$)

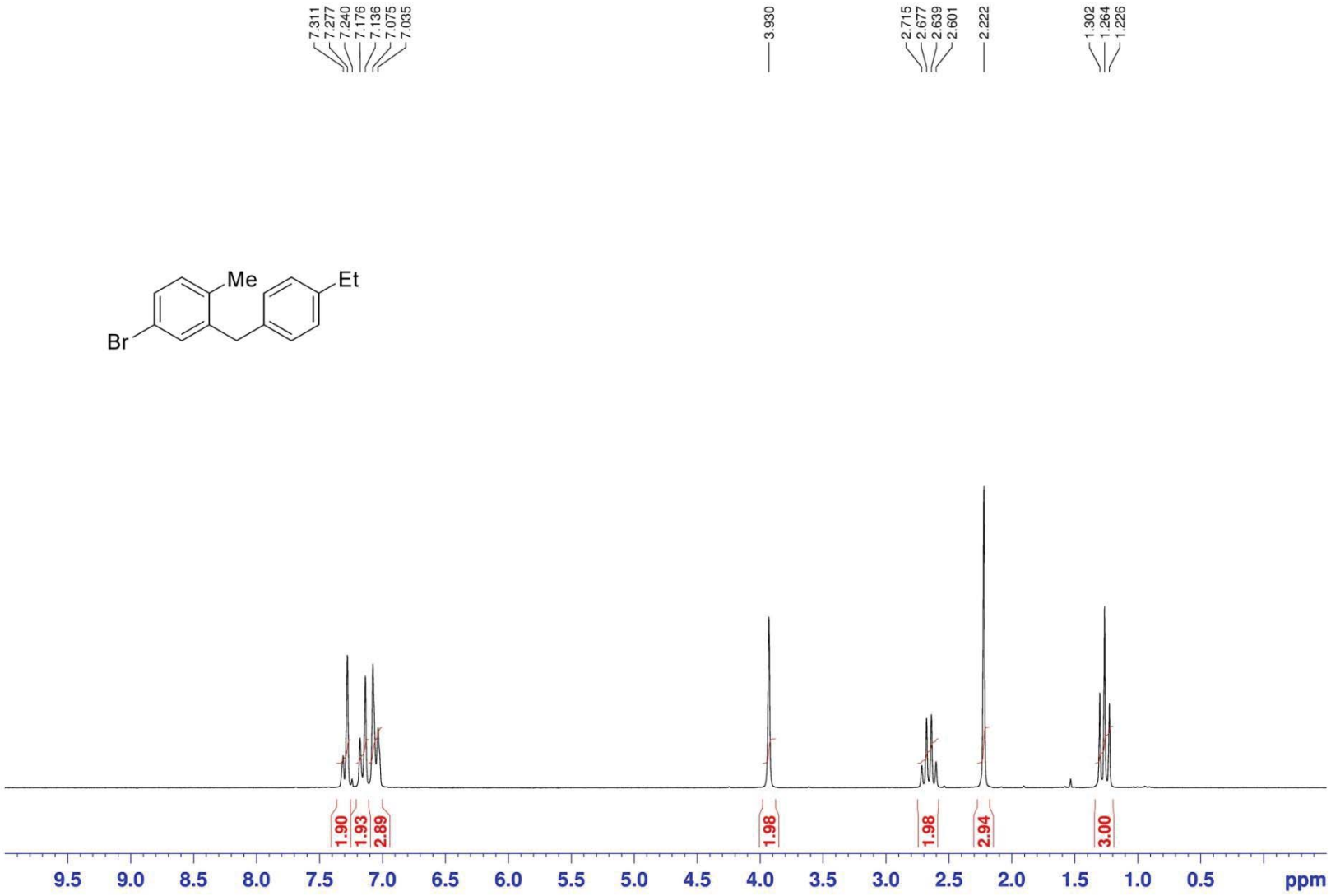

Appendix 19. ^{1}H-NMR spectra of **50e** (200 MHz, $CDCl_3$)

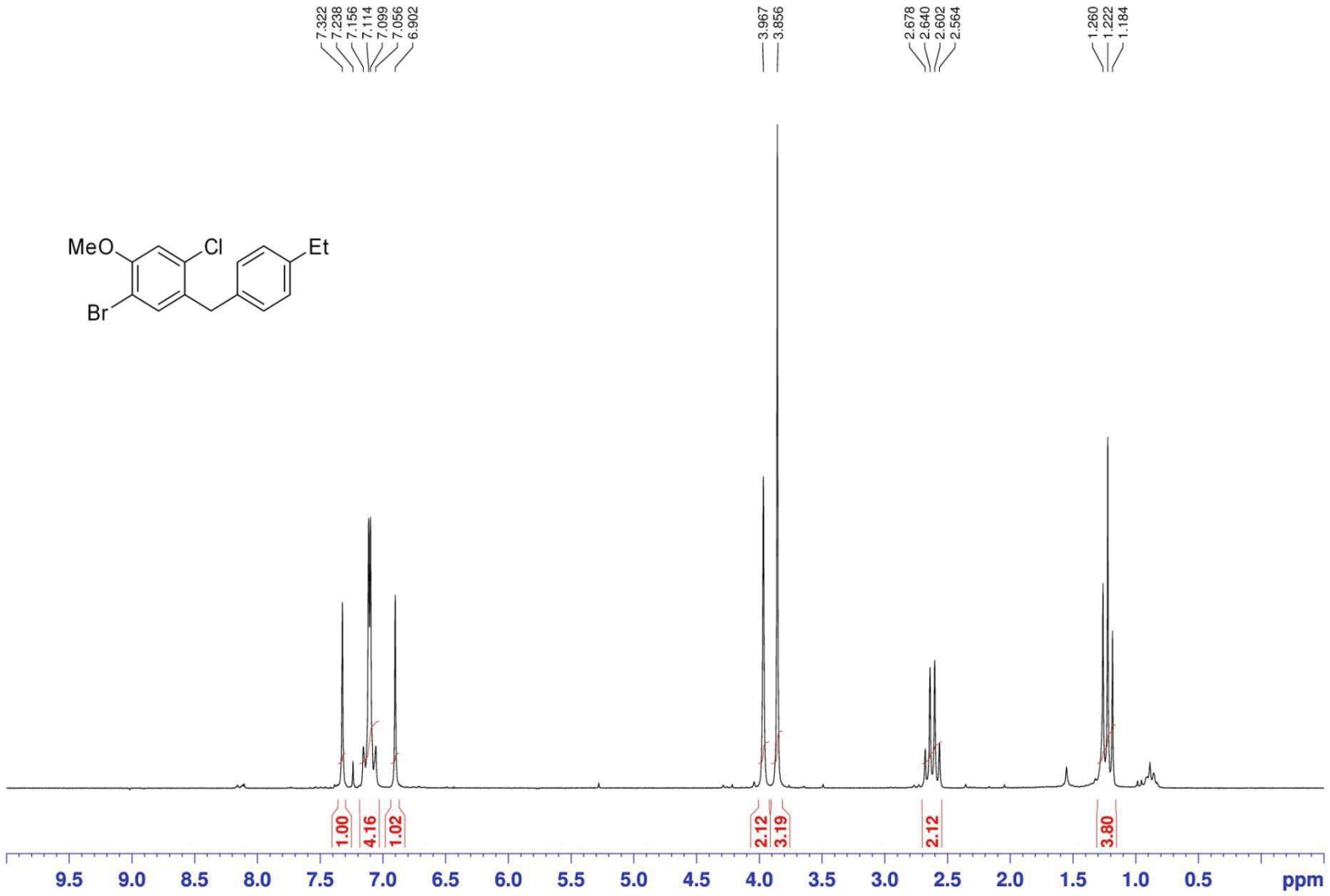

Appendix 20. ^{1}H-NMR spectra of **50g** (200 MHz, $CDCl_3$)

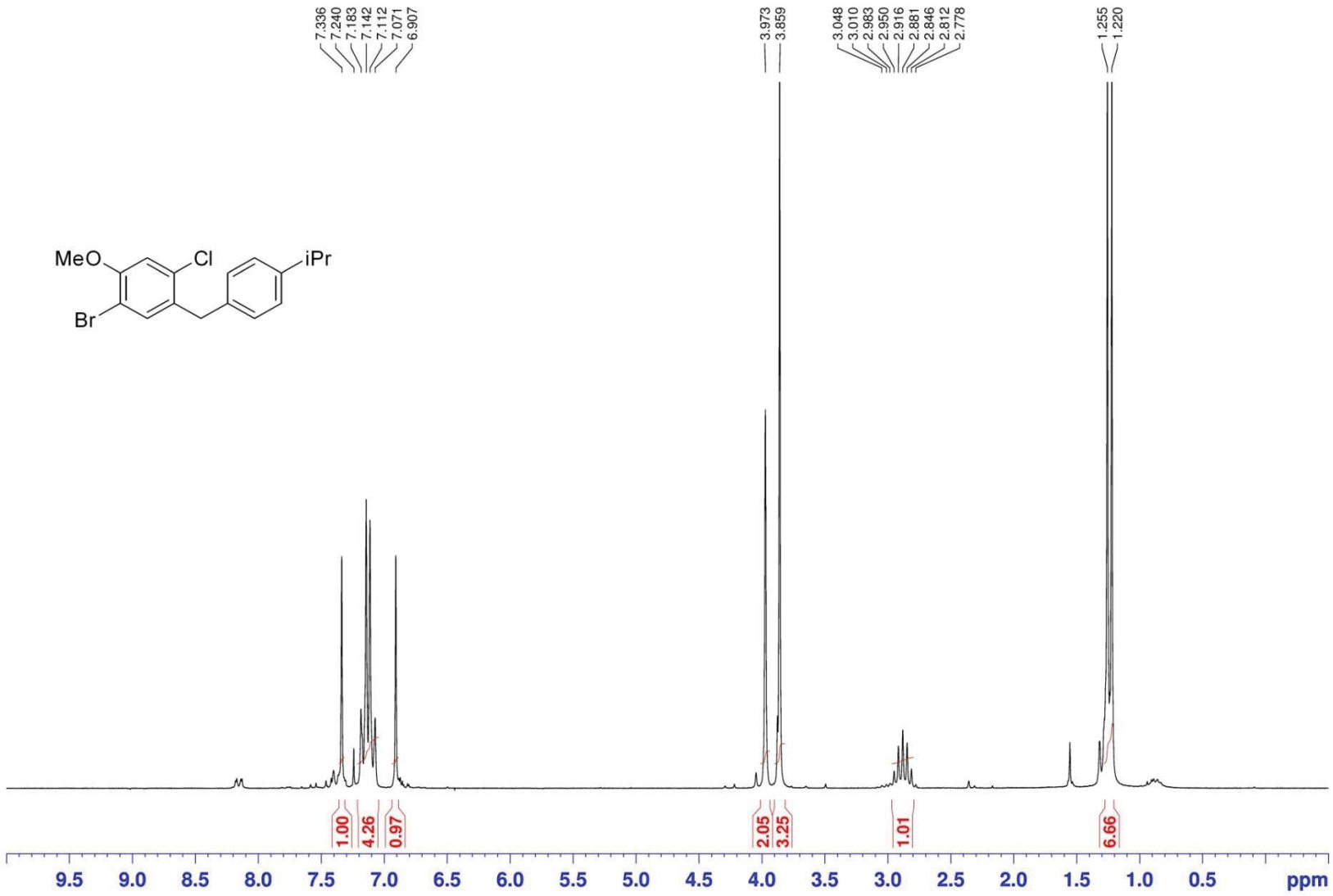

Appendix 21. ^{1}H-NMR spectra of **50h** (200 MHz, $CDCl_3$)

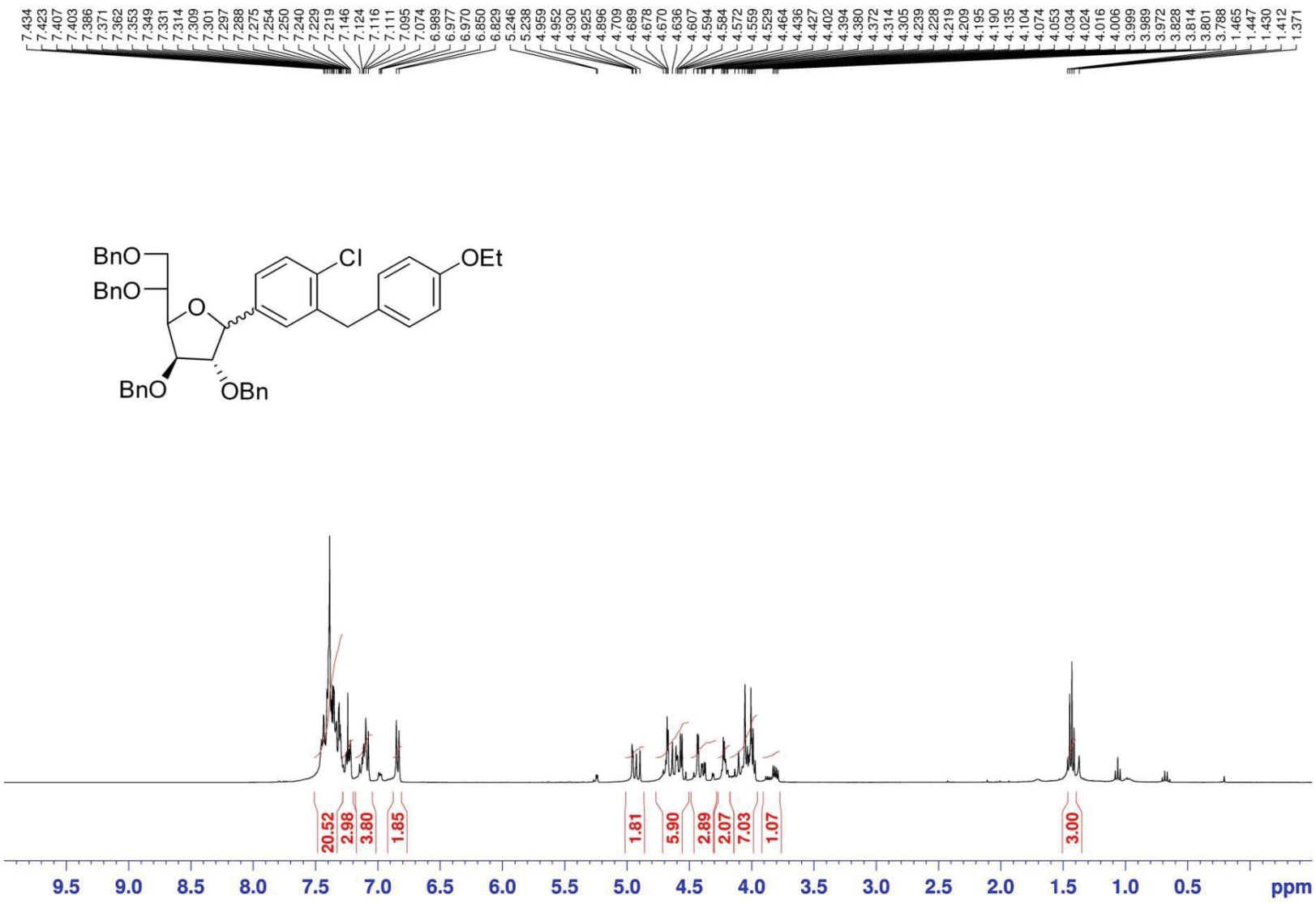

Appendix 22. ^{1}H-NMR spectra of **56a** (400 MHz, $CDCl_3$)

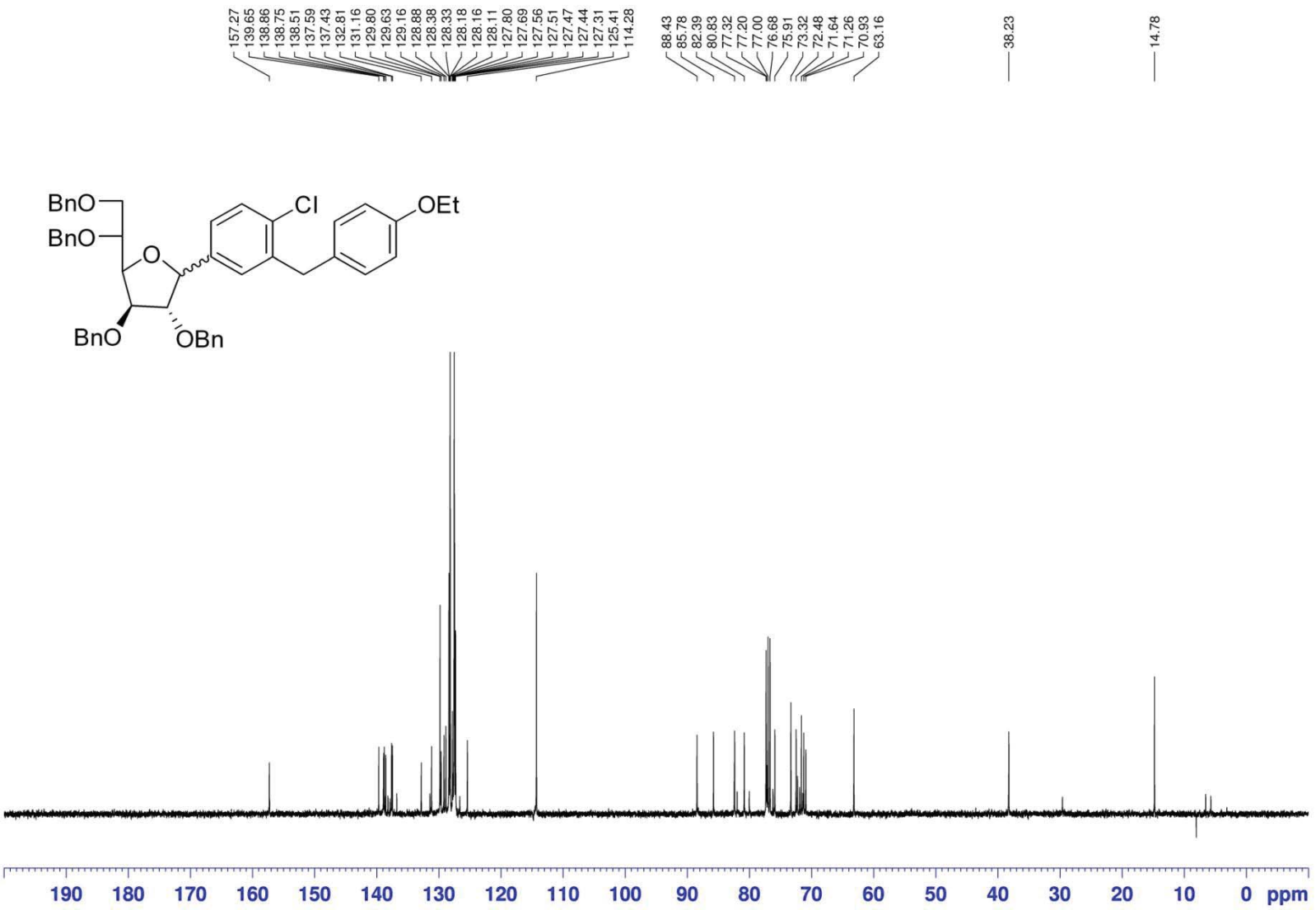

Appendix 23. ^{13}C-NMR spectra of **56a** (100 MHz, $CDCl_3$)

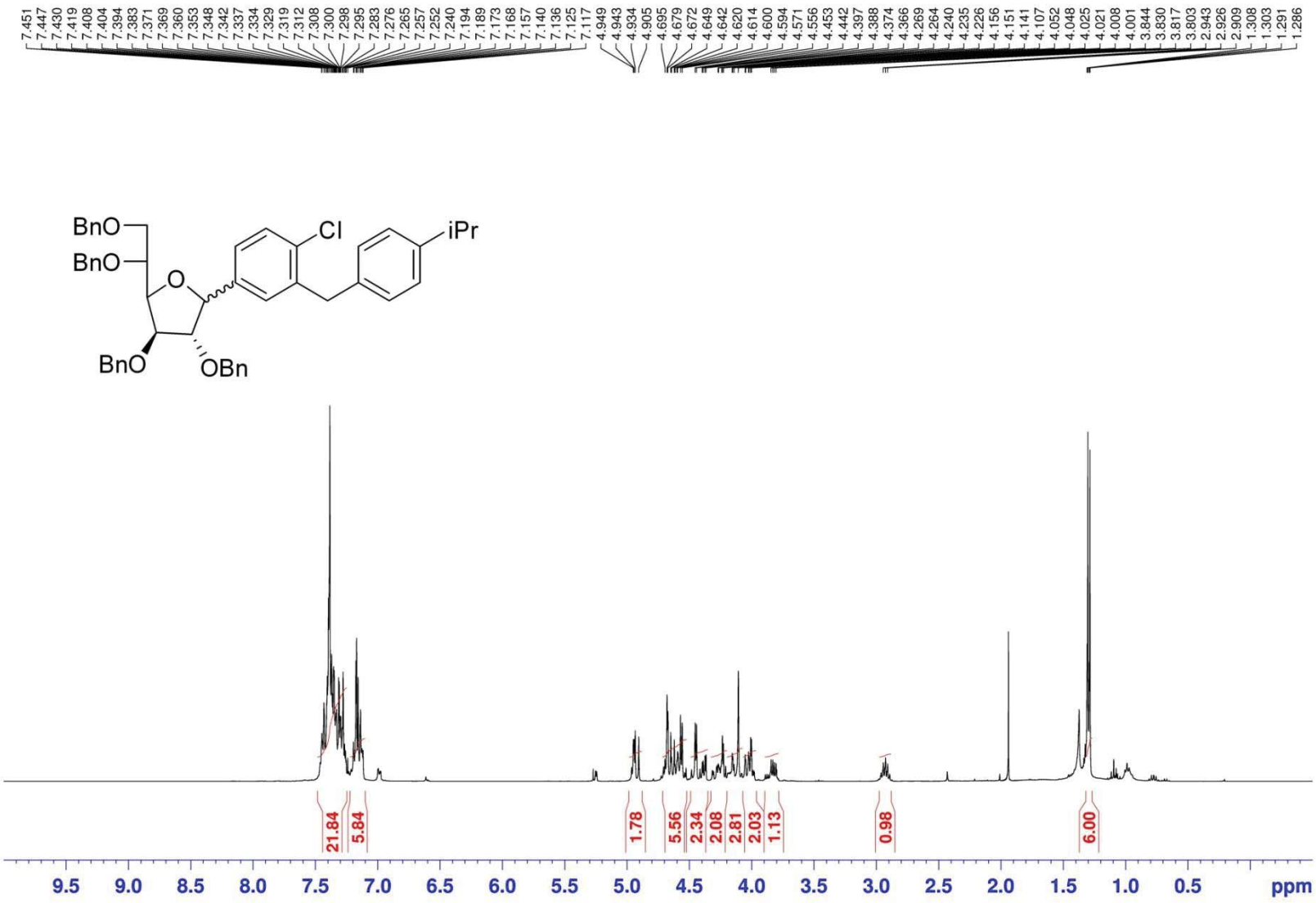

Appendix 24. ^{1}H-NMR spectra of **56b** (400 MHz, $CDCl_3$)

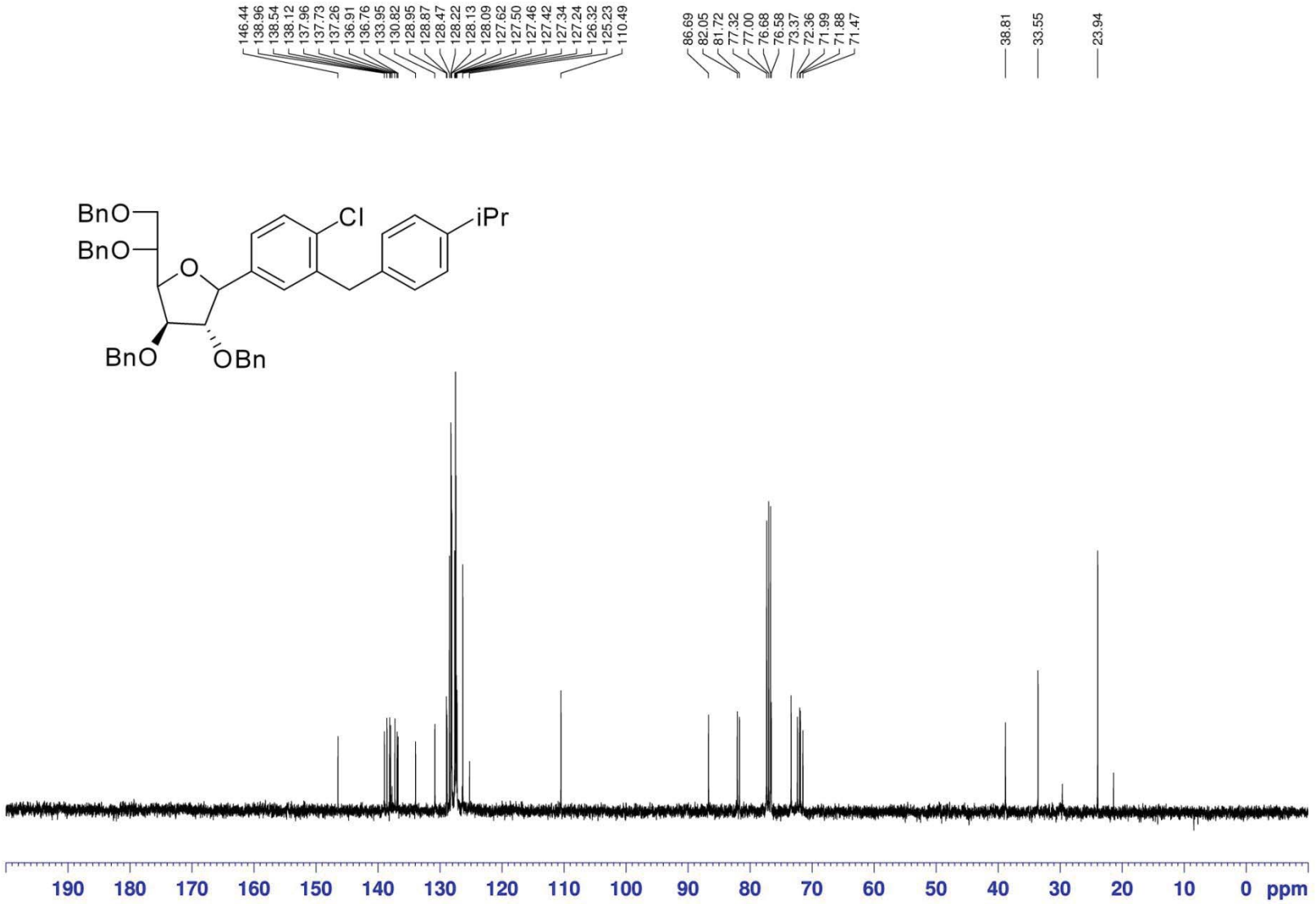

Appendix 25. ^{13}C-NMR spectra of **56b** (100 MHz, $CDCl_3$)

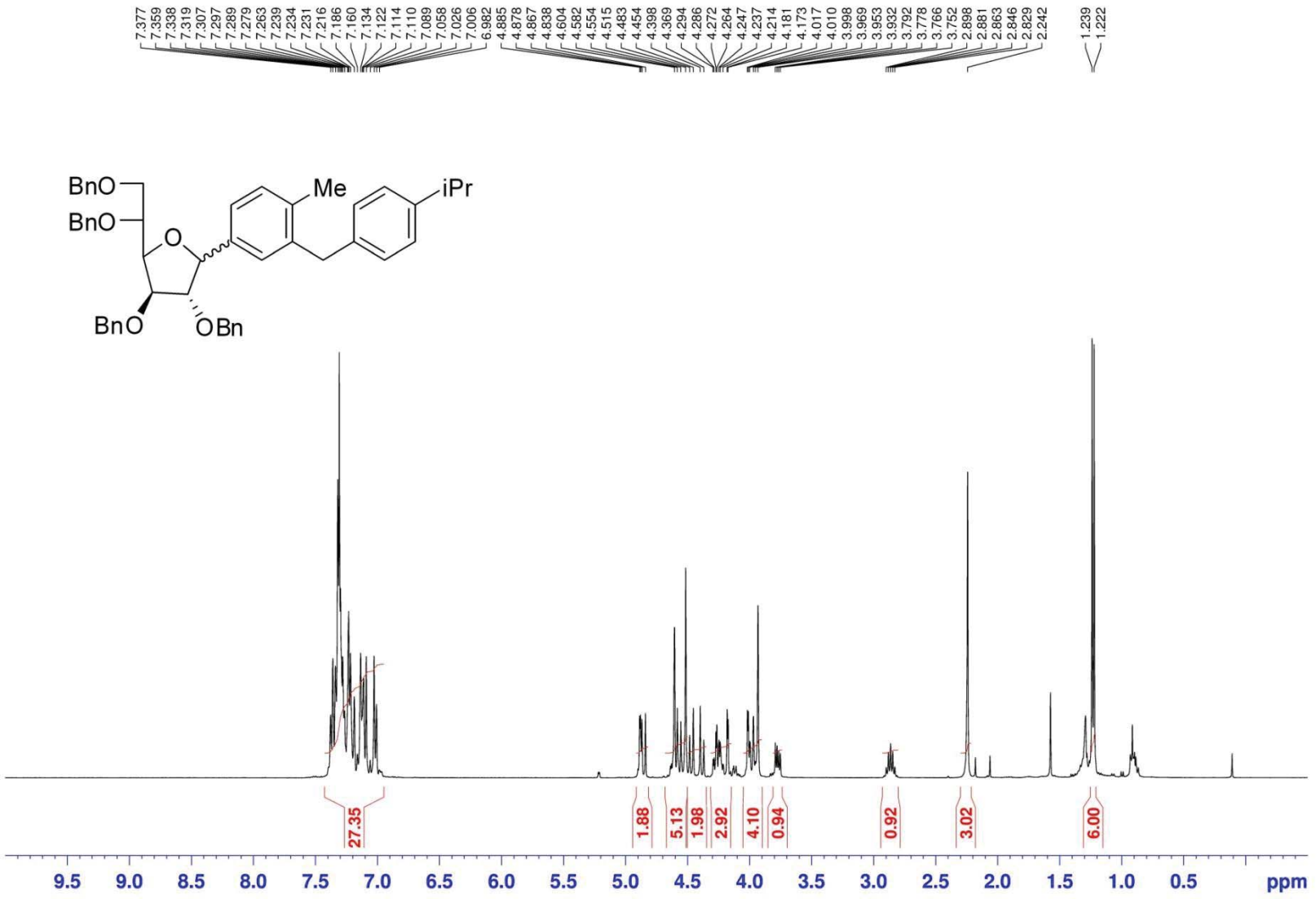

Appendix 26. ^{1}H-NMR spectra of **56d** (400 MHz, $CDCl_3$)

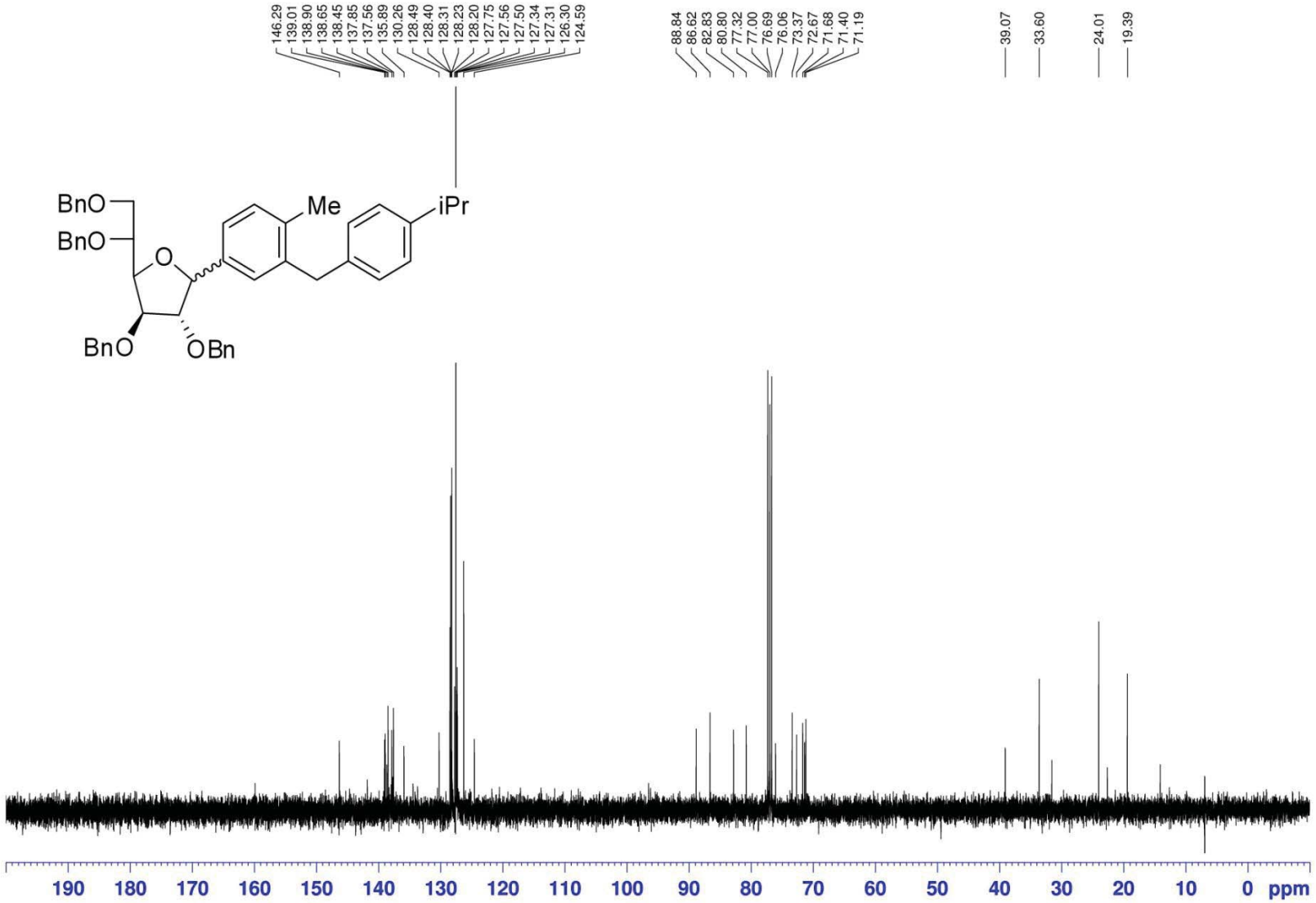

Appendix 27. ^{13}C-NMR spectra of **56d** (100 MHz, $CDCl_3$)

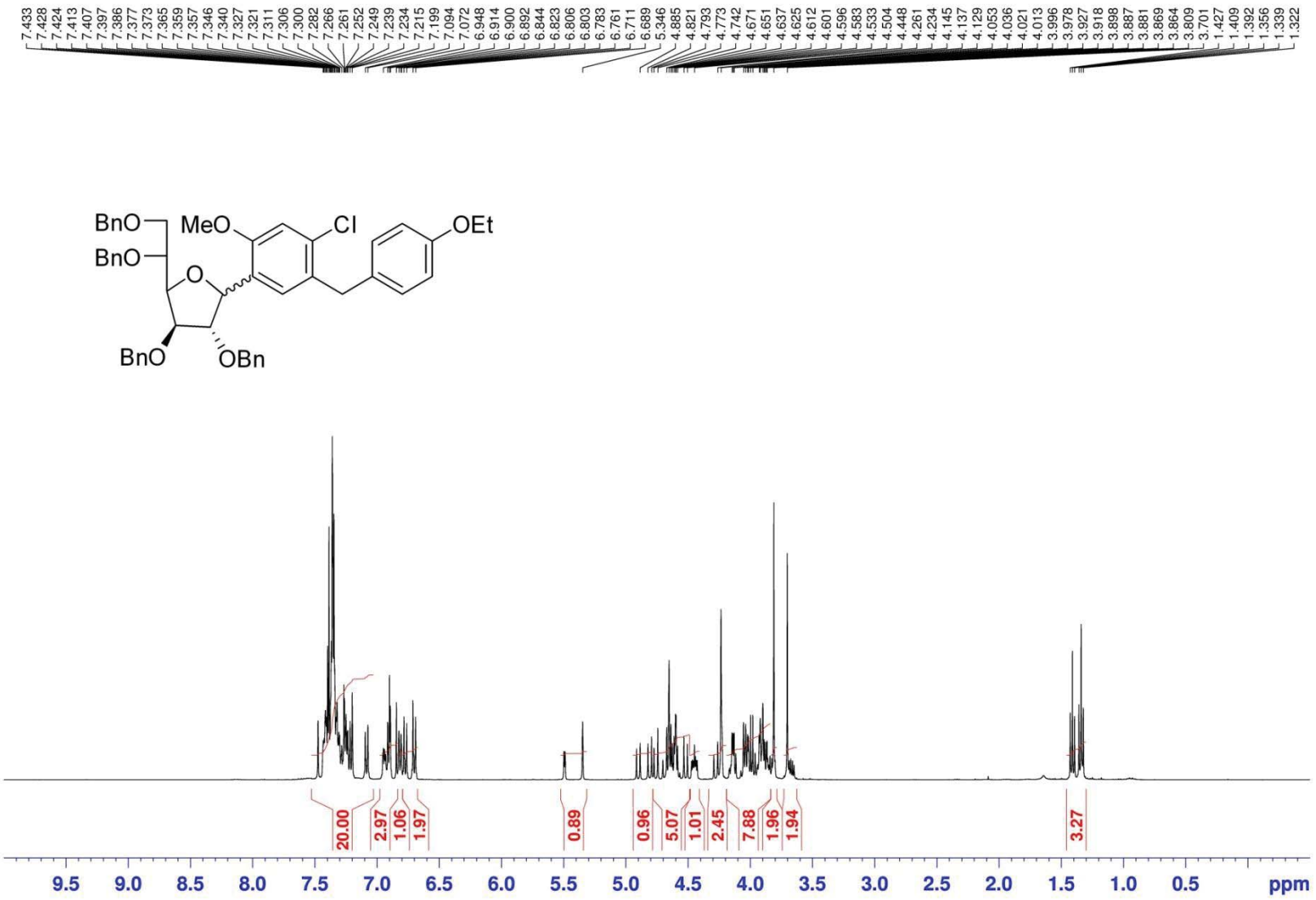

Appendix 28. ^{1}H-NMR spectra of **56f** (400 MHz, $CDCl_3$)

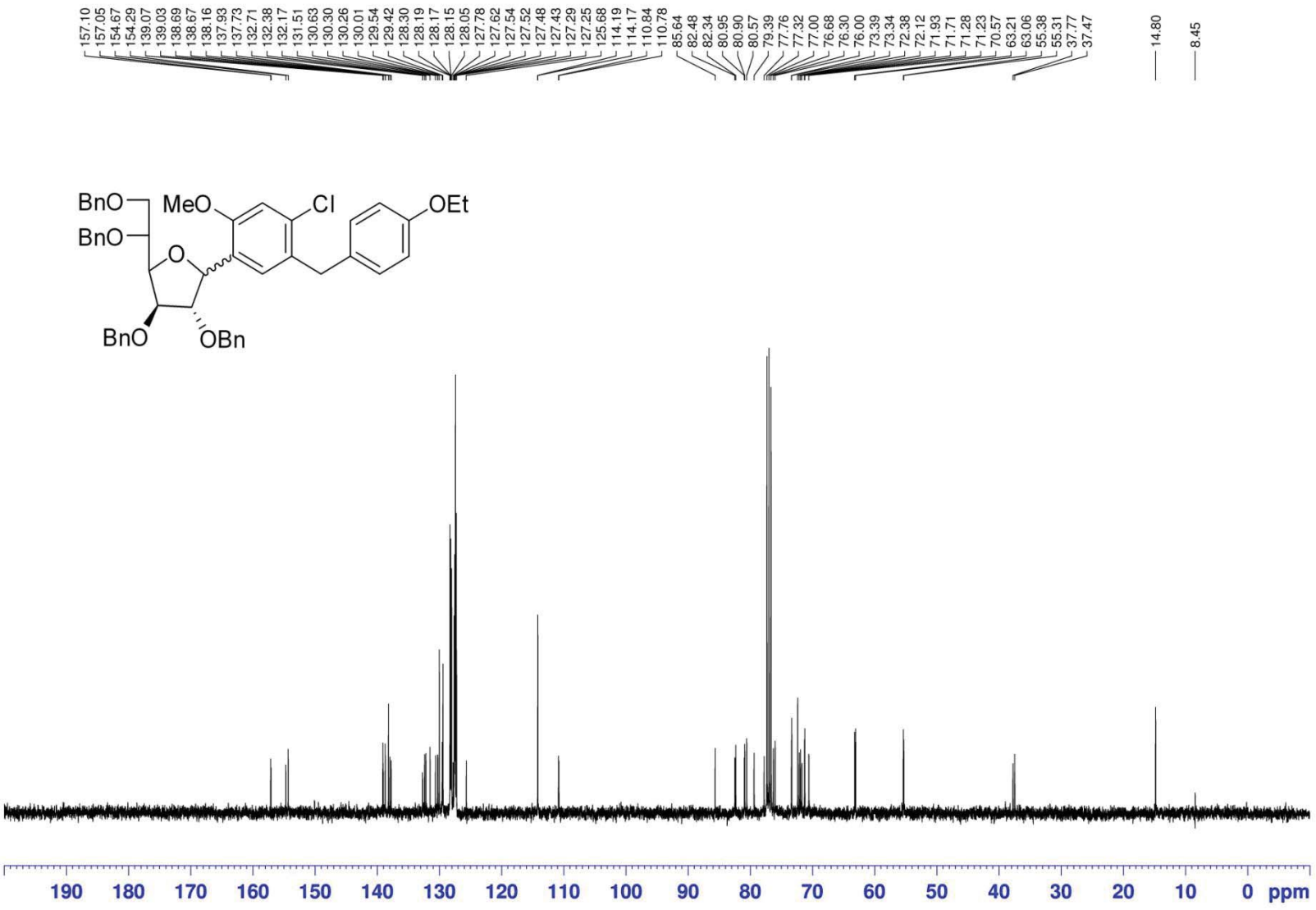

Appendix 29. ^{13}C-NMR spectra of **56f** (100 MHz, $CDCl_3$)

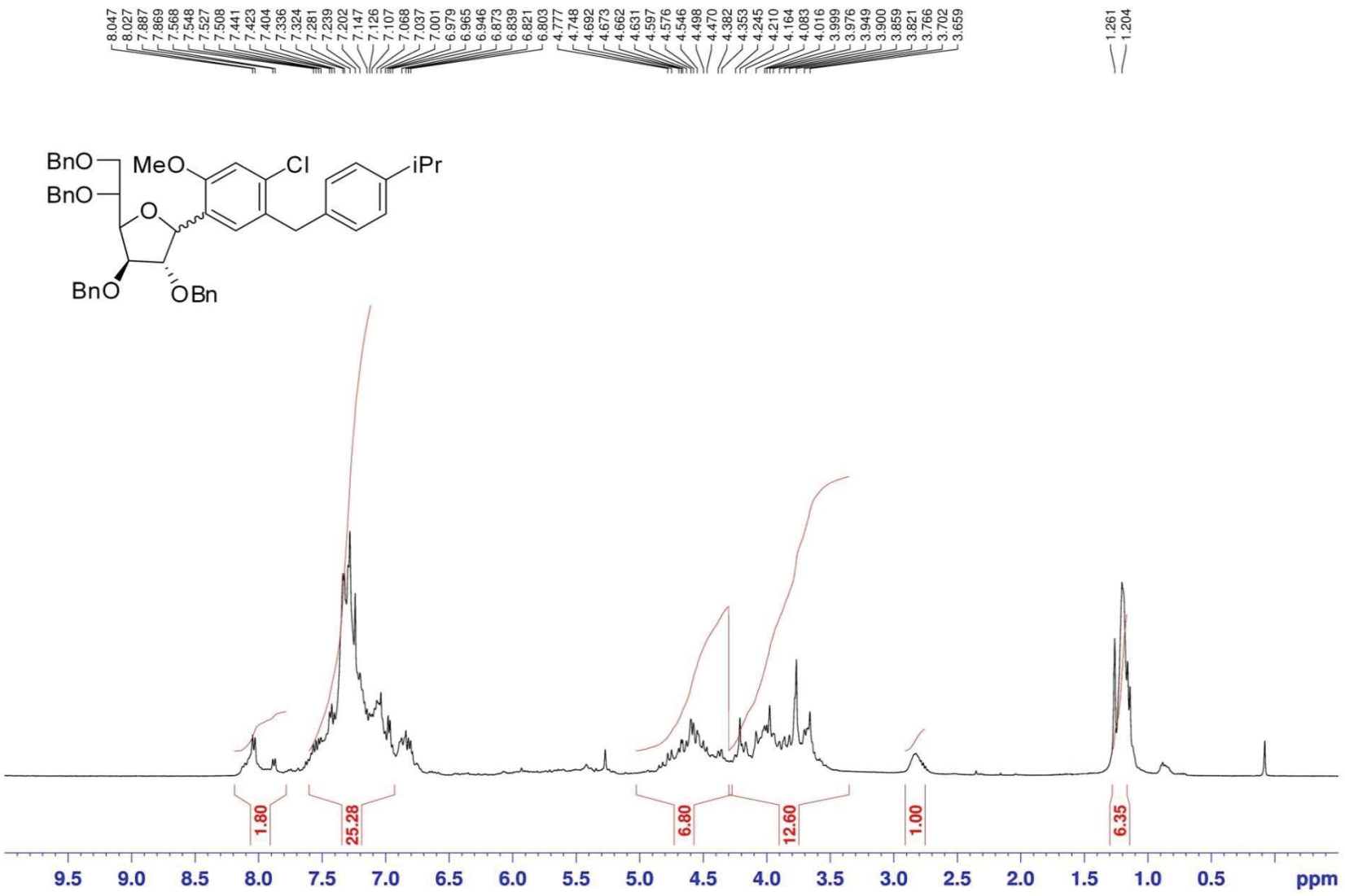

Appendix 30. ^{1}H-NMR spectra of **56h** (400 MHz, $CDCl_3$)

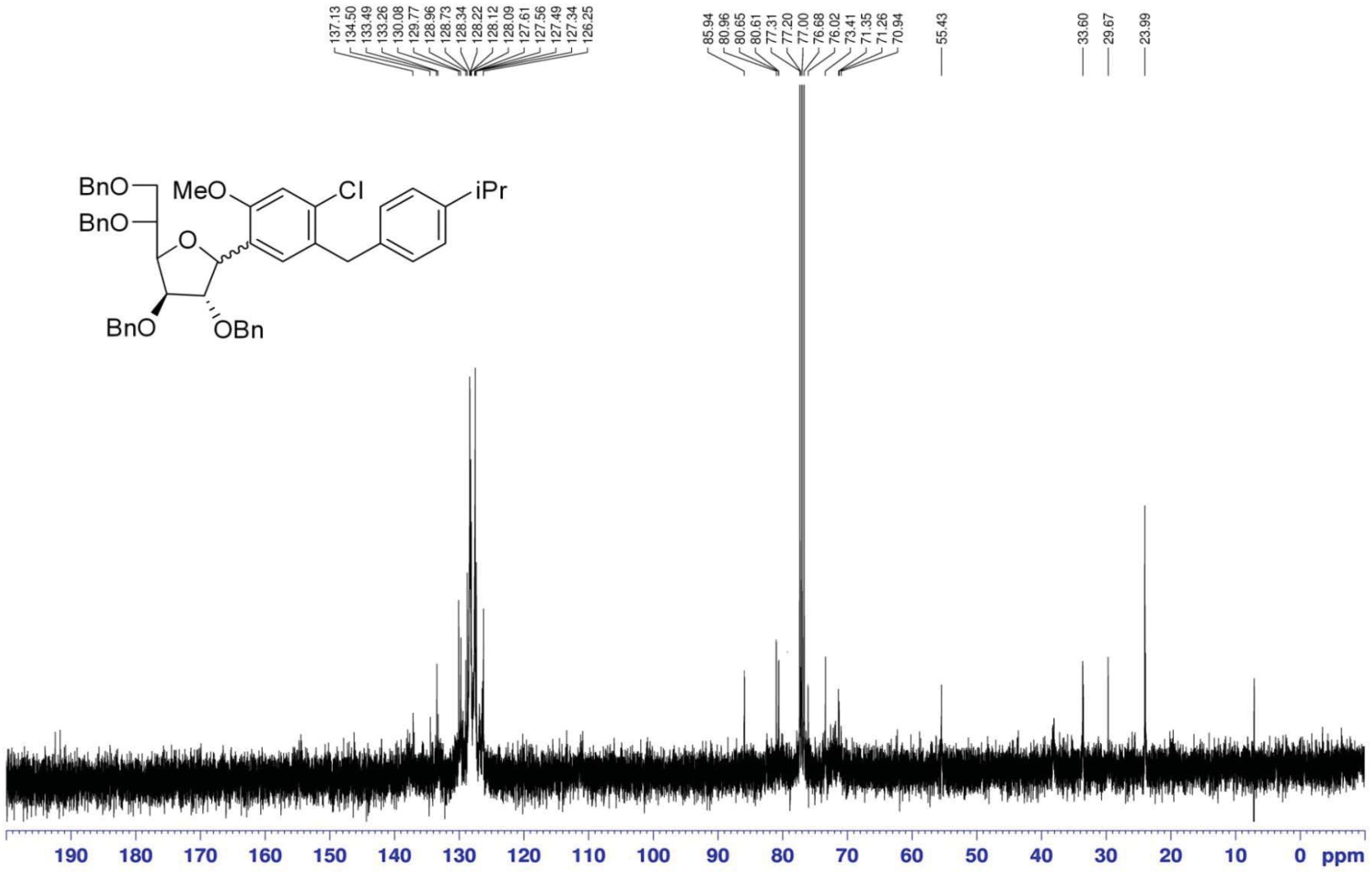

Appendix 31. ^{13}C-NMR spectra of **56h** (100 MHz, $CDCl_3$)

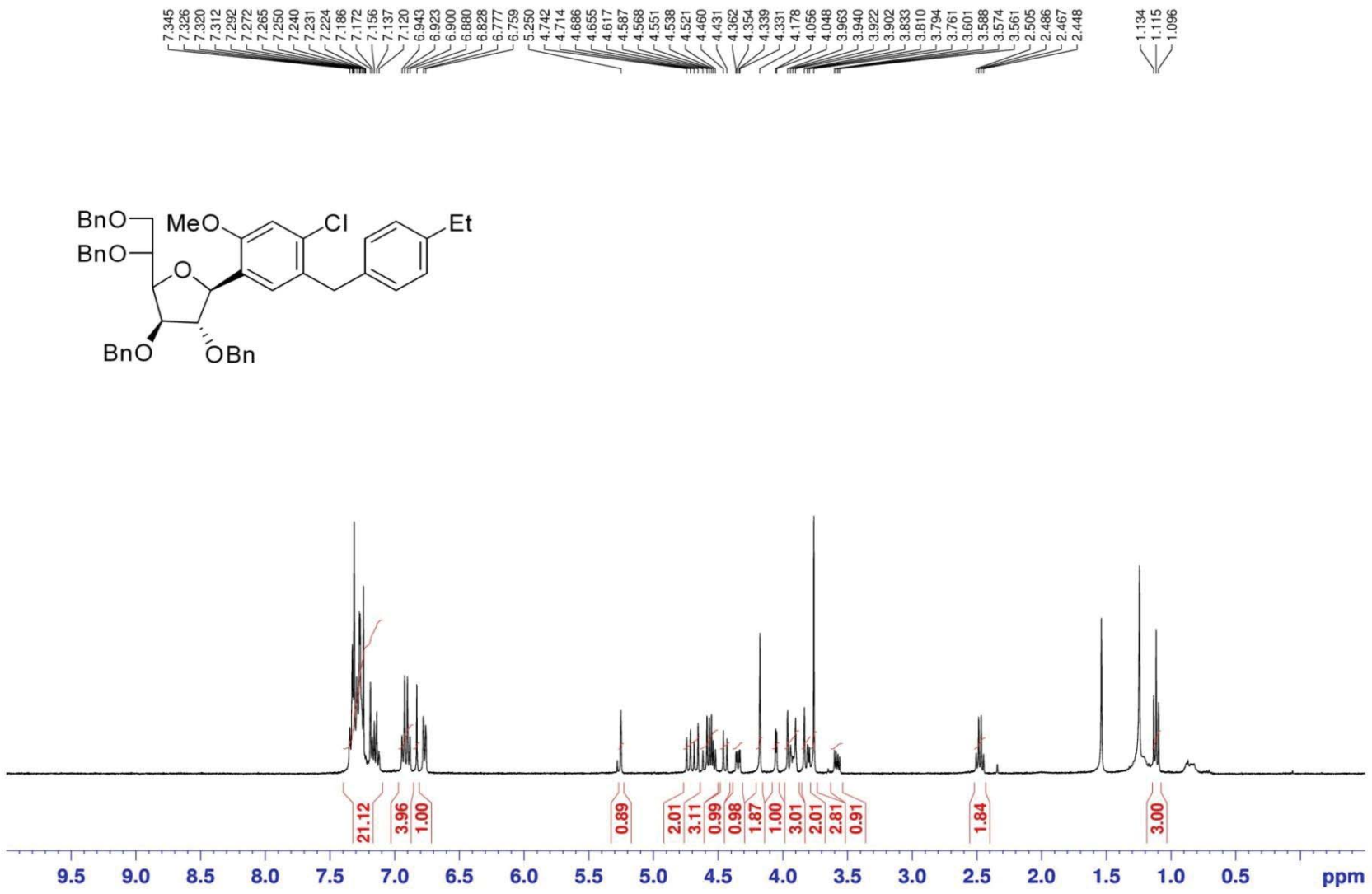

Appendix 32. ^{1}H-NMR spectra of **57g** (400 MHz, $CDCl_3$)

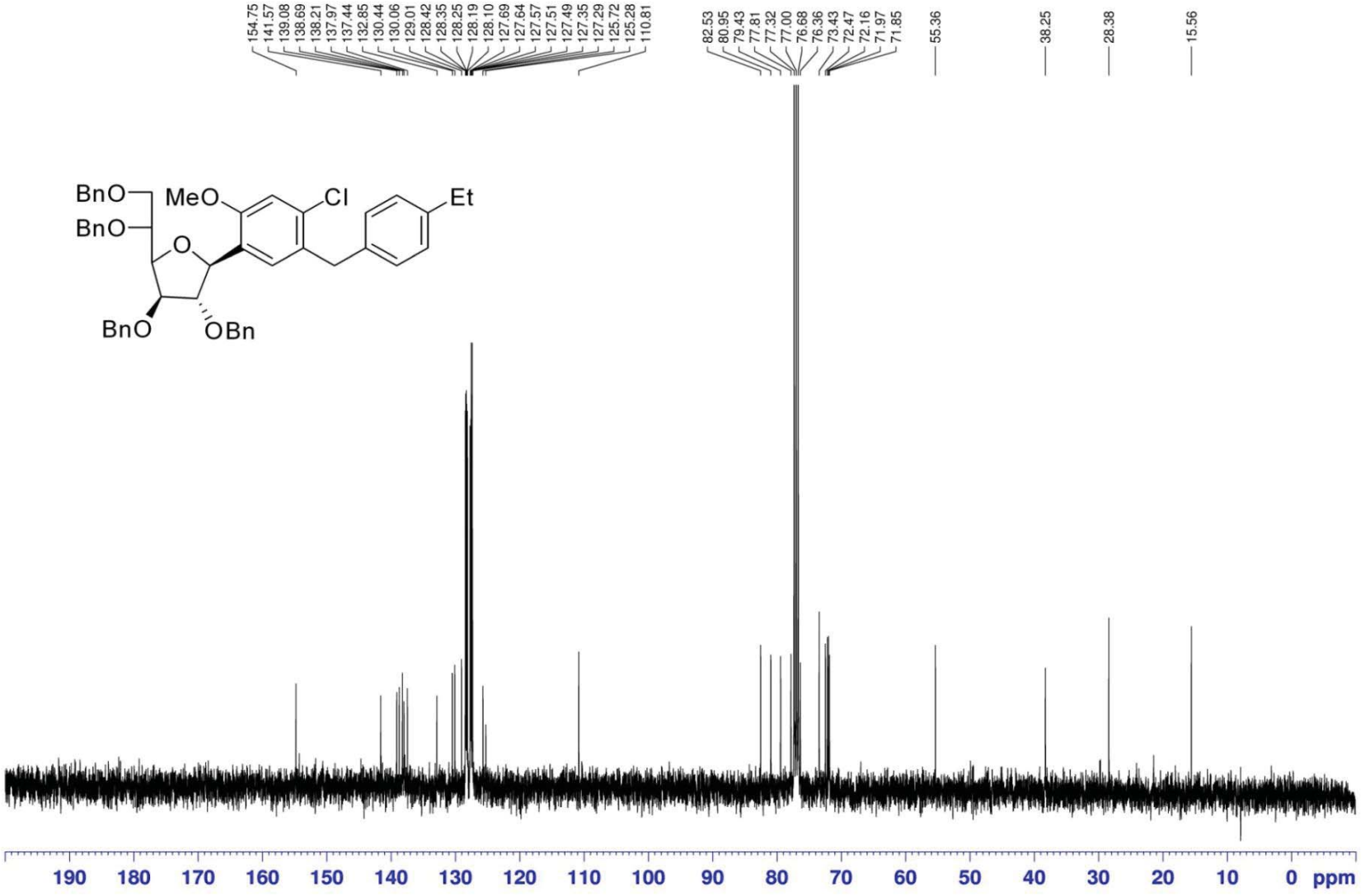

Appendix 33. ^{13}C-NMR spectra of **57g** (100 MHz, $CDCl_3$)

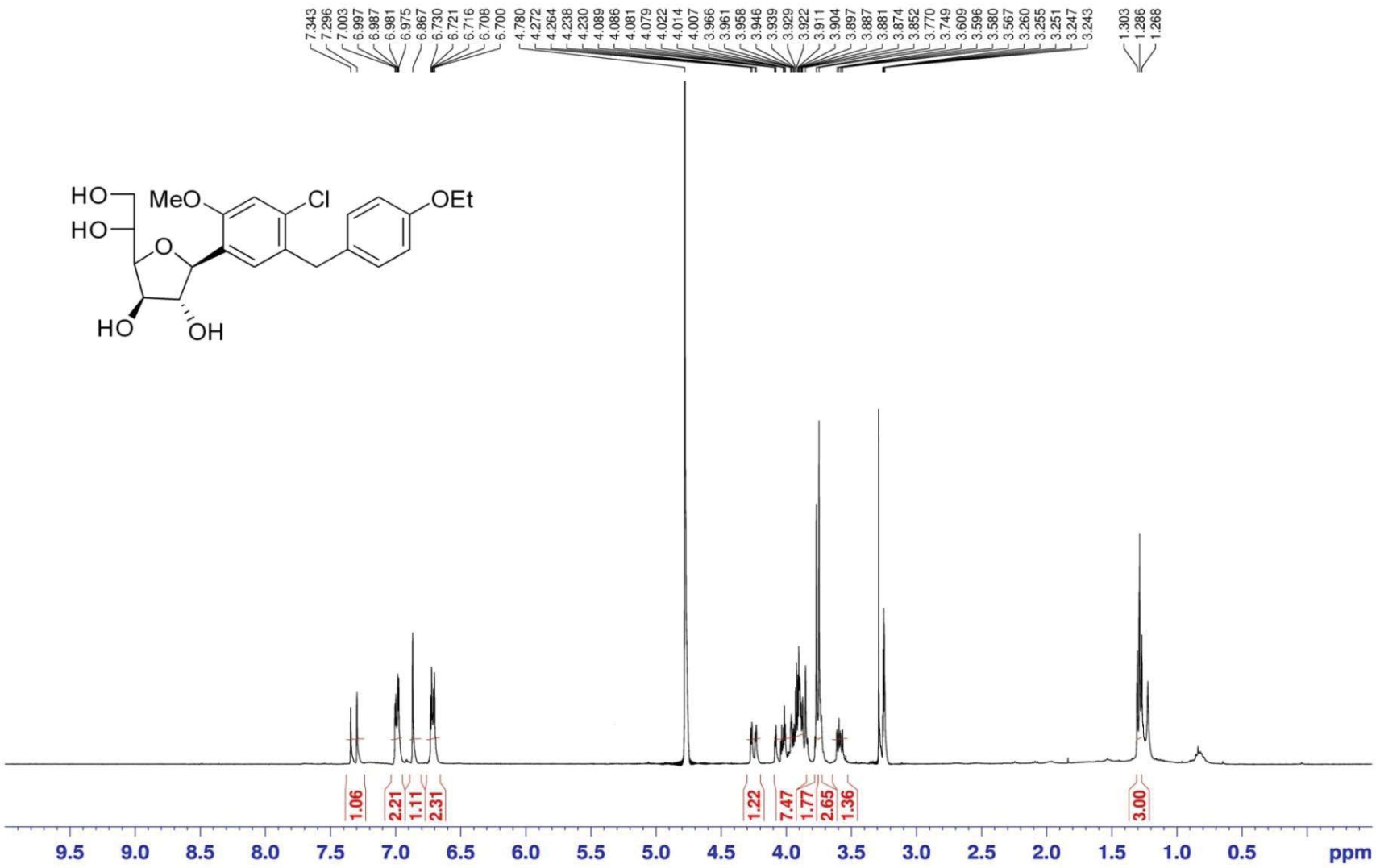

Appendix 34. ^{1}H-NMR spectra of **32f** (400 MHz, d_4-MeOH)

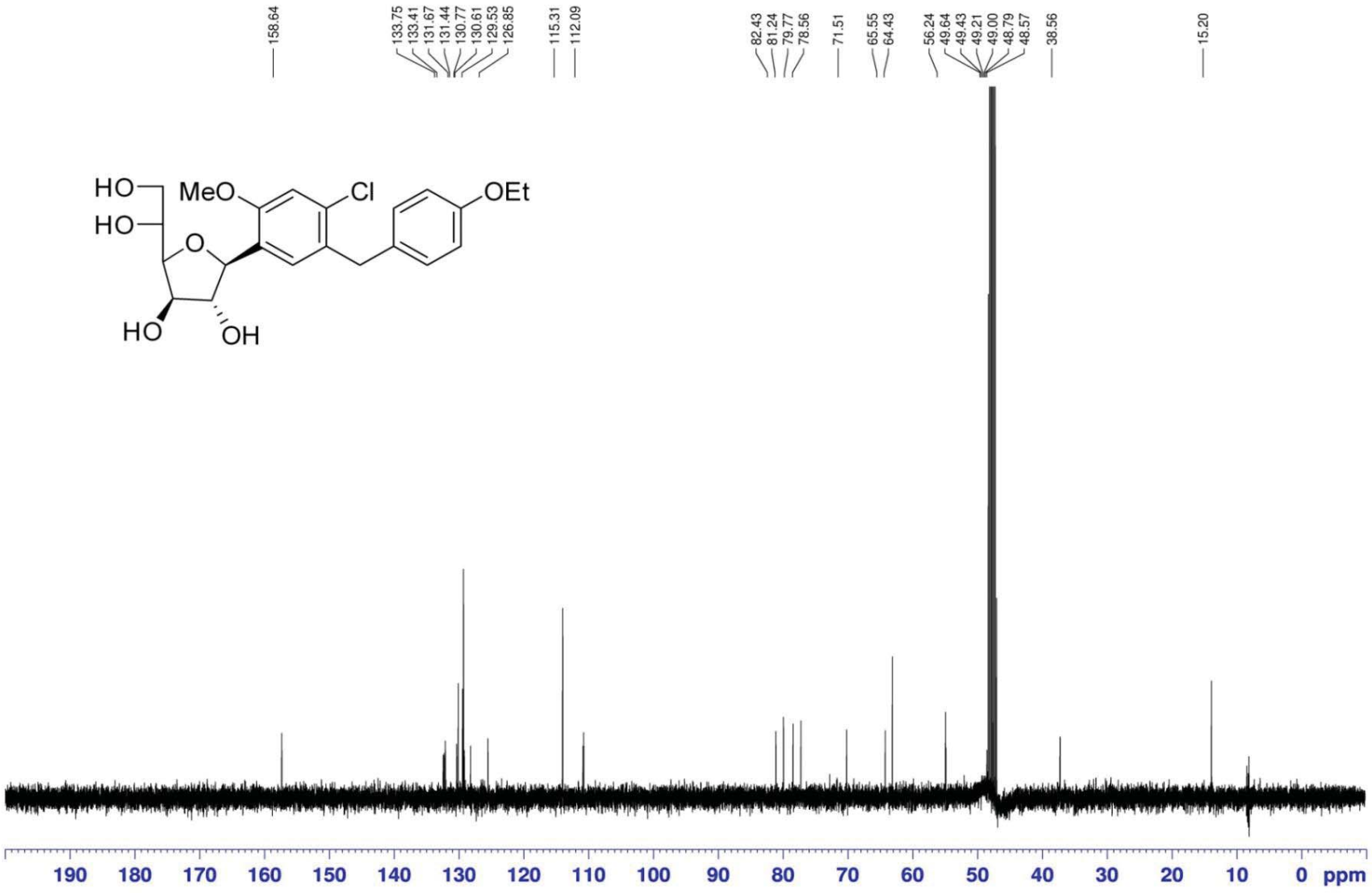

Appendix 35. ^{13}C-NMR spectra of **32f** (100 MHz, d_4-MeOH)

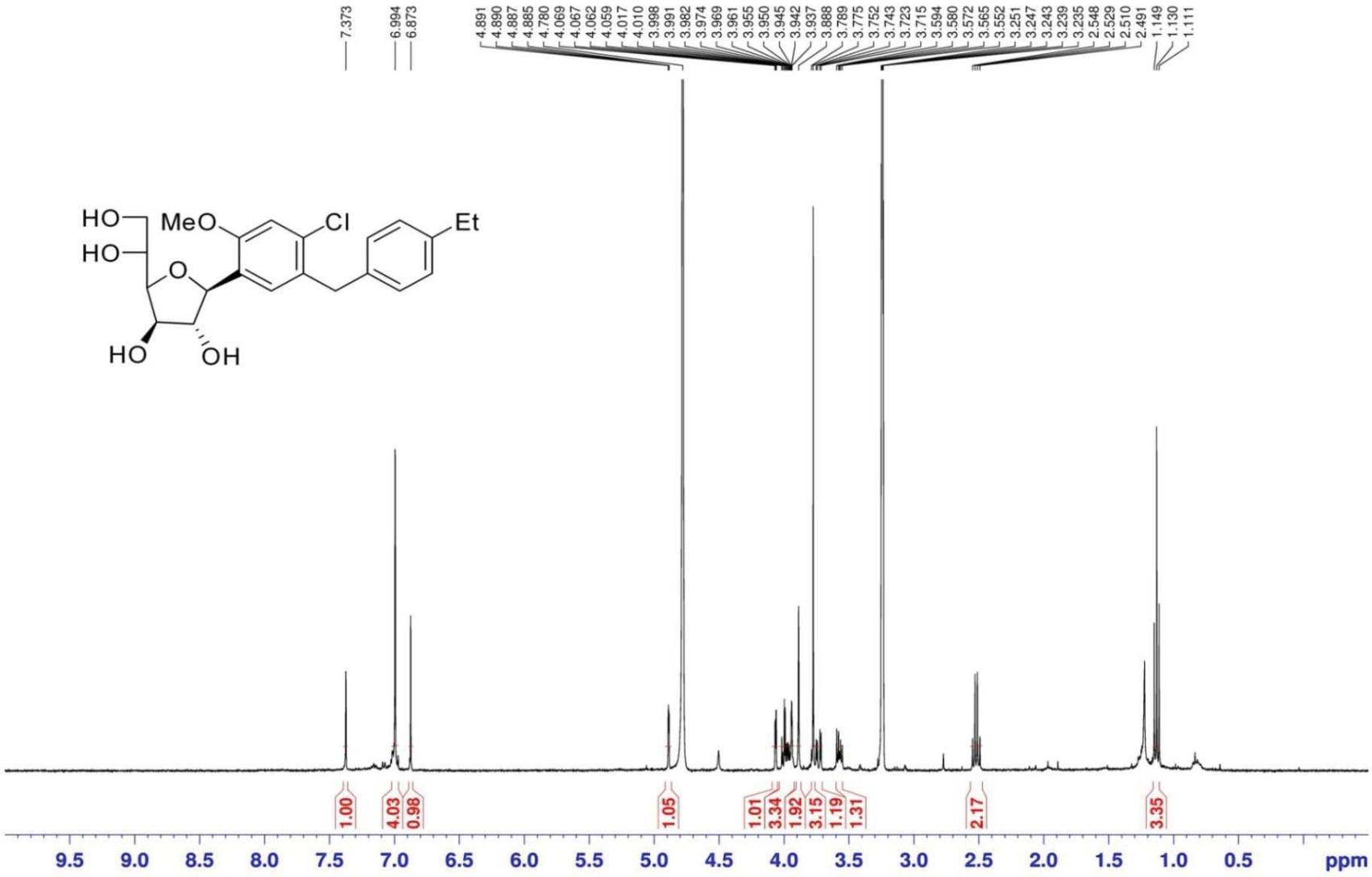

Appendix 36. ^{1}H-NMR spectra of **32g** (400 MHz, d_4-MeOH)

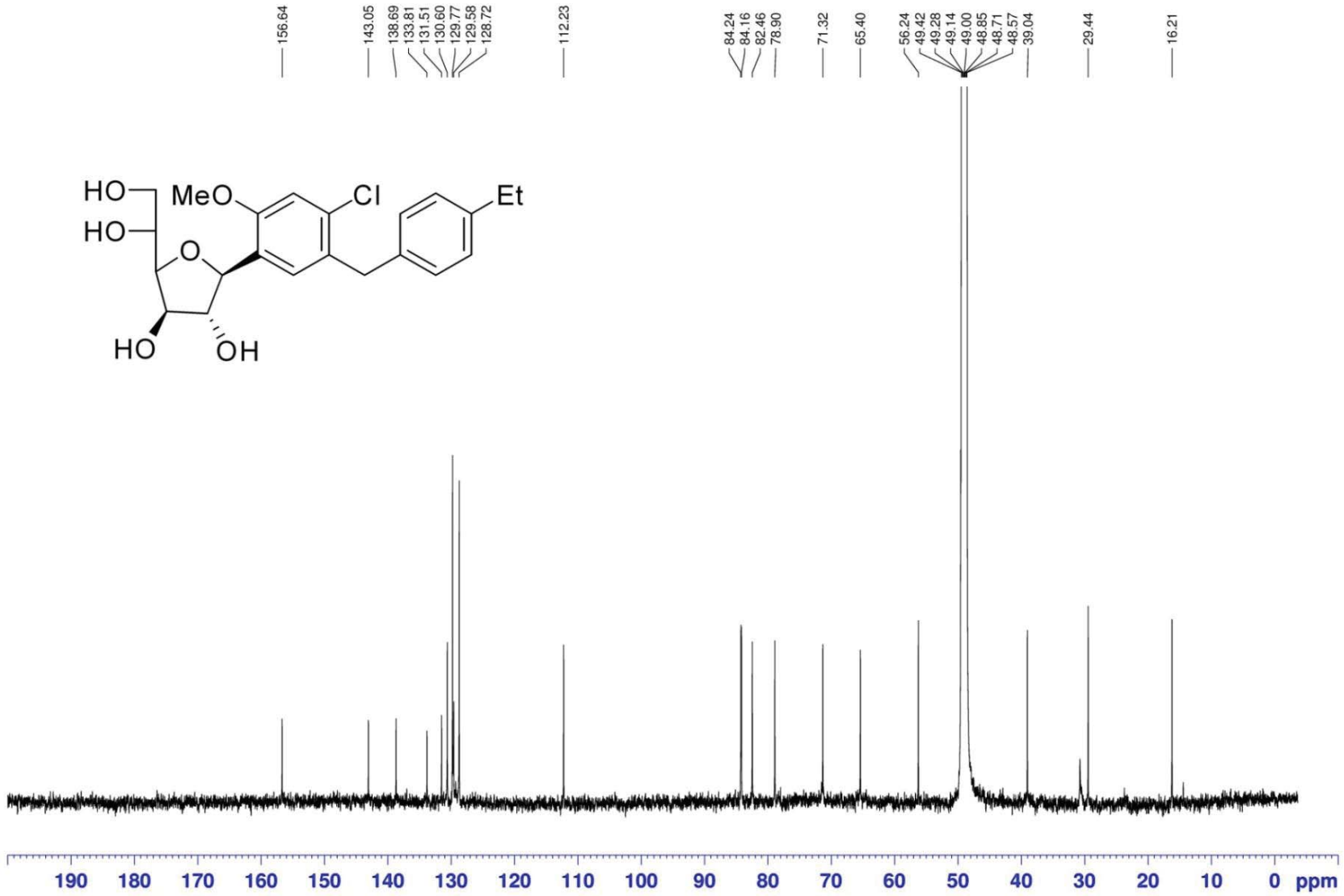

Appendix 37. ^{13}C-NMR spectra of **32g** (150 MHz, d_4-MeOH)

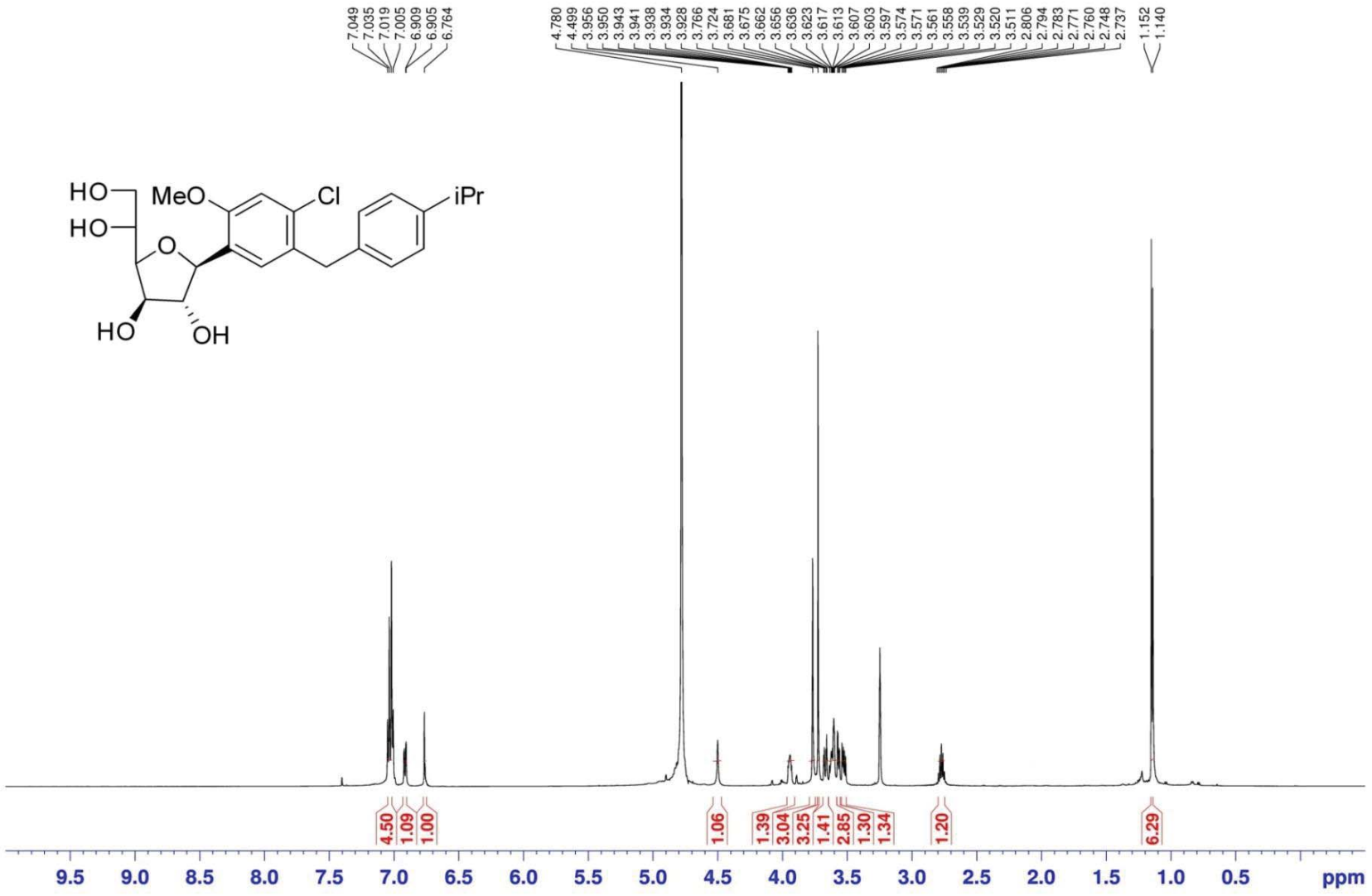

Appendix 38. ^{1}H-NMR spectra of **32h** (600 MHz, d_4-MeOH)

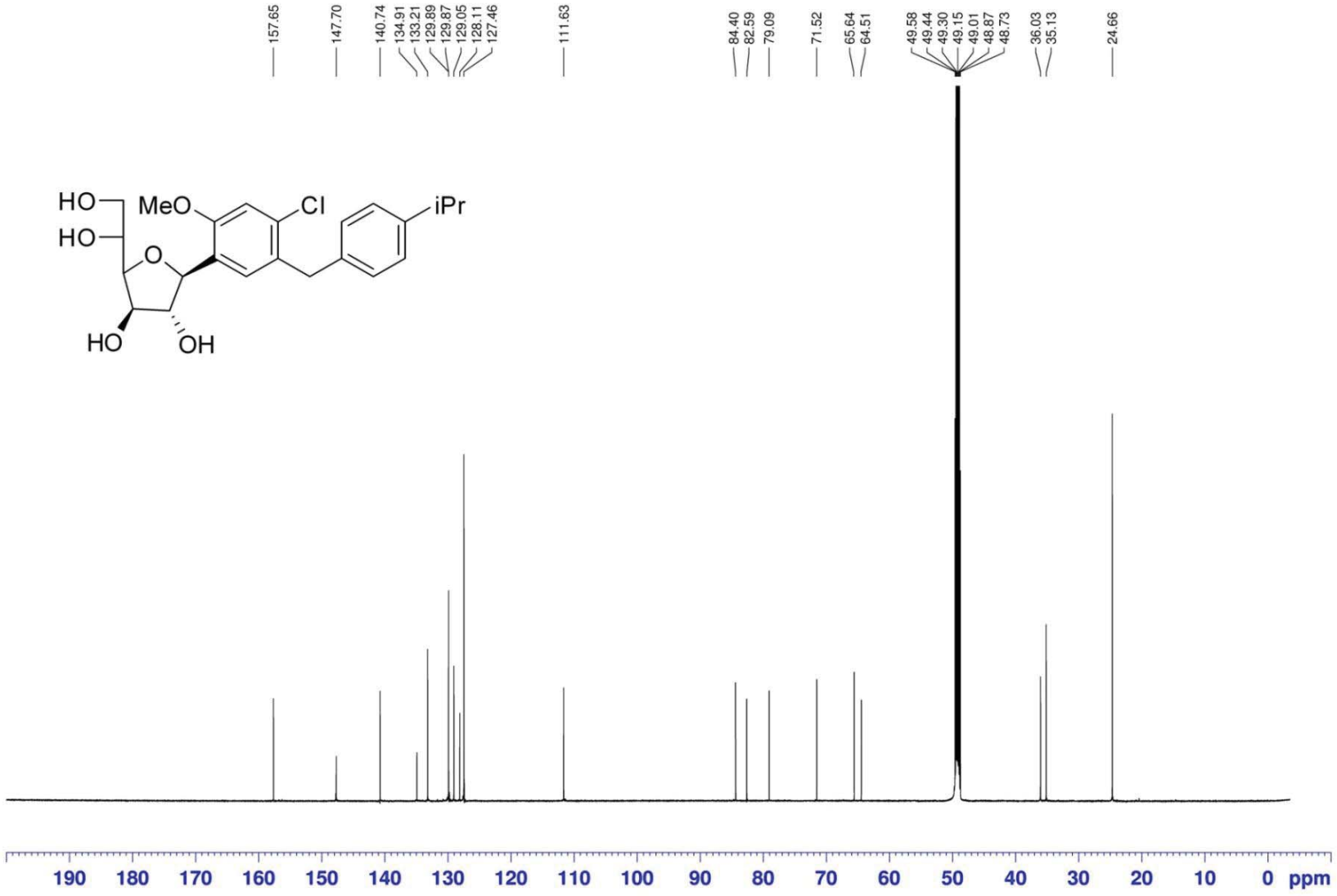

Appendix 39. ^{13}C-NMR spectra of **32h** (150 MHz, d_4-MeOH)

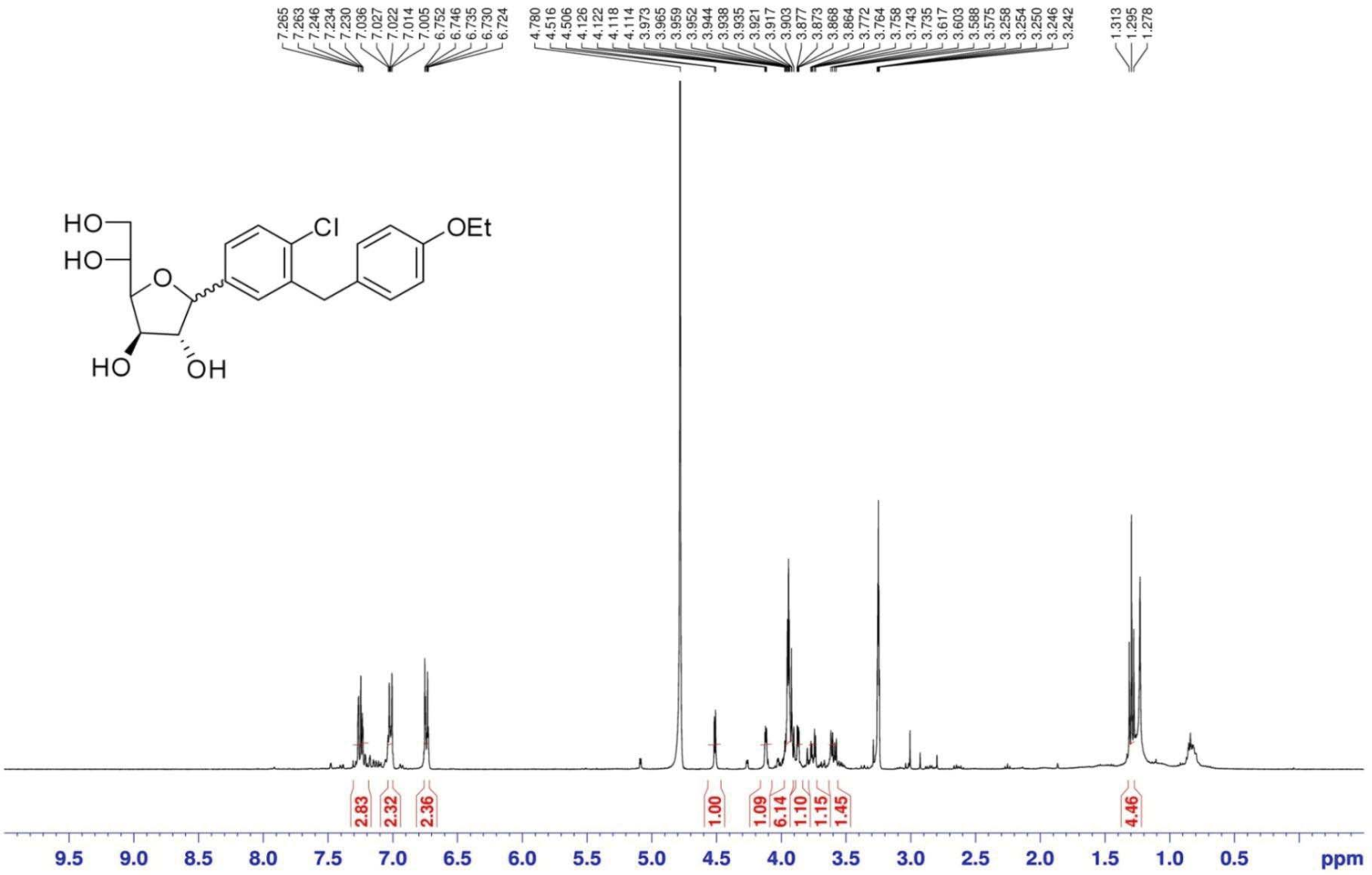

Appendix 40. ^{1}H-NMR spectra of **58a** (400 MHz, d_4-MeOH)

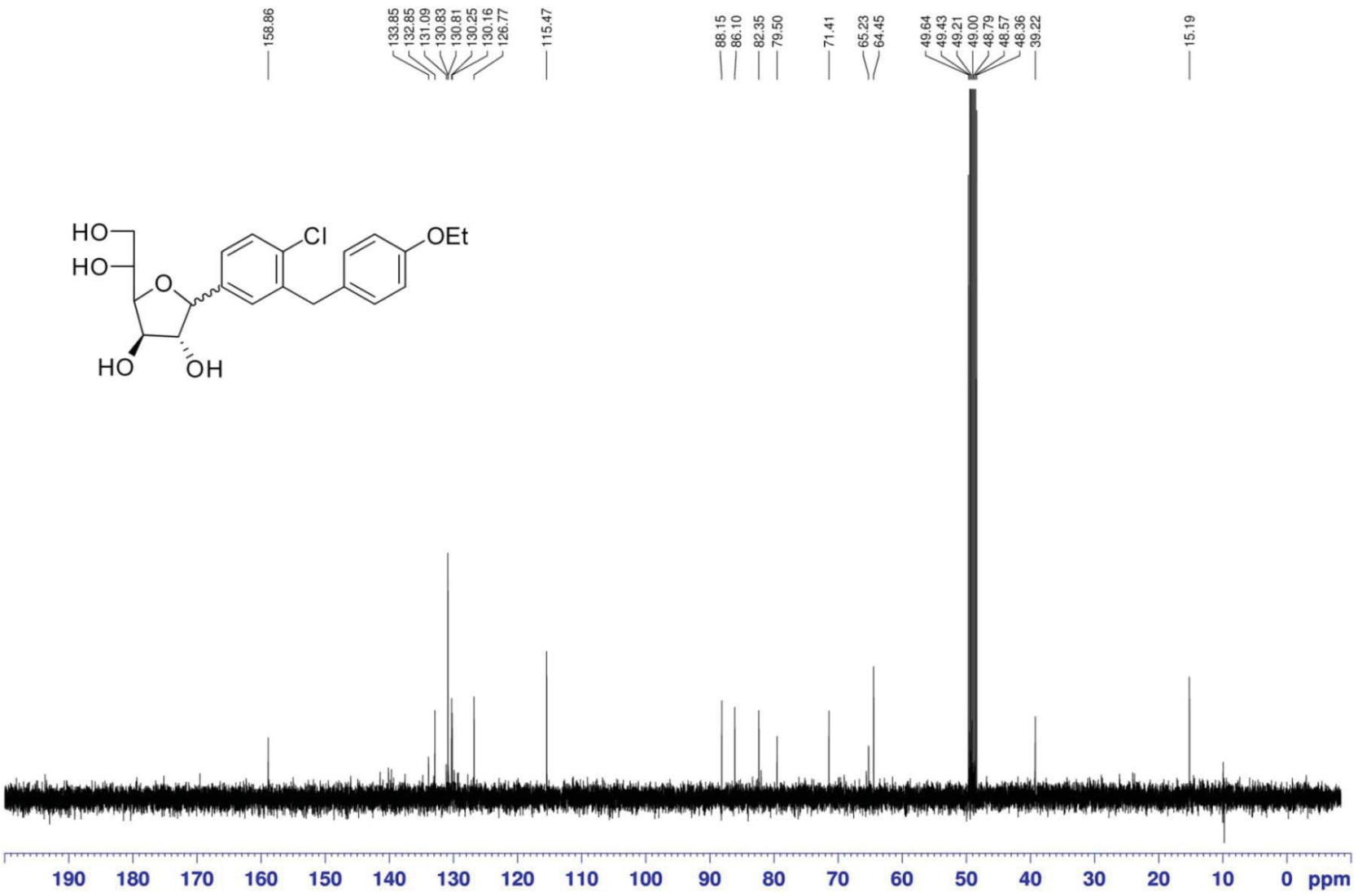

Appendix 41. ^{13}C-NMR spectra of **58a** (100 MHz, d_4-MeOH)

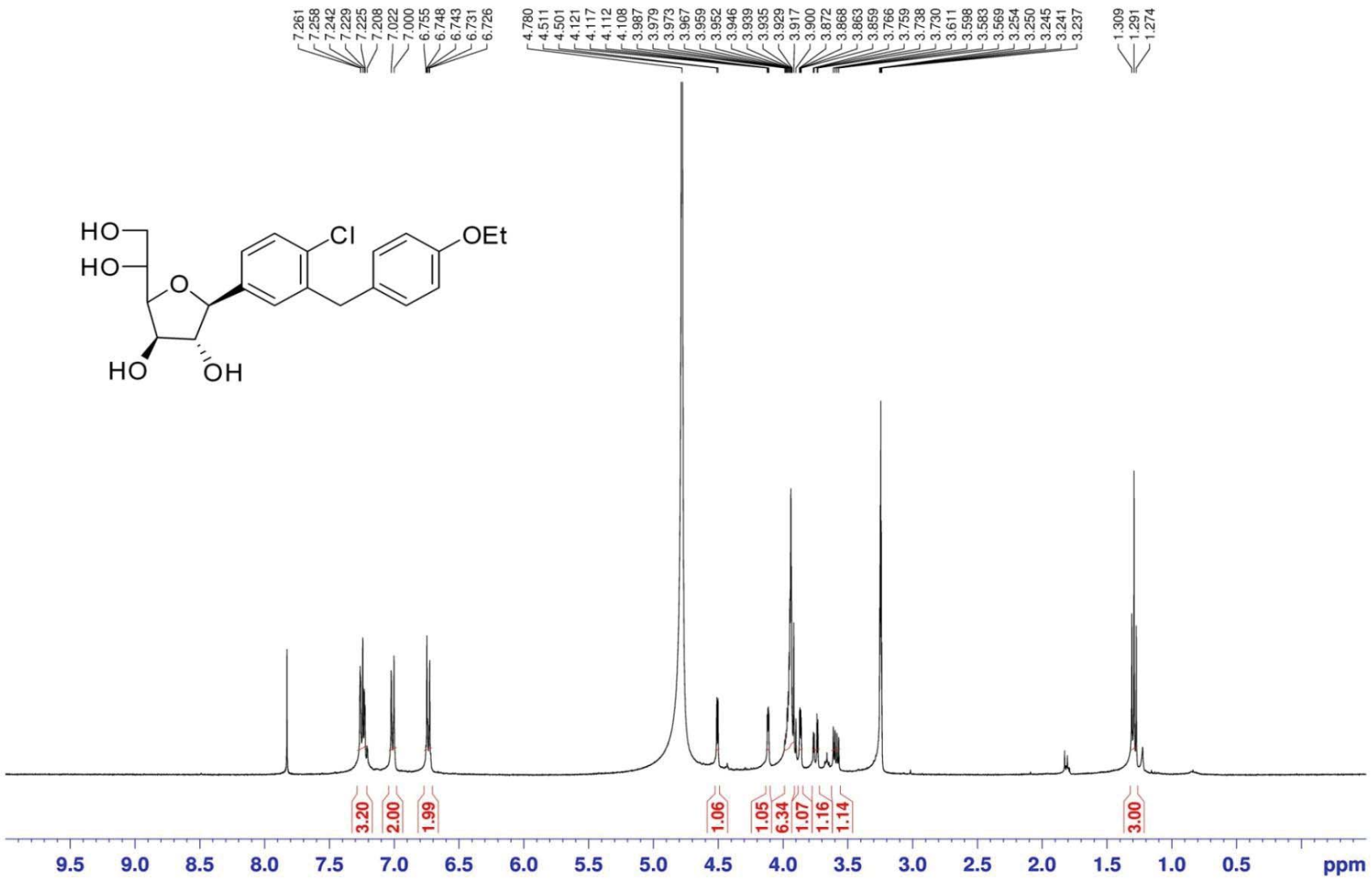

Appendix 42. ^{1}H-NMR spectra of **32a** (400 MHz, d_4-MeOH)

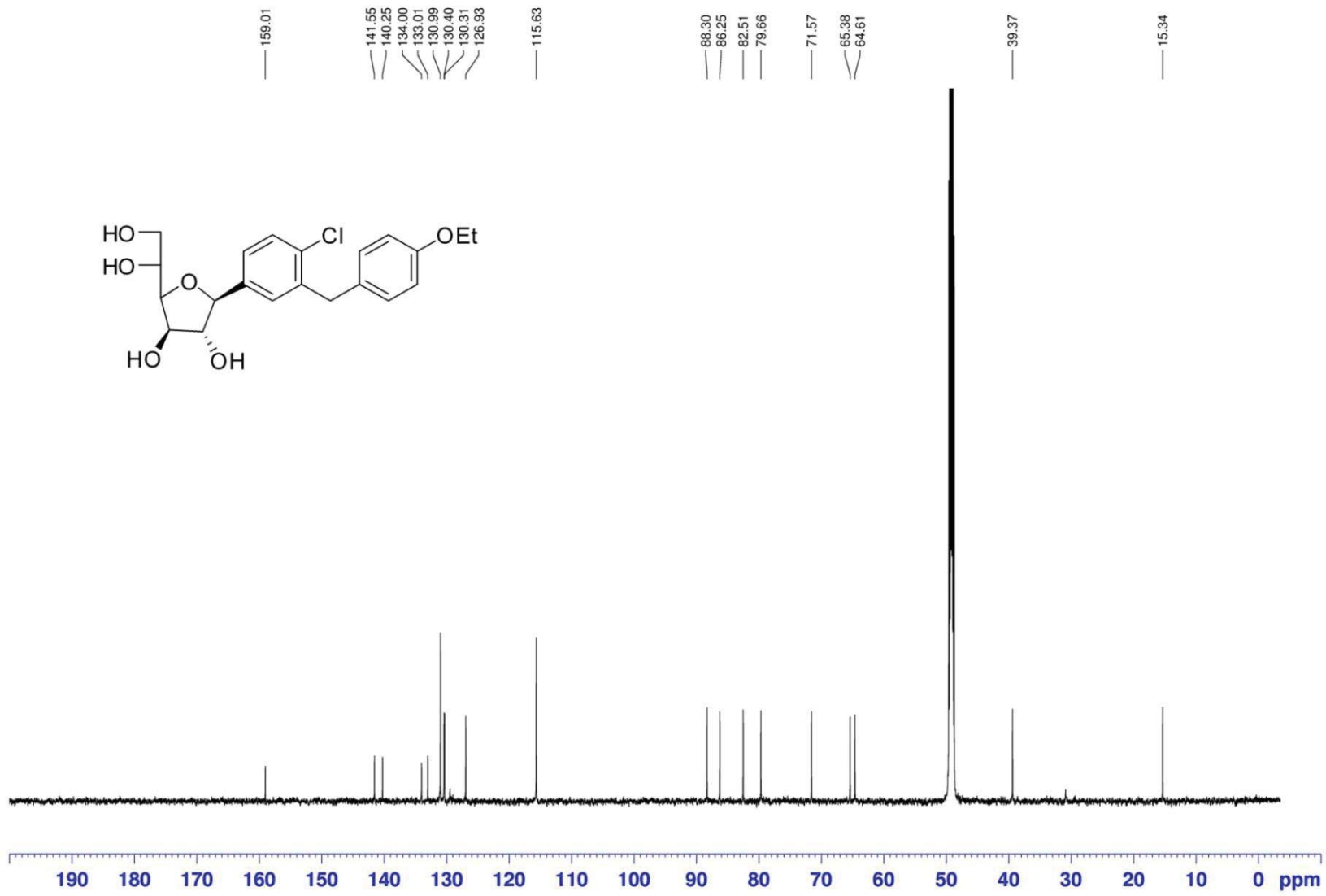

Appendix 43. ^{13}C-NMR spectra of **32a** (150 MHz, d_4-MeOH)

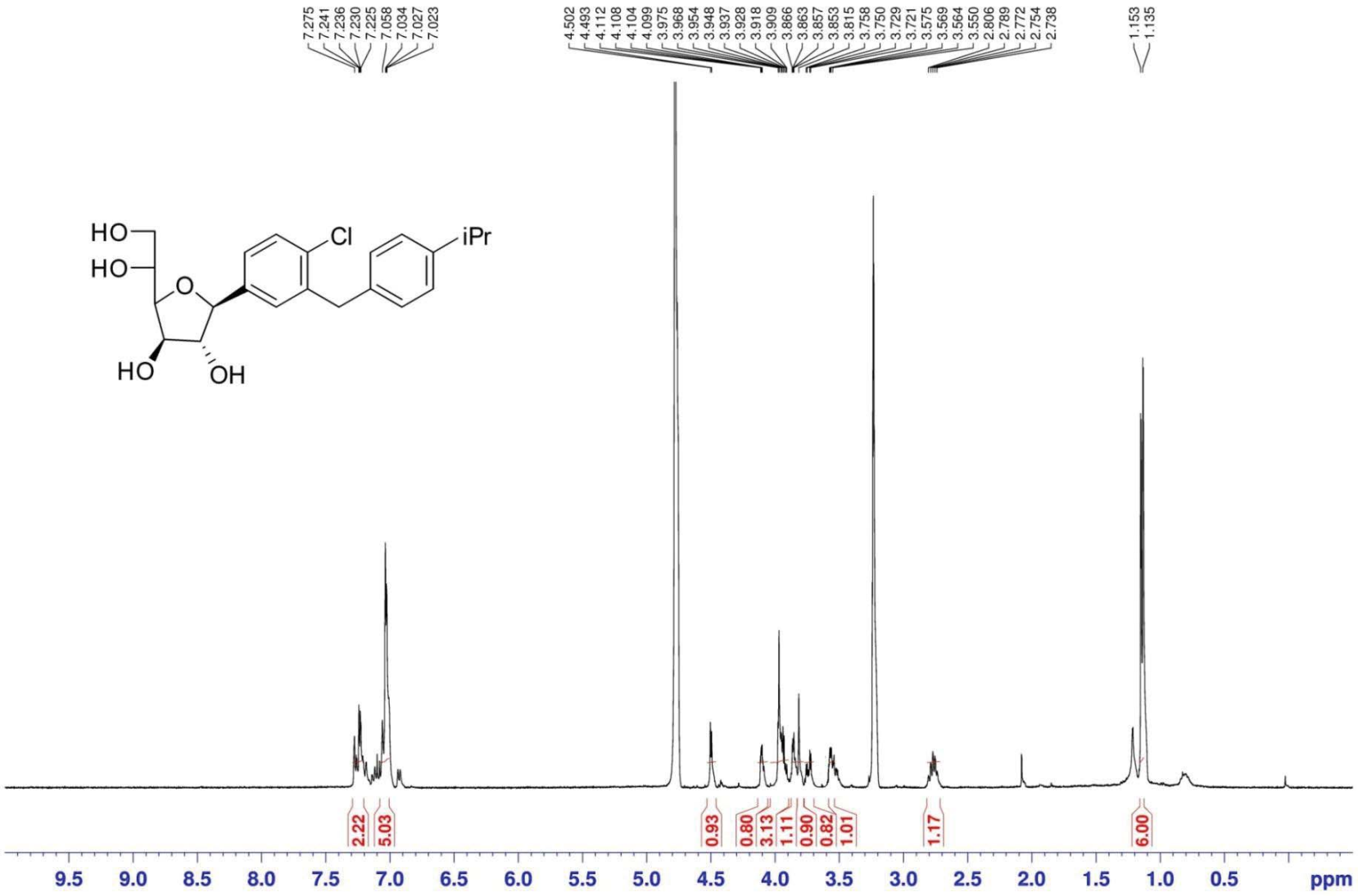

Appendix 44. ^{1}H-NMR spectra of **32b** (400 MHz, d_4-MeOH)

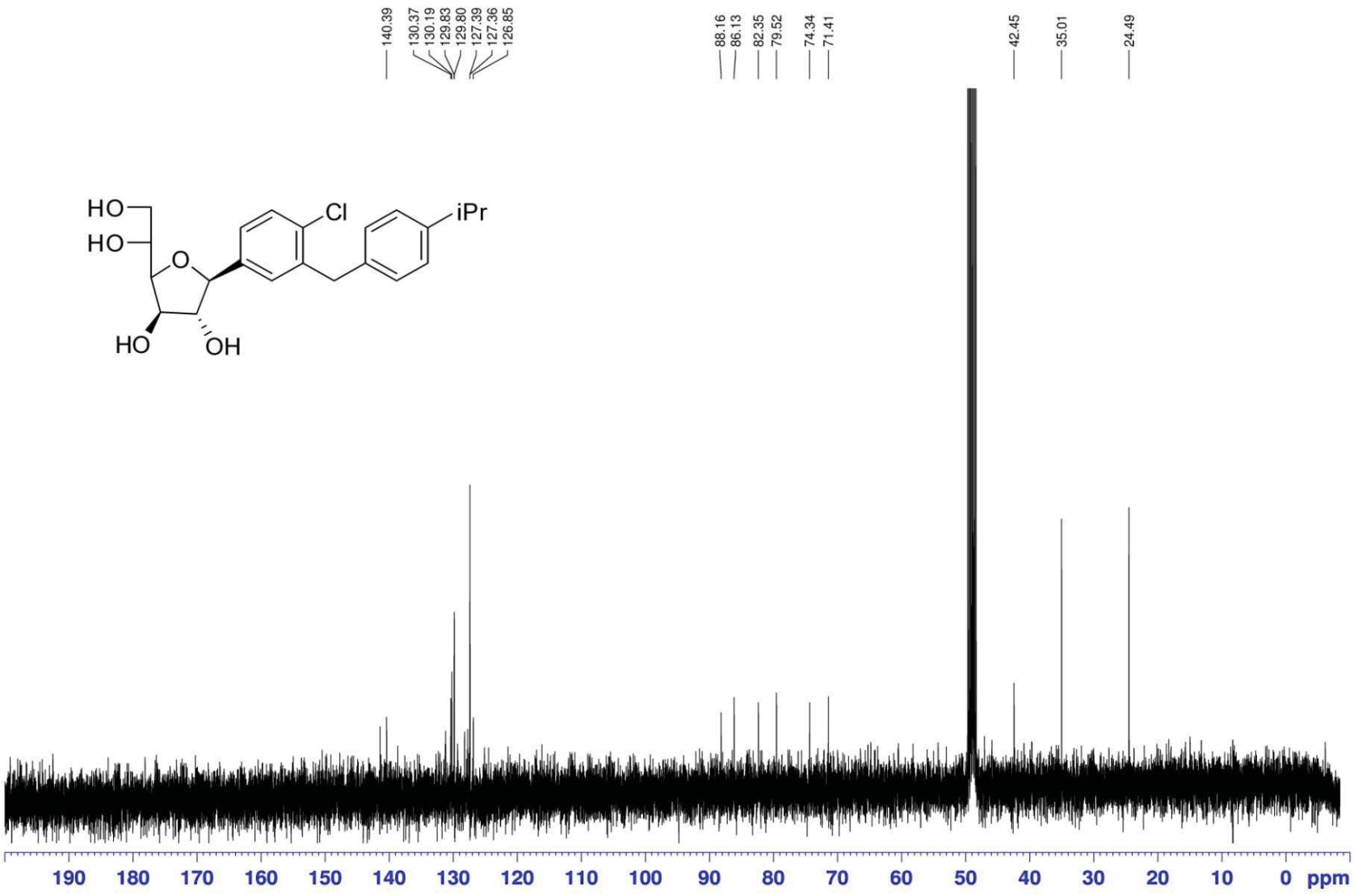

Appendix 45. ^{13}C-NMR spectra of **32b** (100 MHz, d_4-MeOH)

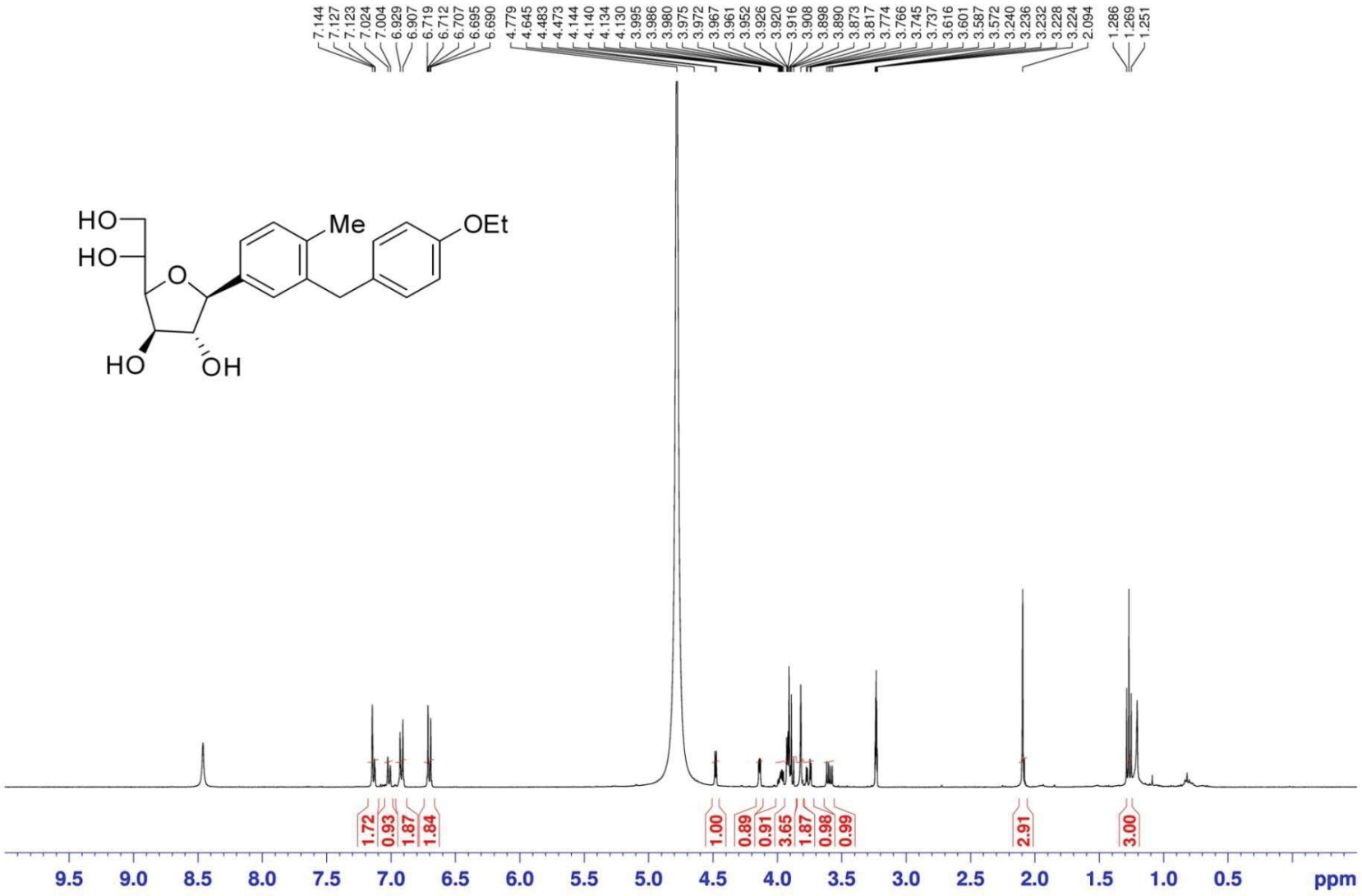

Appendix 46. ^{1}H-NMR spectra of **32c** (400 MHz, d_4-MeOH)

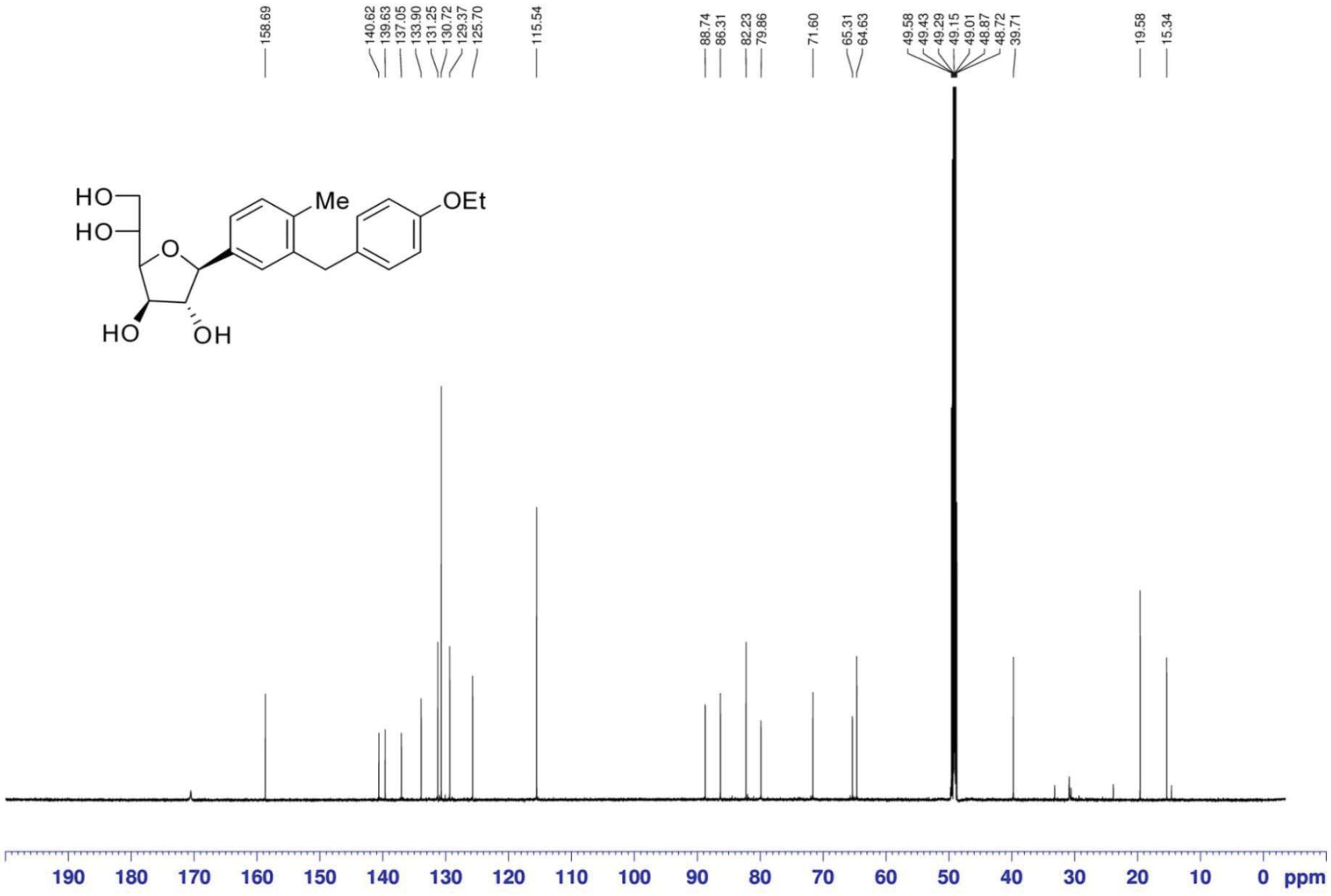

Appendix 47. ^{13}C-NMR spectra of **32c** (150 MHz, d_4-MeOH)

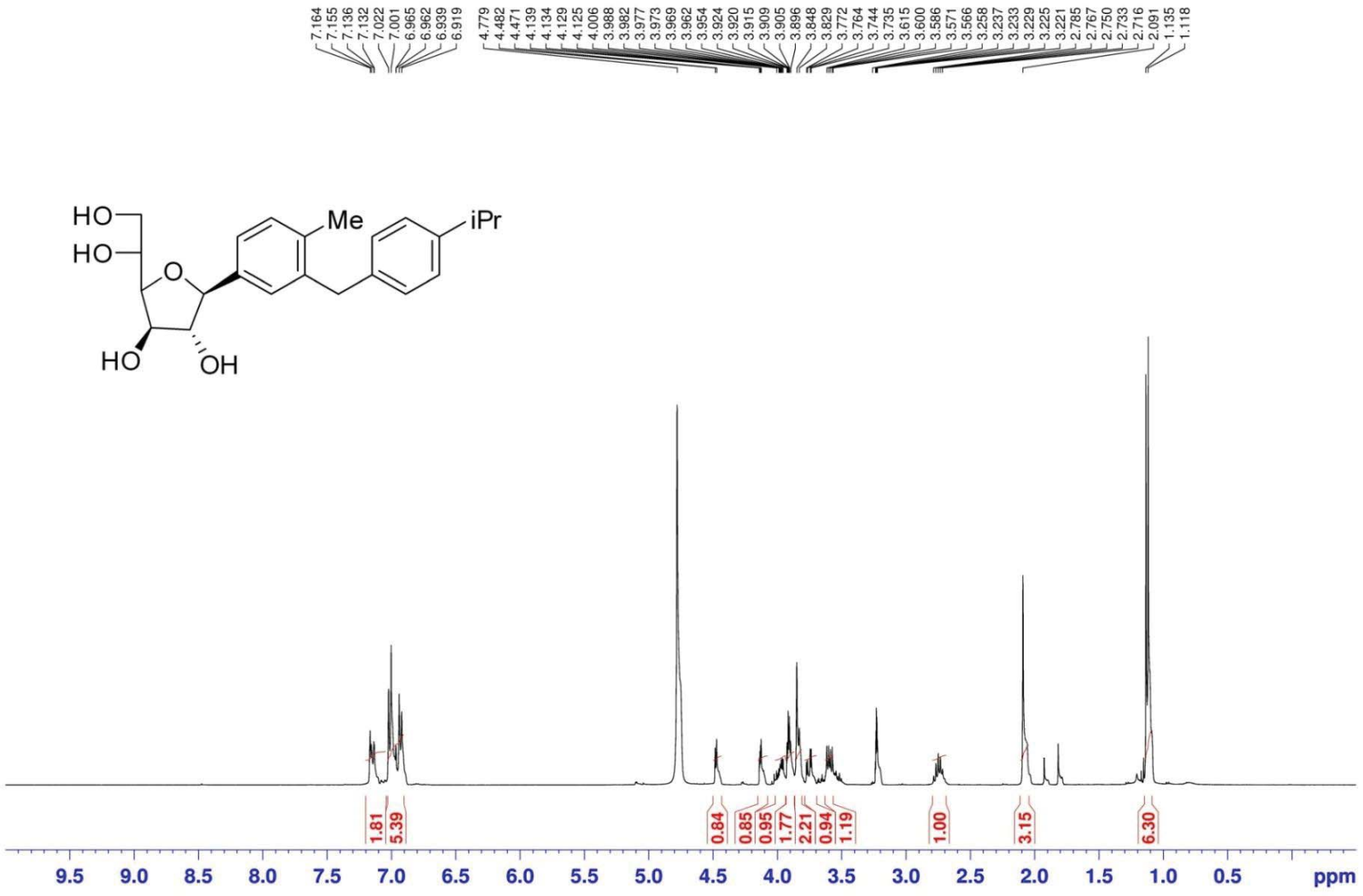

Appendix 48. ^{1}H-NMR spectra of **32d** (400 MHz, d_4-MeOH)

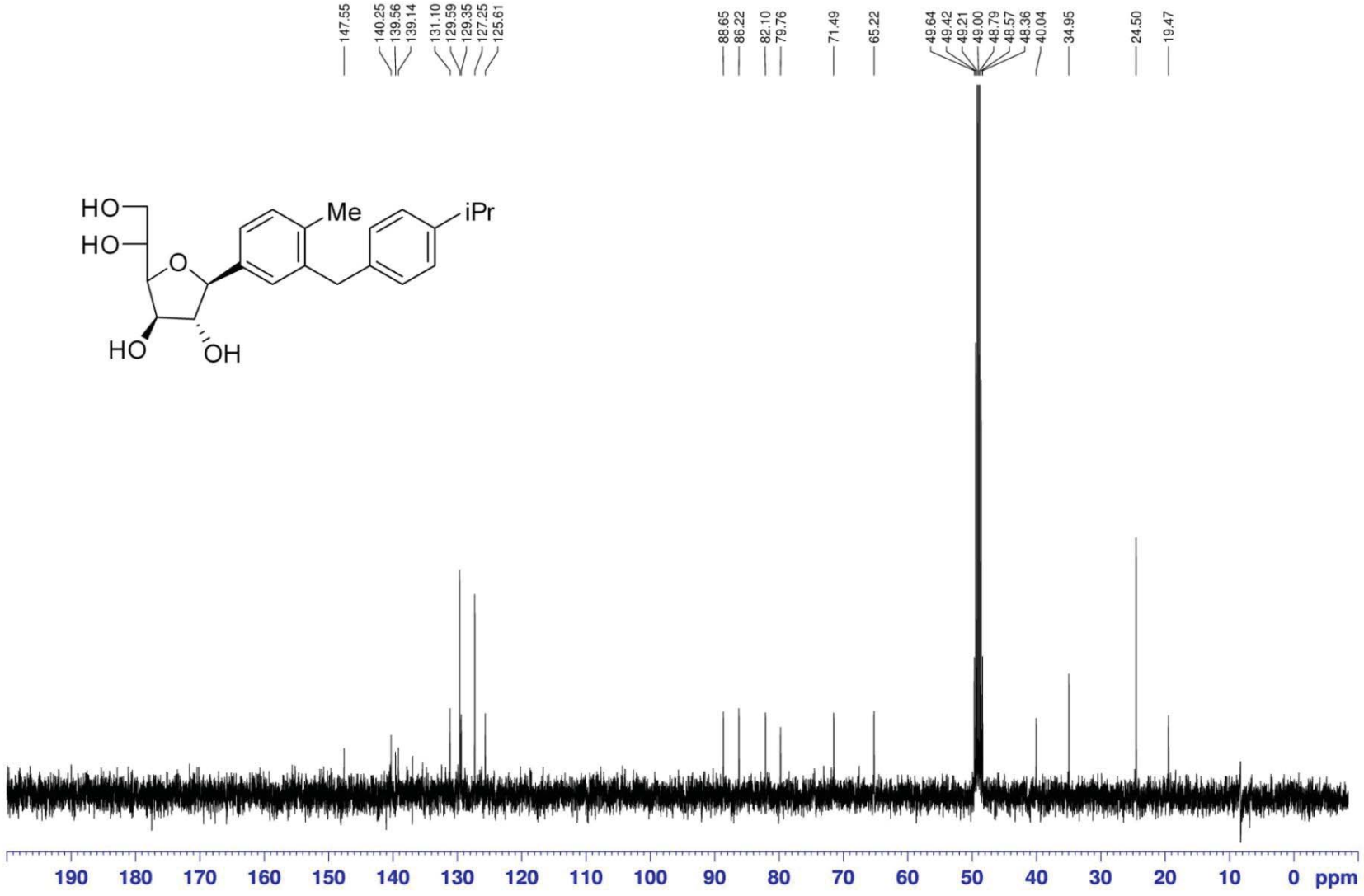

Appendix 49. ^{13}C-NMR spectra of **32d** (100 MHz, d_4-MeOH)

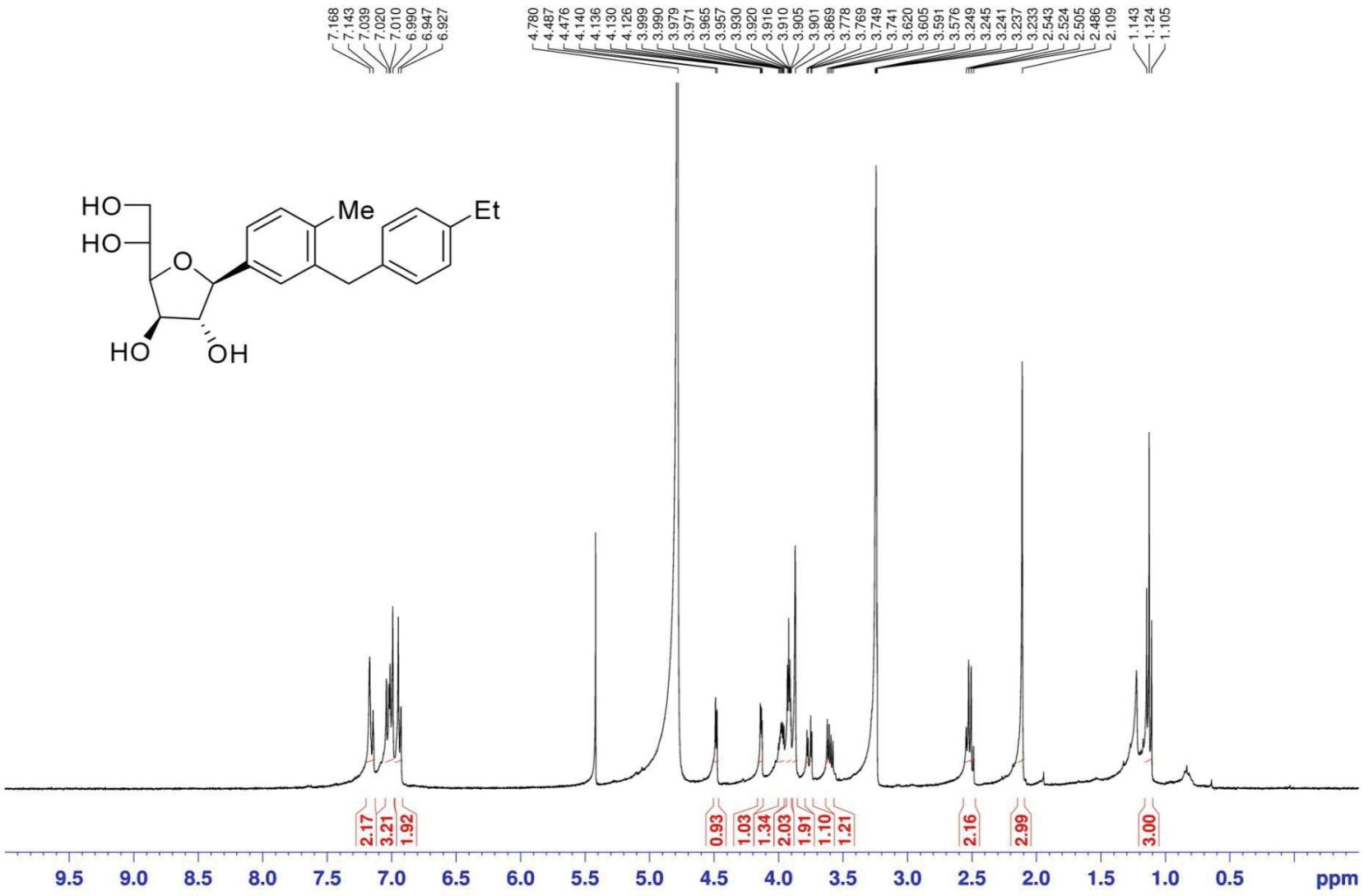

Appendix 50. ^{1}H-NMR spectra of **32e** (400 MHz, d_4-MeOH)

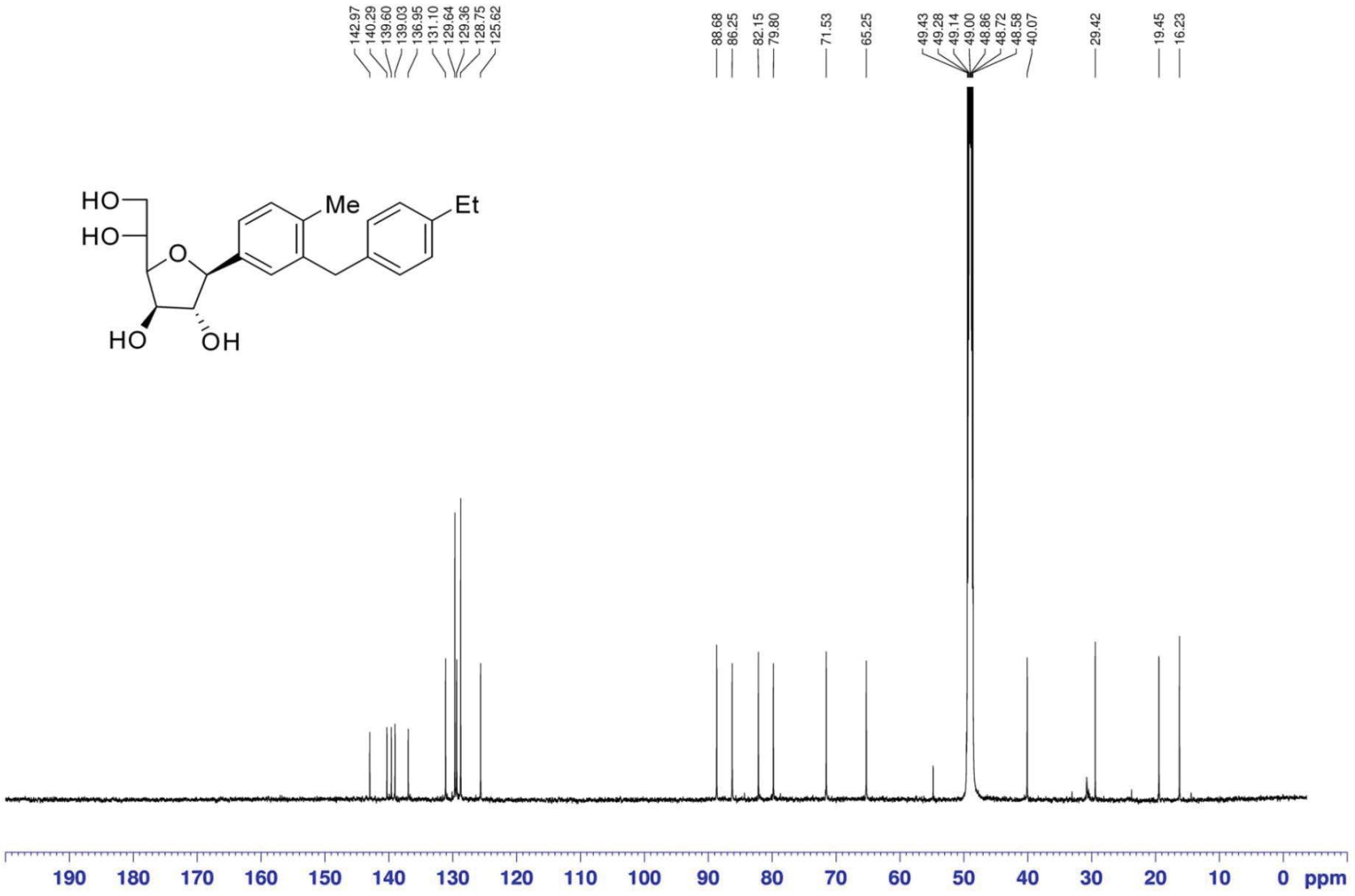

Appendix 51. ^{13}C-NMR spectra of **32e** (150 MHz, d_4-MeOH)

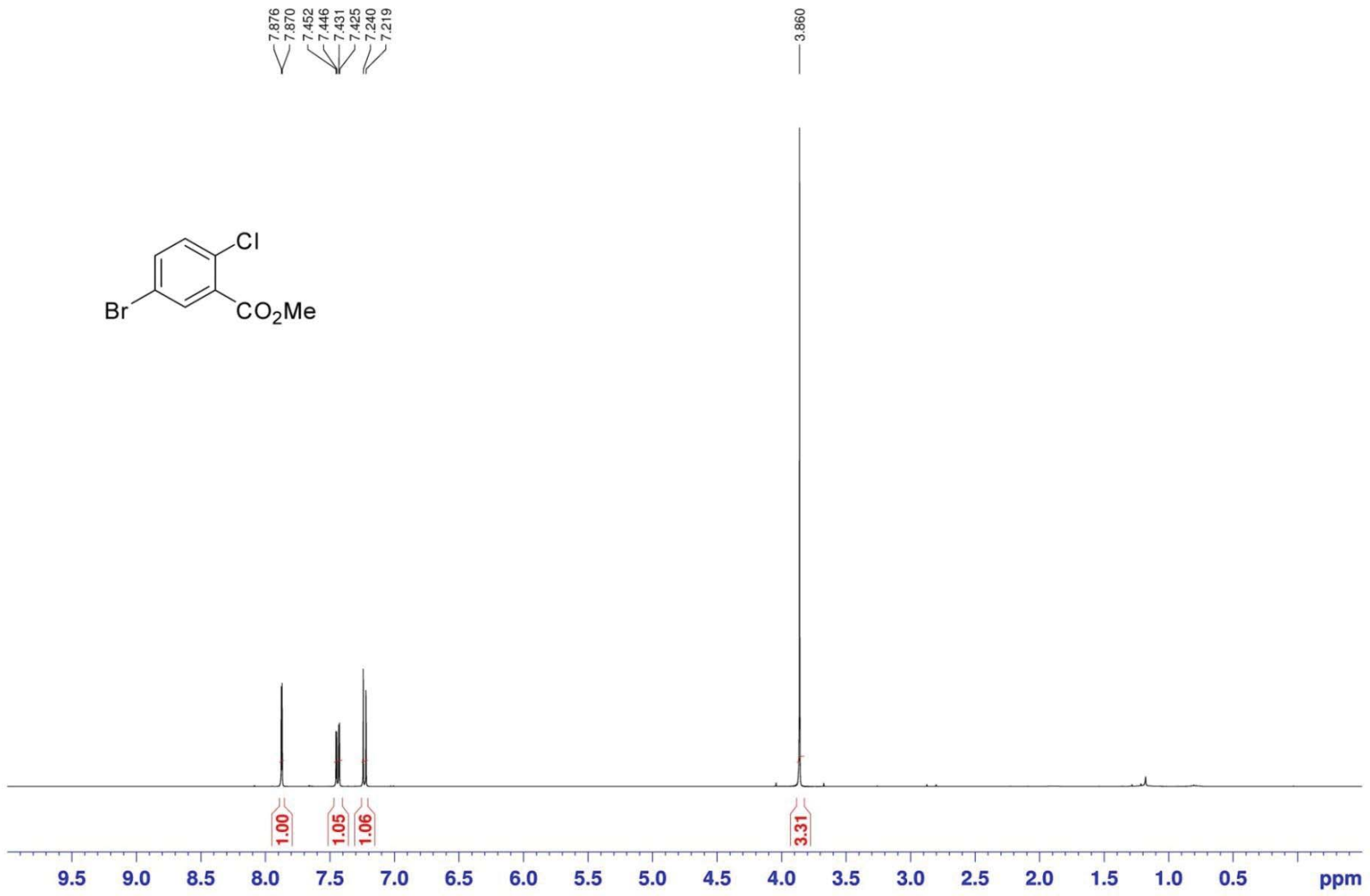

Appendix 52. ^{1}H-NMR spectra of **59** (400 MHz, d_4-MeOH)

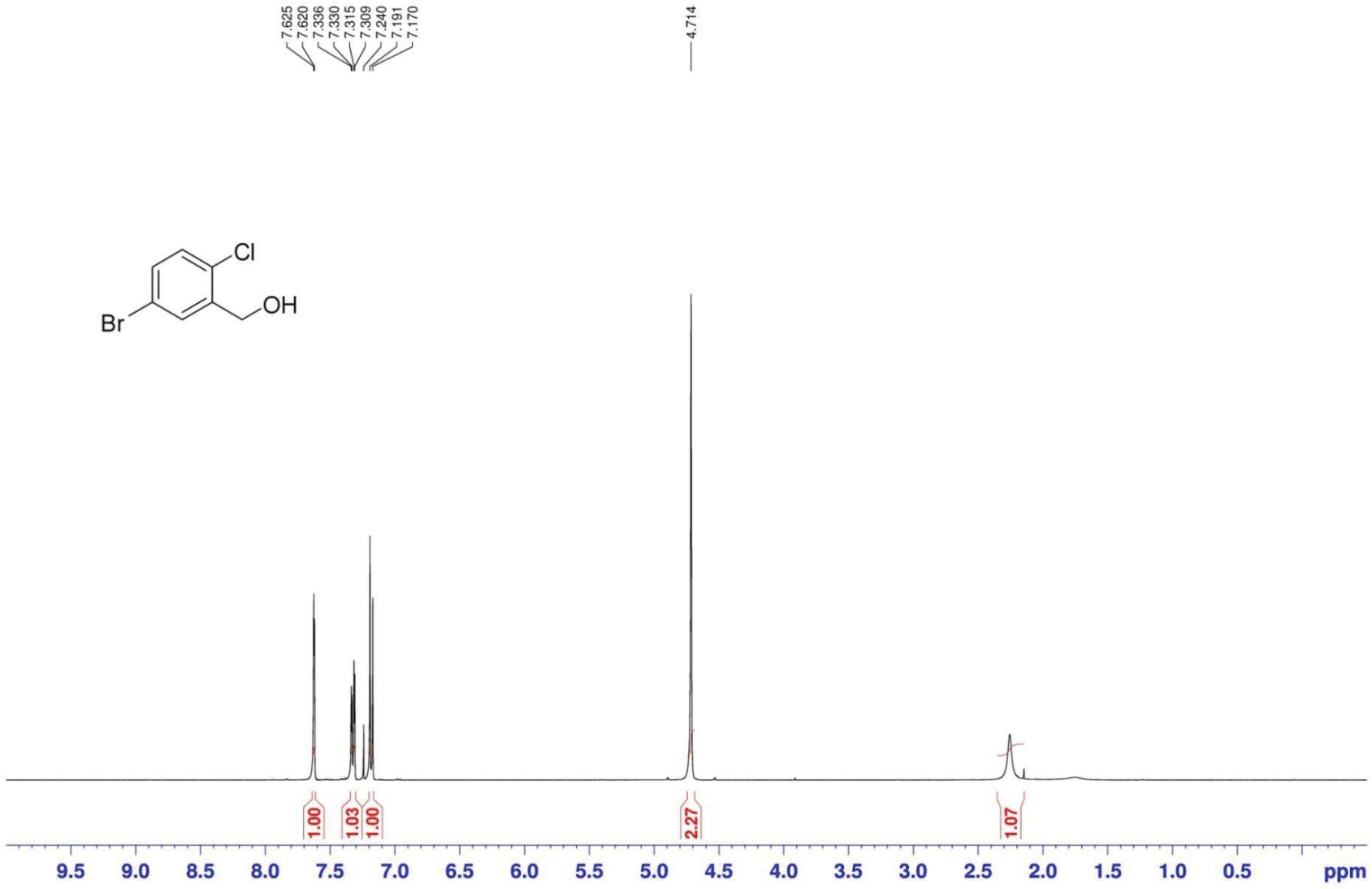

Appendix 53. ^{1}H-NMR spectra of **60** (400 MHz, d_4-MeOH)

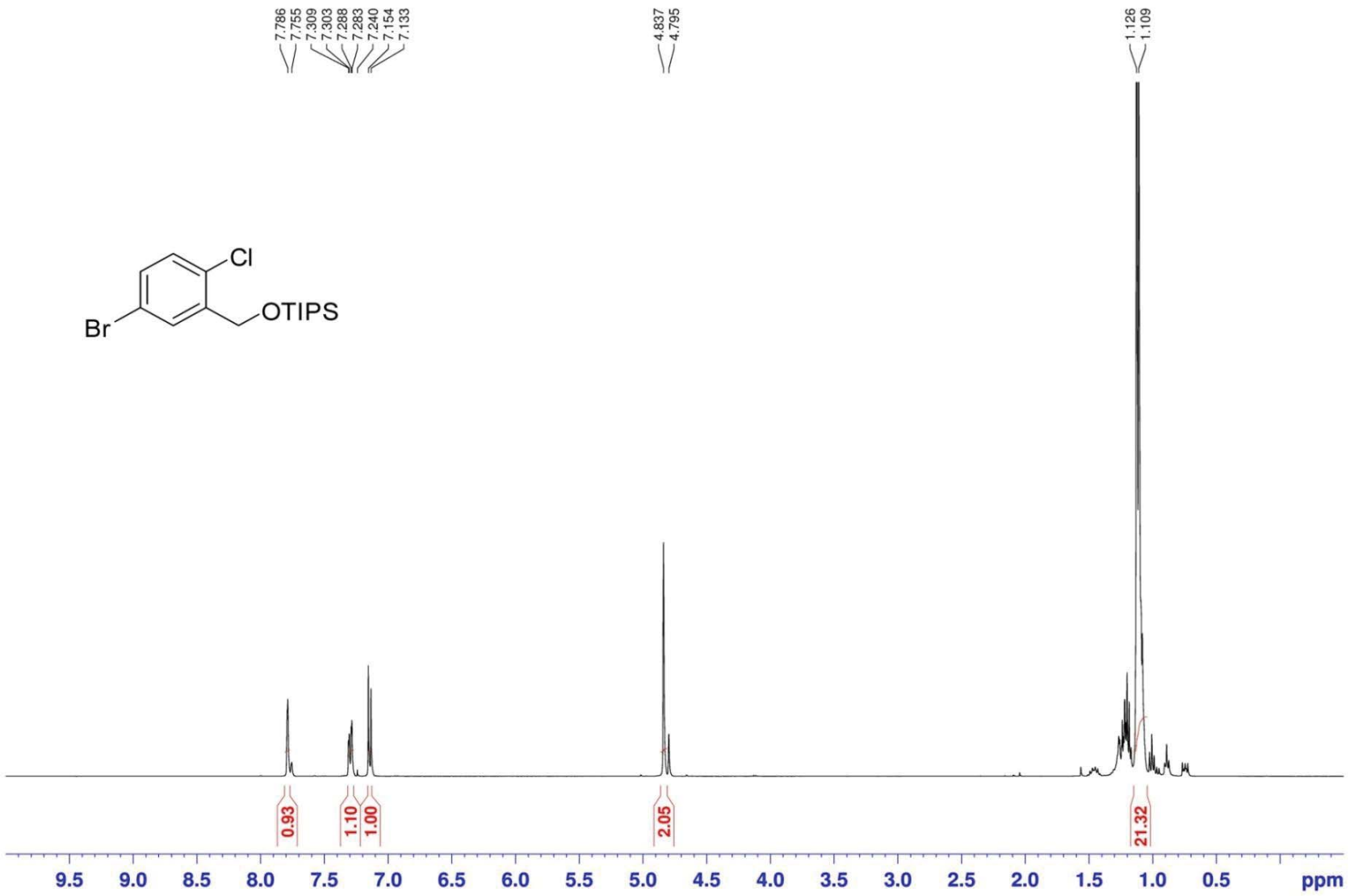

Appendix 54. ^{1}H-NMR spectra of **61** (400 MHz, d_4-MeOH)

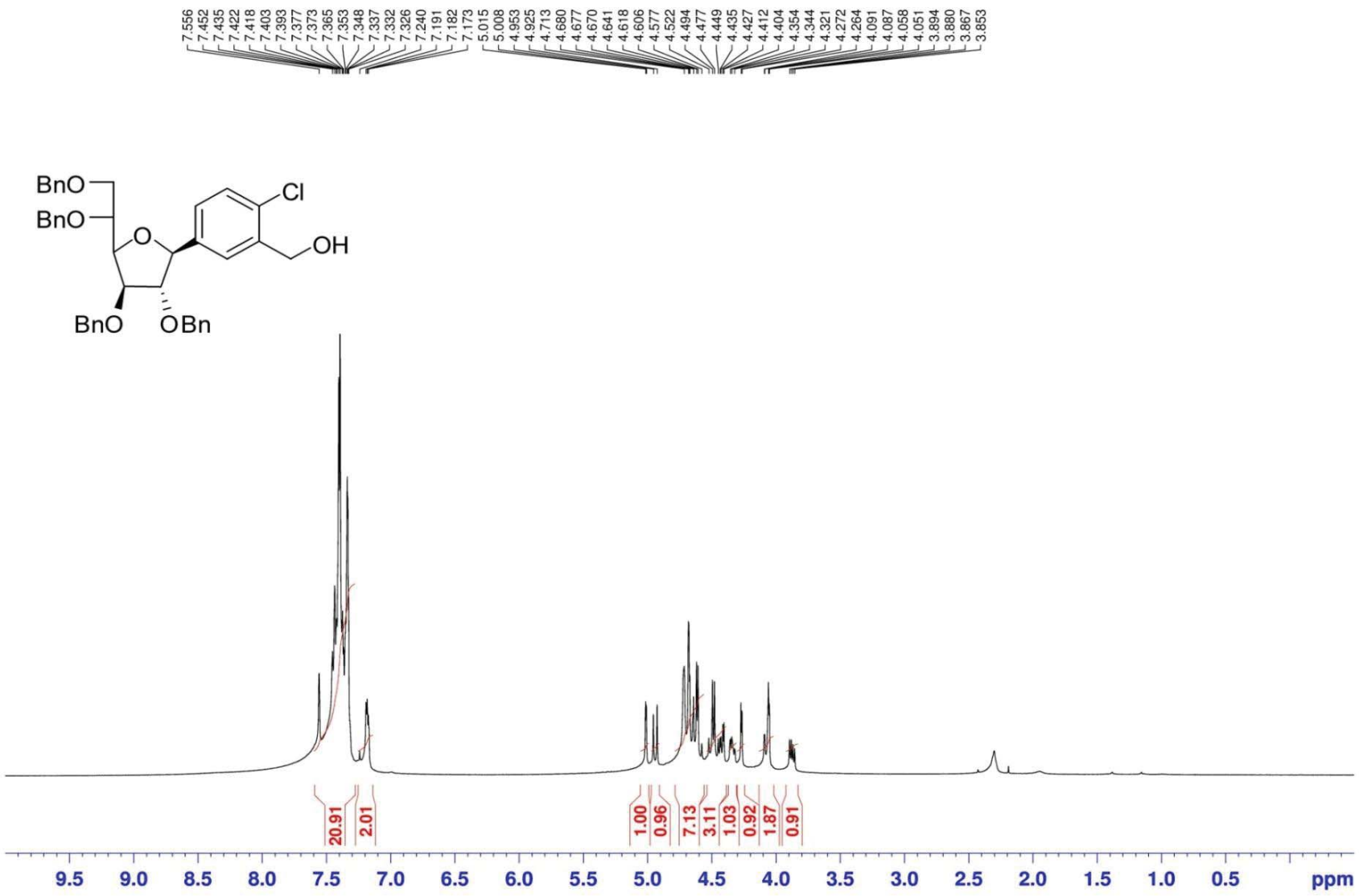

Appendix 55. ^{1}H-NMR spectra of **64** (400 MHz, d_4-MeOH)

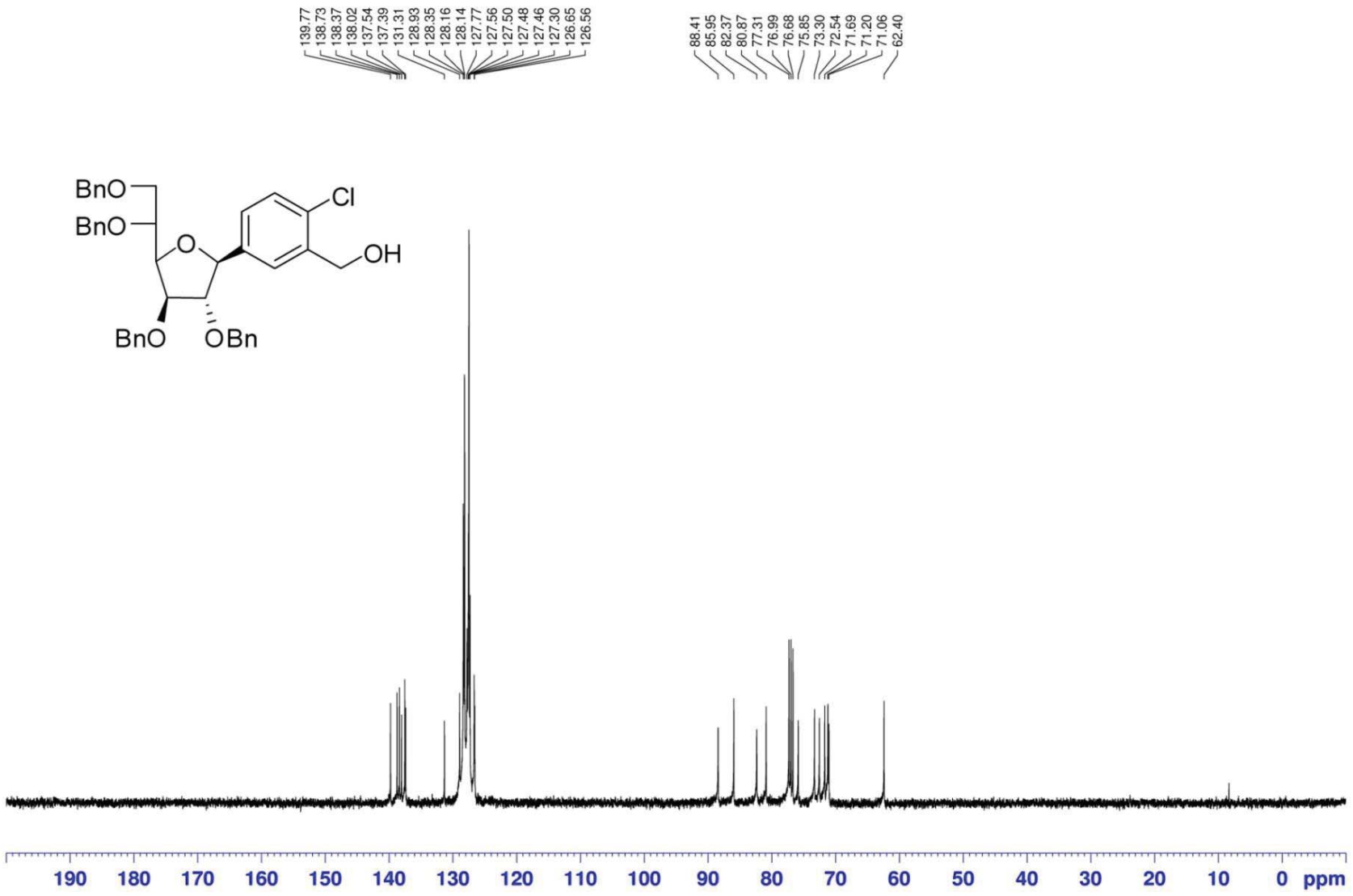

Appendix 56. ^{13}C-NMR spectra of **64** (100 MHz, d_4-MeOH)

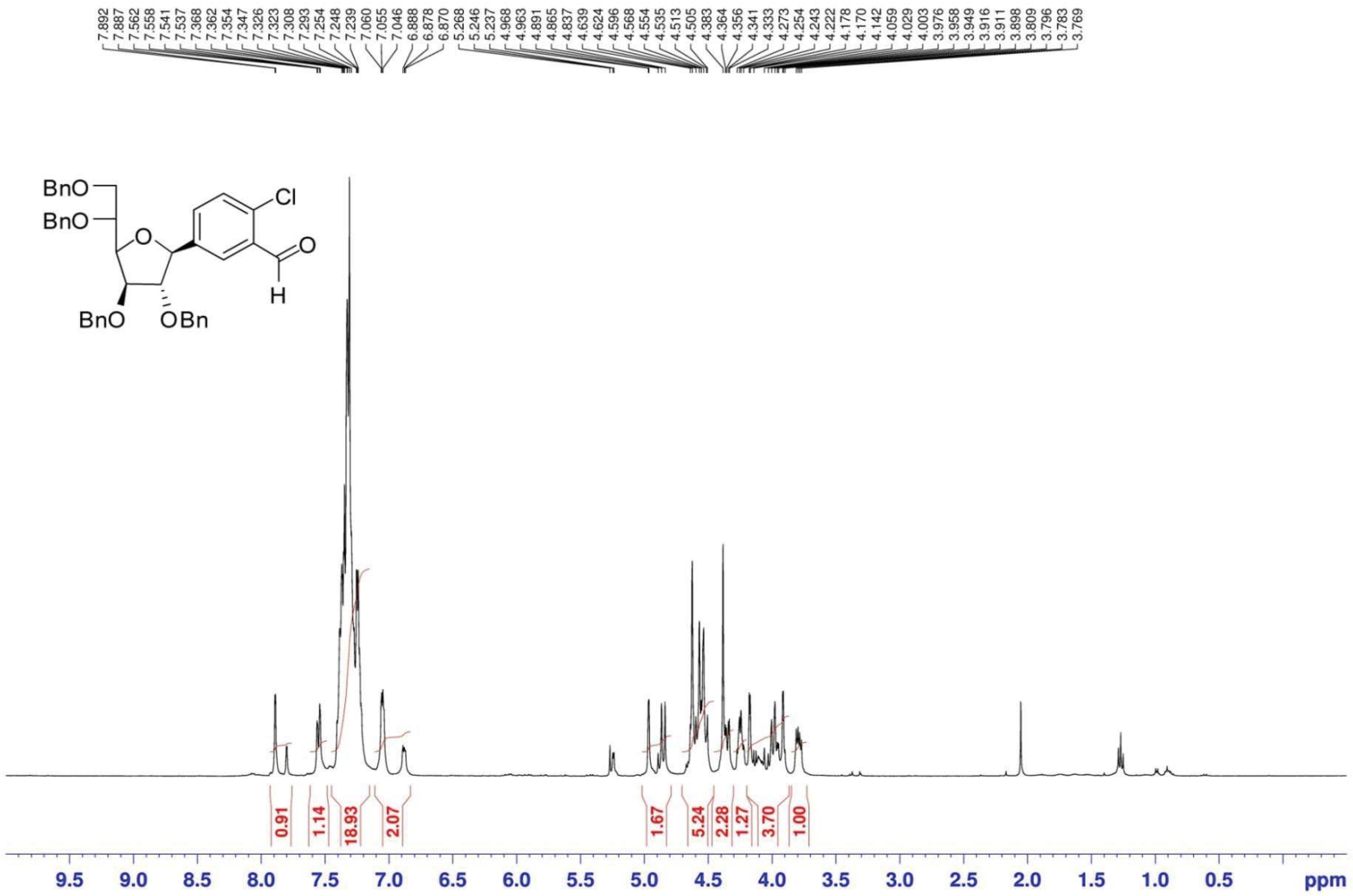

Appendix 57. ^{1}H-NMR spectra of **65** (400 MHz, d_4-MeOH)

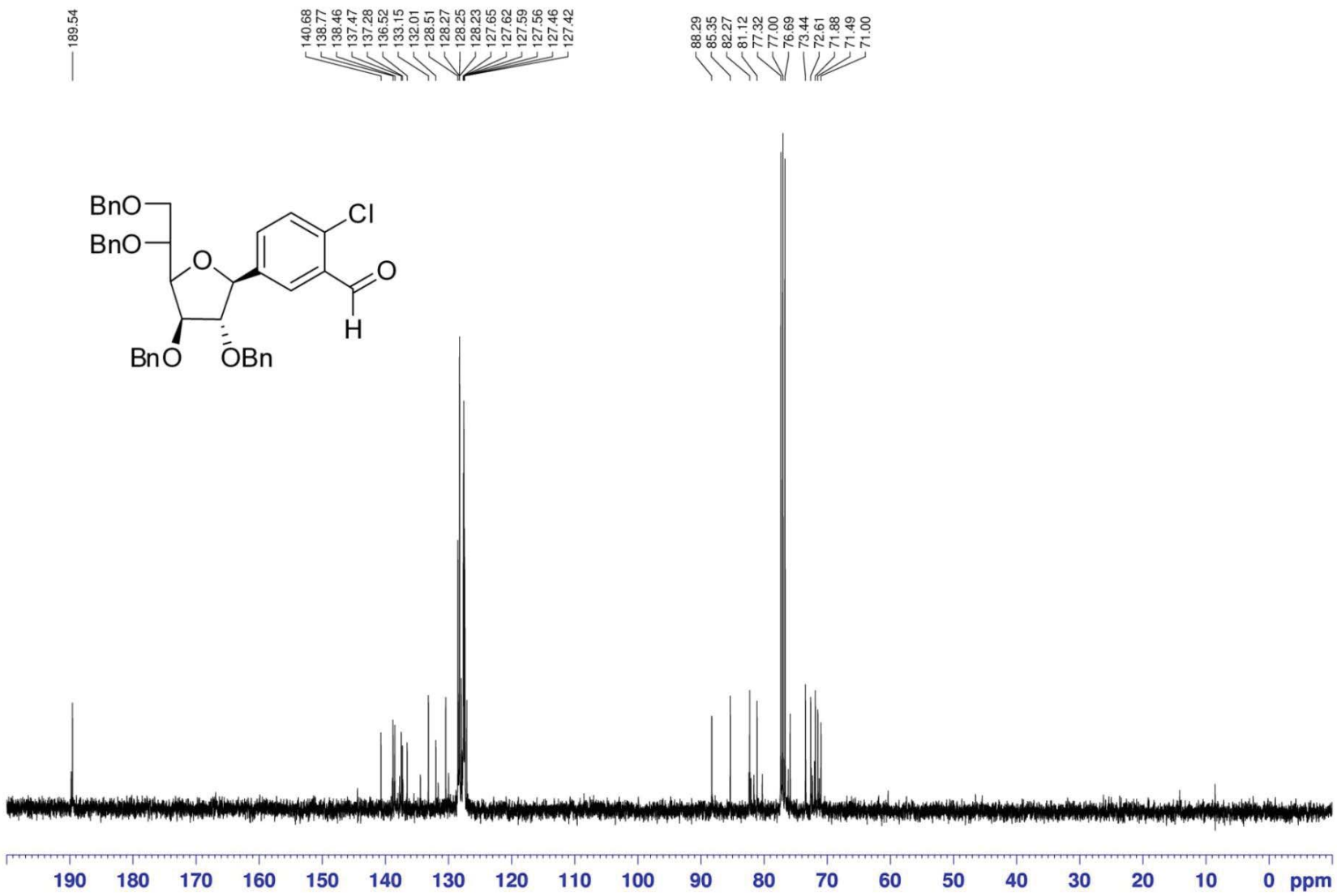

Appendix 58. ^{13}C-NMR spectra of **65** (100 MHz, d_4-MeOH)

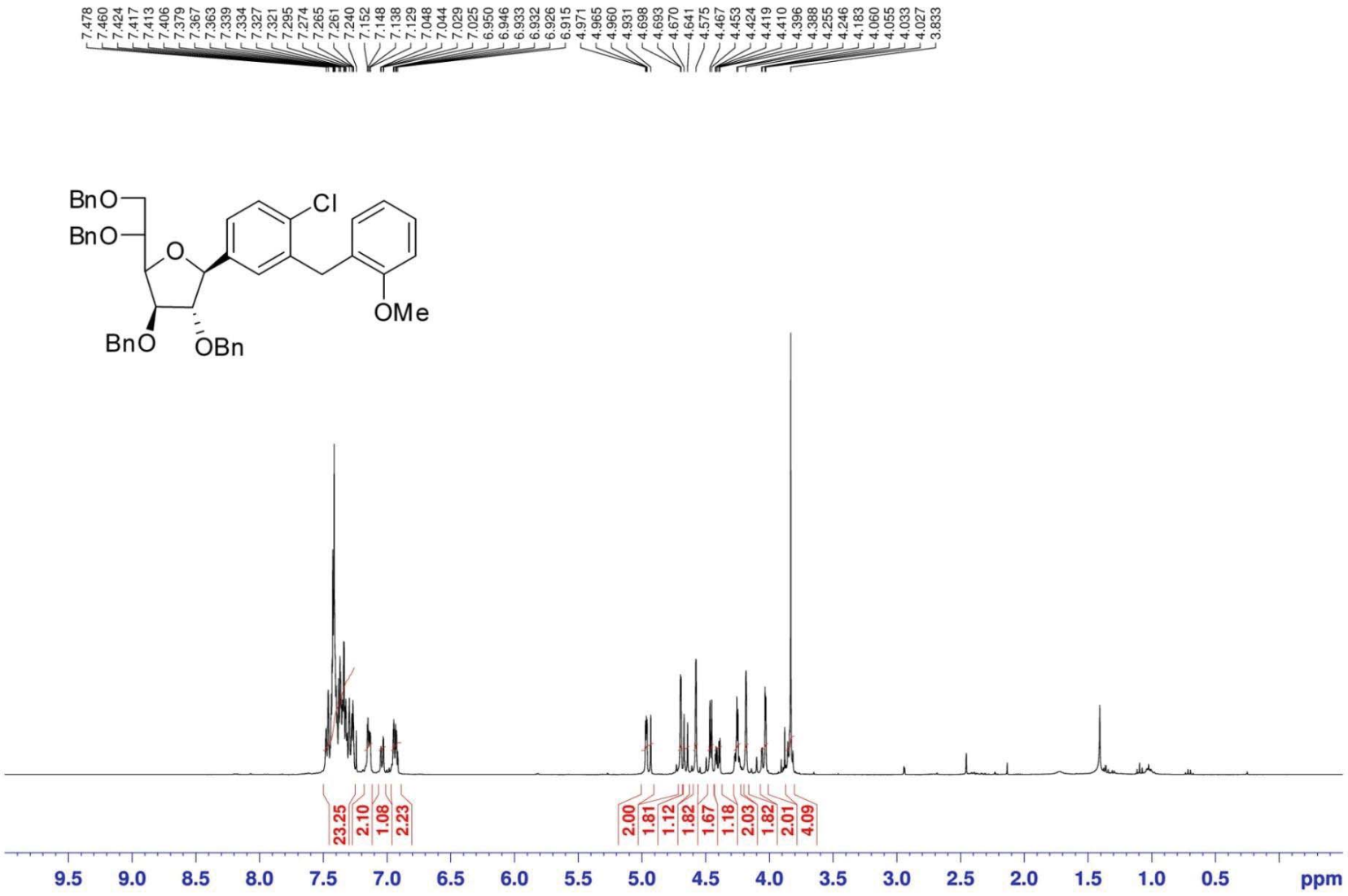

Appendix 59. ^{1}H-NMR spectra of **57i** (400 MHz, $CDCl_3$)

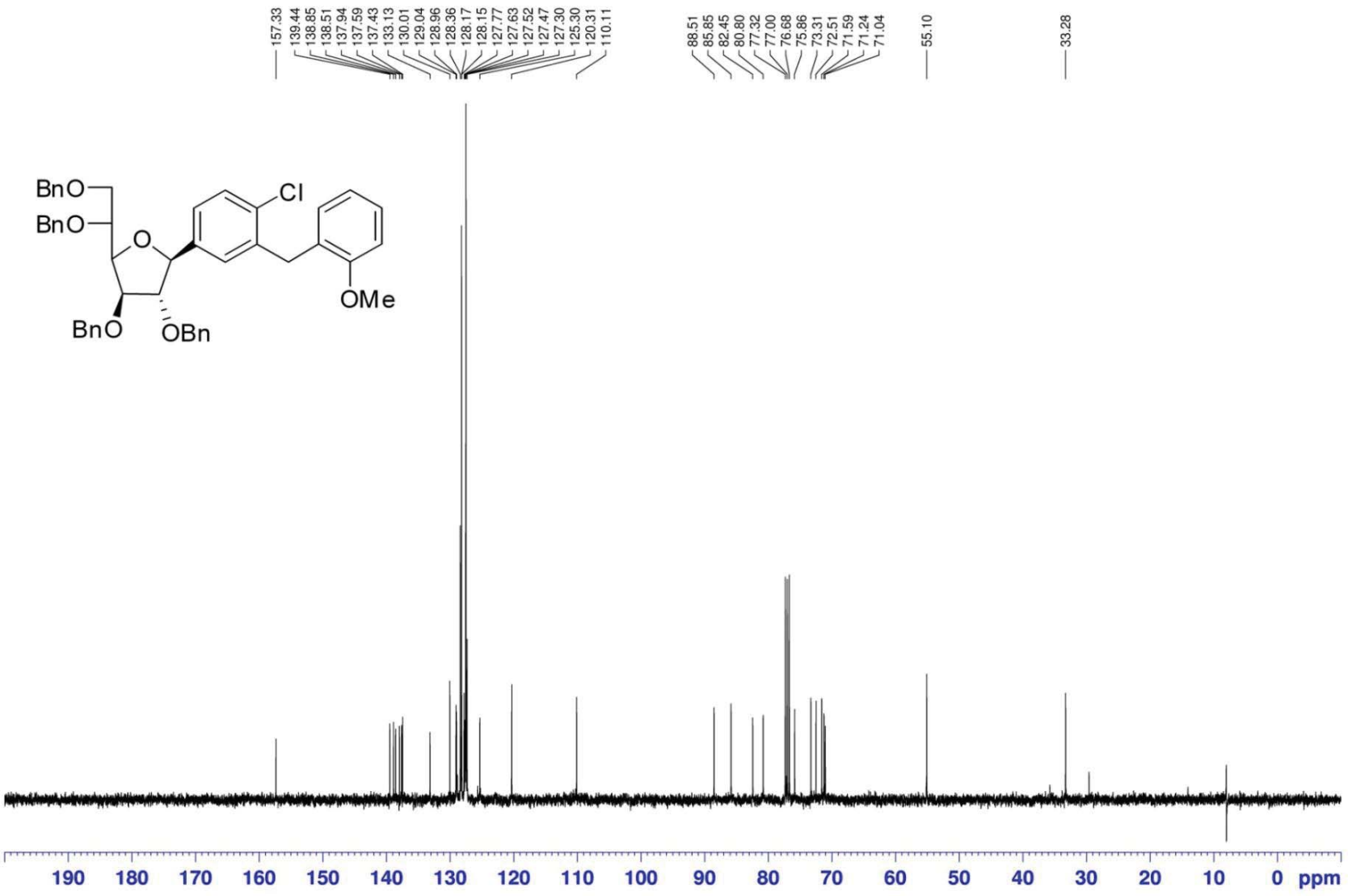

Appendix 60. ^{13}C-NMR spectra of **57i** (100 MHz, $CDCl_3$)

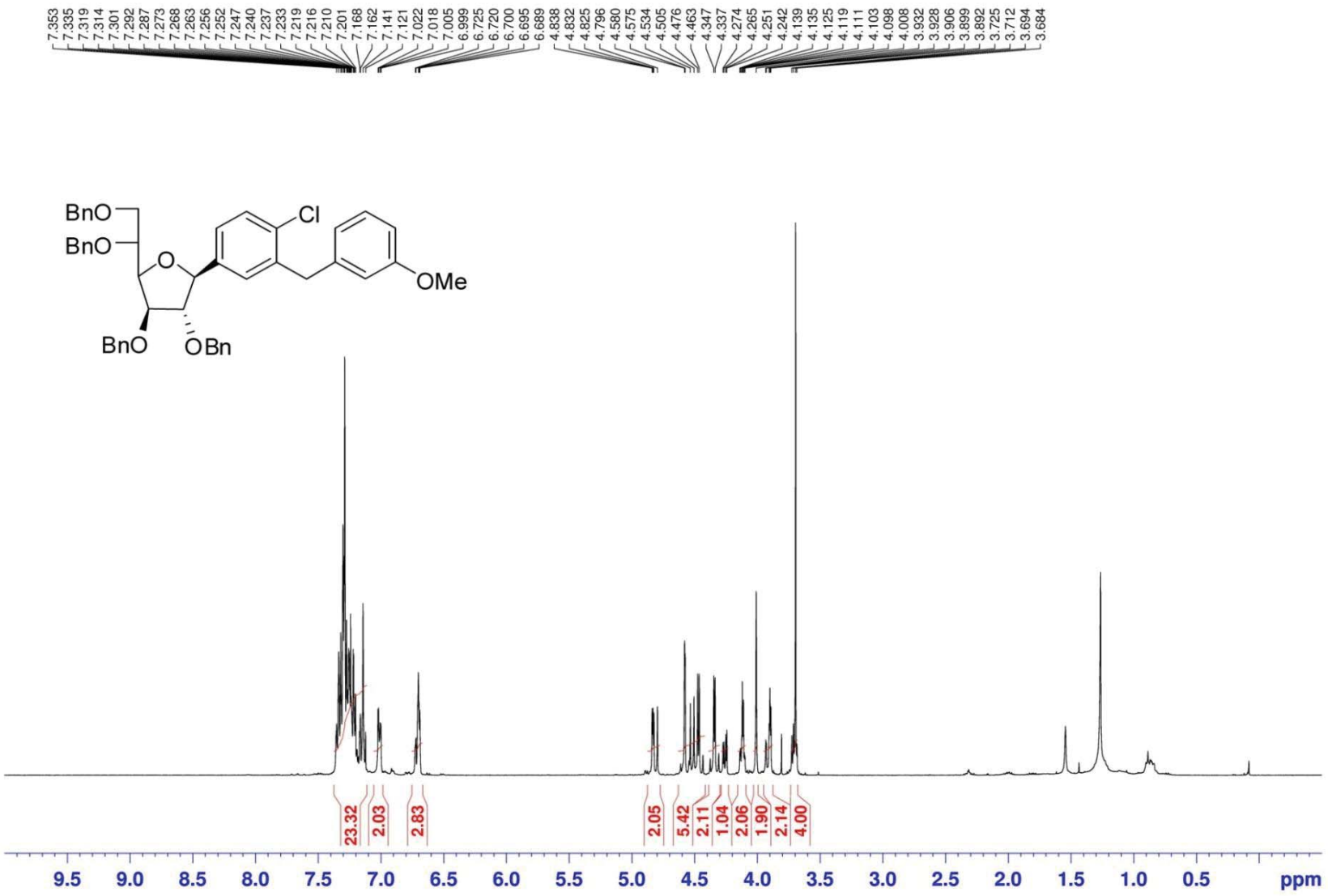

Appendix 61. ^{1}H-NMR spectra of **57j** (400 MHz, $CDCl_3$)

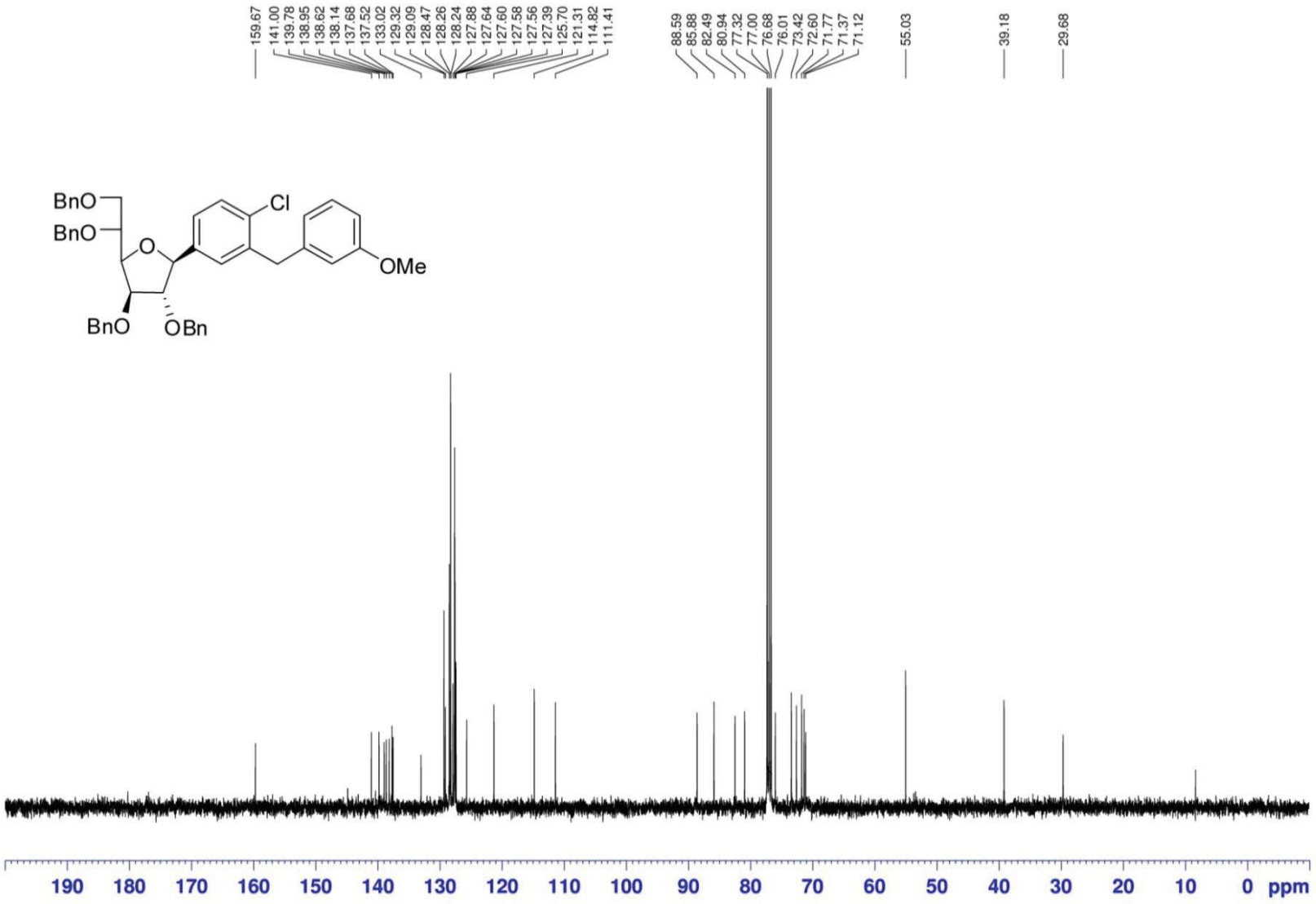

Appendix 62. ^{13}C-NMR spectra of **57j** (100 MHz, $CDCl_3$)

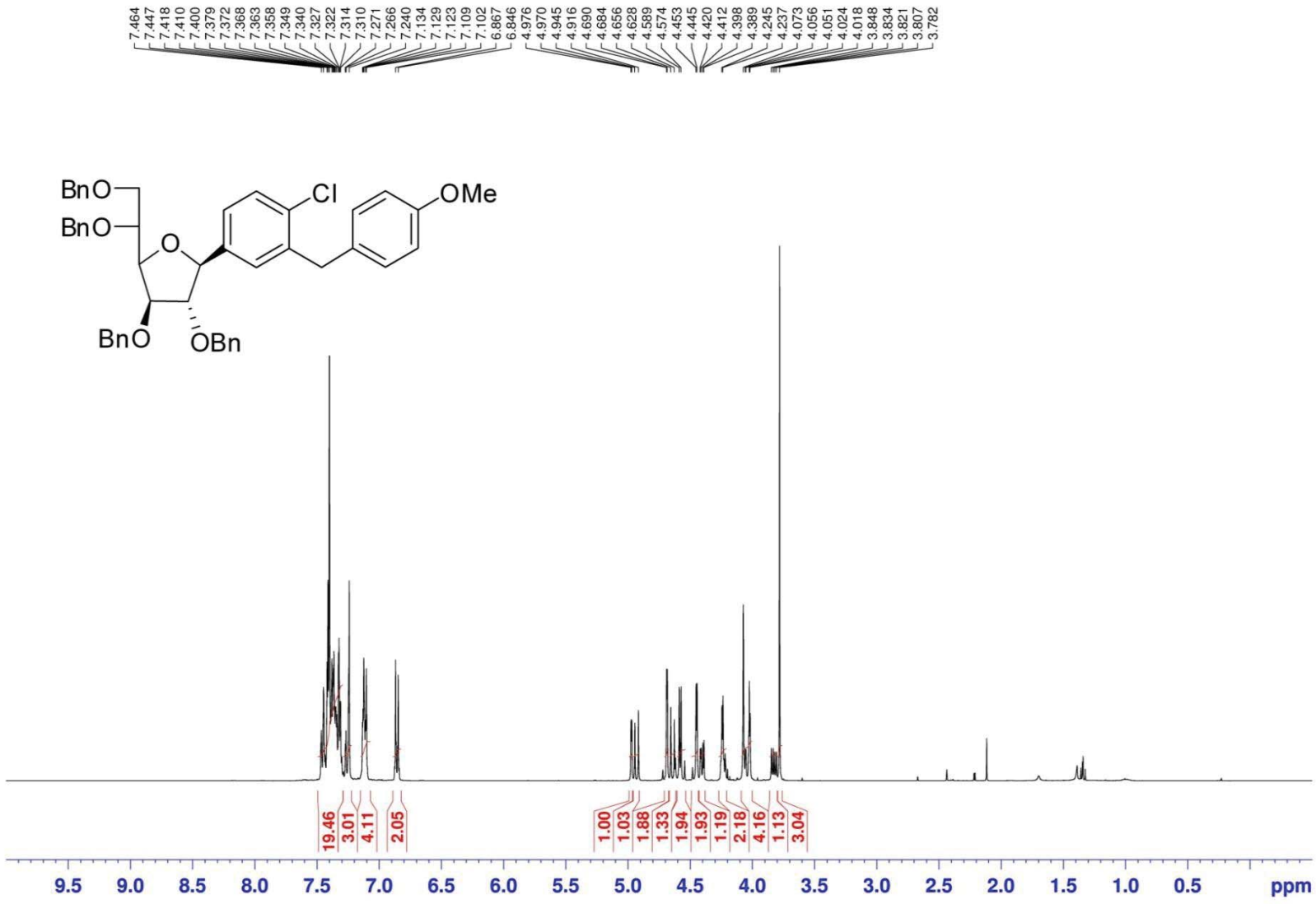

Appendix 63. ^{1}H-NMR spectra of **57k** (400 MHz, $CDCl_3$)

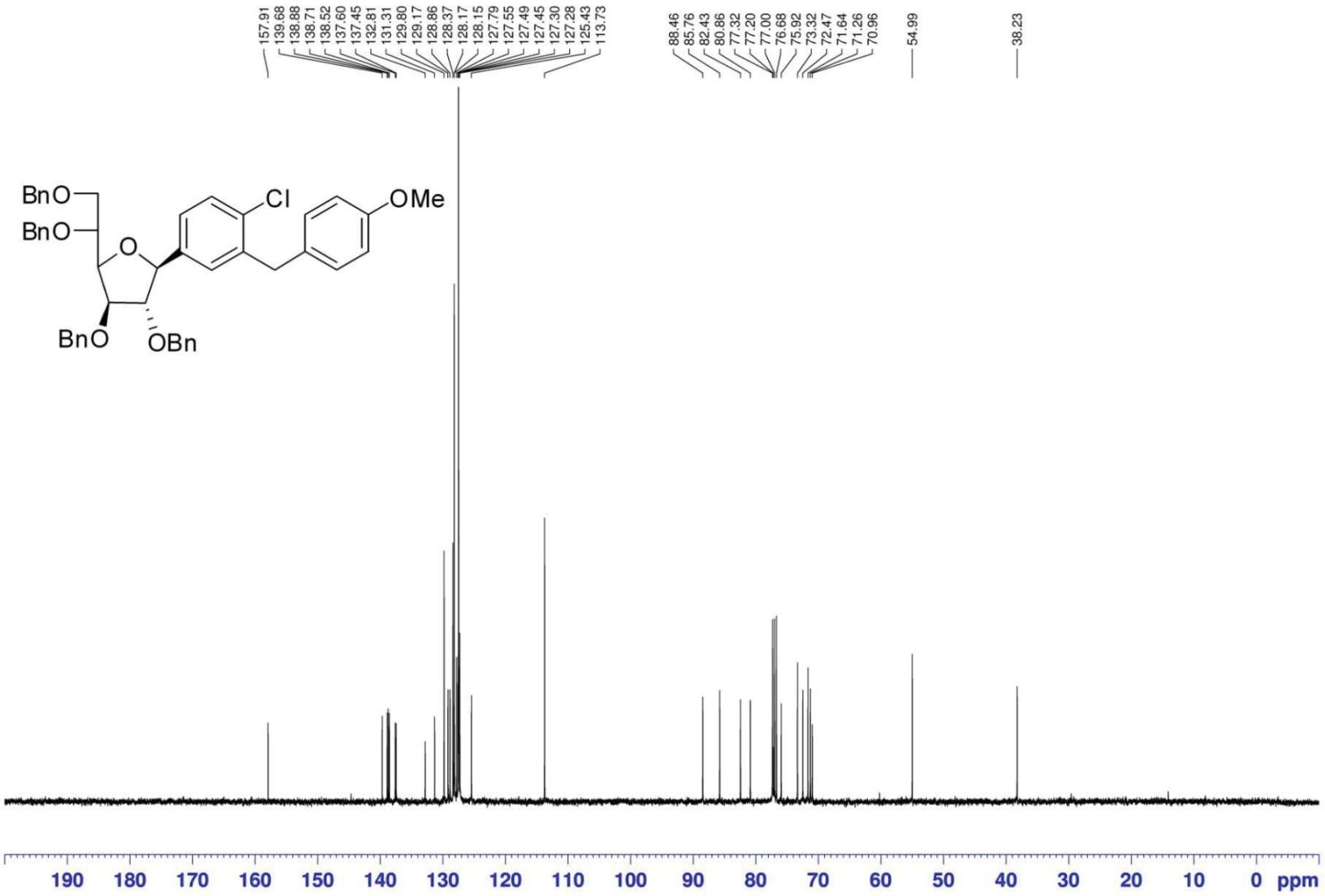

Appendix 64. ^{13}C-NMR spectra of **57k** (100 MHz, $CDCl_3$)

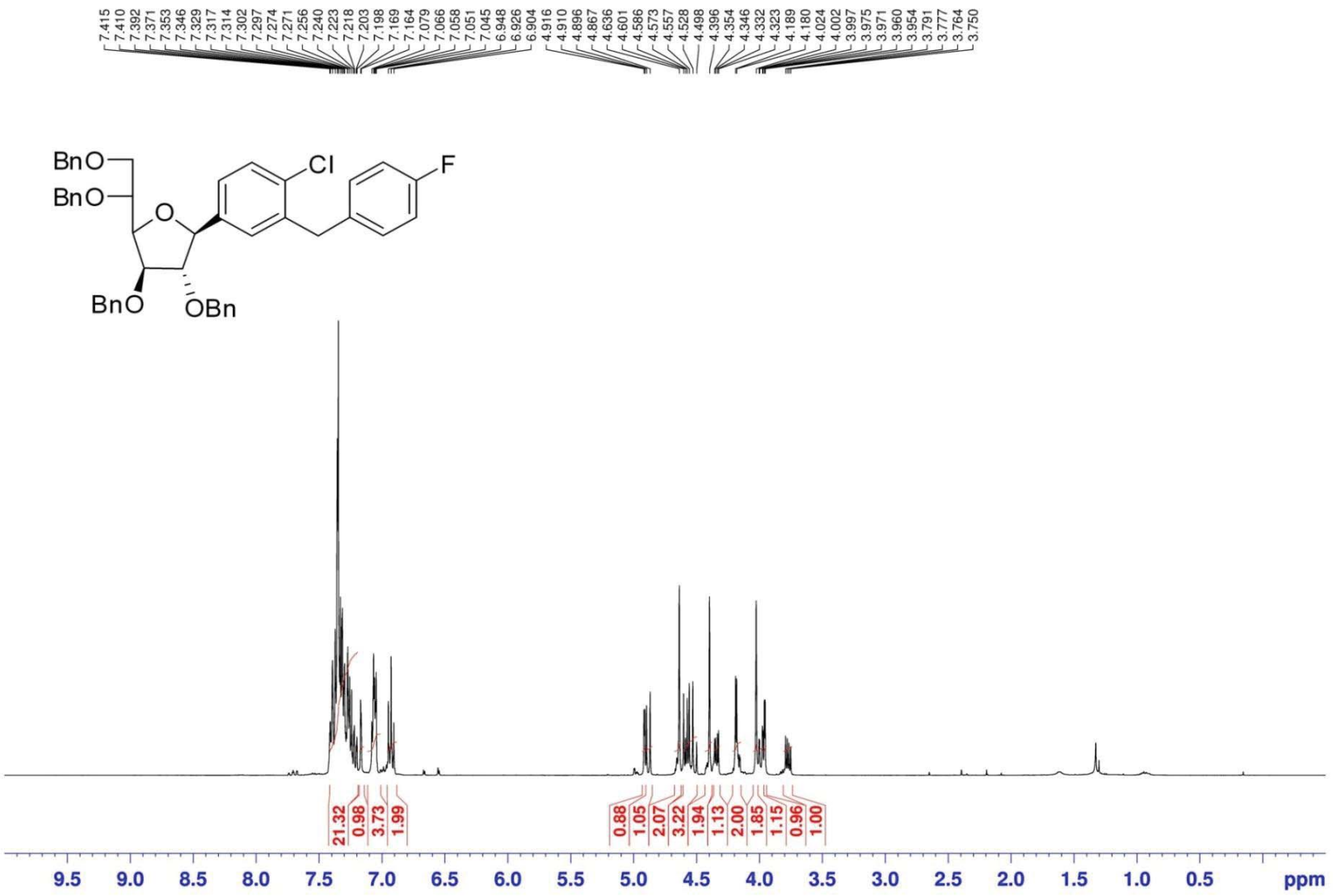

Appendix 65. ^{1}H-NMR spectra of **57l** (400 MHz, $CDCl_3$)

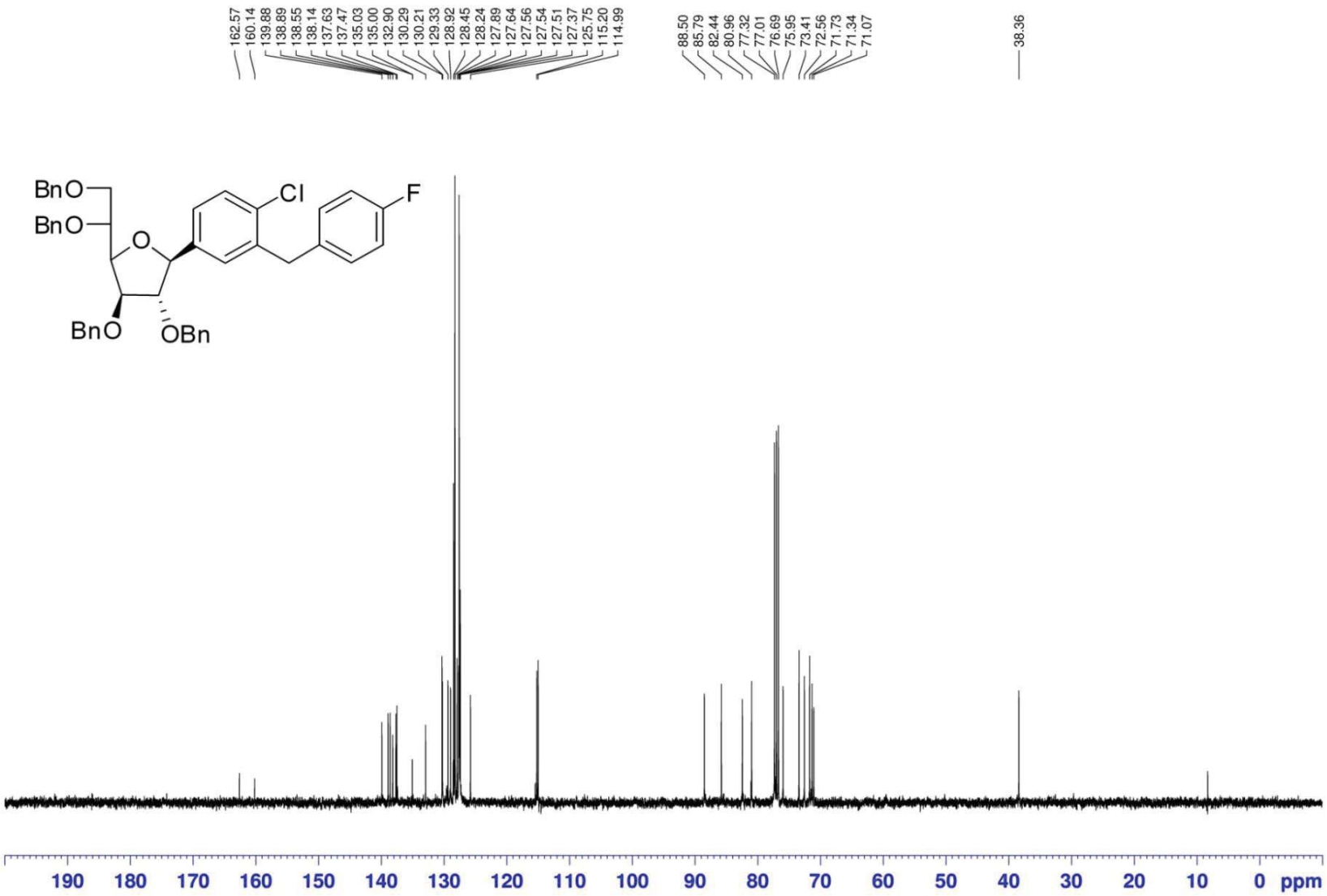

Appendix 66. ^{13}C-NMR spectra of **57l** (100 MHz, $CDCl_3$)

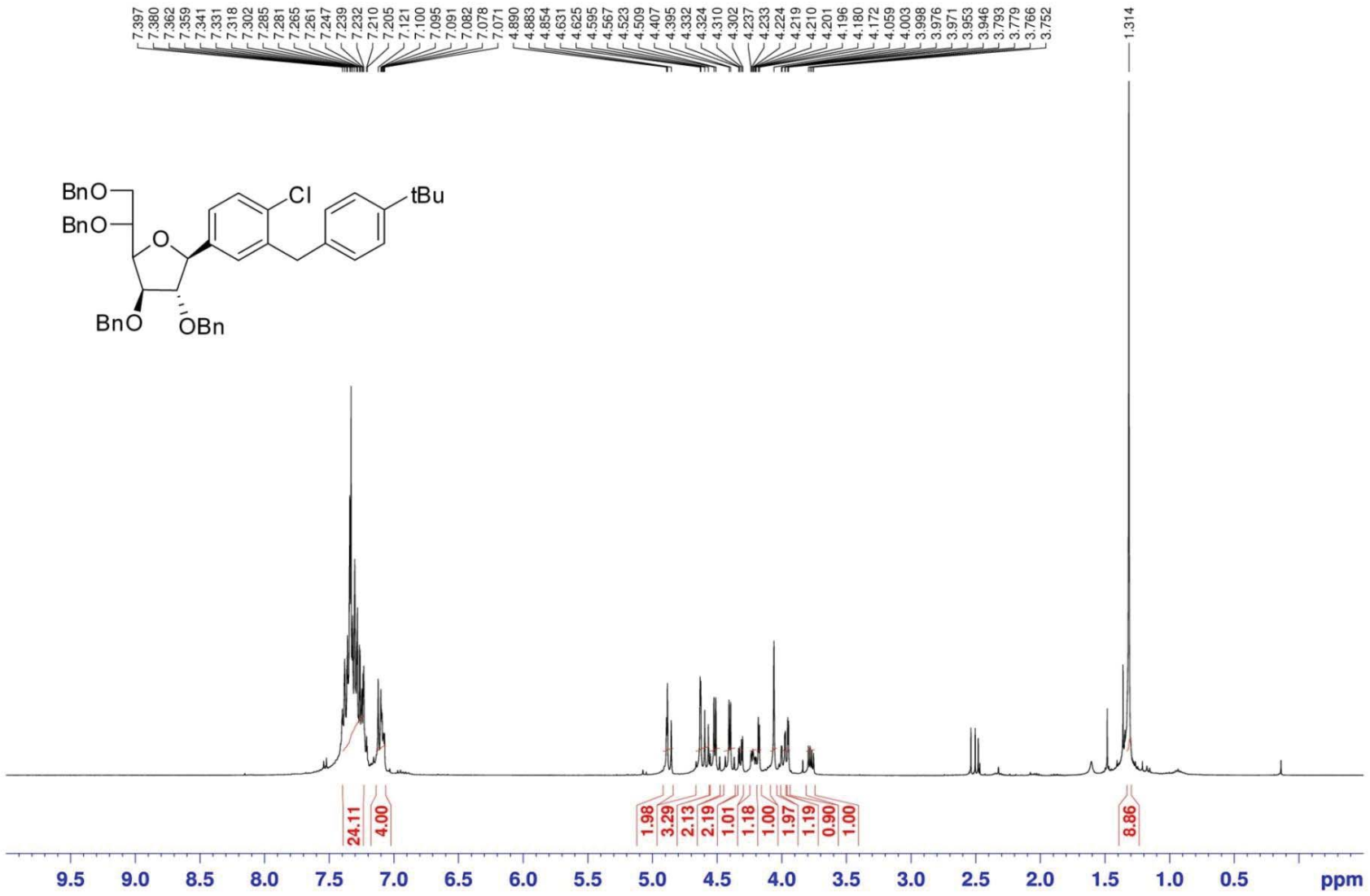

Appendix 67. ^{1}H-NMR spectra of **57m** (400 MHz, $CDCl_3$)

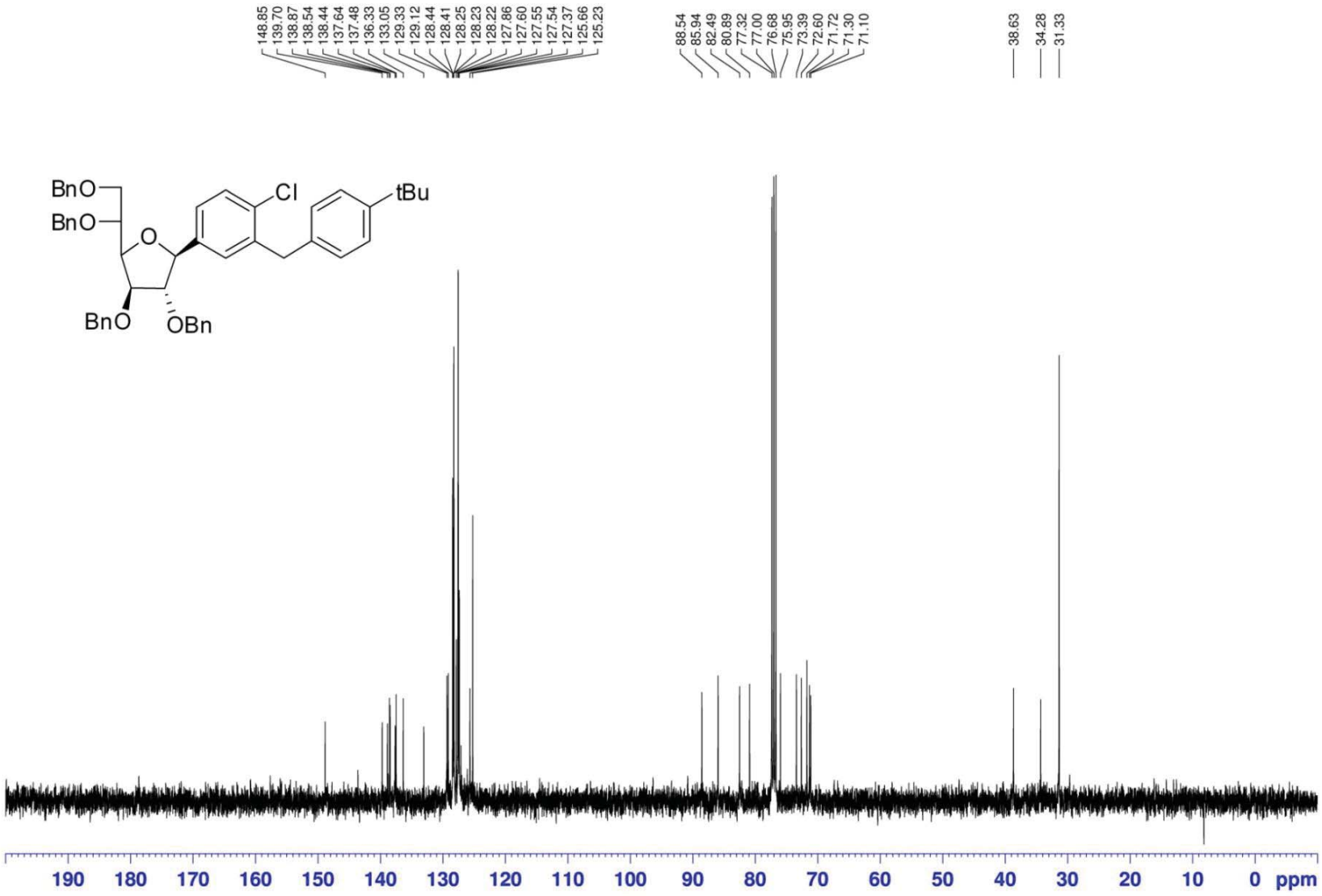

Appendix 68. ^{13}C-NMR spectra of **57m** (100 MHz, $CDCl_3$)

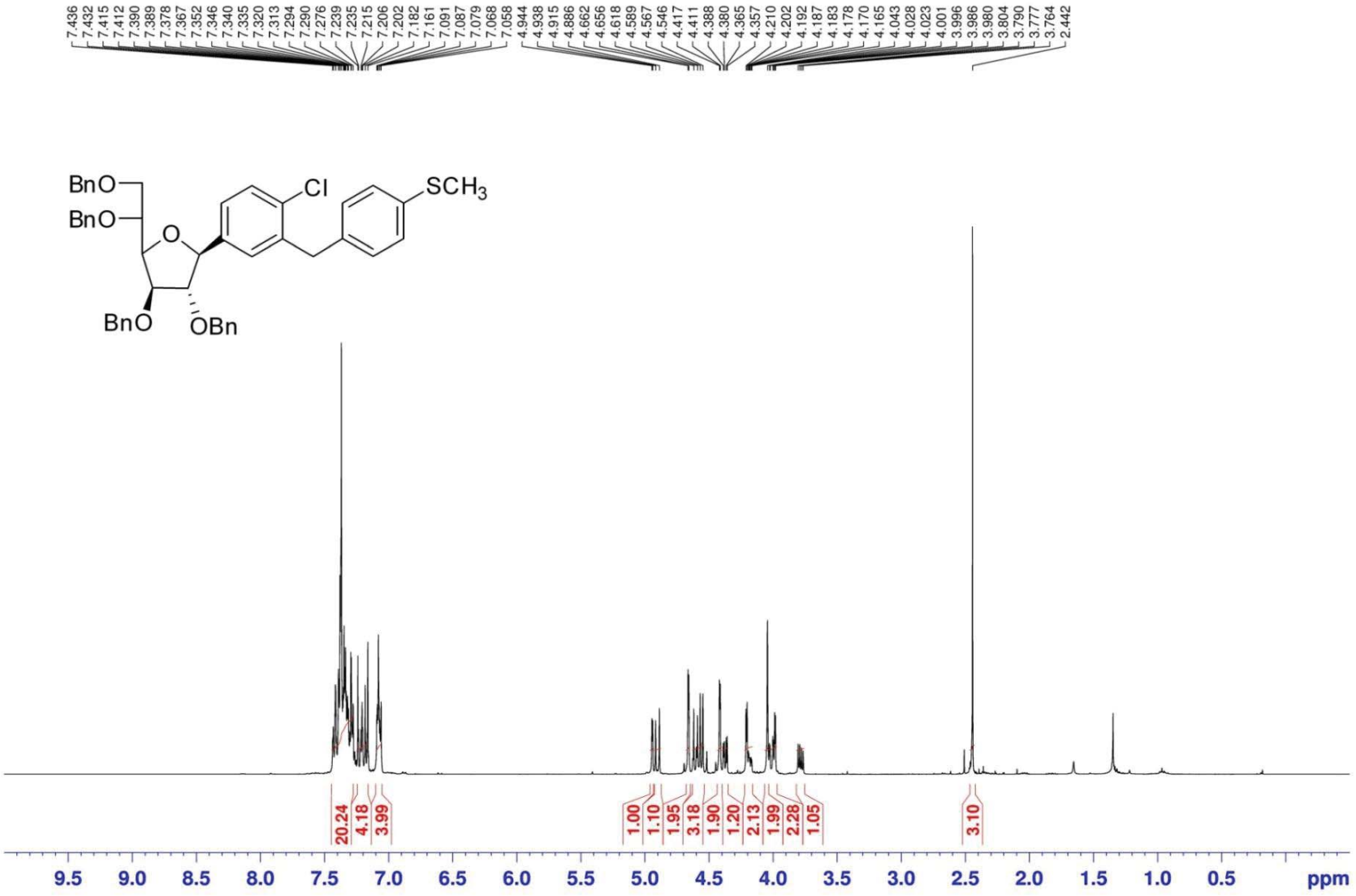

Appendix 69. ^{1}H-NMR spectra of **57n** (400 MHz, $CDCl_3$)

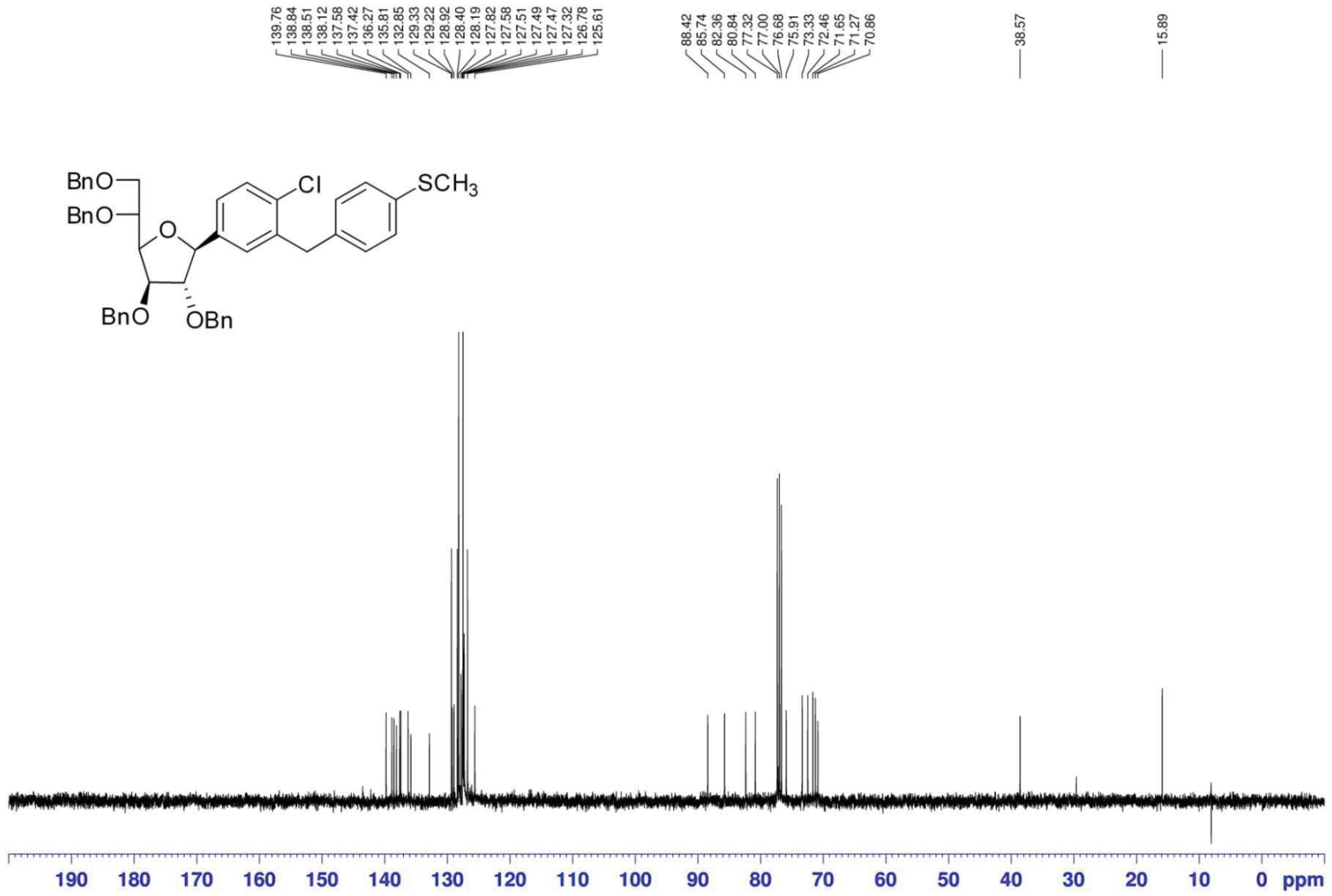

Appendix 70. ^{13}C-NMR spectra of **57n** (100 MHz, $CDCl_3$)

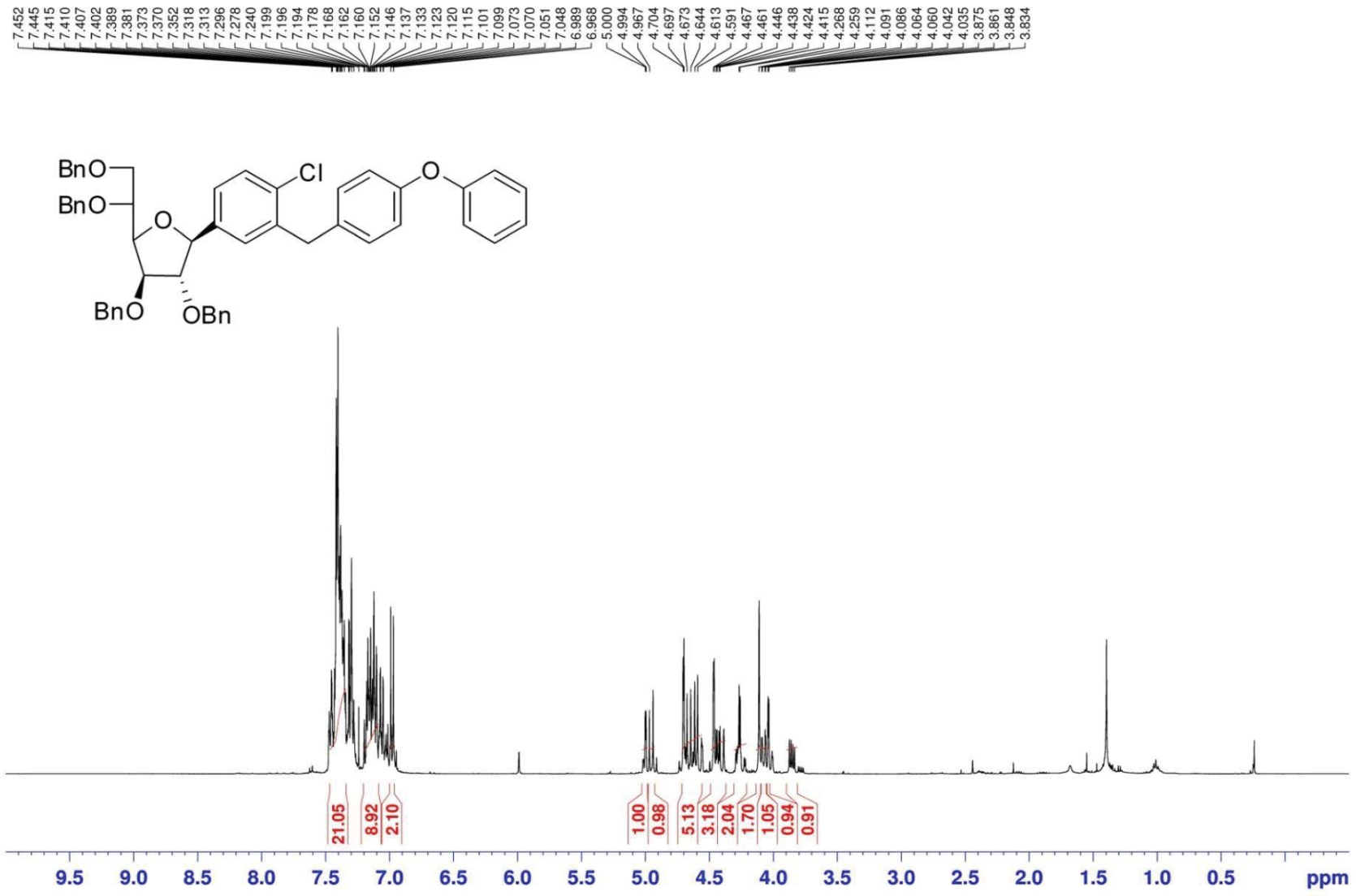

Appendix 71. ^{1}H-NMR spectra of **57o** (400 MHz, $CDCl_3$)

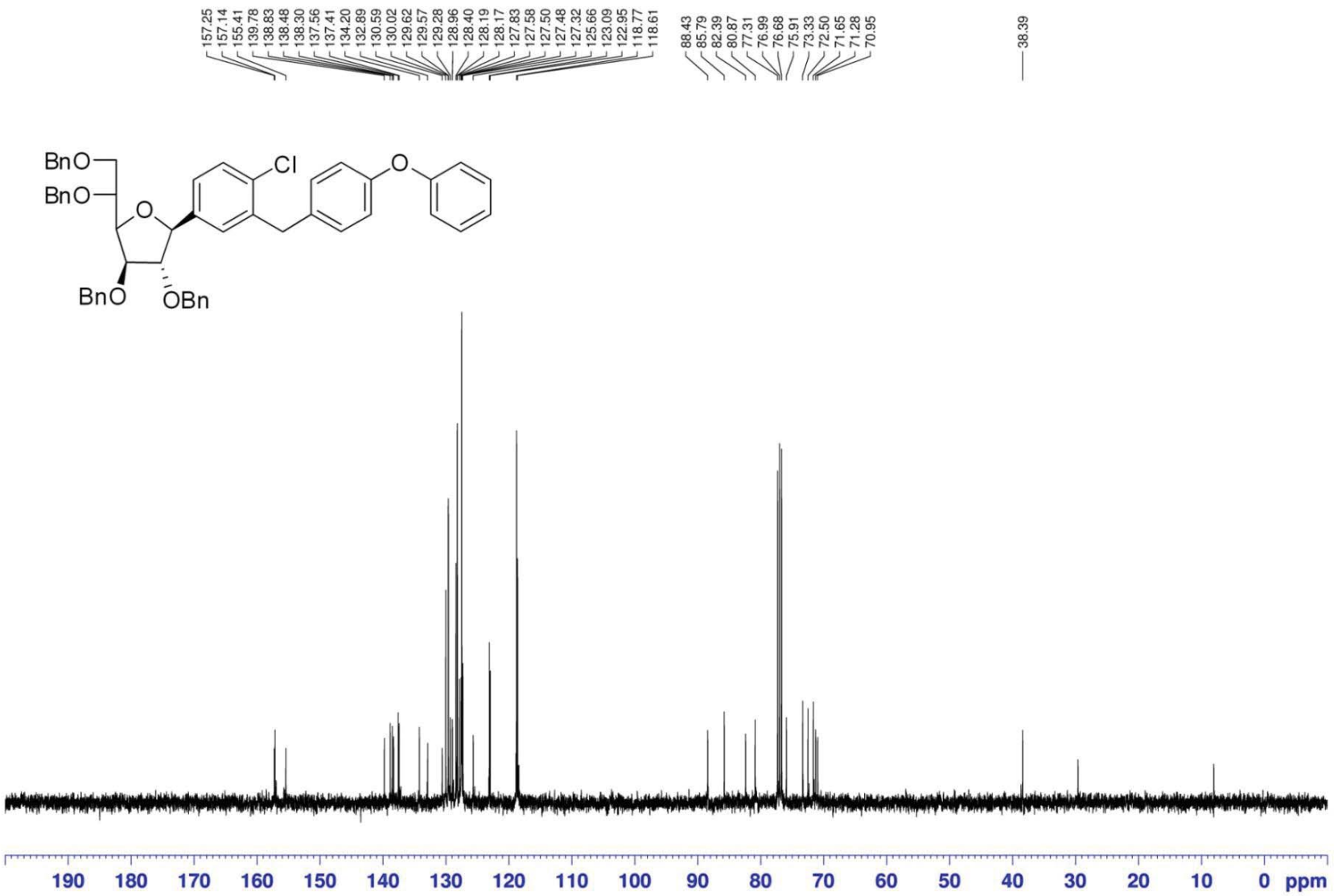

Appendix 72. ^{13}C-NMR spectra of **57o** (100 MHz, $CDCl_3$)

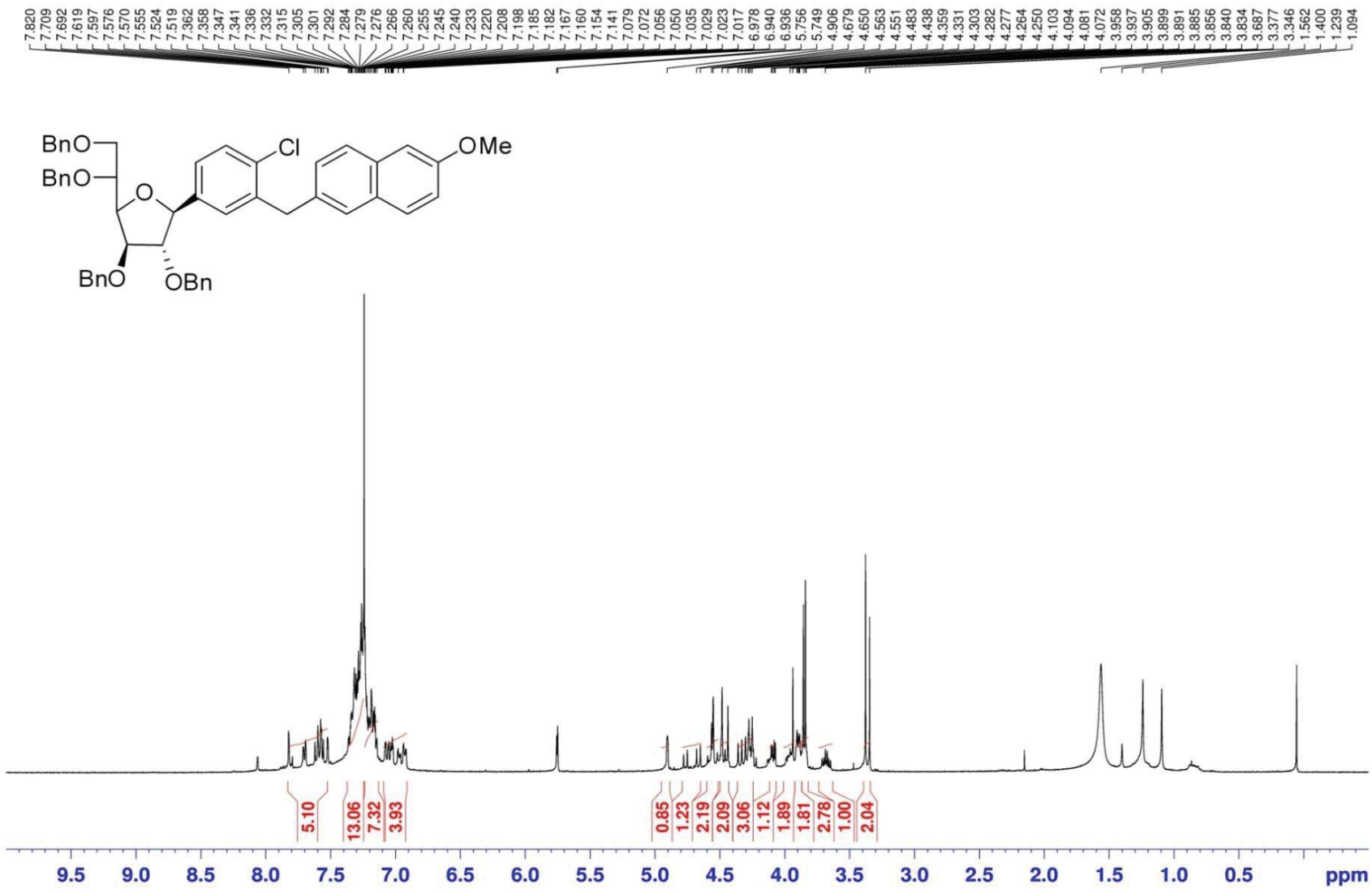

Appendix 73. ^{1}H-NMR spectra of **57p** (400 MHz, $CDCl_3$)

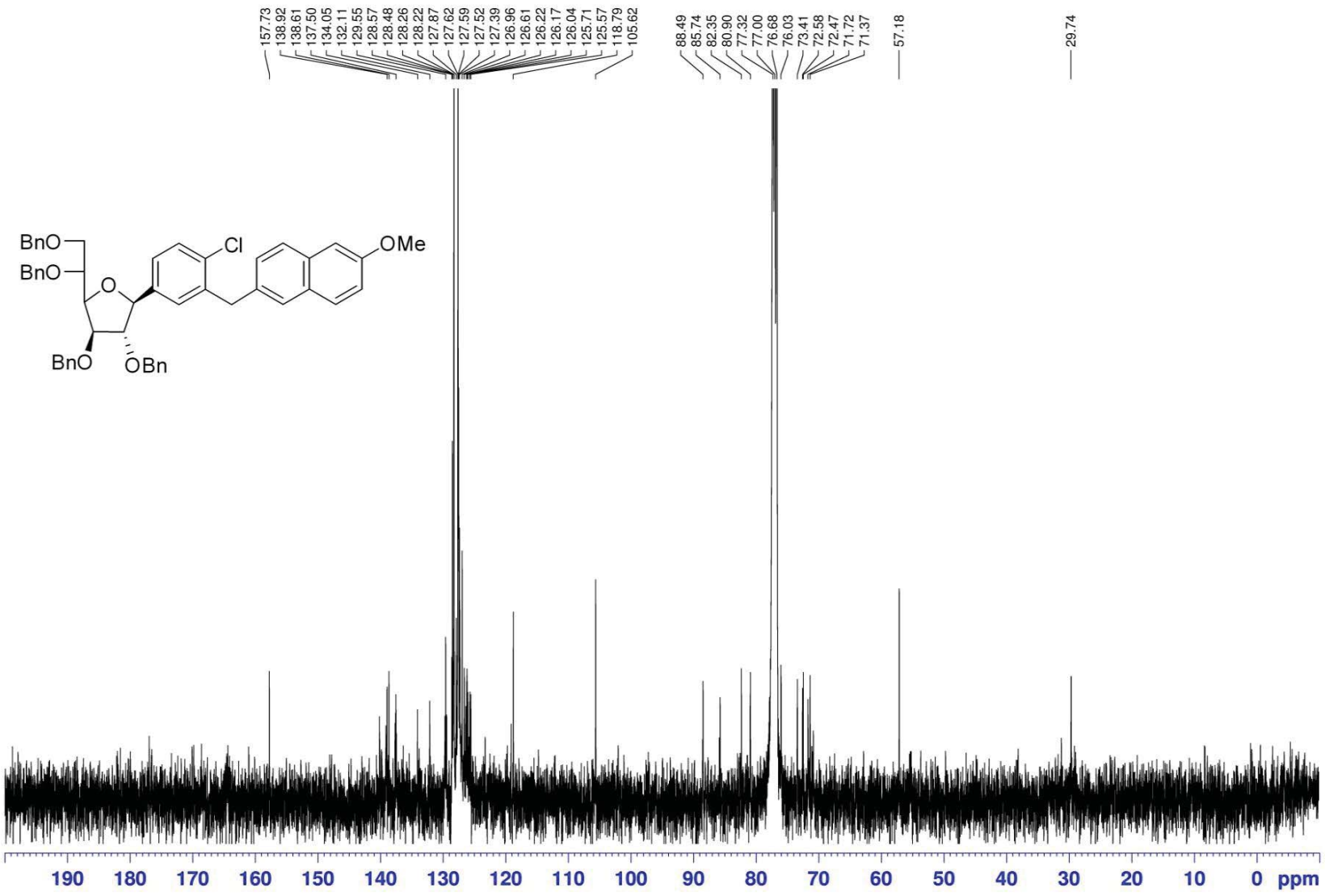

Appendix 74. ^{13}C-NMR spectra of **57p** (100 MHz, $CDCl_3$)

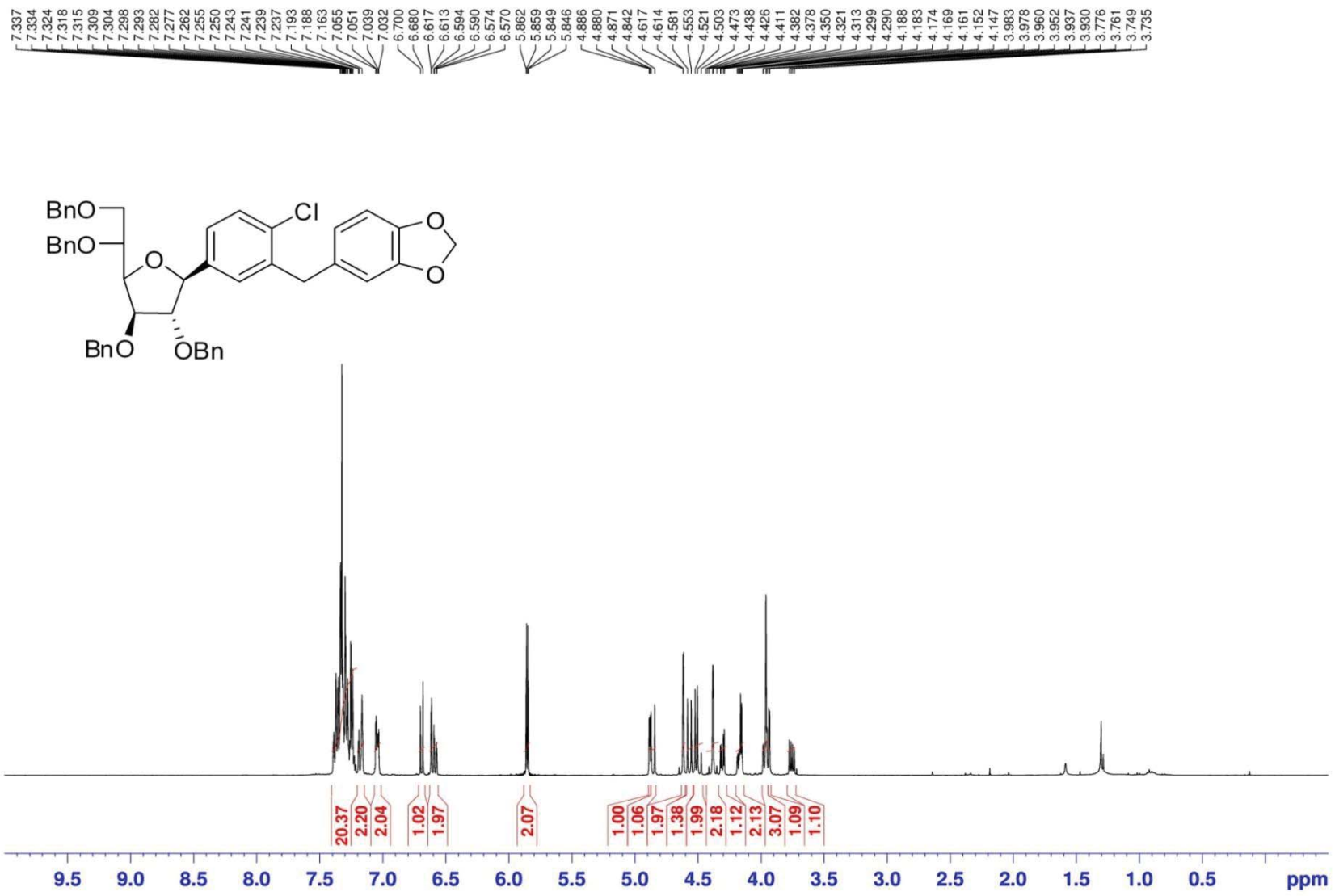

Appendix 75. ^{1}H-NMR spectra of **57q** (400 MHz, $CDCl_3$)

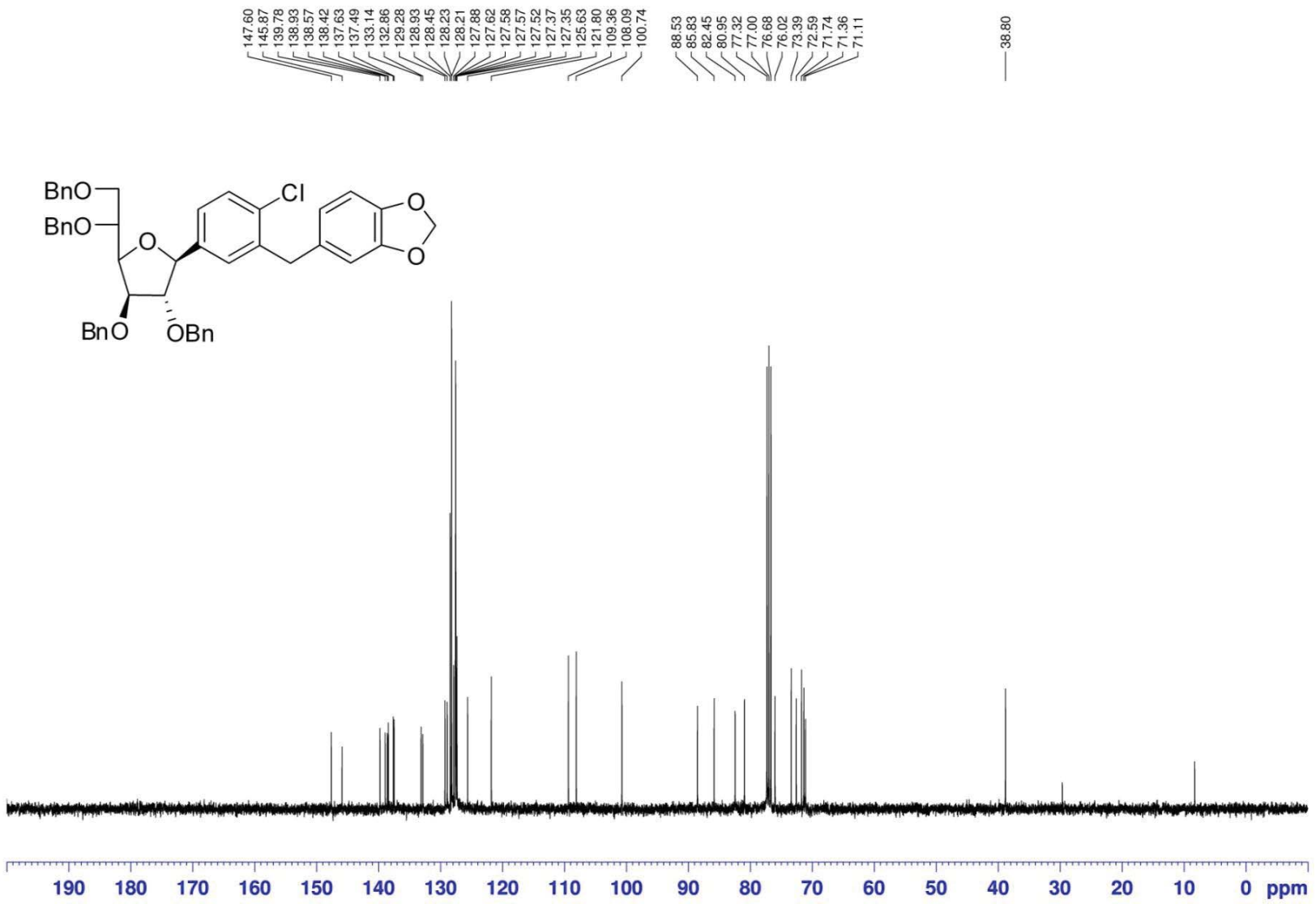

Appendix 76. ^{13}C-NMR spectra of **57q** (100 MHz, $CDCl_3$)

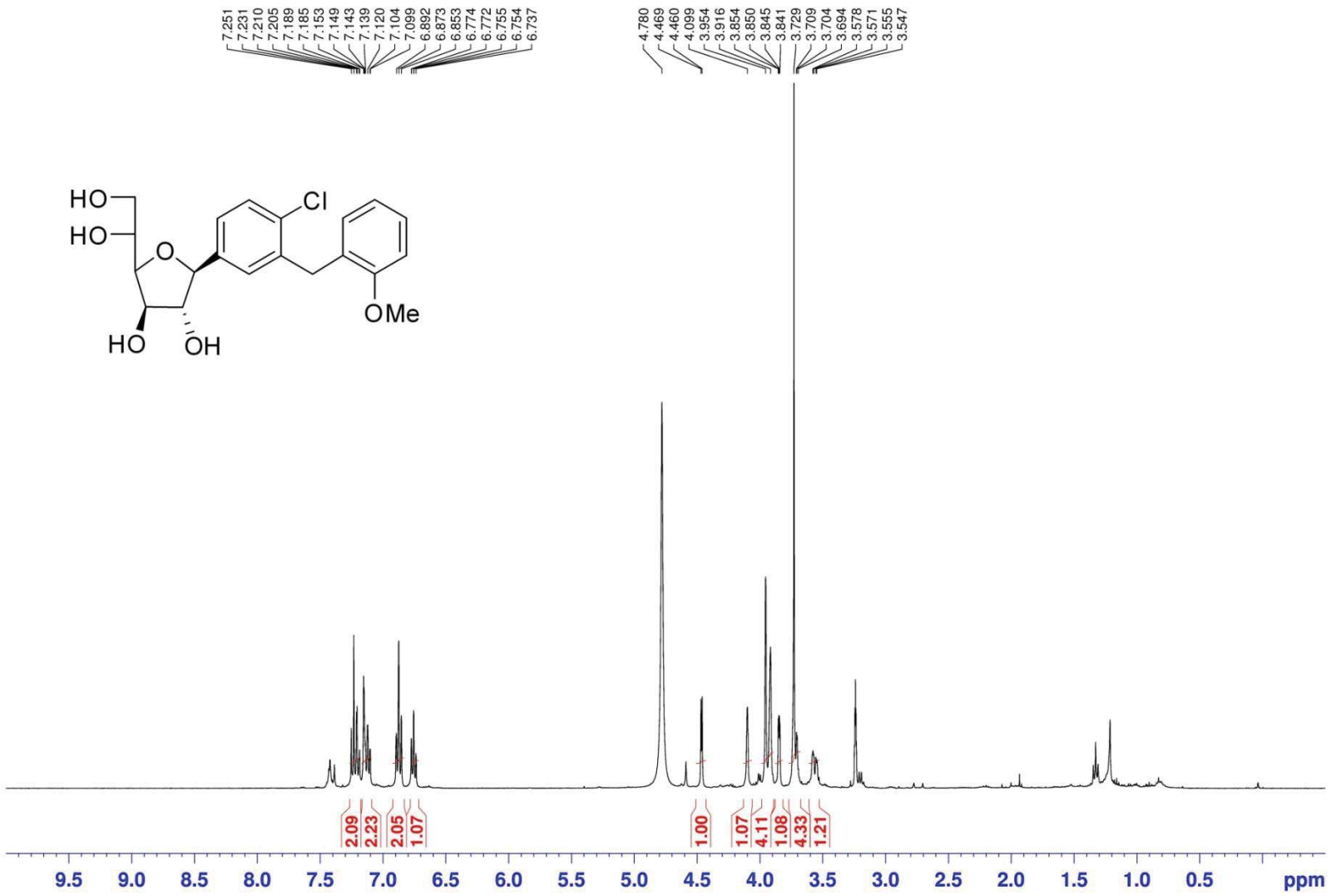

Appendix 77. ^{1}H-NMR spectra of **32i** (400 MHz, d_4-MeOH)

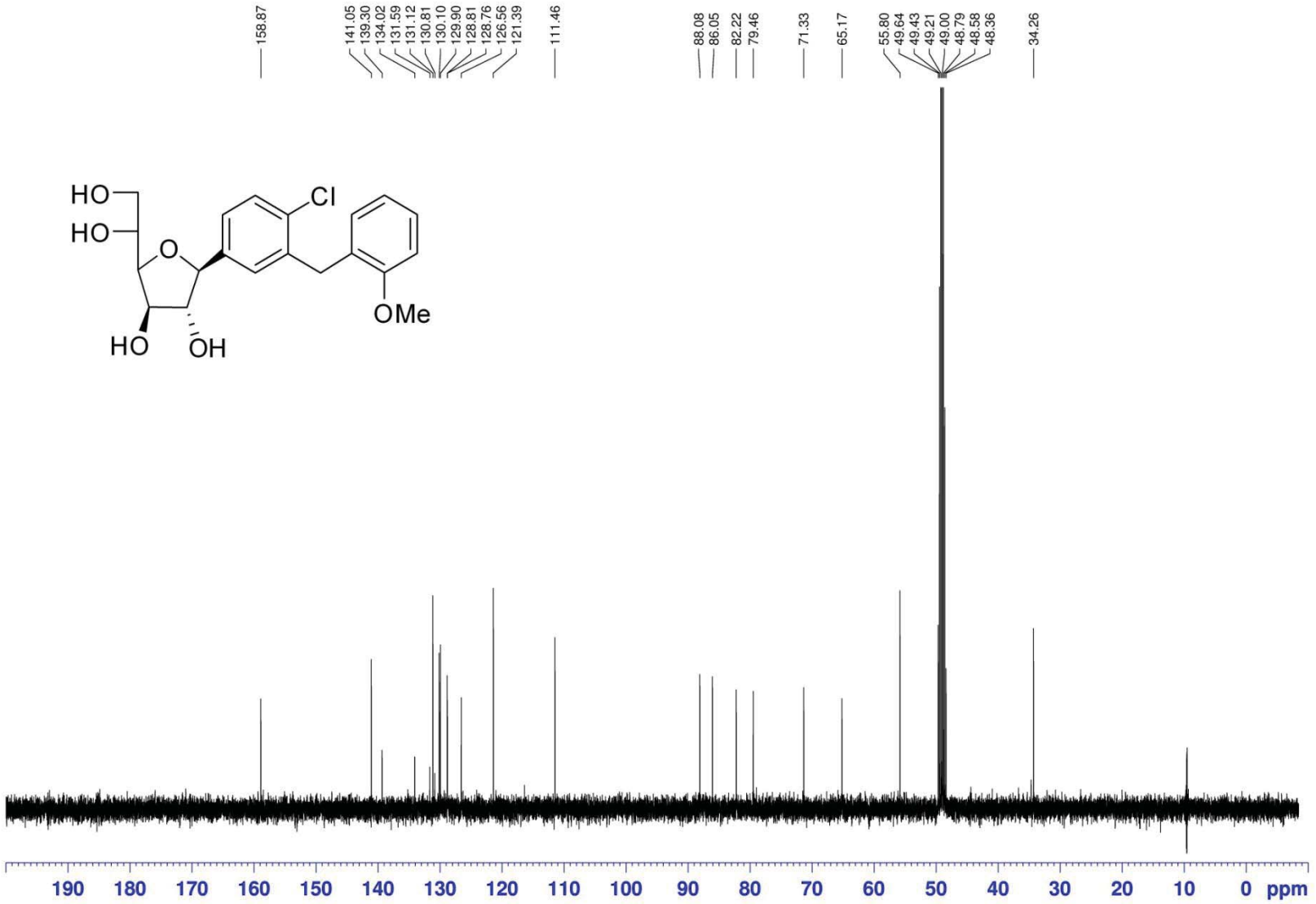

Appendix 78. ^{13}C-NMR spectra of **32i** (100 MHz, d_4-MeOH)

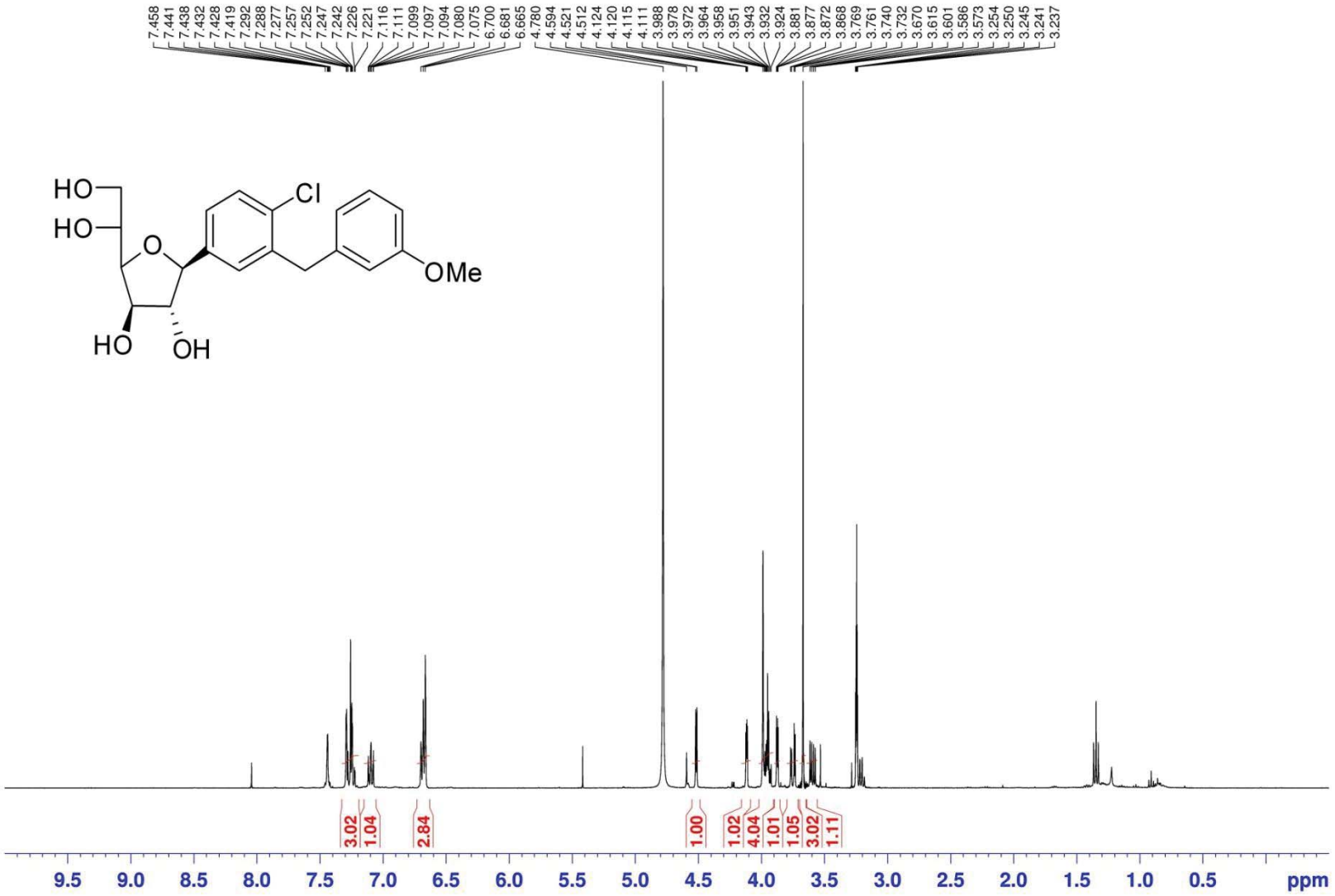

Appendix 79. ^{1}H-NMR spectra of **32j** (400 MHz, d_4-MeOH)

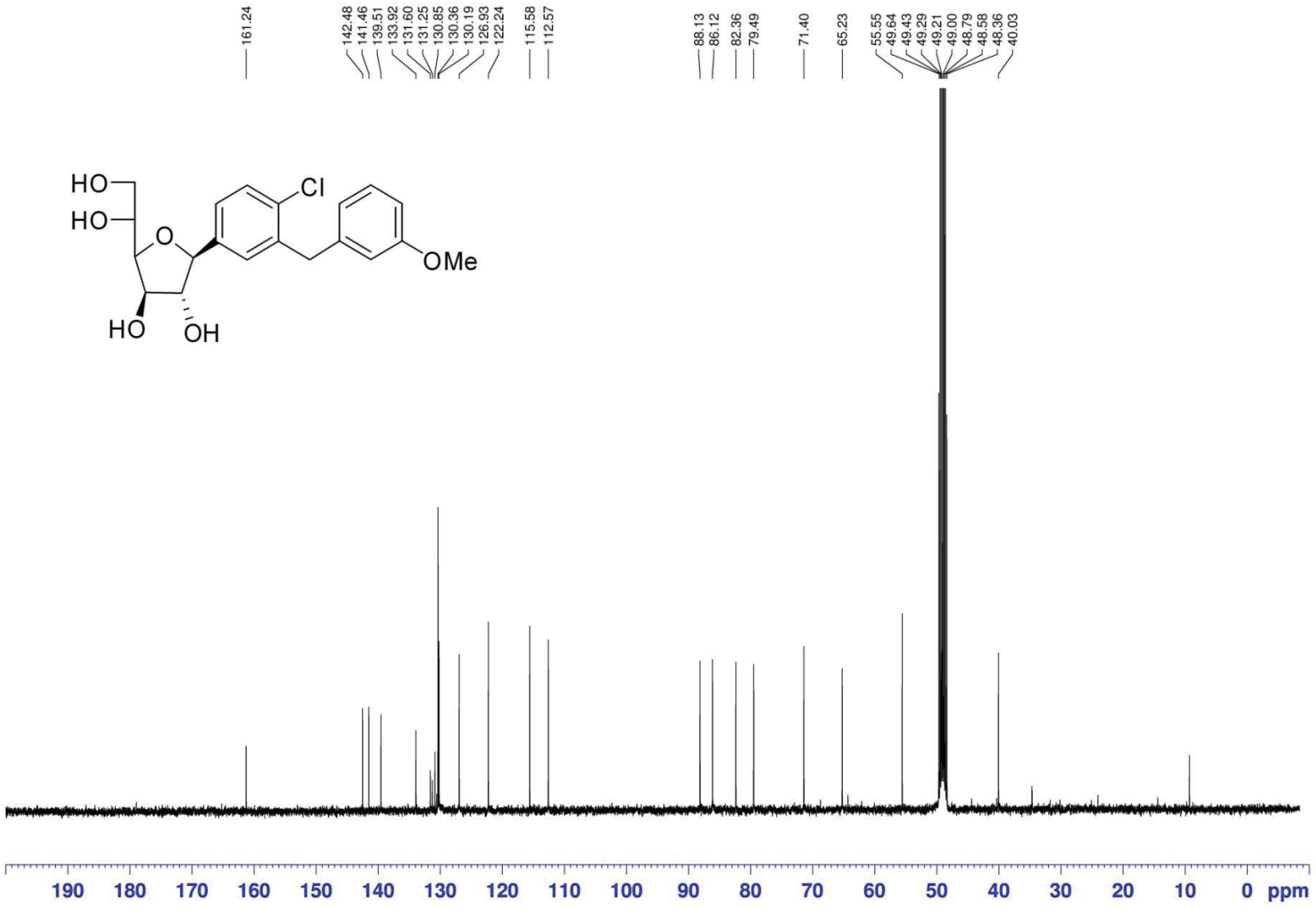

Appendix 80. ^{13}C-NMR spectra of **32j** (100 MHz, d_4-MeOH)

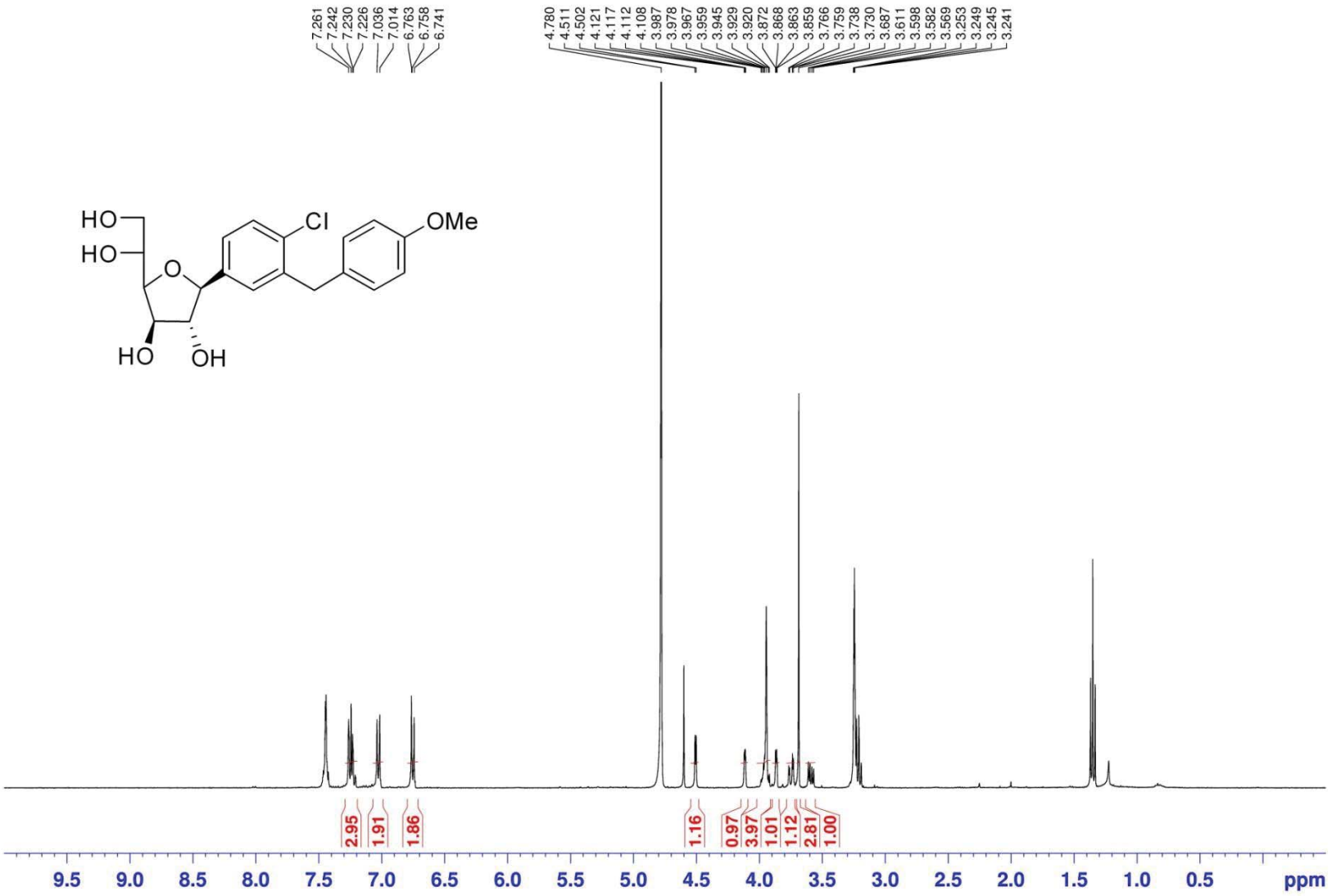

Appendix 81. ^{1}H-NMR spectra of **32k** (400 MHz, d_4-MeOH)

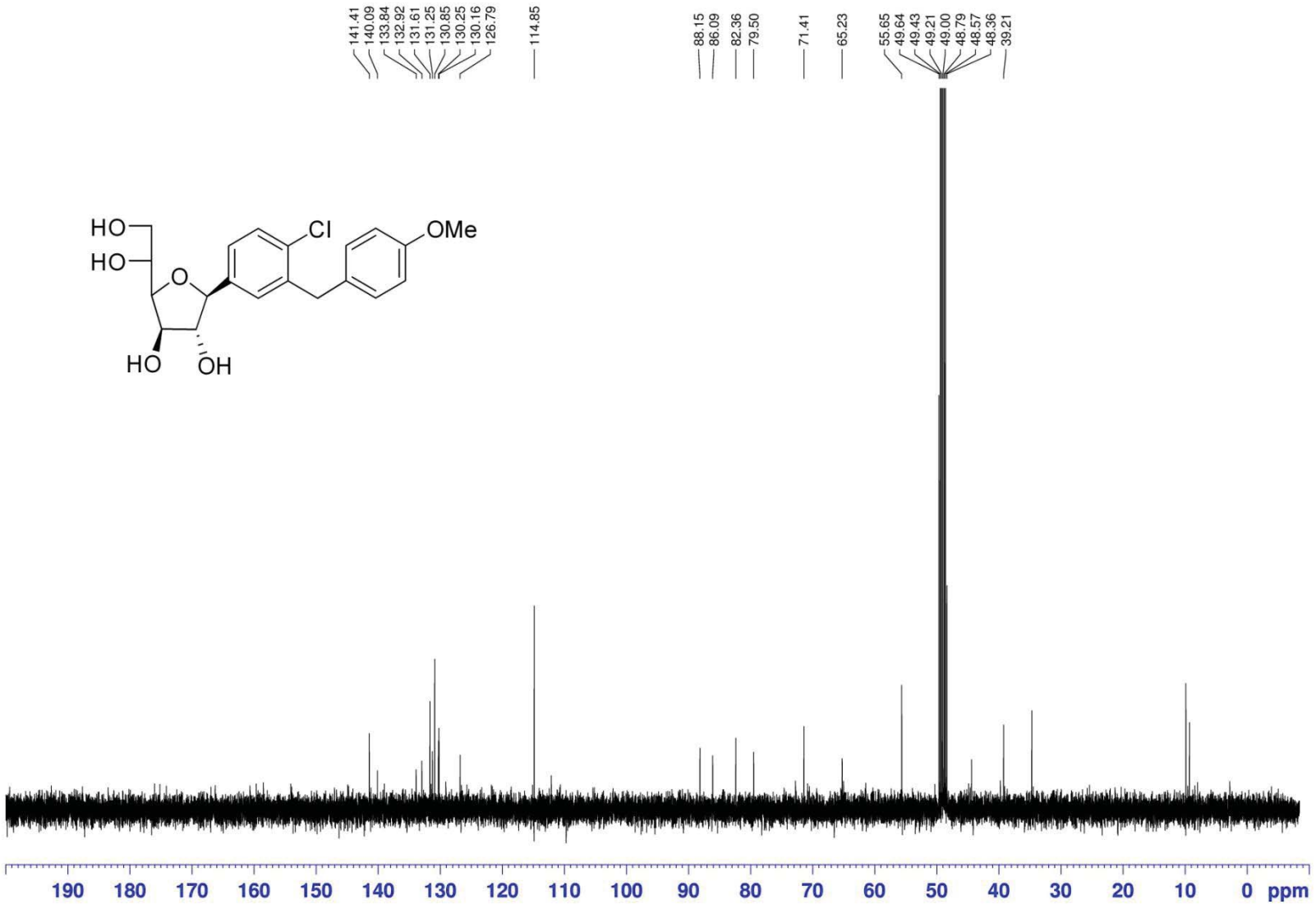

Appendix 82. ^{13}C-NMR spectra of **32k** (100 MHz, d_4-MeOH)

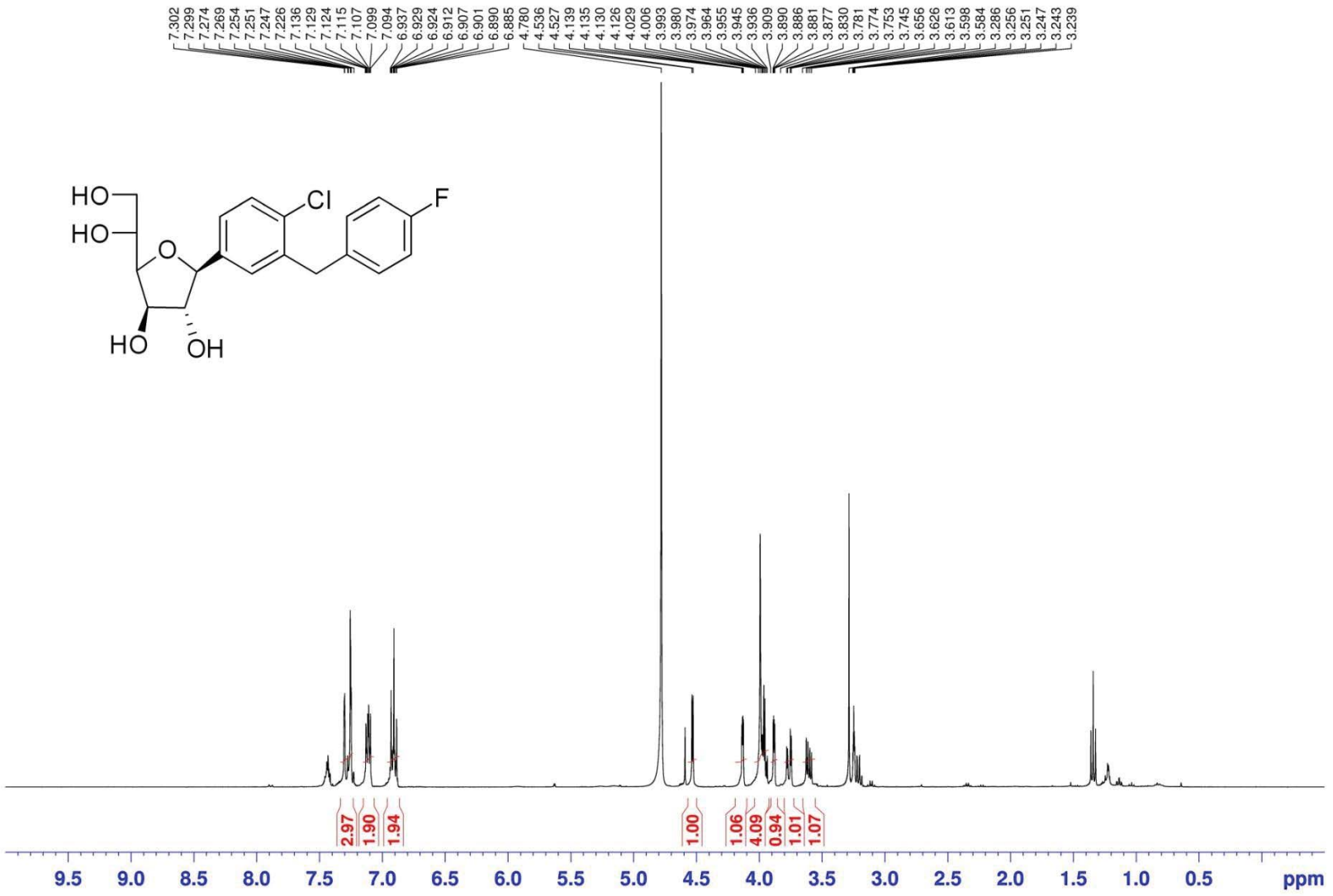

Appendix 83. ^{1}H-NMR spectra of **32l** (400 MHz, d_4-MeOH)

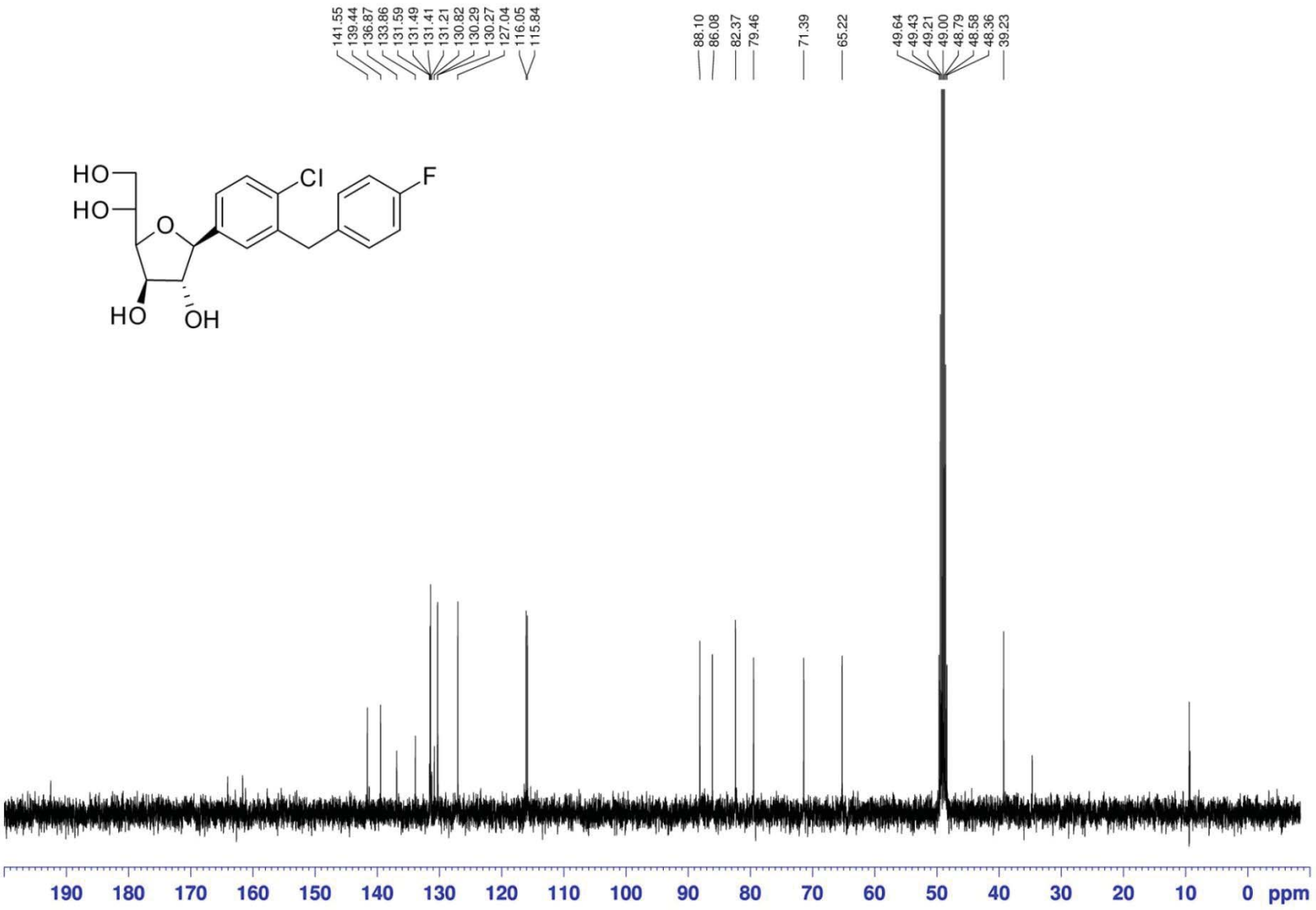

Appendix 84. ^{13}C-NMR spectra of **321** (100 MHz, d_4-MeOH)

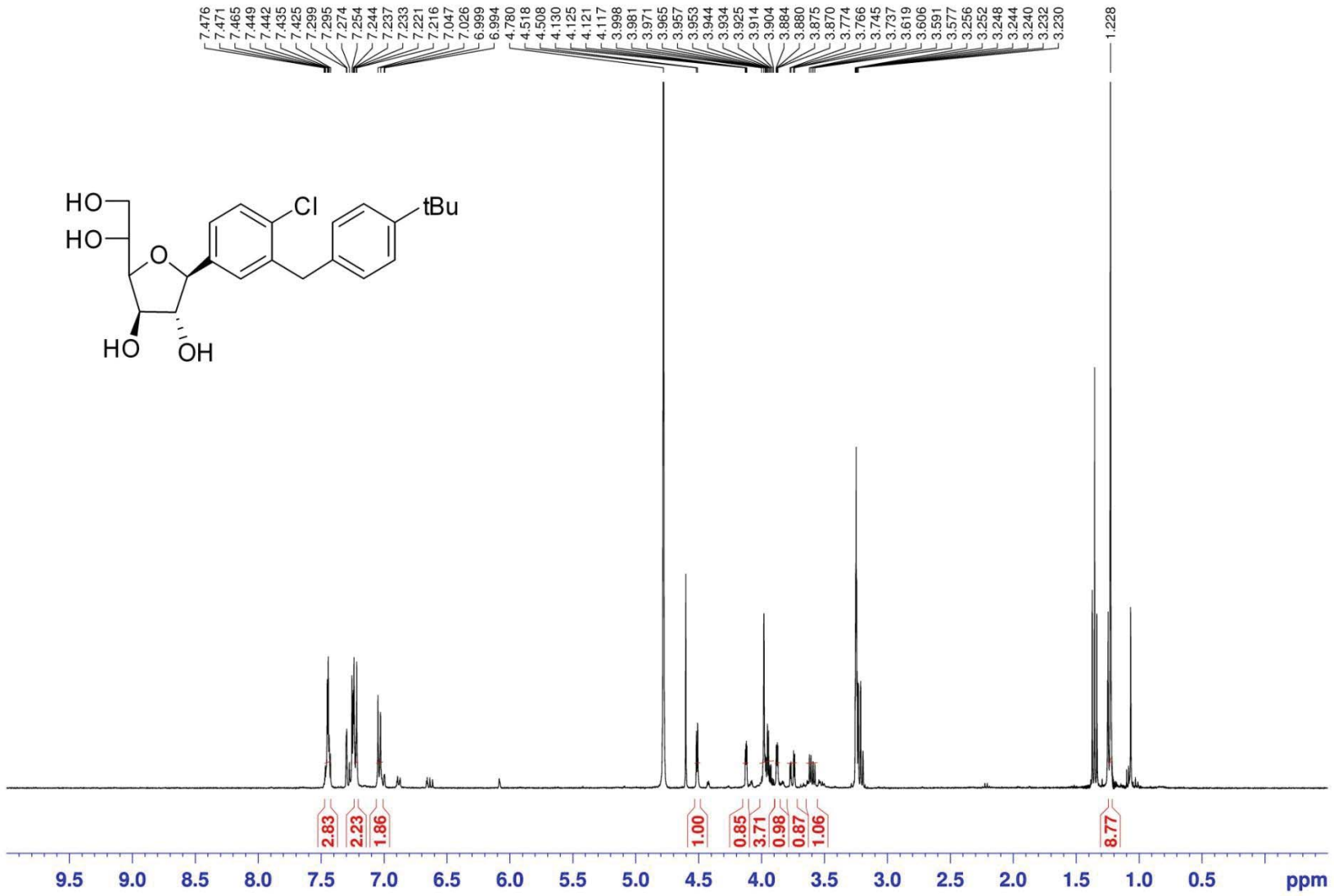

Appendix 85. ^{1}H-NMR spectra of **32m** (400 MHz, d_4-MeOH)

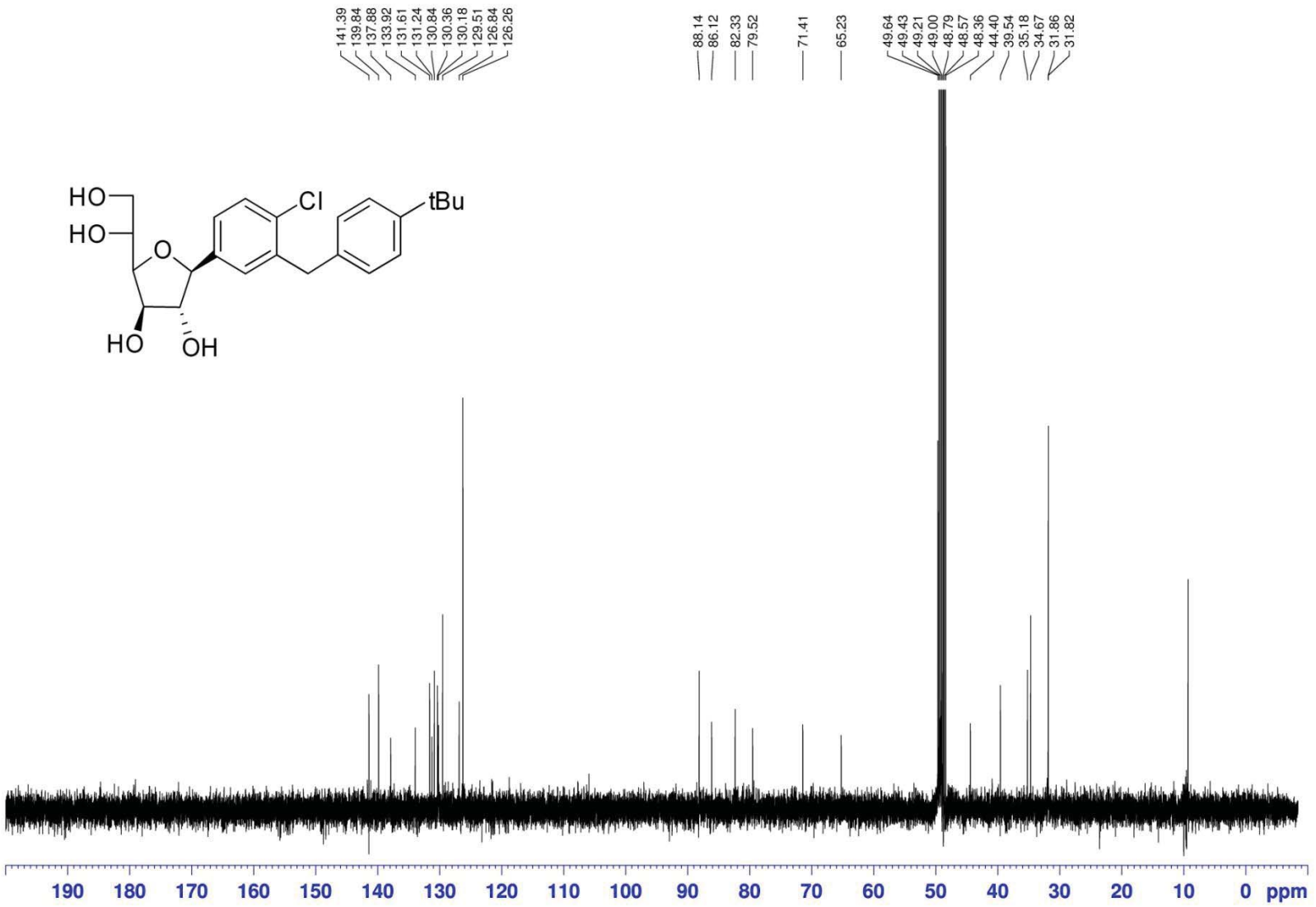

Appendix 86. ^{13}C-NMR spectra of **32m** (100 MHz, d_4-MeOH)

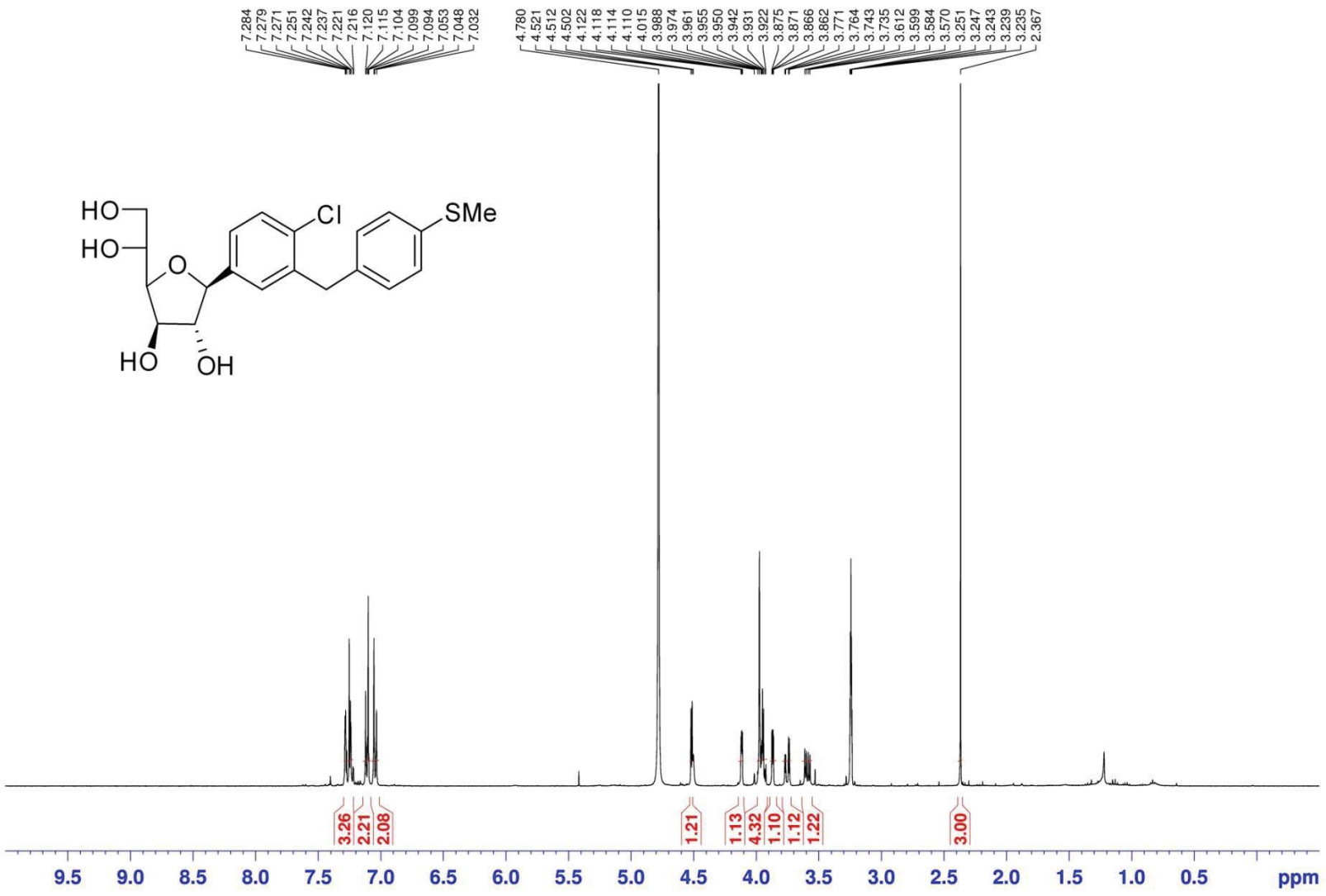

Appendix 87. ^{1}H-NMR spectra of **32n** (400 MHz, d_4-MeOH)

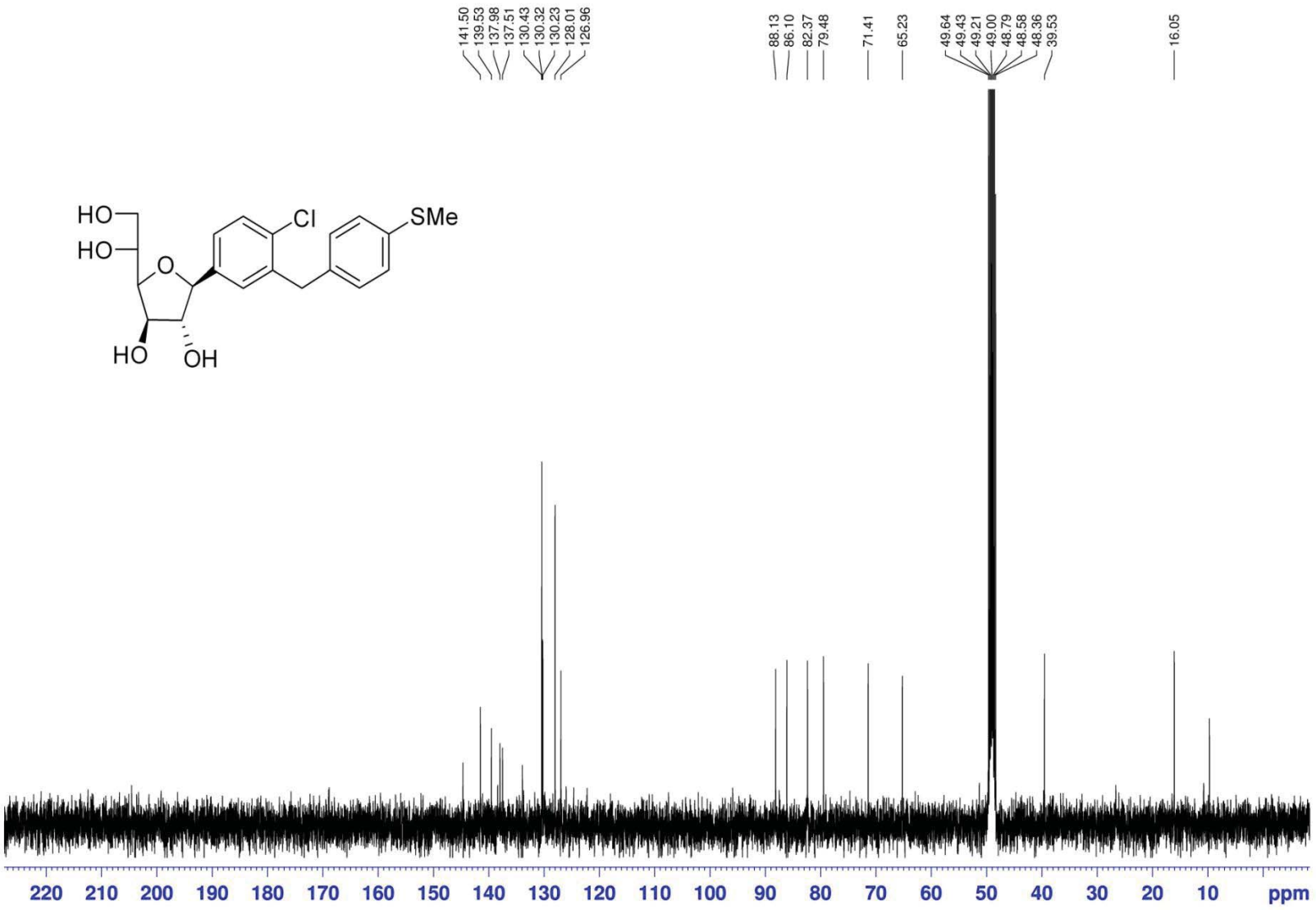

Appendix 88. ^{13}C-NMR spectra of **32n** (100 MHz, d_4-MeOH)

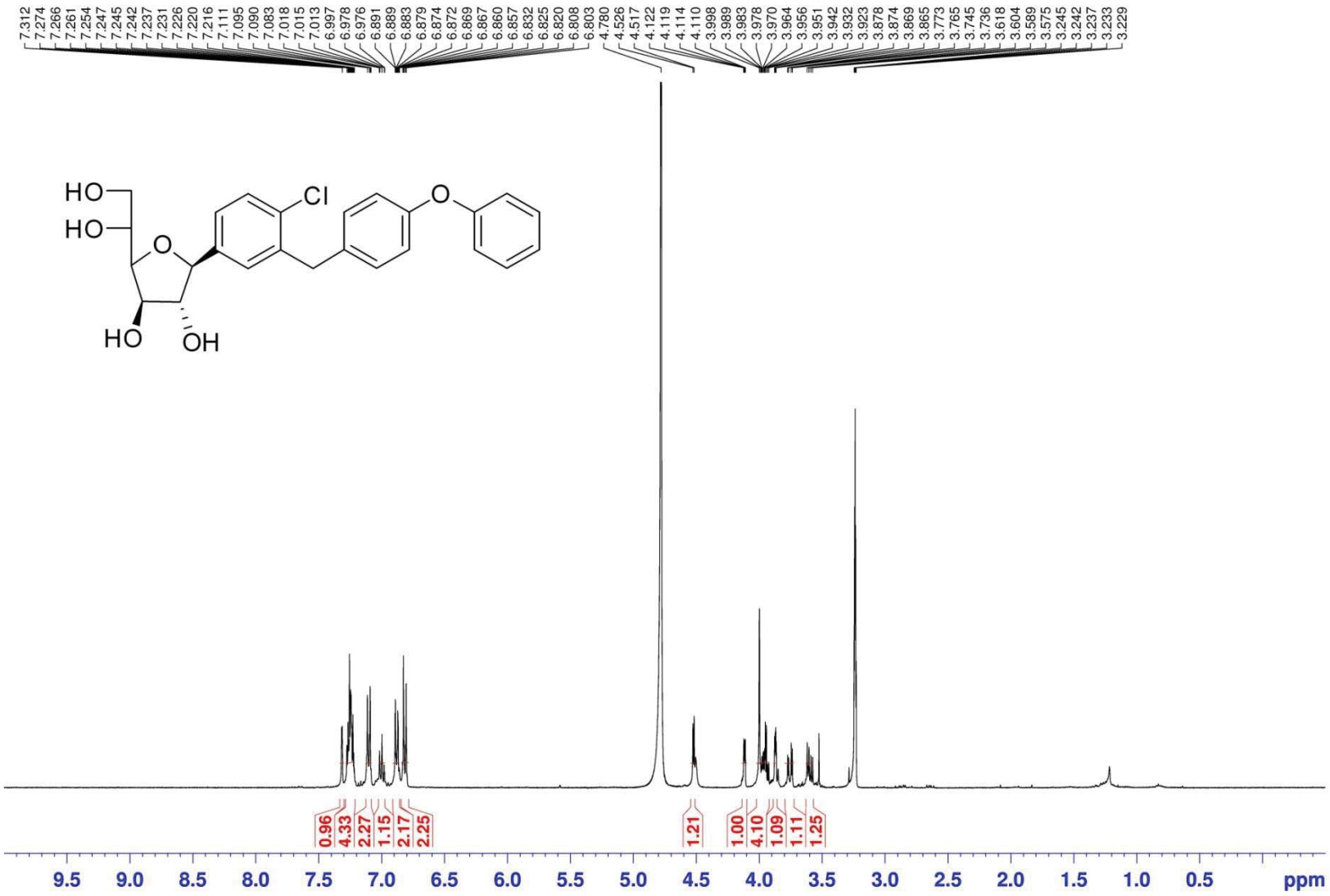

Appendix 89. ^{1}H-NMR spectra of **32o** (400 MHz, d_4-MeOH)

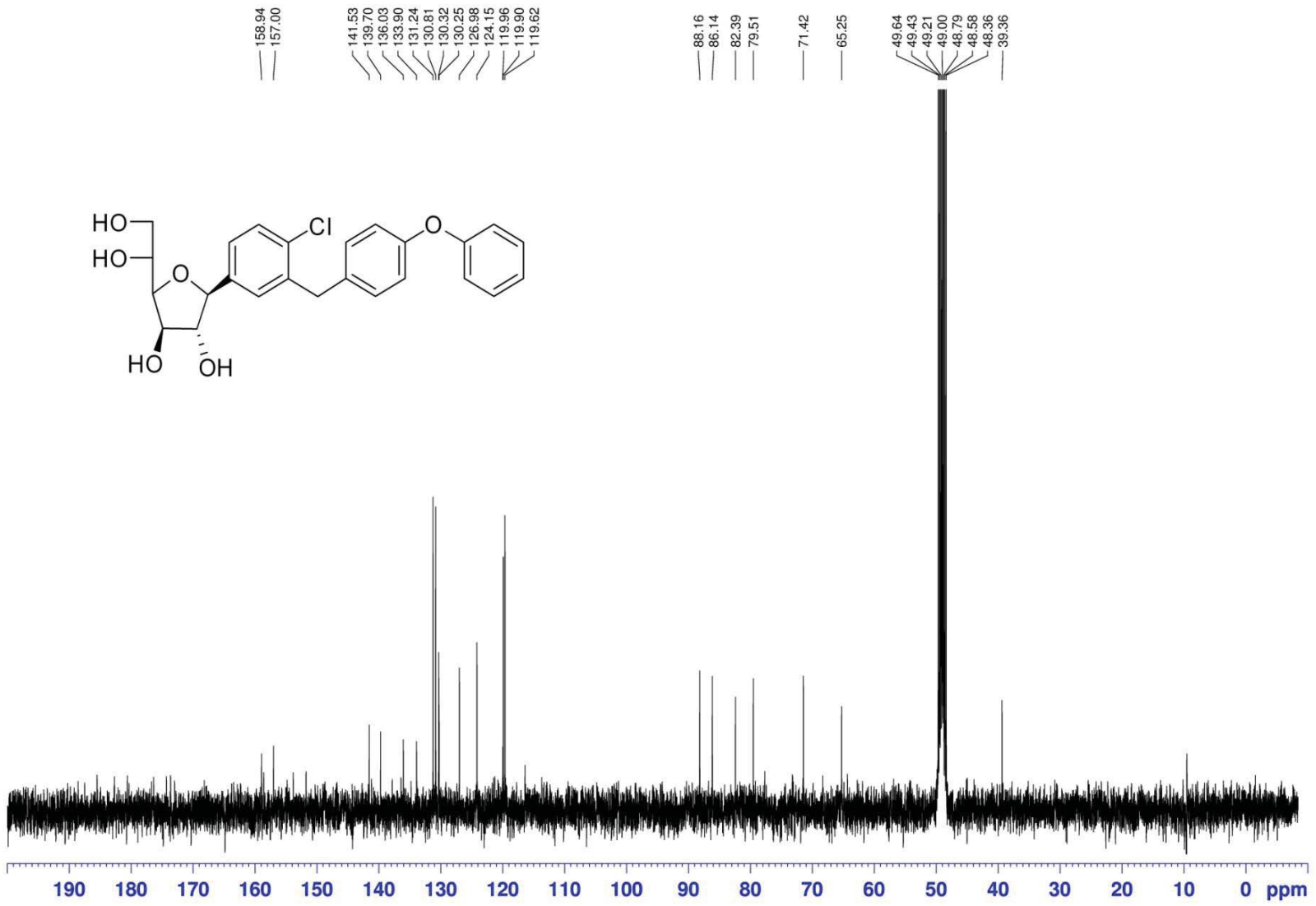

Appendix 90. ^{13}C-NMR spectra of **32o** (100 MHz, d_4-MeOH)

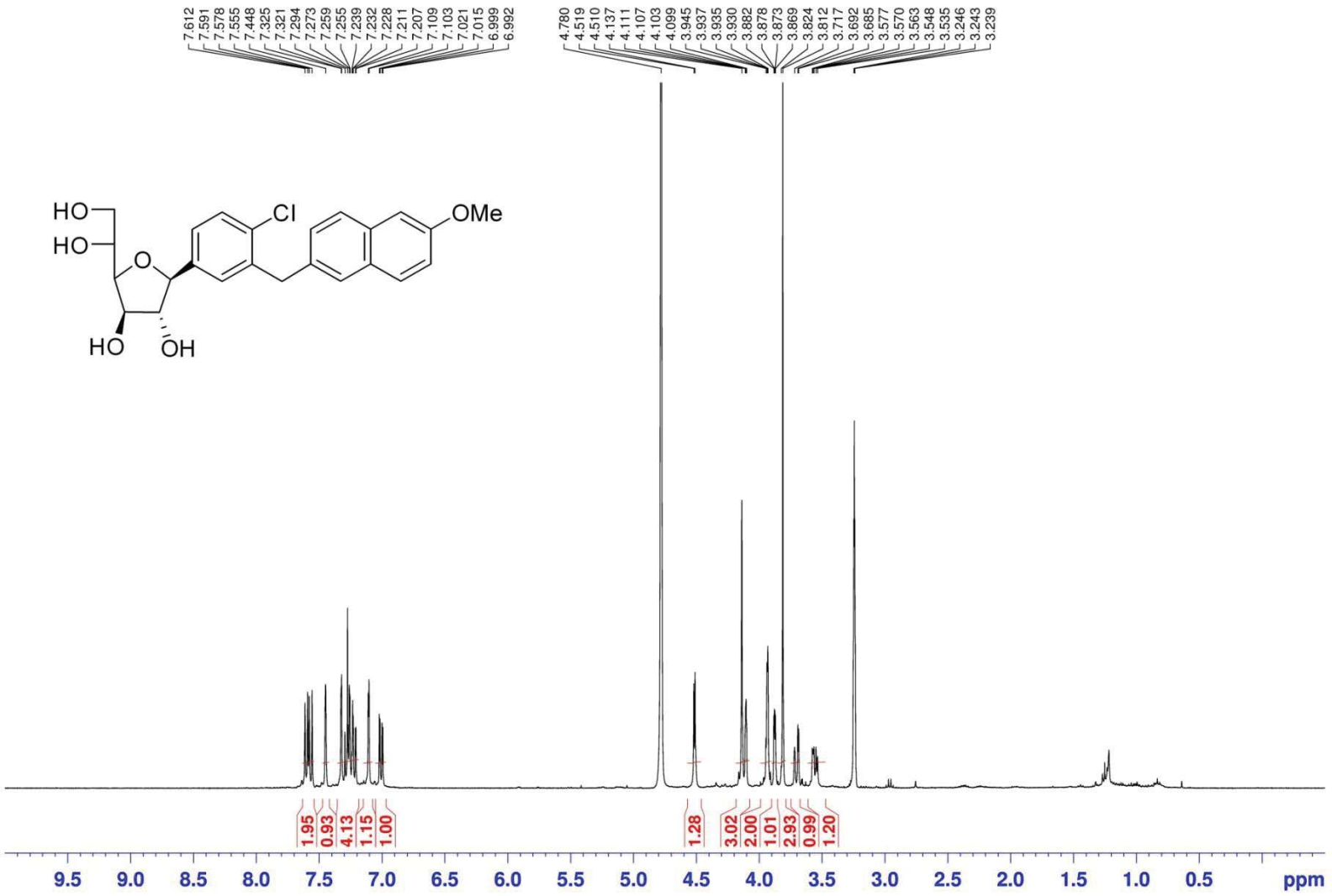

Appendix 91. ^{1}H-NMR spectra of **32p** (400 MHz, d_4-MeOH)

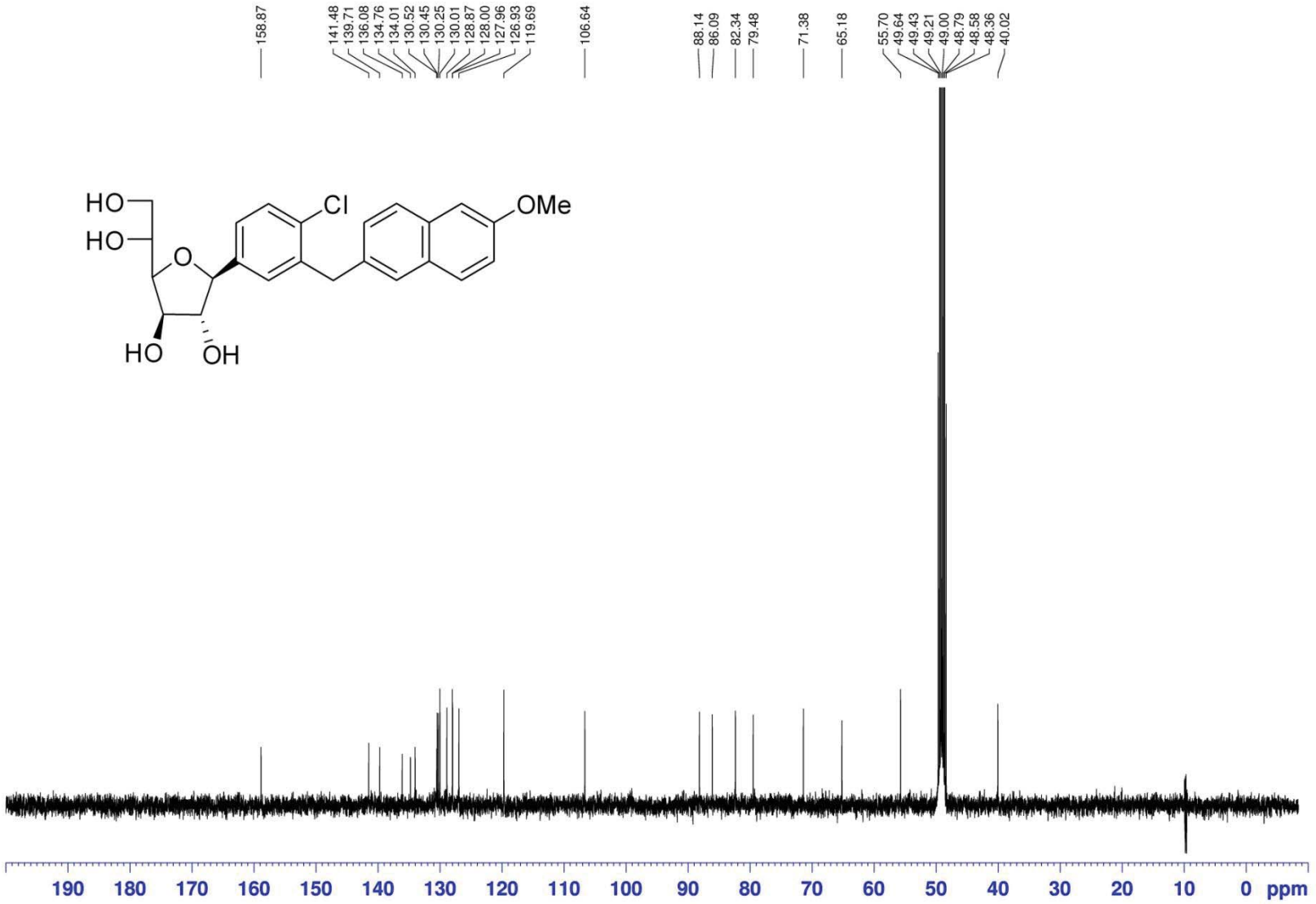

Appendix 92. ^{13}C-NMR spectra of **32p** (100 MHz, d_4-MeOH)

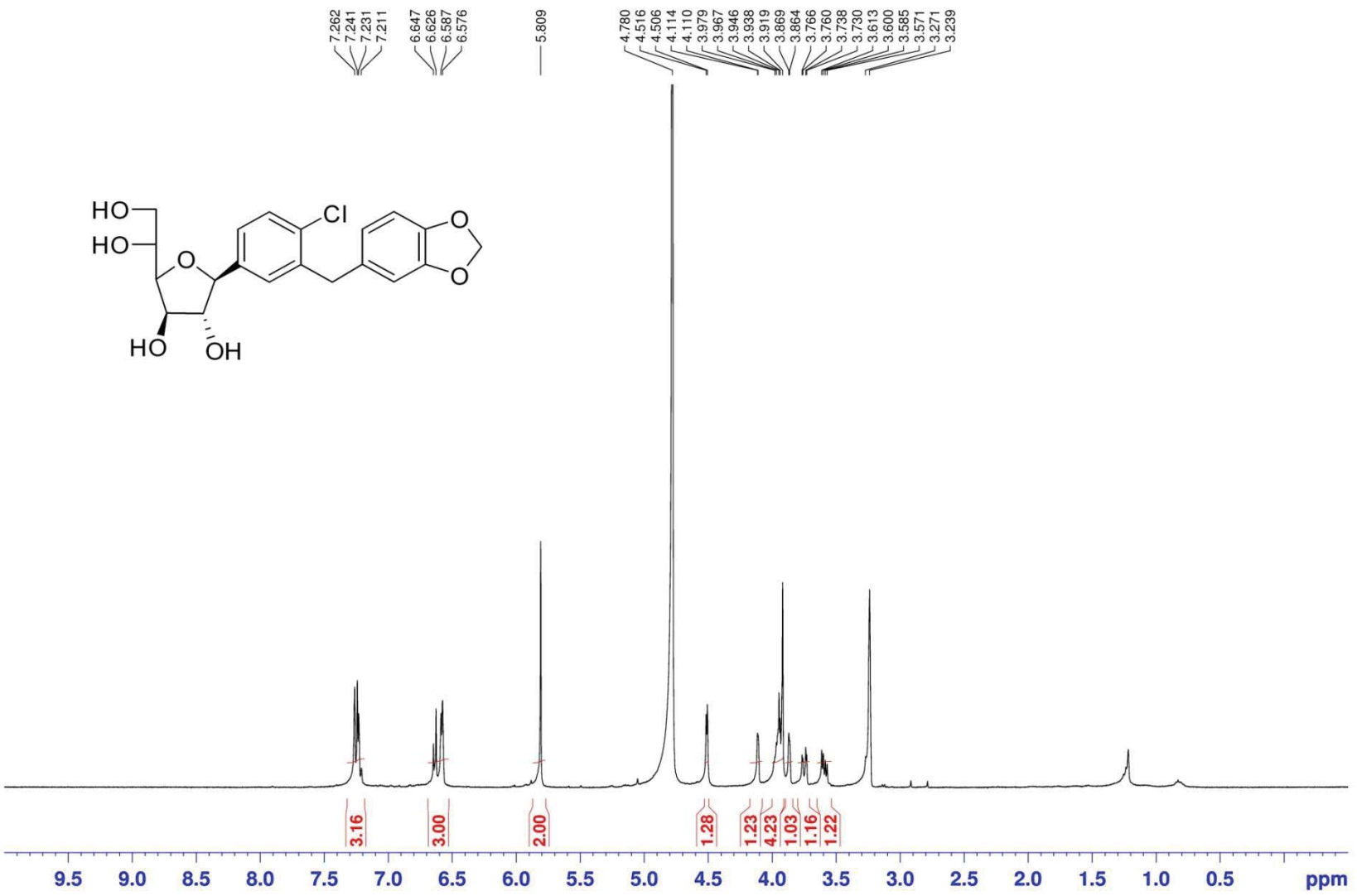

Appendix 93. ^{1}H-NMR spectra of **32q** (400 MHz, d_4-MeOH)

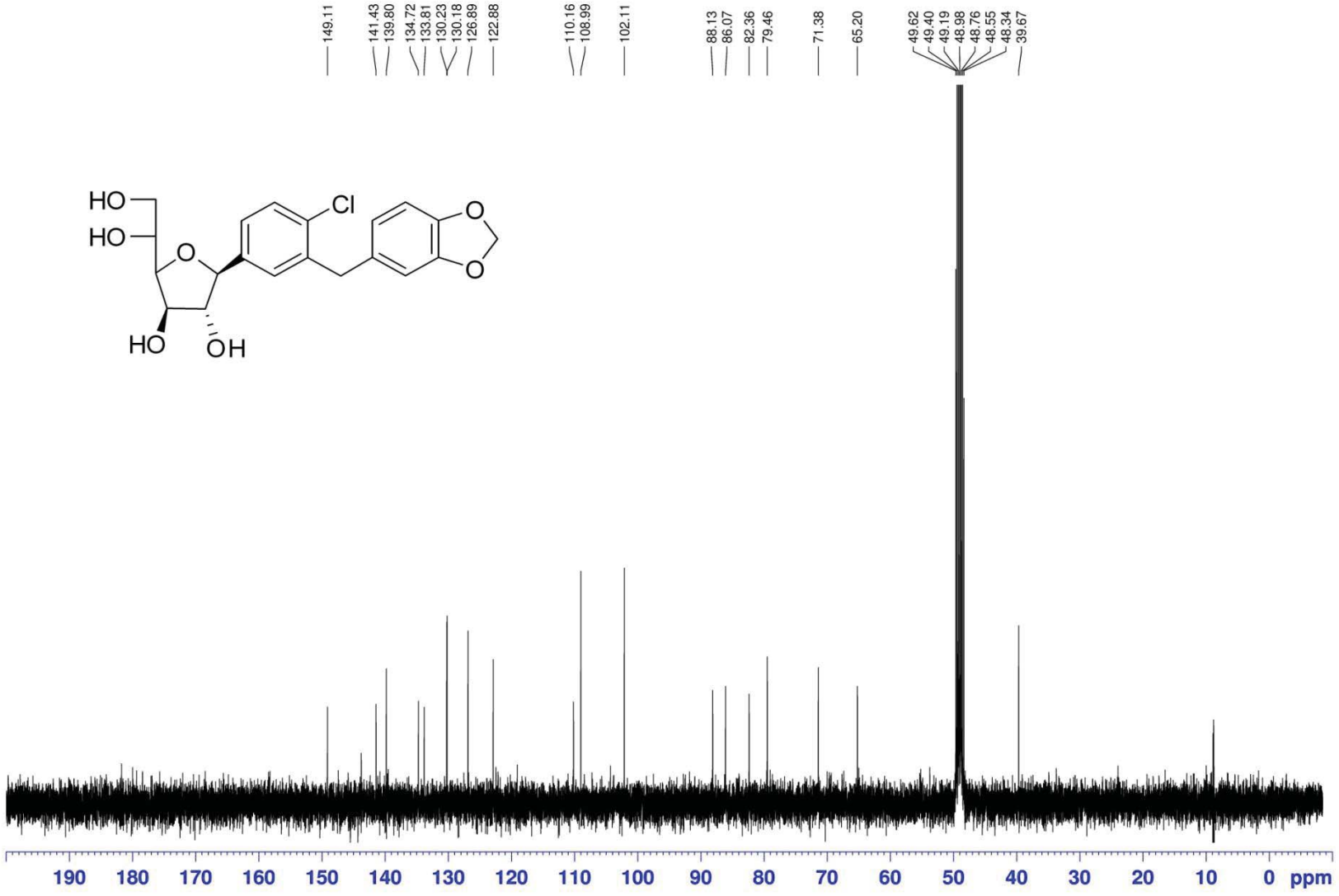

Appendix 94. ^{13}C-NMR spectra of **32q** (100 MHz, d_4-MeOH)